

Characterization of a PKA-like kinase from *Trypanosoma brucei*

**Dissertation der Fakultät für Biologie
der Ludwig-Maximilians-Universität München**

vorgelegt von

Susanne Kramer

Arbeitsgruppe

**Professor Dr. Michael Boshart
Department Biologie I, Bereich Genetik
Ludwig-Maximilians-Universität
München**

eingereicht am

16. Dezember 2004

1. Gutachter

Professor Dr. Michael Boshart
Department Biologie I, Bereich Genetik
Ludwig-Maximilians-Universität
München

2. Gutachter

Professor Dr. Kirsten Jung
Department Biologie I, Bereich Mikrobiologie
Ludwig-Maximilians-Universität
München

Tag der mündlichen Prüfung:

19. April 2005

Erklärung

Ich versichere, daß ich die vorliegende Arbeit, angefertigt am Institut für Genetik des Fachbereichs Biologie der LMU München bei Herrn Professor Dr. Boshart, selbständig durchgeführt und keine anderen als die angegebenen Hilfsmittel und Quellen benutzt habe.

München, am 15.12.2004

(Susanne Kramer)

Erklärung

Ich versichere, daß ich keine Dissertation anderweitig eingereicht habe und mich auch noch keiner Doktorprüfung unterzogen habe.

München, am 15.12.2004

(Susanne Kramer)

Erklärung

Ich versichere, daß ich diese Dissertation oder Teile dieser Dissertation nicht bereits bei einer anderen Prüfungskommission vorgelegt habe.

München, am 15.12.2004

(Susanne Kramer)

Lebenslauf

Name: Susanne Kramer, geb. Schimpf
Adresse: Leipziger Str. 9, 82110 Germering
geboren am: 13.05.1976
Familienstand: verheiratet

SCHULE

1982 – 1995 Polytechnische Oberschule Berlin Marzahn
1990 - 1995 **Gymnasium Scharnebeck**
Abitur 1995 (Note 1.6)

STUDIUM

1995 - 2000 **Freie Universität Berlin**
Studium der Biochemie
1999 Diplomprüfungen (Note 1.0)
10/1999 - 8/2000 Diplomarbeit (Note 1.0)
Priv. Doz. Dr. M. Boshart, AG Molekulare Zellbiologie
Institut für Molekularbiologie und Biochemie, FU Berlin
(Thema: Differentielle Phosphorylierung der katalytischen
Untereinheit der Proteinkinase A bei der Differenzierung
von *Trypanosoma brucei*)

1998 - 1999 **University of Glasgow**
Medical Biochemistry-3(H) (DAAD Stipendium)

PROMOTION

10/2000 – 2/2002 **Promotion**
Professor Dr. M. Boshart, AG Molekulare Zellbiologie
Institut für Molekularbiologie und Biochemie
Freie Universität Berlin
(Thema: Charakterisierung einer Proteinkinase A aus
Trypanosoma brucei)

seit 3/2002 **Fortsetzung der Promotion**
Professor Dr. M. Boshart
Department Biologie I, Bereich Genetik,
Ludwig-Maximilians-Universität München

KONGRESSE und AUSLANDSAUFENTHALTE

9 / 2000	St. Martin de Londre, France, Summerschool: Protein Modules in Signal Transduction (Poster)
12 / 2001	Manchester, GB TrypoFAN Strategy Meeting (Vortrag)
9 / 2001	Woods Hole, USA, Molecular Parasitology Meeting (Poster)
5 / 2003	Schloss Ringberg, Deutschland International Meeting on the Cell and Molecular Biology of Parasitic Protozoa
6 / 2003	Labor J. Mottram, Glasgow (FACS Experimente)

LEHRERFAHRUNG

1997- 1998	Tutorin (Mathematik für Chemiker und Biochemiker, Leitung der Übungen) (Freie Universität Berlin)
seit 2002	Fortgeschrittenenpraktikum Genetik für Biologen (LMU München)

Abstract

The protozoan parasite *Trypanosoma brucei* causes human sleeping sickness and Nagana in domestic animals and depends on the tsetse fly for dissemination. The complex *T. brucei* life cycle requires differentiation from the dividing long slender forms via the cell cycle arrested short stumpy forms (both in the mammalian bloodstream) to the procyclic forms of the insect vector. The signaling pathways that regulate differentiation are unknown but there is evidence for an involvement of cAMP. In search of the putative cAMP receptor, three catalytic and one regulatory PKA-like subunits have been previously cloned from *T. brucei*. The catalytic subunits possess all features of a classical PKA in terms of inhibitor and substrate specificity. It was shown that each of the catalytic PKA-like subunits binds to the regulatory subunit to form a dimeric PKA-like holoenzyme.

Most surprisingly, we found that *T. brucei* PKA-like kinase, despite of its apparent similarities to a PKA, was not activated but instead inhibited by cAMP. Out of several other cyclic nucleotides that were tested on their effects on PKA-like kinase, only cGMP was able to activate the kinase, but in millimolar and thus most likely unphysiological concentrations. Assuming that the activation of PKA-like kinase might depend on its native, subcellular environment, an *in vivo* kinase assay was established in this work. It is based on the immunological detection of the phosphorylated form of the PKA reporter substrate VASP that was transgenically expressed in *T. brucei*. Interestingly, results from the *in vivo* assay did confirm the *in vitro* data, suggesting that *T. brucei* PKA-like kinase is in fact inhibited rather than activated by cAMP.

Even though these findings challenge the original assumption that *T. brucei* PKA-like kinase transmits the differentiation signal mimicked by cAMP antagonists, data from this work nevertheless provide evidence for an involvement of *T. brucei* PKA-like kinase in relaying extracellular cues. This is suggested from an increase in *in vivo* PKA activity in the presence of treatments that have either been shown to induce LS to SS differentiation (etazolate) or to participate in SS to PCF differentiation (cold shock, mild acid stress). In addition, *in vivo* PKA activity was stimulated with the PDE inhibitor dipyrindamole and at hypoosmotic stress.

In the context of a putative role for *T. brucei* PKA-like kinase in the regulation of differentiation, two of the catalytic isoforms (PKAC1 and PKAC2) were of particular interest. We found significant life cycle stage dependent differences in protein expression between the two almost identical isoforms. PKAC1 was nearly exclusively present in bloodstream forms and PKAC2 in procyclic cells. In addition, PKAC1, but not PKAC2 carries a phosphorylation that is restricted to the SS stage. This phosphorylation was mapped to the C-terminal threonine 324 by mass spectrometry. The functions of these life cycle stage dependent differences between PKAC1 and PKAC2 remain unknown. Reverse genetics did not reveal any functional differences between the isoforms, in fact, PKAC1 was even able to complement PKAC2 in procyclic PKAC2 knock-out cells.

Results from several reverse genetic experiments indicate that *T. brucei* PKA-like kinase plays an important role in cell division. Depletion of either PKA-like subunit leads to a cytokinesis block. Depletion of the regulatory PKA-like subunit additionally results in altered basal body segregation. Given that 1) both cytokinesis and basal body movement had been previously suggested to be regulated by the trypanosomal flagellum (Kohl *et al.*, 2003) and 2) the flagellum hosts *T. brucei* PKA-like kinase (C. Krumbholz, this lab) we propose that trypanosomal flagella act as signaling compartments for coordination of cell division.

1. Introduction	1
1.1. <i>Trypanosoma brucei</i>	1
1.1.1. Morphology, phylogeny and pathogenicity	1
1.1.2. Life cycle	2
1.1.3. Cell cycle	4
1.1.4. Unusual biological features	5
1.1.5. <i>T. brucei</i> strains in the laboratory	6
1.1.6. Methods of genetic manipulation	6
1.1.6.1. Gene mutation and deletion	7
1.1.6.2. Expression of transgenes	7
1.1.6.3. RNA interference	8
1.2. Signal transduction in Trypanosomatidae	9
1.3. cAMP signaling	11
1.4. cAMP dependent protein kinases	12
1.5. The <i>T. brucei</i> PKA-like kinase and aims of this Ph.D project	13
2. Materials and Methods	16
2.1. Material	16
2.1.1. <i>Trypanosoma</i> strains	16
2.1.1.1. Wild type strains	16
2.1.1.1. Transgenic strains	16
2.1.2. Bacteria strains	21
2.1.3. Antibodies	21
2.1.3.1. Primary antibodies	21
2.1.3.2. Secondary antibodies	22
2.1.4. Oligos	22
2.1.5. Probes	23
2.1.6. Constructs	23
2.1.7. Enzymes	29
2.1.8. Chemicals	29
2.1.9. Frequently used media and buffers	30
2.1.10. Equipment	31

2.1.11. Kits	31
2.1.12. Software	31
2.2. Methods and Protocols	32
2.2.1. <i>Trypanosoma brucei</i>	32
2.2.1.1. Culture of monomorphic BSF	32
2.2.1.2. Culture of PCF	32
2.2.1.3. Differentiation of monomorphic LS cells into SP cells	32
2.2.1.4. Differentiation of monomorphic BSF into procyclic cells	32
2.2.1.5. Stable transfection of monomorphic BSF cells	32
2.2.1.6. Stable transfection of PCF cells	33
2.2.1.7. Freezing and thawing of <i>T. brucei</i> cells	33
2.2.1.8. Harvest of <i>T. brucei</i> cells	33
2.2.1.9. Methanol fixation and Dapi staining of <i>T. brucei</i> cells	33
2.2.1.10. Paraformaldehyde fixation of <i>T. brucei</i> cells	34
2.2.1.11. Immunofluorescence	34
2.2.2. Nucleic acids	34
2.2.2.1. <i>T. brucei</i>	34
2.2.2.1.1. Isolation of genomic DNA from <i>T. brucei</i>	34
2.2.2.2. <i>E. coli</i>	34
2.2.2.2.1. Preparation of electrocompetent <i>E. coli</i> cells	34
2.2.2.2.2. Transfection of <i>E. coli</i> with plasmid DNA	35
2.2.2.2.3. Isolation of plasmid DNA from <i>E. coli</i>	35
2.2.2.2.4. Long time storage of <i>E. coli</i> cells	35
2.2.2.3. Standard cloning protocols	35
2.2.2.3.1. Agarose Gel electrophoresis	35
2.2.2.3.2. DNA isolation from agarose gel	35
2.2.2.3.3. Modification of DNA	35
2.2.2.3.4. DNA amplification (PCR)	35
2.2.2.3.5. Precipitation of DNA	36
2.2.2.3.6. Quantification of DNA	36
2.2.2.3.7. Sequencing of DNA	36
2.2.2.4. Southern blot analyses	36
2.2.3. Proteins	37
2.2.3.1. Preparation of protein extracts from <i>T. brucei</i>	37
2.2.3.2. Discontinuous SDS Polyacrylamide Gel electrophoresis (SDS PAGE)	37
2.2.3.3. Staining of proteins in Polyacrylamide gels with Coomassie Blue	38

2.2.3.4.	Western blot analyses	38
2.2.3.5.	Affinity purification of antibodies	38
2.2.3.6.	Covalent coupling of anti-Ty1 to protein G sepharose	39
2.2.3.7.	Immunoprecipitation	39
2.2.3.8.	Purification of Ty1-PKAC1 for mass spectrometry	40
2.2.3.9.	<i>In vitro</i> kinase assays	41
2.2.3.10.	<i>In vivo</i> Kinase assays with the PKA reporter substrate VASP	41
3.	Results	42
3.1.	PKAC1 and PKAC2 differ in their life cycle stage dependent posttranslational modifications and expression	43
3.1.1.	<i>Tb</i>PKAC1/2 is posttranslationally modified in SS and PCF cells	43
3.1.1.1.	The stumpy specific modification	44
3.1.1.1.1.	<i>In silico</i> search for potential PKAC1/2 phosphorylation sites	44
3.1.1.1.2.	The stumpy specific phosphorylation was mapped to Thr324 via mass spectrometry	46
3.1.1.1.3.	The stumpy phosphorylation is absent from PKAC2	49
3.1.1.1.4.	The stumpy specific phosphorylation has no influence on PKA activity	50
3.1.1.1.5.	Site directed mutagenesis at Thr324 of PKAC1 results in the loss of the stumpy specific phosphorylation	52
3.1.1.1.6.	Phenotypic analysis of the Thr324 mutant cell lines	53
3.1.1.2.	The PCF modification	57
3.1.2.	Protein expression levels of PKAC1 and PKAC2 in BSF and PCF	58
3.2.	Composition of the <i>T. brucei</i> PKA-like holoenzyme	60
3.2.1.	Coimmunoprecipitation studies with subsequent immunoblotting	60
3.2.1.1.	Generation of cell lines that express epitope tagged subunits	60

3.2.1.2.	Catalytic subunits are only coprecipitated with the regulatory subunit but not with another catalytic subunit	61
3.2.2.	No further coimmunoprecipitated PKAR subunits were detectable on a Coomassie stained gel	64
3.2.3.	No kinase activity was coprecipitated with an inactive PKAC1 (dead mutant)	65
3.3.	Activation of the <i>T. brucei</i> PKA-like kinase	67
3.3.1.	cGMP, not cAMP causes <i>in vitro</i> dissociation of the holoenzyme	67
3.3.2.	cGMP, but not cAMP can activate PKA-like kinase <i>in vitro</i>	68
3.3.3.	<i>T. brucei</i> PKA-like kinase is not activated by cXMP, cIMP, cUMP or cCMP	69
3.3.4.	Detection of <i>in vivo</i> PKA activity with the PKA reporter substrate VASP	70
3.3.4.1.	Transgenic expression of the PKA reporter substrate VASP in <i>T. brucei</i>	70
3.3.4.2.	VASP phosphorylation increases in the presence of the PDE inhibitors dipyridamole and etazolate	72
3.3.4.3.	VASP phosphorylation decreases in the presence of the PKA specific inhibitor KT5720	74
3.3.4.4.	VASP phosphorylation increases with pCPT-cGMP and decreases with pCPT-cAMP	76
3.3.5.	cAMP inhibits PKA <i>in vitro</i>	76
3.4.	Role of <i>T. brucei</i> PKA-like kinase <i>in vivo</i>	79
3.4.1.	Changes in VASP phosphorylation due to different extracellular stresses	79
3.4.1.1.	Effects of increased cell density on VASP phosphorylation	79
3.4.1.2.	VASP phosphorylation increases at low temperatures	80
3.4.1.3.	VASP phosphorylation depends on osmolarity	82
3.4.1.4.	VASP phosphorylation depends on pH	83
3.4.2.	Reverse genetics analyses of <i>T. brucei</i> PKA-like kinase	85
3.4.2.1.	Depletion of PKAR with RNA interference	85
3.4.2.1.1.	Repression of PKAR blocks cellular proliferation	85
3.4.2.1.2.	Repression of PKAR stills allows the complete partition of the nuclei	86
3.4.2.1.3.	Cells can initiate cytokinesis but are unable to complete it	88

3.4.2.1.4.	2K2N cells have increased kinetoplast distances	89
3.4.2.1.5.	The increased kinetoplast distances are not a consequence of cytokinesis block	89
3.4.2.2.	Reverse genetic interference with of PKAC1/2	92
3.4.2.2.1.	Deletion of <i>PKAC2</i> led to reduced growth and block in cytokinesis	92
3.4.2.2.2.	<i>PKAC2</i> is not essential for differentiation into procyclic cells	95
3.4.2.2.3.	Deletion or mutation of one <i>PKAC1</i> allele results in reduced growth and block in cytokinesis	96
3.4.2.2.4.	Gene conversion of the WT <i>PKAC1</i> allele in hemizygote PKAC1 dead mutants	100
3.4.2.2.5.	Depletion of PKAC1/2 with RNAi results in cytokinesis block and cell death	101
3.4.2.2.6.	The PKAC1/2 specific inhibitor KT5720 led to block in cytokinesis and accumulation of 1K2N cells	103
3.4.2.3.	Depletion of PKAC3 results in cytokinesis block and accumulation of 1K2N cells, but not in decreased kinetoplast distances	106
3.5. <i>In silico</i> search for further putative subunits of PKA-like kinases		
3.5.1.	Hidden regulatory subunits ?	111
3.5.1.1.	Search for cNMP binding proteins in the <i>T. brucei</i> genome database	111
3.5.1.1.1.	Three <i>T. brucei</i> proteins have two cNMP binding domains in tandem	112
3.5.1.1.2.	Two of the <i>T. brucei</i> PKAR candidates have highest homologies to PKARs	112
3.5.1.1.3.	Substrate or Pseudosubstrate sequences in the new <i>T. brucei</i> PKAR candidates	114
3.5.1.1.4.	All new PKAR candidates have significant homology to a PKAR specific conserved 14 amino acid stretch in the cNMP binding sites	115
3.5.1.2.	Search for <i>T. brucei</i> proteins with RIIa domains	116
3.5.1.3.	<i>T. brucei</i> might contain up to three further PKAR subunits	117

3.5.2. <i>T. brucei</i> has no further proteins with homologies to catalytic PKA subunits	118
4. Discussion	122
4.1. The catalytic subunits of <i>T. brucei</i> PKA-like kinase	122
4.2. The regulatory subunit of <i>T. brucei</i> PKA-like kinase	123
4.2.1. Holoenzyme formation	123
4.2.2. Activation of the <i>T. brucei</i> PKA-like kinase	126
4.2.2.1. <i>T. brucei</i> PKA-like kinase is activated with cGMP in unphysiologically high concentrations only	126
4.2.2.2. <i>T. brucei</i> PKA-like kinase is inhibited by cAMP	127
4.2.2.3. Establishment of an <i>in vivo</i> kinase assay for <i>T. brucei</i> PKA-like kinase	128
4.2.2.4. The cNMP binding sites of <i>T. brucei</i> PKAR	129
4.3. Functions of <i>T. brucei</i> PKA-like kinase	133
4.3.1. <i>T. brucei</i> PKA-like kinase: a transmitter of environmental stress	133
4.3.1.1. Kinase activity in the presence of the PDE inhibitors dipyridamole and etazolate	133
4.3.1.2. Temperature	134
4.3.1.3. pH value	135
4.3.1.4. Life cycle stage dependent differences in expression and posttranslational modification of PKAC1 and PKAC2	135
4.3.2. Role for <i>T. brucei</i> PKA-like kinase in cell cycle regulation	138
4.3.2.1. <i>T. brucei</i> PKA-like kinase is essential for cytokinesis progression	138
4.3.2.2. Role for <i>T. brucei</i> PKA-like kinase in basal body movement	139
4.3.2.3. The trypanosomal flagellum: a signaling compartment for cell cycle regulation?	140
4.4. The <i>T. brucei</i> PKA-like kinase: current view and outlook	141

Abbreviations	144
References	146
Acknowledgments	162
Attachment	163

1. Introduction

1.1. *Trypanosoma brucei*

1.1.1. Morphology, phylogeny and pathogenicity

Trypanosoma brucei is an eucaryotic parasite that belongs to the order of kinetoplastida. This unicellular organism has a length of approximately 20 μm and a flagellum attached to its cell body. The name giving kinetoplast, containing the DNA of the single mitochondrion, is located near the basal body. (Fig. 1A) Subspecies of *T. brucei* are the causative agents of African trypanosomiasis or sleeping sickness, a disease of tropical Africa that is transmitted by the tsetse fly. Gambian or West African sleeping sickness is due to the infection with *T. brucei gambiense* and Rhodesian or East African sleeping sickness is due to the infection with *T. brucei rhodesiense* (Fig. 1B).

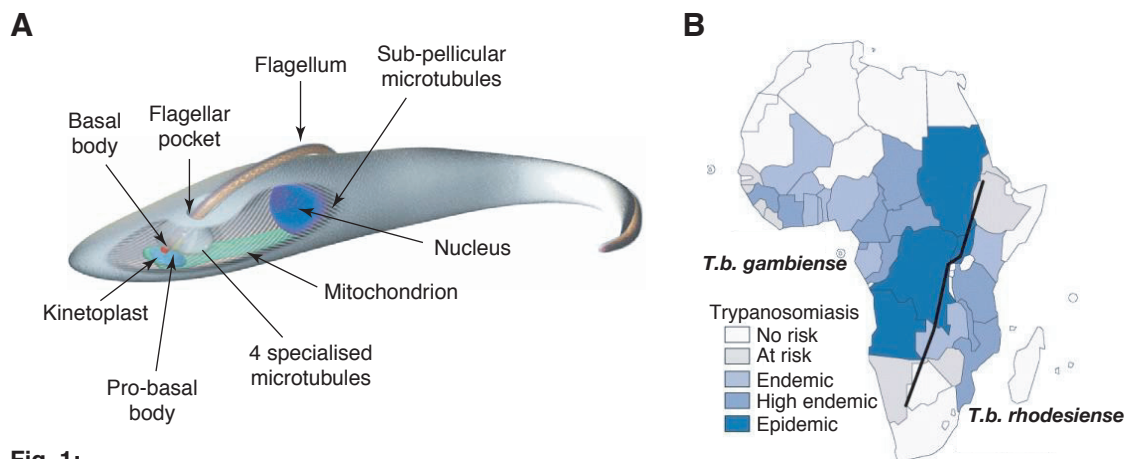


Fig. 1:

A) Schematic representation of a *T. brucei* cell on the basis of electron microscopy studies. The relative positions of organelles such as the nucleus (dark blue), kinetoplast (light blue), mitochondrion (green), basal and probasal bodies (red and yellow respectively) and the flagellum are shown. (Picture taken from Vaughan *et al.* (2003))

B) Geographical extension of *T. b. gambiense* and *T. b. rhodesiense* in Africa. (WHO 1999)

African sleeping sickness is a daily threat to more than 60 million people, in 36 countries of sub-Saharan Africa, 22 of which are among the poorest countries in the world. Only 3 to 4 million of these people have access to medical treatment and surveillance. 45,000 cases of sleeping sickness were reported to the WHO in 1999, but the estimated number of people thought to have the disease is between 300,000 and 500,000 (WHO, 2001). African sleeping sickness can be treated, when diagnosed at an early stage, although

the drugs in use are often too expensive for the African developing countries. At late stages, the disease can only be cured with Melarsoprol that is very toxic but so far the only available drug that can pass the blood brain barrier.

Other *T. brucei* subspecies, among them *T. brucei brucei*, cause the related cattle disease Nagana and are a major economical problem in tropical Africa, but do not affect humans.

1.1.2. Life cycle

Trypanosomes undergo major morphological and metabolic changes during their complex life cycle (Fig. 2). These changes are further characterized by the alternate occurrence of proliferating and cell cycle arrested forms. It is of vital importance for trypanosomes to adapt quickly to new environments as different as the mammal blood and the tsetse fly midgut.

Metacyclic, non-proliferating trypanosomes are transferred via insect bite to the dermal tissue of the mammal where they transform into proliferating long slender (LS) trypanosomes and cause a local inflammation (shanker). Later they invade blood and lymph, which is accompanied by irregular fever and headaches of the affected host. In the second phase of the infection trypanosomes cross the blood brain barrier and reside in the cerebrospinal fluid. At this stage the host is suffering from chronic sleep disorders, apathy, tremor and paralysis.

LS trypanosomes are mainly present at the early stages of the infection. They exclusively metabolize the abundant glucose present in the blood of the mammalian host. Their mitochondrion is not actively engaged in energy production and most respiratory chain enzymes are missing. LS trypanosomes therefore depend entirely on glycolysis which takes place in special organelles, the glycosomes. When cells reach a threshold density, they differentiate into cell cycle arrested short stumpy forms (SS). SS forms differ morphologically from LS cells by their more compact shape and shorter flagellum. They are metabolically preadapted to their life in the tsetse midgut with proline as main energy source. Their mitochondrion is enlarged (Priest and Hajduk, 1994) and mitochondrial enzymes, such as pyruvate dehydrogenase, proline oxidase and α ketoglutarate dehydrogenase are expressed (Flynn and Bowmann, 1973). When SS forms are not taken up by a tsetse fly they die within three to four days. The occurrence of the cell cycle arrested SS forms is thought to be important to control the parasitaemia and prevent an

early death of the host. Since only a fraction of the LS cells differentiates into SS cells, the blood stream form population (BSF) is a mixture of LS and SS cells. This heterogeneous population is termed pleomorphic. The surface of BSF trypanosomes is completely covered with the variant surface glycoprotein (VSG). By antigenic variation (described below) this specific VSG can be exchanged. This process allows clonal variants in the switching population to persist the host immune system. During the bloodmeal of the tsetse fly on an infected mammalian host, SS cells are transmitted back to the tsetse vector into its midgut. There they differentiate into proliferating procyclic cell forms (PCF). This process takes 48 to 72 hours and is called transformation.

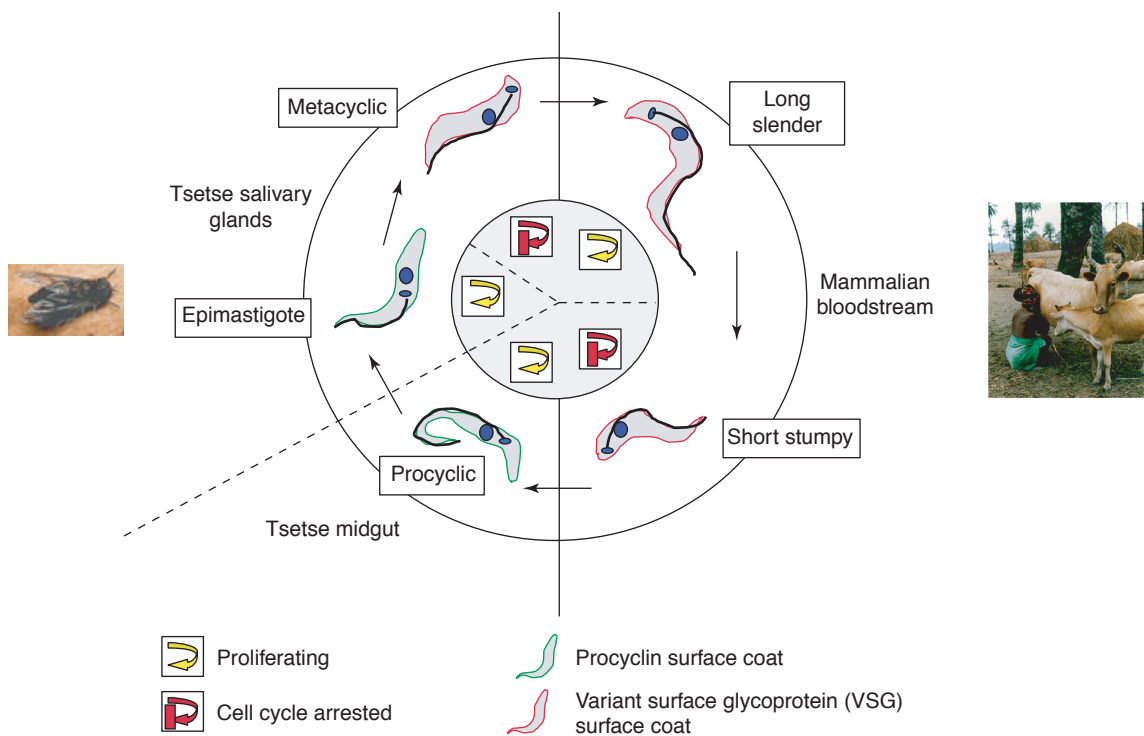


Fig. 2:

Schematic view of the *T. brucei* life cycle. Profound changes in morphology, surface coat, metabolism and cell cycle phase are indicated. (Picture modified from McKean 2003)

The cell surface of PCFs is now covered by procyclin (Roditi *et al.*, 1989). Procyclic cells are longer than BSF cells, they have a very large mitochondrion, which is metabolically active and has a complete respiratory chain (Priest and Hajduk, 1994; Van Weelden *et al.*, 2003; Rivière *et al.*, 2004; Hannaert *et al.*, 2003). After ten days, procyclic cells differentiate into cell cycle arrested proventricular mesocyclic forms (not shown in figure 2) that migrate into the salivary glands. Here they transform into proliferating epimastigote

forms that attach their flagella to the microvilli of the epithelial cells. Epimastigote forms differentiate into metacyclic forms that are cell cycle arrested and express VSG. They are transferred to the mammalian host during the tsetse blood meal and the life cycle starts again.

1.1.3. Cell cycle

Trypanosoma brucei possess an unusually large number of single copy organelles/ compartments such as the kinetoplast, the flagellum, the mitochondrion, the lysosom and the Golgi apparatus. During cell division, these components must replicate and segregate correctly to ensure the survival of the daughter cells. The order and timing of the *T. brucei* cell cycle events have been subjects of extensive studies (reviewed in McKean 2003) and novel cell cycle control mechanisms have been found (Hammarton *et al.*, 2003b; Ploubidou *et al.*, 1999, compare also 1.2.). The cell cycle is initiated with the elongation and maturation of the pro-basal body and the nucleation of a new flagellum. Subsequently, the DNA of the kinetoplast and the nucleus is replicated, whereby kinetoplast S phase initiates before the onset of nuclear S phase and is considerably shorter. Early in G2 phase of the nuclear cycle, basal bodies separate in a microtubule-mediated process also resulting in the separation of the kinetoplasts (Robinson *et al.*, 1991) that are coupled to the basal bodies via the tripartite attachment complex (TAC) (Ogbadoyi *et al.*, 2003). Mitosis occurs with an intranuclear spindle without the disruption of the nuclear envelope. The actual mechanism of chromosome segregation remains unknown, since the number of chromosomes outnumbers the number of kinetochores (Ogbadoyi *et al.*, 2000; Gull *et al.*, 1998). The cell cycle is completed by cytokinesis with the formation of the cleavage furrow along the entire longitudinal axis of the dividing trypanosome.

The *T. brucei* cell cycle can be easily studied when the nuclei and kinetoplasts are stained with the DNA dye DAPI. Thereby the kinetoplast provides a usefull additional marker for the classification of each individual cell to a certain cell cycle phases. Cells are classified as either 1K1N, 2K1N or 2K2N cells, according to the number of their nuclei (N) and kinetoplasts (K). 1K2N cells do not exist since the kinetoplasts always segregate before the nucleus divides. Disruptions of the cell cycle may led to the occurrence of abnormal K/N configurations such as 0K1N, 1K0N (zoid), 1K2N or 4K4N.

1.1.4. Unusual biological features

Kinetoplastida diverged early on during evolution from the eukaryotic main branch. Thus, they possess several unique and unusual biological features that make them very interesting research subjects, not only for parasitologists.

T. brucei first became famous for a process called antigenic variation, a mechanism that the parasite has established to escape the host immune system by frequently changing the cell surface coat (reviewed in Borst 2002; Pays *et al.*, 2001; Cross *et al.*, 1998 and others). Each *T. brucei* cell is completely covered with VSG protein that is transcribed from a telomeric expression site. About 20 of such expression sites exist in each cell, but only one is active at any given time, transcribing only one specific VSG. With a certain frequency, one out of around 1000 different VSG genes that are present in the *T. brucei* genome can replace the VSG gene in the active expression site by reciprocal recombination or gene conversion. The rate of VSG switching is between 10^{-3} to 10^{-2} per division for trypanosomes that have recently passed through the tsetse fly (Turner and Barry, 1989) and 10^{-6} to 10^{-7} for culture adapted trypanosome strains. While most of the trypanosome population express the same VSG molecule at their cell surface and will be finally killed, a small subpopulation is always able to express a different VSG gene and escape the attacks of the immune system.

Another quite unusual feature of this eukaryotic parasite is its mechanism of mRNA processing and gene regulation that involves polycistronic transcription and trans splicing. The protein-coding genes of *T. brucei* are devoid of class II introns and are packed in dense clusters containing both tandem repeats of the same or very similar ORF and completely unrelated ORFs. The intergenic regions are very short. The gene arrays are transcribed in long polycistronic units. Individual mature mRNAs are processed from primary transcripts by the addition of a cap at the 5' end through trans splicing and a poly (A) tail at the 3' end (reviewed in Tschudi *et al.*, 2002). The cap donor is a spliced leader, termed miniexon, arising from the processing of a miniexon donor RNA (141 nucleotides). It is transcribed on arrays of repeated genes. Most interestingly, genes of the same primary transcription unit can show remarkably different expression patterns even though the transcription is regulated from the same promoter (reviewed in Vanhamme and Pays, 1995). This led to the major conclusion that trypanosomes control their gene expression primarily on the posttranscriptional level.

1.1.5. *T. brucei* strains in the laboratory

In vitro culture systems are available for bloodstream and procyclic stage *Trypanosoma brucei* (Brun and Schonemberger, 1979; Hirumi and Hirumi, 1989; Vassella *et al.*, 1996); other developmental stages can only be analyzed in the tsetse host. To avoid the problem that all pleomorphic trypanosomes differentiate into non-proliferating SS forms, most research is done with the so-called monomorphic strains. These cells were adapted to laboratory growth by serial syringe passages between rodents (Ashcroft, 1960). They can be kept at relatively high cell densities and have lost their ability to differentiate into SS forms. However, when monomorphic cells grow to high cell densities, they acquire some functional and metabolic features of short stumpy cells (Braidbach *et al.*, 2002). *In vitro* cultured monomorphic and pleomorphic BSF trypanosomes can be induced to transform into procyclic cells by the addition of citrate or cis-aconitate and by a decrease in cultivation temperature (Brun and Schonemberger, 1981; Simpson *et al.*, 1985; Engstler and Boshart, 2004; reviewed in Matthews and Gull, 1994).

1.1.6. Methods of genetic manipulation

The haploid genome of *T. brucei* is about 35 Mb and varies in size between the different trypanosoma strains in as much as 25%. It contains around 10,000 genes or predicted genes. The DNA of the diploid organism is organized in three size classes of chromosomes: the megabase chromosomes of which there are at least 11 pairs ranging from 1 to 6 Mb in size (numbered I-XI from smallest to largest), several intermediate chromosomes of uncertain ploidy ranging from 200 to 900 kb and about 100 linear minichromosomes of 50 to 150 kb. Around 50% of the DNA sequence is coding. (Reviewed in El Sayed *et al.*, 2000) The 11 megabase chromosomes of the *T. brucei* strain TREU927/4 GUTat10.1 were completely sequenced by the Institute for Genomic Research (TIGR) and the Wellcome Trust Sanger Institute.

The availability of the *T. brucei* genome sequence greatly facilitates the application of reverse genetic methods for the analyses of protein functions. Both monomorphic and pleomorphic BSF and procyclic trypanosomes can be genetically manipulated by DNA transformation (reviewed in McCulloch *et al.*, 2004). Stable transformants are generally obtained by homologous recombination of the DNA of interest together with a dominant selection marker gene into the target locus. In this way genes can be altered or deleted, expression levels changed, transgenes can be introduced and even gene-knock-downs

by inducible expression of double strand RNA (RNA interference) are possible. Two types of targeting vectors that differ in their integration mechanisms are used in *T. brucei*. The ends-in-recombination type (reviewed in Paques *et al.*, 1999 and Symington *et al.*, 2002) is shown in figure 3a. A double strand break is introduced into the cloned targeting sequence usually by a restriction digest. After transforming *T. brucei* with the linear plasmid, the DNA is integrated into the homologous chromosomal sequence by a gene conversion mechanism subsequently followed by a crossing over event. This type of targeting vector results in the duplication of the targeting sequence and is generally used for the insertion of parasite-derived or foreign DNA into novel locations. The second type of targeting vector relies on gene replacement for transformation of the organism (ends-out recombination (Fig. 3b)).

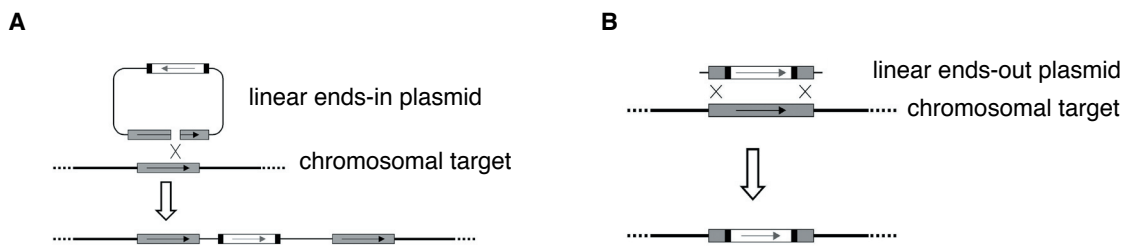


Fig. 3: Mechanism of ends-in recombination (**A**) and ends-out recombination (**B**) to integrate a transformed plasmid into a homologous locus in the *T. brucei* genome. (modified from Mc Culloch *et al.*, 2004)

1.1.6.1. Gene mutation and deletion

For gene mutations and deletions parasites are transformed with DNA that contains both the mutated gene and a selection marker. Both ends of the linear DNA integrate into the genome by homologous recombination and result in the replacement of the WT gene by the mutated gene. For gene mutations, the selection marker is placed in front or behind the gene, whereas for gene deletions, the selection marker is placed in the open reading frame and substitutes part of the gene. Since *T. brucei* is a diploid organism, two rounds of transfections with two different selection markers are necessary to obtain knock-out cells. No promoter is required for the expression of the selection marker, which has the advantage that no downstream genes are affected.

1.1.6.2. Expression of transgenes

The expression of transgenes is achieved in two ways: For constitutive expression, the

gene of interest together with a selection marker is targeted to intergenic regions of *T. brucei* multigenic arrays such as the RNA polymerase I large subunit locus. Alternatively, gene and selection marker are targeted in reverse orientation to chromosomal transcription or to untranscribed regions in the *T. brucei* genome, such as the ribosomal DNA spacer or the silent VSG gene arrays. The promoter must then be included in the expression vector and can be inducible.

The first generation of inducible expression systems for *T. brucei* was developed in 1995 (Wirtz *et al.*, 1995). Two tetracycline repressor binding sites were added to the *T. brucei* derived PARP (procyclin acidic repetitive protein) promoter in an expression vector and the construct was transfected in a cell line that constitutively expressed the prokaryotic tetracycline repressor. From here on both the expression vectors and the expressing cell lines were improved to decrease leakiness and to enable the inducible expression of toxic gene products (Biebinger *et al.*, 1997; Wirtz *et al.*, 1999; Clayton laboratory, unpublished). The cell lines 13-90 (Wirtz *et al.*, 1999), as well as the 1313-514 BSF and PCF cell lines (Clayton laboratory, 2003), constitutively express prokaryotic T7 polymerase and tetracycline repressor and are used for the expression of T7 promoter driven genes or selection markers, examples being pLEW82 and pLEW100 (Wirtz *et al.*, 1999). pLEW82 has a tetracycline inducible T7 promoter that drives both the expression of the target gene and of the selection marker. Since the cell line must be established in the presence of tetracycline, it is only suitable for the expression of non-toxic gene products. By the addition of a second promoter, this problem has been overcome (pLEW100). The selection marker is driven by a constitutively active T7 promoter, while the gene of interest is driven by a tetracycline inducible PARP promoter. To avoid any read-through, this promoter has been placed in the opposite direction to the T7 promoter.

1.1.6.3. RNA interference

RNA interference was first discovered in *C. elegans* (Fire *et al.*, 1998) and shortly thereafter proved to be a very useful tool for inducible gene knockdown in many organisms, among them *T. brucei*. In principle, dsRNA is processed by a ribonuclease III enzyme (DICER) into small interfering RNAs (siRNAs). These siRNAs direct the cleavage of the homologous mRNA via an RNA-induced silencing complex (RISC) (reviewed in Hannon, 2002; Ullu *et al.*, 2004; Tschudi *et al.*, 2003).

Different methods were successfully used for the introduction of dsRNA into

trypanosomes: dsRNA was simply transfected (Ngo *et al.*, 1998) or it was transcribed as inverted repeats from a transfected vector (Shi *et al.*, 2000; Bastin *et al.*, 2000). The easiest way is to transcribe dsRNA from a single vector that has two promoters. These promoters are arranged as inverted repeats and transcribe the target DNA sequence in both directions, generating sense and anti-sense RNA very closely together. An example is the p2T7 vector (used in this work) that has two T7 promoters and is used for inducible RNA interference upon transfection in the 13-90 cell line (LaCount *et al.*, 2000).

1.2. Signal transduction in Trypanosomatidae

The ability to sense environmental signals is of vital importance for all organisms, including trypanosomatidae. In fact, the parasitic flagellates even have some special requirements to signaling pathway since they must frequently respond to extracellular signals as they adapt to new environments within their different hosts.

The following chapter gives an overview on what is currently known about signal transduction mechanisms in Trypanosomatidae. Thereby the focus lies on the control of life cycle and cell cycle, thus the main processes that characterize the life of the single cell organisms.

Cell cycle regulation has been studied in *T. brucei*, *T. cruzi*, *L. major* and *L. mexicana* and orthologues of many key molecules that are involved in cell cycle regulation of higher eukaryotes have been identified. These include cyclins and cyclin dependent protein kinases as well as kinases of the MAP/MOK pathway (reviewed in Hammarton *et al.*, 2003b). Furthermore, the number of cyclins appears to be unusually high in trypanosomatidae. This could be an adaptation to the complexity of the parasitic life cycles with their alternating cell cycle arrested and proliferating stages that might require additional regulations not needed in other eukaryotes. Some of these cyclins and cyclin dependent protein kinases have been characterized. Thereby it was found that *T. brucei* lacks some of the classical cell cycle checkpoints and, interestingly, that cell cycle regulation differs between the life cycle stages of the parasite (Ploubidou *et al.*, 1999; Hammarton *et al.*, 2003a; Li *et al.*, 2003). Thus, the mitotic exit checkpoint is absent in procyclic cells but present in blood stream forms. Cells from both life cycle stages obviously lack the G1 checkpoint, since neither S-phase nor organelle segregation is

prevented in the absence of cytokinesis. Another surprising result was that the nearly synchronous cell cycles of nucleus and kinetoplast are independently regulated (Das *et al.*, 1994; Hammarton *et al.*, 2003a).

Life cycle regulation of kinetoplastida is still poorly understood. There is some evidence that both calcium and cyclic AMP are involved in life cycle regulation of various Trypanosomatidae (Lammel *et al.*, 1996; Stojdl *et al.*, 1996; Sarkar *et al.*, 1995; Strickler *et al.*, 1975; Rangel-Aldao *et al.*, 1987; Gonzales-Perdomo *et al.*, 1988; Vassella *et al.*, 1997; Rolin *et al.*, 1993; Walter *et al.*, 1978). In addition, free fatty acids have been shown to induce differentiation from metacyclic to epimastigote forms in *T. cruzi* (Wainszelbaum *et al.*, 2003). Inositolphosphoceramide is thought to be involved in the differentiation from metacyclic into amastigote *T. cruzi* forms (Salto *et al.*, 2003). Some kinases or kinase activities of *T. brucei* have been suggested to participate in differentiation, including a MAP kinase and a zinc finger kinase (Aboagye-Kwarteng *et al.*, 1991; Parsons *et al.*, 1991; Parsons *et al.*, 1993; Müller *et al.*, 2002; Vassella *et al.*, 2001). However, no connection was yet established between the different factors that are thought to influence differentiation and none of the underlying signaling pathways is known.

In *T. brucei*, the studying of life cycle regulation became feasible with the establishment of an *in vitro* culture system for bloodstream form trypanosomes in our laboratory (Vassella *et al.*, 1996). Thereby it was found that LS to SS differentiation was dependent on a cell density sensing mechanism (Reuner *et al.*, 1997) that is mediated by the so called stumpy induction factor (SIF) (Vassella *et al.*, 1997). SIF is a small molecule (<500 Da) of unknown nature that is released by the parasites themselves, accumulates at high cell densities and mediates differentiation into SS cells via an unknown signaling pathway. There is strong evidence for an involvement of cAMP in this pathway, since firstly, SIF enriched medium induces an 2 to 3 fold increase in intracellular cAMP and secondly, membrane permeable cAMP derivatives and phosphodiesterase inhibitors exactly mimic SIF activity.

1.3. cAMP signaling

Cyclic AMP is the first second messenger that was discovered more than 40 years ago (Rall *et al.*, 1956). Since then it has been detected in most organisms. The components of the cAMP signaling pathway are well described and some are already used as drug targets for various clinical applications.

In higher eukaryotes, the cAMP signaling pathway is initiated by receptor mediated activation of heterotrimeric G-proteins that then either activate or inhibit adenylyl cyclases (ACs). Active ACs synthesize cyclic AMP from ATP. In eukaryotic cells the current view is that the majority of the cAMP signals are mediated via the activation of protein kinase A (PKA) and subsequent phosphorylation of various downstream factors, such as transcription factors, cytoskeletal proteins or metabolic enzymes. Degradation of cAMP to AMP is catalyzed by phosphodiesterases (PDEs).

Dictyostelium is the best examined example for cAMP dependent signaling pathways in lower eukaryotes. In the slime mold, cAMP functions both as first messenger outside the cell and as second messenger inside. It acts on chemotaxis and gene regulation, as well as on differentiation and development (reviewed in Saran *et al.*, 2002). In most of the lower eukaryotes examined to date cAMP regulates differentiation processes and its effects are directly mediated by the activation of a PKA.

The earliest publications on cyclic AMP signaling in Trypanosomatidae range back as far as 1974, when both an AC and a PDE activity was found in *Trypanosoma gambiense* (Walter 1974; Walter *et al.*, 1974). Since then cyclic AMP has been suggested to participate in the regulation of vitally important processes in many kinetoplastida, including life cycle (compare 1.2.) and host-parasite interactions (Dey *et al.*, 1995; Von Kreuter *et al.*, 1995).

There is evidence, that the cAMP signaling pathway of kinetoplastida differs from that of other eukaryotes. In fact, trimeric G-proteins appear to be absent in trypanosomatidae and it is assumed that the extracellular signal is directly sensed by adenylyl cyclases instead. These consist of only one single transmembrane helix with a large extracellular domain (Sanchez *et al.*, 1995; Alexandre *et al.*, 1990; Bieger *et al.*, 2001) and thus have more similarities to mammalian guanylyl cyclases than to mammalian ACs that consist

of two bundles of six transmembrane helices each. Interestingly, *T. brucei* possess more than 100 different genes for adenylate cyclases which is around ten times more than have organisms with much higher complexity (Seebeck, 2001). This strongly implicates that cAMP signaling is a very important signaling pathway in kinetoplastida that might in future even surprise with an unusually high complexity.

Phosphodiesterases have been described in various kinetoplastida (Goncalves *et al.*, 1980; Téllez-Inón *et al.*, 1985; D'Angelo *et al.*, 2004; Zoraghi *et al.*, 2001; Zoraghi *et al.*, 2002; Gong *et al.*, 2001; Kunz *et al.*, 2004; Rascón *et al.*, 2002; Walter *et al.*, 1974; Rascón *et al.*, 2000) and appear to be similar to mammalian PDEs. The best examined examples are the six PDEs from *T. brucei* out of which four have been extensively studied (reviewed in Seebeck, 2001). They all belong to the class I (or mammalian) PDE family and are highly specific for cAMP.

1.4. cAMP dependent protein kinases

The classical cAMP receptor of higher eukaryotes, protein kinase A (PKA), exists in most organisms as a heterotetrameric holoenzyme consisting of two catalytic (C) and two regulatory (R) subunits. Catalytic PKA subunits nearly exclusively consist of a kinase domain and their function is restricted to their kinase activity. Regulatory PKA subunits regulate PKA activity by binding and inhibiting the catalytic subunits in the absence of cAMP. This binding is mainly mediated by a conserved sequence stretch in the R subunit (R R X [A/T/S] Ψ ; Ψ =hydrophobic amino acid) that also exists in PKA substrates (substrate or pseudosubstrate sequence). In addition, regulatory subunits also mediate the formation of the tetrameric PKA holoenzyme by their N-terminal dimerization/docking domain that enables the dimerization of two regulatory PKA subunits. This dimerization/docking domain also binds to A kinase anchoring proteins (AKAPs) that target PKA to specific subcellular locations.

PKA activation is achieved by the release of the catalytic subunits from the holoenzyme complex caused by cAMP induced conformational changes in the regulatory subunits (Fig. 4). PKA substrates include transcription factors, signal transduction components and metabolic enzymes (reviewed in Shabb 2001).

Diversity and presumably specificity of the cAMP signal is achieved by the existence of several different PKAC and PKAR isoforms and AKAPs that are distinctly expressed in

different cells and tissues (reviewed in Skalhegg and Tasken, 2000).

The best examined non-mammalian PKA is that of the slime mold *Dictyostelium*: In contrast to PKAs from higher eukaryotes, it has a dimeric structure out of only one regulatory and one catalytic subunit (Mutzel *et al.*, 1987). PKA activity is regulated by cAMP and also, at the onset of starvation, by transcriptional control (Souza *et al.*, 1999).

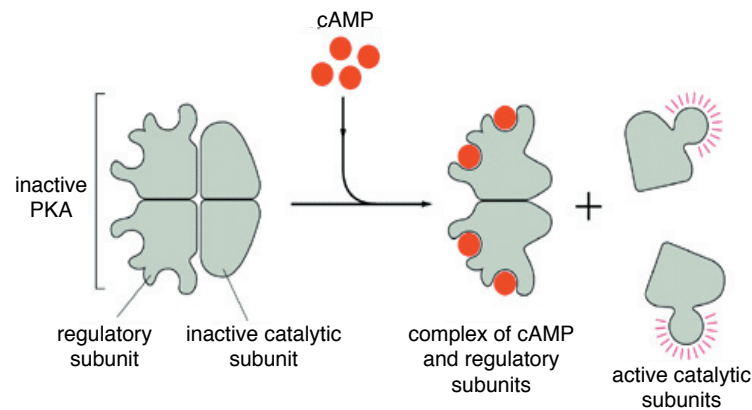


Fig. 4: Activation of protein kinase A

Conformational change of the R subunit is achieved upon binding of two molecules of cAMP. The catalytic subunits are set free and become active. (Picture taken from molecular biology of the cell 3rd edition)

In kinetoplastida, the existence of a cAMP dependent protein kinase still remains unclear, even though several orthologous proteins for catalytic or regulatory PKA subunits have been meanwhile cloned (Siman-Tov *et al.*, 1996; Siman-Tov *et al.*, 2002; Huang *et al.*, 2002; Shalaby *et al.*, 2001). The so far only report about a cAMP dependent kinase activity in kinetoplastida comes from *Trypanosoma cruzi* (Ulloa *et al.*, 1988) but has so far not been reproduced.

1.5. The *T. brucei* PKA-like kinase and aims of this Ph.D. project

Interest in our laboratory on cAMP dependent protein kinases origins from earlier studies on the differentiation of LS to SS trypanosomes, a process that appears to involve cAMP (Vassella *et al.*, 1997; compare 1.2.). In search of the *T. brucei* cAMP receptor, three orthologous proteins for catalytic PKA subunits (PKAC1, PKAC2, PKAC3) and one orthologous protein for a regulatory PKA subunit (PKAR) have been cloned from (T. Klöckner, Ph.D. thesis 1996; C. Schulte zu Sodingen, 2000).

The catalytic PKA-like subunits exhibit all features that characterize a classical cAMP dependent protein kinase. They phosphorylate the PKA specific substrate kemptide and are inhibitable by the PKA specific inhibitor PKI. Recombinant PKAC3 even forms a heterologous holoenzyme complex with mammalian PKA subunits that dissociates in the presence of cAMP (N. Wild, unpublished). Given that *T. brucei* PKA-like kinase is considered as a potential regulator of differentiation, two of the catalytic PKA-like subunits (PKAC1 and PKAC2) are of particular interest: PKAC1 and PKAC2 expression was found to be developmentally regulated (E. Vassella, unpublished). Additionally, life cycle stage dependent posttranslational modifications were detected in these isoforms (S. Schimpf, Diploma thesis 2000, T. Klöckner, Ph.D. thesis 1996).

First aim of this Ph.D. project was therefore to characterize both PKAC1 and PKAC2 biochemically and functionally *in vivo*.

The regulatory PKA-like subunit of *T. brucei* has an unusually long N-terminus that is devoid of a dimerization domain. Apart from that, *TbPKAR* possess all features of a typical PKAR subunit, such as two predicted cNMP binding sites in tandem and a classical inhibitor sequence that mediates the binding to the catalytic subunit. In fact, coimmunoprecipitation studies revealed that *T. brucei* PKAR is able to bind each of the catalytic *T. brucei* PKA-like subunits, which was the first proof for the existence of a PKA-like holoenzyme in *T. brucei* (C. Schulte zu Sodingen, Ph.D. thesis 2000). Given that the *T. brucei* PKA-like kinase appears to possess all characteristics of a classical cAMP dependent protein kinase, it came as a surprise that the kinase was not activable with cyclic AMP. This was not only true for immunopurified PKA-like kinase but also for (PKI-inhibitable) kinase activity in crude cell extracts, thus in the absence of most *in vitro* artefacts.

Second major aim of this Ph.D. project was therefore to discover the mechanism of activation for *T. brucei* PKA-like kinase. This was approached in two different ways: First it was planned to test further cyclic nucleotides on their abilities to activate *T. brucei* PKA-like kinase. The second approach was to establish an *in vivo* assay for PKA activity in *T. brucei*. This way kinase activity can be studied in its native subcellular environment that might be required for kinase activation.

What is the function of this PKA-like kinase that appears to be insensitive towards cyclic AMP? Even though it might possibly not act as the receptor of the cAMP signal that is thought to regulate differentiation, the kinase nevertheless appears to have an important, probably essential function. This is suggested from the failure to genetically knock-out any PKA-like subunit in BSF trypanosomes.

Further major aim of this Ph.D. project was therefore to investigate the function of this interesting, *T. brucei* PKA-like kinase with its yet undefined mechanism of activation. For this, it was aimed to take advantage of the whole spectrum of reverse genetic tools that is currently available for *T. brucei*. Especially the method of inducible gene knock-down by RNA interference that has been recently established in *T. brucei* (compare 1.1.6.3.) was most promising since it allows to functionally analyze even essential genes.

2. Materials and Methods

2.1. Material

2.1.1. Trypanosoma strains

2.1.1.1. Wild type strains

MITat1.2 (NY subclone) monomorphic PCF and BSF Cross and Manning, 1973; Cross, 1975 Note that the Bern subclone of MITat1.2 (l. Roditi) has an additional PKAC allele that has the 5' part of <i>PKAC2</i> and the 3' part of <i>PKAC1</i> (Data not shown in this work).	
MITat1.4	G. Cross, New York
AnTat1.1 (Antwerp Trypanozoon antigen type 1.1)	P. Overath, Tübingen Geigy <i>et al.</i> , 1975; Delauw <i>et al.</i> , 1985

2.1.1.2. Transgenic strains

Transgenic cell lines have been named according to the *T. brucei* community nomenclature rules of Clayton *et al.* (1998). However, in most cases alternative names will be used in this thesis to facilitate reading. In the tables below, these names are indicated in bold letters (headline). In some cases, more than one name exists for the same cell line, which is then shown as “alternative name”. All transgenic cell lines that have been generated in this Ph.D. project are listed. In addition, two cell lines are listed, that have been used but were already available. An overview about all transgenic cell lines used in this work is given in attachment 5.

MITat1.4 Ty1-PKAC1		1
Made by:	Paul Hassan	
Name according to nomenclature:	MITat1.4 $\Delta pkac1::BSD$ / <i>PKAC1::ty1-pkac1 BLE</i>	
Alternative name:	(Pauls MITats)	
Clone or pool number(s):	clone 1	
Date of construction:	2000	
Contains the Constructs:	pTy1- <i>PKAC1</i> p $\Delta PKAC1$ BSD	
Selection markers:	blasticidin [2 μ g/ml]; phleomycin [2 μ g/ml]	
Note:	The cell line was later shown not to be derived from MITat1.4, it is probably MITat1.2 Bern subclone. It was only used for the purification of Ty1-PKAC1 for mass spectrometry.	

Ty1-T324		2
Made by:	S. Kramer	
Name according to nomenclature:	MITat1.2 NY subclone $\Delta pkac1::BSD / PKAC1::ty1-pkac1$ BLE	
Alternative name:	PKAC1 k.o / Ty1-T324	
Clone or pool number(s):	clone K6	
Date of construction:	7 / 2002	
Contains the Construct(s):	p $\Delta PKAC1$ BSD pTy1-PKAC1	
Selection markers:	blasticidin [2 μ g/ml]; phleomycin [2 μ g/ml]	
Note:	-	

Ty1-E324		3
Made by:	S. Kramer	
Name according to nomenclature:	MITat1.2 NY subclone $\Delta pkac1::BSD / PKAC1::ty1-pkac1$ (T324E) BLE	
Alternative name:	-	
Clone or pool number(s):	clone G2	
Date of construction:	7 / 2002	
Contains the Construct(s):	p $\Delta PKAC1$ BSD pTy1-PKAC1-E324	
Selection markers:	blasticidin [2 μ g/ml]; phleomycin [2 μ g/ml]	
Note:	-	

Ty1-A324		4
Made by:	S. Kramer	
Name according to nomenclature:	MITat1.2 NY subclone $\Delta pkac1::BSD / PKAC1::ty1-pkac1$ (T324A) BLE	
Alternative name:	-	
Clone or pool number(s):	clone A1; clone A11, clone A12	
Date of construction:	7 / 2002	
Contains the Construct(s):	p $\Delta PKAC1$ BSD pTy1-PKAC1-A324	
Selection markers:	blasticidin [2 μ g/ml]; phleomycin [2 μ g/ml]	
Note:	-	

T324		5
Made by:	S. Kramer	
Name according to nomenclature:	MITat1.2 NY subclone $\Delta pkac1::BSD / PKAC1::PKAC1$ BLE	
Alternative name:	-	
Clone or pool number(s):	clone K2	
Date of construction:	11 / 2002	
Contains the Construct(s):	p $\Delta PKAC1$ BSD pPKAC1-T324	
Selection markers:	blasticidin [2 μ g/ml]; phleomycin [2 μ g/ml]	
Note:	-	

A324		6
Made by:	S. Kramer	
Name according to nomenclature:	MITat1.2 NY subclone $\Delta pkac1::BSD / PKAC1::pkac1(T324A)$ BLE	
Alternative name:	-	
Clone or pool number(s):	clone A3	
Date of construction:	11 / 2002	
Contains the Construct(s):	p $\Delta PKAC1$ BSD pPKAC1-A324	
Selection markers:	blasticidin [2 μ g/ml]; phleomycin [2 μ g/ml]	
Note:	-	

E324		7
Made by:	S. Kramer	
Name according to nomenclature:	MITat1.2 NY subclone $\Delta pkac1::BSD / PKAC1::pkac1(T324E)$ BLE	
Alternative name:	-	
Clone or pool number(s):	clone G2-2	
Date of construction:	2 / 2003	
Contains the Construct(s):	p $\Delta PKAC1$ BSD pPKAC1-E324	
Selection markers:	blasticidin [2 μ g/ml]; phleomycin [2 μ g/ml]	
Note:	-	

HA-PKAC2		8
Made by:	S. Kramer	
Name according to nomenclature:	MITat1.2 NY subclone $PKAC2::ha-pkac2$ NEO	
Alternative name:	-	
Clone or pool number(s):	HA-S2; HA-S4	
Date of construction:	2 / 2002	
Contains the Construct(s):	pHA-PKAC2NEO	
Selection markers:	neomycin [2 μ g/ml]	
Note:	-	

Ty1-PKAC1		9
Made by:	S. Kramer	
Name according to nomenclature:	MITat1.2 NY subclone $PKAC1::ty1-pkac1$ BLE	
Alternative name:	-	
Clone or pool number(s):	clone 1; clone 2	
Date of construction:	1 / 2004	
Contains the Construct(s):	pTy1-PKAC1	
Selection markers:	pheomycin [2 μ g/ml]	
Note:	-	

Ty1-PKAC3		10
Made by:	S. Kramer	
Name according to nomenclature:	MITat1.2 NY subclone <i>RRNA::ty1-pkac3 HYG</i>	
Alternative name:	-	
Clone or pool number(s):	Pool	
Date of construction:	2 / 2004	
Contains the Construct(s):	pTSAribTy1-PKAC3	
Selection markers:	hygromycin [4 µg/ml]	
Note:	-	

Ty1-PKAR		11
Made by:	C. Schulte zu Sodingen	
Name according to nomenclature:	MITat1.2 "single marker" <i>T7POL TETR NEO RDNA::ty1-PKAR BLE</i>	
Alternative name:	pLew82PKARwttag	
Clone or pool number(s):	C2	
Date of construction:	See C. Schulte zu Sodingen	
Contains the Construct(s):	pLew82Ty1-PKAR	
Selection markers:	phleomycin [4 µg/ml], select in the presence of tetracycline	
Note:	-	

Ty1-PKAC1 dead		12
Made by:	S. Kramer	
Name according to nomenclature:	MITat1.2 NY subclone <i>PKAC1::ty1-pkac1(N165A) BLE</i>	
Alternative name:	-	
Clone or pool number(s):	clone 11, clone 12, clone 14	
Date of construction:	1 / 2004	
Contains the Construct(s):	pTy1-PKAC1dead	
Selection markers:	phleomycin [2 µg/ml]	
Note:	The mutation is frequently repaired by gene conversion using the WT <i>PKAC1</i> allele as template.	

PKAC2 knock-out		13
Made by:	S. Kramer	
Name according to nomenclature:	MITat1.2 NY subclone <i>Δpkac2::NEO / Δpkac2::HYG</i>	
Alternative name:	<i>PKAC2</i> null mutant	
Clone or pool number(s):	clone 2-1	
Date of construction:	6 / 2002	
Contains the Construct(s):	pΔPKAC2HYG pΔPKAC2NEO	
Selection markers:	hygromycin [1 µg/ml]; neomycin [1 µg/ml]	
Note:	This is the only existing clone. Cells were first transfected with pΔPKAC2HYG and subsequently with pΔPKAC2NEO.	

PKAC2 hemizygous knock-out		14
Made by:	S. Kramer	
Name according to nomenclature:	MITat1.2 NY subclone $\Delta pkac2::HYG$	
Alternative name:	PKAC2 WT/k.o.	
Clone or pool number(s):	clone 2	
Date of construction:	5 / 2002	
Contains the Construct(s):	p Δ PKAC2HYG	
Selection markers:	hygromycin [1 μ g/ml]	
Note:	-	

PKAC1 hemizygous knock-out		15
Made by:	S. Kramer	
Name according to nomenclature:	MITat1.2 NY subclone $\Delta pkac1::BSD$	
Alternative name:	PKAC1 WT/k.o.	
Clone or pool number(s):	clone 5	
Date of construction:	6 / 2002	
Contains the Construct(s):	p Δ PKAC1BSD	
Selection markers:	blasticidin [1 μ g/ml]	
Note:	-	

13-90 p2T7 PKAR		16
Made by:	S. Kramer	
Name according to nomenclature:	MITat1.2 13-90 <i>T7POL TETR NEO HYG RDNA::T7POL PKAR BLE</i>	
Alternative name:	-	
Clone or pool number(s):	clone 1, clone 4, clone 6, clone 8	
Date of construction:	12 / 2000	
Contains the Construct(s):	p2T7 PKAR	
Selection markers:	hygromycin [5 μ g/ml]; neomycin [2.5 μ g/ml]; phleomycin [2.5 μ g/ml]	
Note:	-	

1313-514 p2T7TAblue PKAC3		17
Made by:	S. Kramer	
Name according to nomenclature:	MITat 1.2. 1313-514 <i>T7POL TETR NEO BLE RDNA::T7POL PKAC3 HYG</i>	
Alternative name:	-	
Clone or pool number(s):	clone 1, clone 4, clone 8	
Date of construction:	4 / 2004	
Contains the Construct(s):	p2T7TAblue PKAC3	
Selection markers:	hygromycin [2 μ g/ml]; neomycin [2 μ g/ml]; phleomycin [0.2 μ g/ml]	
Note:		

VASP		18
Made by:	S. Kramer	
Name according to nomenclature:	MITat1.2 NY subclone <i>RRNA::VASP HYG</i>	
Alternative name:	-	
Clone or pool number(s):	clone 1 (only one clone available)	
Date of construction:	9 / 2003	
Contains the Construct(s):	pTSAribVASP	
Selection markers:	hygromycin [4µg/ml];	
Note:		

1313-514 p2T7TAblue PKAC1/2		19
Made by:	S. Kramer	
Name according to nomenclature:	MITat 1.2 1313-514 <i>T7POL TETR NEO BLE RDNA::T7PRO PKAC1 HYG</i>	
Alternative name:	-	
Clone or pool number(s):	clone 2, clone 3	
Date of construction:	4 / 2004	
Contains the Construct(s):	p2T7TAblue <i>PKAC1/2</i>	
Selection markers:	hygromycin [2 µg/ml]; neomycin [2µg/ml]; phleomycin [0.2 µg/ml]	
Note:		

2.1.2. Bacteria Strains

<i>E. coli</i> DH5 α	<i>F⁻ endA1 hsdR17 (r_k⁻ m_k⁺) supE44 thi-1 recA1 gyrA (Nal^r) relA1 Δ(lacZYA-argF)_{U169} (f80lacZΔM15)</i>
M15	<i>Nal^S Str^S rif^S lac⁻ ara⁻ gal⁻ mtl⁻ F⁻ recA⁺ uvr⁺</i>

2.1.3. Antibodies

2.1.3.1. Primary antibodies

name	organism	origin	western	IF
anti-PKAC1/2	rabbit	T. Klöckner (Ph.D. thesis, 1996)	1:500	
anti-PKAR	rabbit	C. Schulte zu Sodungen (Ph.D. thesis, 1996)	1:500	
anti-HA Hybridoma (clone 12CA5) concentrated hybridoma supernatant	mouse	M. van den Boogard	undiluted	
anti-Ty1 IgG1-Hybridoma (BB2)	mouse	K. Gull lab (Manchester)	1:50	
anti-Ty1 Ascites	mouse	M. van den Boogard	1:300	
anti-VASP AB19728	rabbit	kind gift from Thomas Renné and Ulrich Walter (Medizinische Universitätsklinik Würzburg) Halbrügge <i>et al.</i> , 1990	1:5000	
anti-VASP M4	rabbit	immunoGlobe Antikörpertechnik GmbH	1:5000	
anti-PFR (L13D6)	mouse	K. Gull lab (Manchester)	1:2000	1:10

anti-NUP	mouse	K. Ersfeld and K. Gull		undiluted
Anti-Digoxigenin-AF Fab fragments	sheep	Roche	1:5000	

2.1.3.2 Secondary antibodies

Anti-rabbit-IgG-alkaline phosphatase	Böhringer Mannheim
Anti-mouse-IgG-alkaline phosphatase	Böhringer Mannheim
Odyssey Infrared Imaging Goat-Anti-Mouse IRDye800	LI-COR
Odyssey Infrared Imaging Goat-Anti-Mouse Alexa680	LI-COR
Odyssey Infrared Imaging Goat-Anti-Rabbit IRDye800	LI-COR
Odyssey Infrared Imaging Goat-Anti-Rabbit Alexa680	LI-COR
Alexa 488 goat Anti-Mouse	Molecular Probes

2.1.4. Oligos

Name	Sequence	Gene	Origin
C3-ATG	cgggatccATGACGACAACCTCCAC	<i>PKAC1</i>	T. Klöckner
C3-Stop	ggggtaccgtcgaCTAAAAACCACGGAATG	<i>PKAC1</i>	T. Klöckner
PKA-N153>A.u. <i>Eco31I</i>	ACT GAG GTC TCG GCT CTG CTA CTT GAT GGG AAG	<i>PKAC1</i>	S. Kramer
<i>PKAC1</i> seq.I.19/7/01	GCA GTG AAA ACC AAG AAA GGG	<i>PKAC1</i>	S. Kramer
PKA-N153->A.I. <i>Eco31I</i>	ACT GAG GTC TCT GAG CCT CAG GTT TCA AGT CAC G	<i>PKAC1</i>	S. Kramer
<i>PKAC1</i> .II.L.11/7/01	GCG CAC GCC CAT ACG TCA TTA TTC AGC	<i>PKAC1</i>	S. Kramer
3.7.01 5'lower Ala	GGC ACG GTC TCG GGG CTA GTG GAG GAG	<i>PKAC1</i>	S. Kramer
4.7.01 5'upper	TAA TGG AGT TGT CAC ACC		S. Kramer
<i>PKAC1</i> .II.(T>A). <i>Eco31I</i> .U.11/7/01	GTG TCG GTC TCA GCC CCT TCG CAA CAG GTT GCA TTC	<i>PKAC1</i>	S. Kramer
<i>PKAC1</i> .II.L.11/7/01	GCG CAC GCC CAT ACG TCA TTA TTC AGC	<i>PKAC1</i>	S. Kramer
3.7.01 5'lower Glu	GGC ACG GTC TCG GTT CTA GTG GAG GAG	<i>PKAC1</i>	S. Kramer
<i>PKAC1</i> .II.(T>E). <i>Eco31I</i> .U.11/7/01	GTG TCG GTC TCA GAA CCT TCG CAA CAG GTT GCA TTC	<i>PKAC1</i>	S. Kramer
19.11.01 <i>ty1</i> /upper	CGGTGAGGTCCATACTAAC	<i>PKAC1</i>	S.Kramer
HA-Sall- <i>TbPKAC2</i> upp	AGT TCG AGT CGA CGT ACC CAT ACG ACG TCC CAG ACT ACG CTG AAC CGC AAA CGT ATG TG	<i>PKAC2</i>	S. Kramer
<i>TbPKAC2</i> -Cterm.lower	CTT TAC GAG ATC CCG AGC	<i>PKAC2</i>	S. Kramer
34-ATG	CGG GAT CCA TGC TGT TGG TGT TAC TT	<i>PKAC2</i>	T. Klöckner
34-STOP	GGG GTAC CTA AAA CCC ACG GAA CT	<i>PKAC2</i>	T. Klöckner
<i>PKAC3</i> <i>Hind</i> Ty1ATG.u.	CTG GAA GCT TAT GAC CGG TGA GGT CCA TAC TAA CCA GGA CCC ACT TGA CAA GTC GGA TGG GTG CTT G	<i>PKAC3</i>	S. Kramer
<i>PKAC3</i> - <i>Bam</i> HI	CTG GGG ATC CTC AGA TCC TCG TGT ATTC	<i>PKAC3</i>	S. Kramer
VASP- <i>Hind</i> III.u	ACG TAA GCT TAT GAG CGA GAC GGT CAT C	VASP	S. Kramer

VASP- <i>Bam</i> HI-I	ACG TGG ATC CTC AGG GAG AAC CCC GCT T	VASP	S. Kramer
-----------------------	--	------	-----------

2.1.5. Probes

	Length [bp]	binds to	construction
PKAC1/2	1005	full length <i>PKAC1</i>	PCR product from pC3-1 with the oligos C3-ATG and C3-Stop
PRP8	1139	3' part of <i>PRP8</i>	<i>Xho</i> I/ <i>Bgl</i> II fragment from pC3-1
MCP	1029	3' part and 3'UTR of <i>MCP</i>	<i>Xho</i> I/ <i>Sal</i> I fragment from pC34-1

2.1.6. Constructs

For increased clarity all constructs that have been made or used in this work are described together in this chapter rather than in the result section. Complete sequences of all constructs are available on the attached CD as GCK files.

Overview about the plasmids that were made or used in this Ph.D. project			
1	pTy1- <i>PKAC1</i>	15	pLew82 Ty1- <i>PKAR</i>
2	pTy1- <i>PKAC1</i> -dead	16	p2T7 <i>PKAR</i>
3	pTy1- <i>PKAC1</i> -A324	17	pSL301/ <i>PKA-R-YFP_3'_tr1a</i>
4	pTy1- <i>PKAC1</i> -E324	18	p2T7_tiA_GFP
5	p <i>PKAC1</i> -T324	19	pTSAr ib -Ty1- <i>PKAC3</i>
6	p <i>PKAC1</i> -A324	20	pTSAr ib VASP
7	p <i>PKAC1</i> -E324	21	Ph.D615neo gamma
8	pΔ <i>PKAC1</i> BSD	22	pBlueScript_VASP
9	pΔ <i>PKAC2</i> NEO	23	p2T7 <i>PKAC3</i>
10	pΔ <i>PKAC2</i> HYG	24	p2T7TA blue
11	pC34-1	25	p2T7TA blue <i>PKAC3</i>
12	p <i>PKAC2</i> NEO	26	p2T7TA blue <i>PKAC1/2</i>
13	pHA- <i>PKAC2</i> NEO	27	p2T7 <i>PKAC1/2</i>
14	pC3-1		

pTy1- <i>PKAC1</i>		1
Construction:	See N. Wild (p <i>Tb</i> PKA alpha N-Ty1 <i>Phleo</i> origin.)	
Date of construction:	unknown	
Made by:	N. Wild	
Short description:	Upon transfection, one WT <i>PKAC1</i> allele is replaced by Ty1 epitope tagged <i>PKAC1</i> .	
Digest for transfection:	<i>Hind</i> III / <i>Sda</i> I	
Selection marker:	phleomycin [2 μg/ml]	

pTy1-PKAC1-dead		2
Construction:	N153 of PKAC1 was mutated to alanine with the type II restriction enzyme <i>Eco31I</i> . Two PCR reactions with the template <i>pTy1-PKAC1</i> were performed using the oligos PKA-N153->A.u. <i>Eco31I</i> and <i>PKAC1</i> seq.l.19/7/01 (A) and PKA-N153->A.l. <i>Eco31I</i> and <i>PKAC1</i> seq.u.19/7/01 (B). The PCR products were digested with <i>Eco31I</i> / <i>Bam</i> HI (A) and <i>Eco31I</i> / <i>Xba</i> I (B) and both ligated into the <i>Xba</i> I / <i>Bam</i> HI digested backbone of <i>pTy1-PKAC1</i> . The success of the mutagenesis was confirmed by sequencing (18.6.03).	
Date of construction:	6 / 2003	
Made by:	S. Kramer	
Short description:	For expression of catalytically inactive Ty1-PKAC1 (dead mutant).	
Digest for transfection:	<i>Hind</i> III / <i>Sda</i> I	
Selection marker:	phleomycin [2 µg/ml]	

pTy1-PKAC1-A324		3
Made by:	S. Kramer	
Construction:	Thr324 of Ty1-PKAC1 was mutated to alanine with the type II restriction enzyme <i>Eco31I</i> . Therefore two PCR reactions with the template <i>pTy1-PKAC1</i> were performed using the oligos 5'lower Ala and 4.7.5'upper (A) and <i>PKAC1</i> .II.(T>A). <i>Eco31I</i> .U.11/7/01 and <i>PKAC1</i> .II.L.11/7/01 (B). The PCR products were digested with <i>Eco31I</i> / <i>Xba</i> I (A) and <i>Eco31I</i> / <i>Bam</i> HI (B) and both ligated into the <i>Xba</i> I / <i>Bam</i> HI prepared backbone of the vector <i>pTy1-PKAC1</i> . The success of the site directed mutagenesis was controlled by sequencing.	
Date of construction:	7/ 2001	
Short description:	Threonine 324 of Ty1-PKAC1 was mutated to alanine for functional analysis of the stumpy specific phosphorylation.	
Digest for transfection:	<i>Hind</i> III / <i>Sda</i> I	
Selection marker:	phleomycin [1 µg/ml]	

pTy1-PKAC1-E324		4
Made by:	S. Kramer	
Construction:	Thr324 of Ty1-PKAC1 was mutated to alanine with the type II restriction enzyme <i>Eco31I</i> . Therefore two PCR reactions with the template <i>pTy1-PKAC1</i> were performed using the oligos 5'lower Glu and 4.7.5'upper (A) and <i>PKAC1</i> .II.(T>E). <i>Eco31I</i> .U.11/7/01 and <i>PKAC1</i> .II.L.11/7/01 (B). The PCR products were digested with <i>Eco31I</i> / <i>Xba</i> I (A) and <i>Eco31I</i> / <i>Bam</i> HI (B) and both ligated into the <i>Xba</i> I / <i>Bam</i> HI prepared backbone of the vector <i>pTy1-PKAC1</i> . The success of the site directed mutagenesis was controlled by sequencing.	
Date of construction:	7/ 2001	
Short description:	Threonine 324 of Ty1-PKAC1 was mutated to glutamate for functional analyses of the stumpy specific phosphorylation.	
Digest for transfection:	<i>Hind</i> III / <i>Sda</i> I	
Selection marker:	phleomycin [1 µg/ml]	

pPKAC1-T324		5
Made by:	S. Kramer	
Construction:	The <i>Ty1</i> epitope tag of p <i>Ty1</i> - <i>PKAC1</i> was removed by digestion with <i>AgeI</i> and subsequent religation.	
Date of construction:	9 / 2002	
Short description:	Targeting construct for <i>PKAC1</i> without <i>Ty1</i> epitope tag. Used as control for the functional analysis of the stumpy specific phosphorylation.	
Digest for transfection:	<i>Hind</i> III / <i>SdaI</i>	
Selection marker:	phleomycin [1 µg/ml]	

pPKAC1-A324		6
Made by:	S. Kramer	
Construction:	The <i>Ty1</i> epitope tag of p <i>Ty1</i> - <i>PKAC1A324</i> was removed by digestion with <i>AgeI</i> and subsequent religation.	
Date of construction:	9 / 2002	
Short description:	Targeting construct for <i>PKAC1</i> (T324->A) without <i>Ty1</i> epitope tag. Used for the functional analysis of the stumpy specific phosphorylation.	
Digest for transfection:	<i>Hind</i> III / <i>SdaI</i>	
Selection marker:	phleomycin [1 µg/ml]	

pPKAC1-E324		7
Made by:	S. Kramer	
Construction:	The <i>Ty1</i> epitope tag of p <i>Ty1</i> - <i>PKAC1E324</i> was removed by digestion with <i>AgeI</i> and subsequent religation. The construct was controlled by restriction analyses.	
Date of construction:	9 / 2002	
Short description:	Targeting construct for <i>PKAC1</i> (T324->E) without <i>Ty1</i> epitope tag. Used for the functional analysis of the stumpy specific phosphorylation.	
Digest for transfection:	<i>Hind</i> III / <i>SdaI</i>	
Selection marker:	phleomycin [1 µg/ml]	

pΔPKAC1BSD		8
Made by:	Paul Hassan (pA5A3BSDnew)	
Construction:	See P. Hassan	
Date of construction:	See P. Hassan	
Short description:	For deletion of one <i>PKAC1</i> allele.	
Digest for transfection:	<i>EcoRI</i> / <i>Bgl</i> II	
Selection marker:	blastocidin [1-2 µg/ml]	

pΔPKAC2NEO		9
Made by:	Paul Hassan (pB5B3NEO)	
Construction:	See P. Hassan	
Date of construction:	See P. Hassan	
Short description:	Deletion of one <i>PKAC2</i> allele.	
Digest for transfection:	<i>EcoRI</i> / <i>Xmn</i> I	
Selection marker:	neomycin [1-2 µg/ml]	

pΔPKAC2HYG		10
Made by:	Paul Hassan (pB5B3HYGnew)	
Construction:	See P. Hassan	
Date of construction:	See P. Hassan	
Short description:	Deletion of one <i>PKAC2</i> allele.	
Digest for transfection:	<i>XcmI</i> / <i>XmnI</i>	
Selection marker:	hygromycin [1-2 μg/ml]	

pC34-1		11
Made by:	T. Klöckner	
Construction:	See T. Klöckner	
Date of construction:	See T. Klöckner	
Short description:	Bacterial cloning vector, contains <i>PKAC2</i> with 3' and 5' UTR and <i>MCP</i> .	
Digest for transfection:	-	
Selection marker:	-	

pPKAC2NEO		12
Made by:	S. Kramer	
Construction:	The neomycin phosphotransferase gene of pΔ <i>PKAC2Neo</i> was isolated as <i>BglII</i> / <i>XbaI</i> fragment, treated with Klenow polymerase and cloned into the <i>BsaBI</i> site of pC34-1.	
Date of construction:	12 /2001	
Short description:	targeting construct for <i>PKAC2</i> , intermediate construct for the construction of pHA- <i>PKAC2NEO</i>	
Digest for transfection:	was never transfected	
Selection marker:	neomycin [1-2 μg/ml]	

pHA-<i>PKAC2NEO</i>		13
Made by:	S. Kramer	
Construction:	The HA epitope tag was introduced at the <i>Sall</i> site of <i>PKAC2</i> by pcr amplification with the primers HA- <i>Sall-TbPKAC2</i> and <i>TbPKAC2-Cterm.I</i> . The PCR product was digested with <i>Sall</i> and <i>EcoRI</i> and exchanged against the <i>Sall/EcoRI</i> fragment of p <i>PKAC2NEO</i> .	
Date of construction:	1/2001 – 2 /2001	
Short description:	Targeting construct for epitope labeling of <i>PKAC2</i> with the HA tag. Upon transfection into trypanosomes one <i>PKAC2</i> allele is replaced by the N-terminal HA-epitope tagged <i>PKAC2</i> . The construct was partly sequenced.	
Digest for transfection:	<i>Clal</i> / <i>BstZ17I</i>	
Selection marker:	neomycin [1-2 μg/ml]	

pC3-1		14
Made by:	T. Klöckner	
Construction:	See T. Klöckner	
Date of construction:	See T. Klöckner	
Short description:	Bacterial cloning vector that contains the <i>PRP8</i> sequence; used in this work as template for amplification of the <i>PRP8</i> probe.	
Digest for transfection:	-	
Selection marker:	-	

pLEW82 Ty1-PKAR		15
Made by:	C. Schulte zu Sodingen (<i>TbRlwttag</i>)	
Construction:	See C. Schulte zu Sodingen	
Date of construction:	See C. Schulte zu Sodingen	
Short description:	expression of Ty1-PKAR in the presence of tetracycline	
Digest for transfection:	<i>NotI</i>	
Selection marker:	phleomycin [1-5 µg/ml] only in presence of tetracycline!	
p2T7 PKAR		16
Made by:	S. Kramer	
Construction:	The N-terminal <i>PKAR</i> fragment (501 bp) was mobilized from pSL301/PKA-R-YFP_3'_tr1a (C. Krumbholz) with <i>EagI</i> and <i>HindIII</i> , the <i>EagI</i> site was filled with Klenow polymerase. The RNAi vector p2T7_tiA_GFP was equally prepared with <i>BamHI</i> (filled with Klenow polymerase) and <i>HindIII</i> and both vector and insert were ligated.	
Date of construction:	11 / 2000	
Short description:	Construct for inducible RNAi targeted against <i>TbPKAR</i>	
Digest for transfection:	<i>NotI</i>	
Selection marker:	phleomycin [3 µg/ml]	
pSL301/PKA-R-YFP_3'_tr1a		17
Made by:	C. Krumbholz	
Construction:	See C. Krumbholz	
Date of construction:	See C. Krumbholz	
Short description:	Contains <i>PKAR</i> N-terminus; was used for the construction of p2T7-PKAR	
Digest for transfection:	-	
Selection marker:	-	
p2T7_tiA_GFP		18
Made by:	LaCount <i>et al.</i> (2000)	
Construction:		
Date of construction:		
Short description:	Original RNAi vector, contains <i>GFP</i>	
Digest for transfection:	<i>NotI</i>	
Selection marker:	phleomycin [3 µg/ml]	
pTSArib-Ty1-PKAC3		19
Made by:	S. Kramer	
Construction:	The <i>Ty1</i> epitope tag was introduced with PCR. <i>PKAC3</i> was amplified from Ph.D615neo gamma with the primers <i>PKAC3HindTy1ATG.u.</i> and <i>PKAC3-BamHI</i> and cloned <i>HindIII</i> / <i>BamHI</i> in the equally prepared pTSArib.	
Date of construction:	12 / 2003	
Short description:	Overexpression of <i>Ty1</i> epitope tagged <i>PKAC3</i> .	
Digest for transfection:	<i>SphI</i>	
Selection marker:	hygromycin [4 µg/ml]	

pTSArivVASP		20
Made by:	S. Kramer	
Construction:	VASP was amplified from pBlueScript_VASP with the oligos VASP-HindIII.u and VASP-BamHI-I. The VASP fragment was cloned <i>BamHI/HindIII</i> in the equally prepared pTSAriv.	
Date of construction:	7 / 2003	
Short description:	Expression of transgenic VASP in <i>T. brucei</i> as <i>in vivo</i> PKA substrate.	
Digest for transfection:	<i>SphI</i>	
Selection marker:	hygromycin [4 µg/ml]	

Ph.D615neo gamma		21
Made by:	C. Schulte zu Sodingen	
Construction:	See C. Schulte zu Sodingen	
Date of construction:	See C. Schulte zu Sodingen	
Short description:	Used as template for <i>Ty1</i> epitope tagging of <i>PKAC3</i> .	
Digest for transfection:	not transfected in this work	
Selection marker:	neomycin	

pBlueScript_VASP		22
Made by:	Haffner <i>et al.</i> ,1995	
Construction:	Cloned via <i>SmaI</i> / <i>PstI</i>	
Date of construction:		
Short description:	Clone p14/1 in pBlueScript 1 SK(-), Acc. No. Z46389	
Digest for transfection:		
Selection marker:		

p2T7 PKAC3		23
Made by:	T. Riek	
Construction:	see T. Riek	
Date of construction:	see T. Riek	
Short description:	The <i>PKAC3</i> fragment of this plasmid was recloned into p2T7TA blue.	
Digest for transfection:	<i>NotI</i>	
Selection marker:	phleomycin [2.5 µg/ml]	

p2T7TA blue		24
Made by:	C. Clayton (unpublished)	
Construction:		
Date of construction:		
Short description:	original construct from the Clayton laboratory	
Digest for transfection:	<i>NotI</i>	
Selection marker:	hygromycin [2 µg/ml]	

p2T7TA blue PKAC3		25
Made by:	S. Kramer	
Construction:	The N-terminal fragment of <i>PKAC3</i> was transferred from p2T7 <i>PKAC3</i> (T. Riek) into p2T7TA blue using the <i>Xho</i> I and <i>Bam</i> HI site.	
Date of construction:	3 / 2004	
Short description:		
Digest for transfection:	<i>Not</i> I	
Selection marker:	hygromycin [2 µg/ml]	

p2T7TA blue PKAC1/2		26
Made by:	S. Kramer	
Construction:	The N-terminal fragment of <i>PKAC1</i> (corresponding to amino acids 10 to 216) was recloned from p2T7 <i>PKAC1/2</i> (P. Hassan) into p2T7TA blue using the <i>Xho</i> I and <i>Bam</i> HI sites.	
Date of construction:	3 / 2004	
Short description:		
Digest for transfection:	<i>Not</i> I	
Selection marker:	hygromycin [2 µg/ml]	

p2T7 PKAC1/2		27
Made by:	Paul Hassan	
Construction:	see Paul Hassan	
Date of construction:		
Short description:	used to reclone <i>PKAC1</i> into p2T7TAblue	
Digest for transfection:	<i>Not</i> I, not transfected in this work	
Selection marker:	phleomycin [3 µg/ml]	

2.1.7. Enzymes

Restriction endonucleases	NEB, Frankfurt; MBI Fermentas, St. Leon-Rot
T4 DNA Ligase	NEB, Frankfurt
Alkaline phosphatase, Calf Intestinal (CIP)	NEB, Frankfurt
Klenow Fragment of DNA Polymerase I	NEB, Frankfurt
<i>Pfu</i> DNA Polymerase	MBI Fermentas, St. Leon-Rot
Expand High Fidelity PCR System	Roche, Basel
Expand long Template PCR System	Roche, Basel
<i>Pwo</i> DNA Polymerase	Roche, Basel
<i>Taq</i> DNA Polymerase	Roche, Basel

2.1.8. Chemicals

Standard chemicals	Merck, Darmstadt; Roth, Karlsruhe
Radiochemicals	Amersham Bioscience, Freiburg
Medium additives	Difco, Detroit, USA; Gibco BRL, Eggenstein

Fine chemicals	Roche, Basel; Cayla, Toulouse; Fluka, Neu Ulm; Merck, Darmstadt; Pharmacia, Freiburg; Serva, Heidelberg; Sigma, Deisenhofen
Cyclic nucleotides	Biolog, Bremen

2.1.9. Frequently used media and buffers

All media were prepared with double distilled water and subsequently sterilized by filtration. FCS was incubated for 1 hours at 56 °C before use.

HMI9 medium:	(Hirumi and Hirumi, 1989; modified by Vassella and Boshart (1996) Iscoves modified medium for 1 l; 3.024 g NaHCO ₃ ; 136 mg hypoxanthine; 82.2 mg bathocuproine sulfonate; 0.2 mM 2-mercaptoethanol; 39 mg thymidine; 100,000 u penicillin; 100 mg streptomycin; 182 mg cysteine; 10% FCS
SDM79 medium:	SDM79 basic medium was prepared as described by Brun and Schonenberger (1979) with the following modifications: Instead of folic acid we used 9.1 g p-aminobenzoic acid folic and 1.82 g biotin as well as vitamin-mix. The medium was supplemented with 7.5 mg hemin, 100,000 u penicillin, 100 mg streptomycin, 0.1 mM glycerine and 10% FCS. Quantiities refer to 1 l of medium.
Conditioned SDM79:	PCF cells were harvested at a cell density between 1 x 10 ⁷ and 2 x 10 ⁷ cells/ml. The supernatant (conditioned SDM79) was sterilized by filtration.
DTM:	DTM basic medium (Overath <i>et al.</i> , 1986) was supplemented as described in Ziegelbauer <i>et al.</i> (1990) with the following modification: 10 mM glycerine was used instead of glycine. 28.2 mg bathocuproin sulphonate, 182 mg cysteine and 7.5 mg hemin were added. Quantities refer to 1 l of medium.
Cytomix:	10 mM K ₂ HPO ₄ /KH ₂ PO ₄ pH 7.6; 2 mM EGTA; 120 mM KCl; 150 μM CaCl ₂ ; 25 mM HEPES; 5 mM MgCl ₂ ; 0.5% glucose; 1 mM hypoxanthine; 100 μg/ml BSA
DNA loading dye (10 x):	0.1 M EDTA pH 8; 0.5% Bromophenol blue; 0.5% Xylencyanol blue; 40% saccharose
Laemmli buffer (2 x):	125 mM Tris-HCl pH 6.8; 0.1% SDS; 10% v/v glycerol; 0.004% Bromophenol blue; 0.2% 2-Mercaptoethanol
Laemmli buffer (6 x):	350 mM Tris-HCl pH 6.8; 0.28% SDS; 30% v/v glycerol; 0.6 M DTT; 0.012% Bromophenol blue; 0.6% 2-Mercaptoethanol
EB buffer:	10 mM Tris-HCl pH 8; 10 mM NaCl; 10 mM EDTA; 0.5% SDS
LB medium and agar plates:	10 g/l tryptone; 5 g/l yeast extract; 10 g/l NaCl; pH 7 For agar plates 16 g agar was added to 1 l LB medium.
MOPS buffer:	200 mM MOPS and 80 mM NaOAc (pH 7.0); 1 mM EDTA
SDS electro-phoresis buffer:	25 mM Tris-Base; 200 mM glycine; 3.46 mM SDS
SSC (1x):	15 mM sodium citrate pH 7; 150 mM NaCl
SOB-medium:	20 g/l tryptone; 5 g/l yeast extract; 10 mM NaCl; 2.5 mM KCl; 10 mM MgCl ₂ ; 10 mM MgSO ₄ ; pH 7
PBS:	10 mM Na ₂ HPO ₄ and 1.8 mM KH ₂ PO ₄ (pH 7.4); 140 mM NaCl; 2.7 mM KCl
TAE:	40 mM Tris-HCl and 40 mM NaOAc (pH 8.0); 1 mM EDTA
TBS/TBST:	20 mM Tris-HCl pH 7.6; 137 mM NaCl; ad 0.05% Tween for TBST
TDB	20 mM Na ₂ HPO ₄ ; 2 mM NaH ₂ PO ₄ pH 7.7; 20 mM glucose; 5 mM KCl; 80 mM NaCl; 1 mM MgSO ₄ ;
TE:	10 mM Tris-HCl pH 7.6; 1 mM EDTA

2.1.10. Equipment

Stratagene Stratacooler		Stratagene, Heidelberg
Odyssey IR-Scanner		Licor, Lincoln (Nebraska, USA)
Casy® I Cell analyzer (Modell TTC)		Schärfe System, Reutlingen
Electro Cell Manipulator 630 BTX		San Diego, California
Gene Amp PCR System 2400		Perkin Elmer, Weiterstadt
Spectrophotometer DU 640		Beckman Instruments, München
ABI PRISM 3100 Genetic Analyzer		Applied Biosystems, Norwalk (USA)
Geldoc 2000		Bio-Rad, München
Stratalinker™		Stratagene, Heidelberg
Hybridization Oven Mini-oven MKII		MWG Biotech, Ebersberg
Microscopes	Axioskop	Zeiss, Jena
	Axiovert	Zeiss, Jena
	Diavert	Leitz, Wetzlar
	Invert-Microscope IM35	Zeiss, Jena
Gene Pulser		Bio-Rad, München
Liquid Scintillation Counter		Beckman Instruments, München
Sonifier 250 (Branson)		Heinemann, Schwäbisch Gmünd
Vacuum Concentrator		Bachofer, Reutlingen
Centrifuge Sorvall RC5C		DuPont-Sorvall, Bad Homburg
Centrifuge 2K15 (with cooling device)		Sigma, Deisenhofen
Table centrifuge Biofuge B		Heraeus Christ, Hanau

2.1.11. Kits

peq Gold RNA pure Kit	peqLab, Erlangen
Qiagen Plasmid Purification Kit	Qiagen, Hilden
Quiax II Gel extraction Kit	Qiagen, Hilden
PCR purification Kit	Qiagen, Hilden
Prime-It® RmT Random Primer Labeling Kit	Stratagene, Heidelberg
DIG DNA Labeling and Detection Kit	Roche, Basel
ECL Chemiluminescence Detection Kit	Amersham, Freiburg

2.1.12. Software

Gene Construction Kit 2	Textco, New Hampshire (USA)
IP-lab 3.9.1	Scanalytics, Fairfax (USA)
Oligo 4.0	National Biosciences, Plymouth (USA)

2.2. Methods and Protocols

2.2.1. *T. brucei*

2.2.1.1. Culture of monomorphic BSF

Monomorphic *Trypanosoma* strains were cultured in HMI9 medium at 37 °C, 5% CO₂ in a humidified incubator. Logarithmically growing cells were generally kept at cell densities below 7 x 10⁵ cells/ml. Cell densities were counted regularly with the Neubauer cell chamber.

2.2.1.2. Culture of PCF

Procyclic trypanosoma strains were cultured in SDM79 at 27°C. The cell density was kept between 2 x 10⁶ and 2 x 10⁷ cells/ml. Cells may be diluted to lower cell densities, when they are already culture adapted or when the medium is supplemented with 20-50% conditioned SDM79. Cell densities were measured with the CASY cell counter.

2.2.1.3. Differentiation of monomorphic LS cells into SP cells

The laboratory adapted monomorphic trypanosoma strains are not able to differentiate into SS cells. However, when grown to high cell densities, monomorphic strains have some properties of SS cells (Breidbach *et al.*, 2002), among them they exhibit the life cycle stage specific PKA phosphorylation that was examined in this work. These monomorphic cells at high cell densities will be further referred to as SP cells, for stationary phase. To get SP trypanosomes, logarithmically growing monomorphic BSF cells were grown from <10⁴ cells/ml to cell densities of about 5 x 10⁶ cells/ml without dilution.

2.2.1.4. Differentiation of monomorphic BSF into procyclic cells

Logarithmically growing monomorphic BSF cells were transformed into SP cells, harvested and resuspended in SDM79 at a cell density of 2 x 10⁶ cells/ml. The transformation was induced by addition of 6 mM cis-aconitate and cultivation at 27 °C. Monomorphic MITat1.2 cells do transform into PCF but usually die around 10 days after the induction of the transformation. In contrast, pleomorphic strains like AnTat1.1 proceed in the life cycle.

2.2.1.5. Stable transfection of monomorphic BSF cells

Monomorphic BSF cells at cell densities between 5 and 8 x 10⁵ were harvested, washed once in cytomix (37 °C) and resuspended in cytomix (37 °C) at a cell density of 1 x 10⁷ / 400 µl. For each transfection, 400 µl of cell suspension was transferred into a sterile cuvette together with 10 µg linearized plasmid DNA [1 µg/µl]. The electroporation was performed with the electro cell manipulator 630 (BTX, San Diego, California) at 1.5 kV, 175 Ω and 25 µF. After electroporation, cells were transferred immediately into 50 ml HMI9 (37 °C). 18 hours after the transfection the selection marker was added in the appropriate concentration. Transfectants were usually visible 4-6 days later. If clonal transfections were needed, cells were serially diluted on 24 well tissue culture plates immediately after

the transfection. Each construct was transfected between 5 to 10 times in parallel.

2.2.1.6. Stable transfection of PCF cells

Logarithmically growing PCF cells at cell densities between 5×10^6 and 1×10^7 were harvested, washed once in cytomix (4° C) and resuspended in cytomix (4 °C) at a cell density of $1 \times 10^7 / 400 \mu\text{l}$. For each transfection, $400 \mu\text{l}$ of cell suspension was transferred into a sterile cuvette together with $10 \mu\text{g}$ linearized plasmid DNA [$1 \mu\text{g}/\mu\text{l}$]. The electroporation was done with the electro cell manipulator 630 (BTX, San Diego, California) at 1.5 kV, 175Ω and $25 \mu\text{F}$. After electroporation, cells were transferred immediately into 10 ml 30% conditioned SDM79 (pre warmed to 27 °C) and cultivated. The selection marker was added 18 hours later. Transfectants were visible after 12 to 14 days. If clonal transfectants were needed, 5 ml of a 1:1, 1:10 and 1:100 dilution of the transfected cells were plated on 96 well tissue culture plates ($50 \mu\text{l}$ per well) as soon as the selection marker was added. Each construct was transfected only once or twice.

2.2.1.7. Freezing and thawing of *T. brucei* cells

For freezing 5×10^6 BSF or 5×10^7 PCF cells were harvested and resuspended in cold culture medium with 10% glycerol v/v (0 °C) in cryotubes. Cells were slowly cooled down to $-80 \text{ }^\circ\text{C}$ with the Strata Cooler and transferred to liquid nitrogen for long term storage. Cells were thawed quickly in a 37° C water bath, washed once in 10 ml culture medium and transferred to warm culture medium. If necessary, selection markers were added earliest one hour after the thawing. In some cases PCF cells require conditioned medium after thawing.

2.2.1.8. Harvest of *T. brucei* cells

Cells were generally harvested by centrifugation at 4 °C and 1400 g (BSF) or 900 g (PCF) for 10 minutes. For transfection, BSF cells were harvested at 37 °C. According to requirements, cells may be washed once or twice in an appropriate buffer (TDB, PBS) at the respective temperature.

2.2.1.9. Methanol fixation and Dapi staining of *T. brucei* cells

Approximately 5×10^5 cells were resuspended in $50 \mu\text{l}$ of medium, spread on a glass microscope slide, air-dried, and fixed overnight in methanol at $-20 \text{ }^\circ\text{C}$. Slides were removed, the methanol was allowed to evaporate, and $40 \mu\text{l}$ of $0.1 \mu\text{g} / \text{ml}$ DAPI (4,6-Diamidino-2-phenylindole) in Vectashield Mounting Medium (Vector Laboratories, Burlingame) was added to the slide and spread by the addition of the coverslip. Slides were examined under UV light (350 nm excitation).

2.2.1.10. Paraformaldehyde fixation of *T. brucei* cells

0.4% Paraformaldehyde: 4 g paraformaldehyde were resuspended in sterile PBS, pH 7.0. 1 ml 1M NaOH was added and the solution was heated at 80°C until the paraformaldehyde was completely solved. 1 ml aliquots were stored at -20°C.

1-5 x 10⁶ cells were harvested, resuspended in 0.2 ml DTM w/o FCS and carefully mixed with 0.3 ml 4% paraformaldehyde. The fixation was carried out at 4 °C over night.

2.2.1.11. Immunofluorescence

Paraformaldehyde fixed cells were washed once in PBS and incubated in 0.5 ml 0.1 M Na₂HPO₄ / NaH₂PO₄ pH 7.2 / 0.1 M glycine for 15 minutes. For permeabilization, 0.5 ml 0.2% triton v/v was added for exactly 5 minutes. Cells were washed once in 0.5 ml PBS / 1% BSA w/v and incubated with the primary antibody in PBS / 1% w/v BSA for one hour at 4 °C. After two washing steps in PBS / 1% w/v BSA cells were incubated with the secondary antibody in PBS / 1% w/v BSA for one hour at 4 °C in the dark. Cells were washed twice in PBS / 1% w/v BSA and once in PBS. All centrifugations were carried out for 10 minutes at 600 g and 4 °C.

2.2.2. Nucleic acids

2.2.2.1. *T. brucei*

2.2.2.1.1. Isolation of genomic DNA from *T. brucei*

2.5x10⁷ to 1x 10⁸ cells were harvested, washed in PBS and lysed in 500 µl EB-buffer / 100 µg Proteinase K at 37 °C for at least two hours without resuspending the cell pellet. The DNA was purified by phenol extraction: 1 ml phenol (pH 8) was added to the lysed cells. After mixing (10 minutes on overhead shaker), the aqueous layer was separated from the organic layer by centrifugation (5 min, 20000 g) and removed into a fresh tube. The procedure was repeated with 1 ml phenol / chloroform (pH 8) and finally with chloroform to remove traces of phenol. The DNA was precipitated with 1 volume isopropanol and 1/25 volume 5 M NaCl and washed with 70% ethanol.

2.2.2.2. *E. coli*

2.2.2.2.1. Preparation of electrocompetent *E. coli* cells

5 ml of an *E. coli* overnight culture was transferred to 500 ml LB medium and grown to an optical density (OD₆₀₀) between 0.6 and 0.8. The bacteria were cooled down on ice for 20 minutes and harvested by centrifugation (4000 g, 15 min, 4 °C). The cell pellet was resuspended in 500 ml sterile ddH₂O (4 °C) and incubated on ice for 30 minutes. Cells were washed once in 250 ml ddH₂O (4 °C) (4000 g, 15 min, 4 °C) and once in 25 ml 10% glycerine (4 °C). The bacteria pellet was resuspended in 3 ml 10% glycerine, aliquoted in Eppendorf reaction tubes, frozen in liquid nitrogen and finally stored at -80 °C for up to 12 months. All resuspension steps were carried out very carefully.

2.2.2.2.2. Transfection of *E. coli* with plasmid DNA

The electroporation of *E. coli* cells was carried out according to the method of Dower *et al.* (1988). 40 μ l competent cells were thawed on ice, mixed with 1-3 μ l of DNA, incubated on ice for one minute and placed into a cuvette (4 °C). The electroporation was done with the GenePulser (Bio-Rad) at 25 μ F, 2.5 kV and 200 Ω . Cells were transferred into 1 ml SOB-medium (37 °C) immediately after the transfection and incubated for 45 min at 37 °C on a shaker. Cells were plated to LB agar plates with the appropriate antibiotics (usually ampicillin) and incubated overnight at 37 °C.

2.2.2.2.3. Isolation of plasmid DNA from *E. coli*

Small amounts of plasmid DNA was isolated from *E. coli* using a standard alkaline lysis protocol (Sambrook *et al.*, 1989). Higher quantities of plasmid DNA (100-500 μ g) were isolated with the Qiagen plasmid purification kit as described by the manufacturers.

2.2.2.2.4. Long time storage of *E. coli* cells

1 ml of *E. coli* overnight culture was added to 1 ml of glycerine buffer (25 mM Tris-HCl pH 8.0; 65% glycerine; 0.1 M MgSO₄) in cryotubes and stored at -80 °C.

2.2.2.3. Standard cloning protocols

2.2.2.3.1. Agarose gel electrophoresis

DNA fragments were separated on agarose gels (1% agarose, 1 μ g/ml ethidiumbromid) in TAE buffer with 10 V/cm. Samples were mixed with 0.1 volume 10 x DNA loading buffer. Sizes of DNA fragments were determined by comparison with DNA ladders (GeneRuler 1 kb ladder (MBI) and others). DNA was visualized with the Geldoc 2000 or on a UV illuminator.

2.2.2.3.2. DNA isolation from agarose gels

DNA was extracted from agarose gels with the Qiaex II Gel Extraction Kit (Qiagen) according to the instructions of the manufacturer.

2.2.2.3.3. Modification of DNA

The following methods were performed as described at Sambrook *et al.* (1989) or as described by the manufacturers of the used enzymes: DNA cleavage with restriction endonucleases, Ligation of DNA fragments, dephosphorylation of DNA with alkaline phosphatase and Klenow enzyme reaction.

2.2.2.3.4. DNA amplification (PCR)

DNA was amplified by polymerase chain reaction with either *Pfu* DNA Polymerase, Expand High Fidelity PCR System, Expand long Template PCR System, Pwo DNA Polymerase or Taq DNA Polymerase as described by the manufacturers of the enzymes / kits. The choice of polymerase was dependent on the application (length of PCR product, required

accuracy etc.). The Gene Amp PCR System 2400 (Perkin Elmer) was used for cycling. Primers were designed with the Oligo 4.0 Software (National Biosciences, Plymouth) that also calculates the ideal annealing temperatures. PCR products were purified with the PCR Purification Kit (Qiagen).

2.2.2.3.5. Precipitation of DNA

DNA was precipitated by addition of 1 volume isopropanol and 0.1 volume 3 M sodium acetate (pH 7.0) and subsequent centrifugation at 20,000 g for 20 minutes at 4 °C. The DNA pellet was washed once with 70% ethanol, allowed to dry and resuspended in either ddH₂O or TE buffer. Precipitation of genomic DNA was done with 0.08 volume 5 M NaCl instead of sodium acetate.

2.2.2.3.6. Quantification of DNA

Purity and quantity of nucleic acids were determined by measuring the absorption at 260 and 280 nm. An OD₂₆₀ of 1 is equivalent to 50 µg/ml dsDNA. The ratio of OD₂₆₀/OD₂₈₀ indicates the purity of the preparation and is ideally 1.8. The measurements were done with the spectrophotometer DU 640.

2.2.2.3.7. Sequencing of DNA

DNA was sequenced either at the SeqLab Sequence Laboratories (Göttingen) (hot shot sequencing) or on the Abi PRISM 3100 Genetic Analyzer (Applied Biosystems, Norwalk (USA)). Samples were prepared as required by SeqLab or as described by Applied Biosystems.

2.2.2.4. Southern blot analyses

Restriction enzyme digests of genomic DNA were separated on a 0.8% agarose gel together with a DNA size marker. After documentation (Geldoc 2000), the gel was soaked in 0.25 N HCl for 15 minutes (depurination), in 0.5 M NaOH/ 1.5 M NaCl for 30 minutes (DNA denaturation) and in 1 M Tris-HCl pH 7.4/1.5 M NaCl for 30 minutes (neutralization). The DNA was transferred to a nylon membrane over night in 20 x SSC by capillary forces as described by Sambrook *et al.* (1989). The DNA was covalently bound to the damp membrane by UV crosslinking (Stratalinker, autocrosslink function). The detection was done either with radioactive or digoxigenine labeled probes:

Radioactive detection:

The radioactive labeling of the probe was carried out with the Prime-It RmT Random Primer Labeling Kit according to the instructions of the manual. The prehybridization of the membrane was done in QuickHyb (Stratagene) for one hour at 65°, followed by the hybridization for another hour. The membrane was rinsed three times with 2 x SSC/ 0.1% SDS and washed three times in 0.1 x SSC/ 0.1% SDS (65 °C) for 30 minutes each. The detection was done either by autoradiography or with the phosphorimager.

Digoxigenine labeling:

Probes were labeled with Digoxigenine with the aid of the DIG DNA Labeling and Detection Kit as described by the manufacturer. Membranes were prehybridized with DIG Easy Hyb solution for at least one hour. Hybridization with the DIG labeled probe was carried out overnight in fresh DIG Easy Hyb solution. The membrane was rinsed three times with 2 x SSC/ 0.1% SDS and washed three times in 0.1 x SSC/ 0.1% SDS (65 °C) for 30 minutes each. The membrane was incubated 1 min in buffer 1 (Tris-HCl 100 mM pH 7.5 / 150 mM NaCl), 30 min in buffer 1 / 0.5% blocking reagent, 1 min in buffer 1, 30 min with anti-DIG-AP in buffer 1, 3 x 10 min in buffer 1 and 2 min in buffer 3 (Tris-HCl 100 mM pH 9.5 / NaCl 100 mM / MgCl₂ 50 mM). For detection the membrane was overlaid with 4 mM NBT / 4 mM BCIP in buffer 3 and incubated without light for 1 to 12 hours, until bands were visible. The reaction was stopped with Tris-HCl pH 8.0 / EDTA 1 mM.

2.2.3. Proteins

2.2.3.1. Preparation of protein lysates from *T. brucei*

BSF or PCF cells were harvested by centrifugation (10 min, 1400 g, 4 °C), resuspended in ice cold PBS and transferred to an 1.5 ml Eppendorf tube. Cells were centrifuged (30", 10000 g, 4 °C) and the cell pellet was resuspended in an appropriate volume of PBS. An equal volume 2 x Laemmli buffer was added, the lysate was incubated at 100 °C for 3 to 5 minutes and finally ultrasonificated for 20" (Branson Sonifier 250, output control 7). Usually 1 x 10⁶ cells to 5 x 10⁶ cells were used for 10 µl of final cell lysate (one lane on SDS PAGE), depending on the abundance of the protein and the antibody used for detection. Cell lysates were stored at -20 °C and were stable for about 12 months.

2.2.3.2. Discontinuous SDS polyacrylamide gel electrophoresis (SDS PAGE)

separation gel (10%):	acrylamide/ bisacrylamide 37.5:1 (rotiphorese Gel 30)	20 ml
	1.5 M Tris-HCl pH 8.8; 0.4% SDS	15 ml
	H ₂ O bidest	25 ml
	10% w/v APS	0.2 ml
	TEMED	0.04 ml
stacking gel	acrylamide/ bisacrylamide 37.5:1 (rotiphorese Gel 30)	1.95 ml
	0.5 M Tris-HCl pH 6.8; 0,4% SDS	3.75 ml
	H ₂ O bidest	9.15 ml
	10% w/v APS	75 µl
	TEMED	15 µl

The separation of proteins by their differences in molecular weight was done in the one dimensional discontinuous gel electrophoresis (Laemmli, 1970). 10% acrylamide gels out of separation gel and stacking gel were poured according to the instructions above. The gel electrophoresis was carried out in SDS electrophoresis buffer at 130 Volt. For size markers, See Blue™ Pre-Stained Standard (Invitrogen) (250, 98, 64, 50, 36, 30, 16, 6, 4 kDa) or SeeBlue® Plus2 Pre-Stained Protein Standard (Invitrogen) (250, 148, 98, 64, 50, 36, 22, 16, 6, 4 kDa) were used.

2.2.3.3. Staining of proteins in polyacrylamide gels with Coomassie Blue

SDS gels were stained in Coomassie solution (0.1% Coomassie Brilliant Blue R250; 10% acetic acid; 50% methanol) for 10 minutes to 12 hours and destained in 10% v/v HCl (3 times 10 minutes) on a shaker. Gels were packed in cellophane paper avoiding air bubbles, wetted with 10% glycerol and dried over night.

2.2.3.4. Western blot analyses

The electrophoretic transfer of proteins from SDS gels to PVDF membranes was done with the semi dry technique according to Kyhse-Andersen (1984). The blot was assembled from the cathode to the anode as follow: 6 Whatman papers wetted in anode buffer I (300 mM Tris pH 10.4; 20% methanol), 3 Whatman papers wetted in anode buffer II (30 mM Tris pH 10.4; 20% methanol), PVDF membrane (preequilibrated in methanol), gel, 6 Whatman papers wetted in cathode buffer (25 mM Tris pH 9.4; 20% methanol; 40 mM 6-aminohexanoic acid). The blotting was done with a current density of 0.8 mA/cm² for one hour. The immunological detection of the proteins was either done with enhanced chemiluminescence (ECL) or with the Licor Western blot detector according to the following protocols:

ECL:

- Incubate membrane with TBST/ 5% skim milk powder for 1 hour at RT
- Incubate membrane in TBST/ 1% skim milk powder/ primary antibody for 1 hour at RT
- Wash membrane two times short and 3 times 10 minutes in TBST
- Incubate membrane in TBST/ 1% skim milk powder / secondary antibody (peroxidase coupled)
- Wash membrane two times short and 3 times 10 minutes in TBST
- Treat membrane according to the instructions of the ECL Chemiluminescence Detection Kit (Amersham) and detect bands with autoradiography.

LiCor Western blot detector:

- Incubate membrane with PBS/ 5% skim milk powder for 1 hour at RT
 - Incubate membrane in PBS 0.1% Tween/ 1% skim milk powder / primary antibody for 1 hour at RT.
 - Wash membrane two times short and 3 times 10 minutes in PBS 0.2% Tween.
 - Incubate membrane in PBS 0.1% Tween / 1% skim milk powder / secondary antibody (IRDye800 or Alexa 680) in the dark.
 - Wash membrane two times short and 3 times 10 minutes in PBS 0.2% Tween in the dark.
 - Dry membrane between two Whatman papers
 - Scan membrane with the Odyssey IR Scanner according to the instructions of the manufacturer. If necessary, bands can be quantified with the Odyssey Software.
- Dried membranes were stored in the dark and can be rescanned for about 12 months.

Antibodies were removed from the membrane by incubation in stripping buffer (100 mM 2-mercaptoethanol; 62.5 mM Tris-HCl; 2% v/v SDS; pH 6.7) at 50 °C for 30 min and subsequently washed 2 x 10 minutes in either TBST or PBS.

2.2.3.5. Affinity purification of antibodies

Antiserum was affinity purified according to the method of Olmsted (1981). 250 µg

recombinant protein were transferred to a 9 cm wide well of an SDS gel, separated and transferred to a PVDF membrane. The membrane was stained with Ponceau solution (0.1% PonceauS in 1% acetic acid) and the protein band was cut out. The membrane strip was incubated in 5% skim milk powder/ PBS for 1 hour, washed 3 times short and 3 times 10 minutes in PBS and incubated for 3-4 hours with 1 ml antiserum at RT. Subsequently the stripe was washed 3 times short and 3 times 10 minutes in PBS and the antibody was eluted by addition of 1 ml 0.2 M glycine/ 1 mM EGTA pH 2.2 for exactly 10 minutes. The eluate was transferred to an Eppendorf tube that contained 200 μ l 1 M Tris-HCl pH 8.0 for neutralization. For stabilization, 200 μ g / ml BSA was added and the eluate was dialyzed for 12-24 hours against PBS, changing the PBS three times. The antibody was stored at 0 °C in the presence of 0.02% NaN₃.

2.2.3.6 Covalent coupling of anti-Ty1 to protein G sepharose

For immunoprecipitations, anti-Ty1 was covalently coupled to protein G sepharose beads (Amersham Pharmacia, Uppsala (Sweden); 50% slurry). 1 ml protein G-sepharose beads were preequilibrated in “borate buffer low” (50 mM boric acid; 3 M NaCl, pH 9.0) and mixed with 500 μ l anti-Ty1 hybridoma supernatant for 3 hours at RT. Subsequently, the supernatant was removed by centrifugation (1400 g, 3 min) and the antibody containing protein G-sepharose beads were washed twice in 10 ml “borate buffer” low and resuspended in 10 ml “borate buffer high” (200 mM boric acid; 3 M NaCl, pH 9.0). After addition of dimethylpimelimidate (cross-linker) at 20 mM the beads were incubated for 30 min at RT on a shaker, washed once in 10 ml 0.2 M ethanolamine and incubated for 2 hours in 10 ml 0.2 M ethanolamine at RT. The beads were washed twice with 10 ml PBS/ 0.02% NaN₃, resuspended in 400 μ l PBS/ 0.02% NaN₃ and stored at 4 °C. The antibody containing sepharose beads can be used for immunoprecipitations for at least 2 years.

2.2.3.7. Immunoprecipitation

IP stock buffer	50 mM Tris-HCl pH 7.5; 2 mM EGTA; 150 mM NaCl
IP buffer	IP stock buffer complemented with 1 mM NaVO ₄ ; 0.5% aprotinin; 2 μ g/ml leupetin and 1 mM PMSF (prepare freshly)
IP* buffer	IP + 0.2% Nonidet P40
IP2* buffer	IP + 0.4% Nonidet P40
Washing buffer	10 mM Tris-HCl pH 7.0; 5 mM Mg-acetate; 150 mM NaCl
Washing buffer *	10 mM Tris-HCl pH 7.4; 5 mM Mg-acetate, 2.5 mM NaF

The immunoprecipitation procedure was carried out either on ice or at 4 °C using ice cold buffers only. Solutions that contained protein G/A sepharose beads were generally pipetted with a cut pipette tip, to avoid shearing of the beads.

Cell pellets of 5 x 10⁷ cells were thawed on ice, resuspended in 100 μ l IP buffer and mixed with 100 μ l IP2* buffer for cell lysis. Lysates were incubated on ice for 10 minutes and the

non-soluble cell components were pelleted by centrifugation (20,000 g , 20 min, 4 °C). The supernatant extract was transferred to a fresh tube.

If the required antibody is already coupled to protein G sepharose beads, 20 μ l of these beads were mixed with the supernatant for 1 hour to overnight on an over head mixer. Ty1-PKAR was precipitated quantitatively only with an overnight incubation while for most proteins one hour of immunoprecipitation was sufficient. If the required antibody is not coupled to protein G sepharose beads, the supernatant is mixed with the antibody (e.g. 200 μ l HA hybridoma supernatant) for 1 hour and then with 20 μ l protein G sepharose beads (equilibrated in IP* buffer) for an additional hour or overnight. In the case of the HA antibody, the high antibody volume results in lower NP40 concentrations (0.1%) in the final precipitation reaction that were not corrected.

After short centrifugation (30" microfuge) the supernatant was removed and if necessary concentrated with Microcon 30 tubes (Amicon) to control for the completeness of the precipitation by Western blot analysis. For kinase assays, the protein loaded beads were washed twice in IP* buffer, twice in washing buffer and once in washing buffer* and finally resuspended in the appropriate volume washing buffer*. For other experiments (e.g. coimmunoprecipitation) the beads were washed three times in IP* buffer and twice in IP buffer. Generally it was not necessary to eluate the protein from the beads for the applications used in this work. Samples for Western blots were prepared by heating an aliquot of the immunoprecipitate (IP) or the supernatant (SN) in an equal volume of 2 x Laemmli buffer at 95°C for 5 min.

2.2.3.8. Purification of Ty1-PKAC1 for mass spectrometry

For mass spectrometry, Ty1-PKAC1 was purified by immunoprecipitation from the cell line MITat1.4 Ty1-PKAC1 (P. Hassan) essentially as described above, with the following modifications:

60 to 240 tubes with 2×10^8 cells each were resuspended in 200 μ l IP buffer, lysed with 200 μ l IP* buffer, incubated for 10 minutes on ice and centrifuged (20000 g, 20 min, 4 °C). The supernatants of 60 tubes were pooled in a 50 ml falcon tube and incubated with 500 μ l Ty1-Protein G-sepharose beads overnight. The beads were washed once in 50 ml IP* buffer, twice in 50 ml IP* buffer without protease and phosphatase inhibitors and twice in 50 ml PBS. The beads were cooked in an equal volume of 2 x Laemmli buffer and transferred to an SDS gel (large size) using 2-8 lanes depending on the amount of cells. The gel was stained in Coomassie solution (0.1% Coomassie Brilliant Blue R250; 10% acetic acid; 50% methanol) for one hour to overnight and destained in 10% v/v acetic acid until bands were visible. A typical Coomassie stained gel is shown in figure 5. The phosphorylated and unphosphorylated PKAC1 bands were cut with a sterile scalpel and transferred to a fresh tube. A small part of the gel band was reheated at 100°C in an approximately equal volume of 2 x Laemmli buffer and analyzed on a Western blot to ensure that the correct bands were cut. The PKAC1 containing gel slices were then sent to E. Krause (MDC, Berlin Buch) for mass spectrometry.

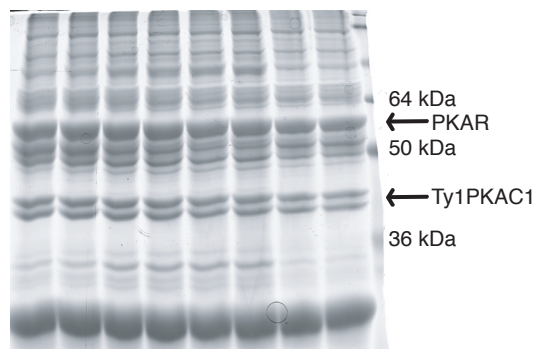


Fig. 5: Purification of immunoprecipitated Ty1-PKAC1 on SDS gel for mass spectrometry: Ty1-PKAC1 was immunoprecipitated from 4.8×10^{10} cells and applied to SDS PAGE (8 lanes). The gel was stained with Coomassie. The Ty1-PKAC1 double bands (phosphorylated and unphosphorylated) and the PKAR bands are marked with arrows.

2.2.3.9. *In vitro* Kinase assays

PKA kinase assay using a peptide as substrate:

5 x MES buffer:	250 mM MES pH 6.9; 2 mM EGTA; 5 mM Mg-acetate; 50 mM NaCl
reaction mix:	500 μ l 5 x MES buffer; 250 μ l DTT [100 mM]; 125 μ l BSA [10 mg/ml]; 25 μ l peptide substrate [5 mM]; 241.6 μ l ATP [1 mM]; γ - 32 P-ATP [5 μ l = 50 μ Ci]; ad 1.5 ml

Either kemptide (LRRASLG; Kemp et al., 1976; Kemp et al., 1977) or an optimized PKA substrate (RRRRSIIIFI, Songyang *et al.*, 1994) were used as peptide substrates. Both are equally well substrates for *T. brucei* PKA-like kinase (data not shown). Each assay was usually done in triplicates and at least once in the presence of 5 μ M PKI 5-24 to control for the specificity of the reaction. 30 μ l reaction mix were added to each tube that already contained 10 μ l of H₂O or additives such as PKI or cNMPs. The assay was started with the addition of 10 μ l immunoprecipitated kinase, which equals protein from 1×10^6 to 2×10^6 cells. Samples were shaken slightly at 30°C for 15 min. Afterwards, 30 μ l of each sample was transferred to phosphocellulose (P81 Whatman) filter (2 x 2 cm). The filters were washed four times 10 min in 75 mM phosphoric acid and once in acetone. The radioactivity of the bound peptide substrate was measured in a liquid scintillation counter.

2.2.3.10. *In vivo* Kinase assays with the PKA reporter substrate VASP

Transgenically expressed human VASP has been used as a reporter substrate to measure *T. brucei* PKA activity *in vivo*. Since the assay has been established in this work its exact performance varies between the different experiments and the exact conditions are shown in the legend of each figure.

The protocol described below has been found most suitable and already considers some results from this work for example the activation of PKA-like kinase by a decrease in temperature.

- Culture VASP expressing trypanosomes to a cell density between $5 \cdot 10^5$ and $7 \cdot 10^5$ cells/ml. (Note: lower cell densities might result in problems of VASP detection on the Western blot)
- Fill Eppendorf tubes with 1 ml of VASP cells, incubate at 37°C while slightly shaking. No more than 10 samples should be handled in one assay.
- Perform the experiment. If possible, the duration of an experiment should not exceed 10 minutes. All cells should remain at the 37°C shaker for the same time, this means that during kinetic experiments the substance of interest is added at different time points. Note that a control must always be performed in parallel for each assay. It is not sufficient to consider the null value as a control.
- Harvesting: Centrifuge samples (10,000 g, 30", 37°C) and remove the supernatant by suction (fast!). Add $4 \mu\text{l}$ 6x Laemmli buffer to the cells and incubate at 95°C for 5 minutes.
- Analyze the extent of VASP phosphorylation from a quantitative Western blot.

3. Results

3.1. PKAC1 and PKAC2 differ in their life cycle stage dependent posttranslational modifications and expression

Three related protein kinase A homologues to catalytic subunits of PKAs from other organisms have been cloned from the genome of the *T. brucei* strain AnTat in this laboratory (T. Klöckner, Ph.D. thesis 1996). From these, PKAC1 and PKAC2 are remarkably similar. Their amino acid sequences are 98% identical and the only differences lie at their N- and C-termini. The genes for PKAC1 and PKAC2, located at adjacent gene loci, most likely arose from a single precursor gene during an evolutionary recent gene duplication event. Antibodies raised against small peptides of the distinct N-termini of PKAC1 and PKAC2 were not able to discriminate between the isoforms (T. Klöckner, Ph.D. thesis 1996). The available antibody (anti-PKAC1/2) recognizes both, PKAC1 and PKAC2 (T. Klöckner, Ph.D. thesis 1996). For this reason, PKAC1 and PKAC2 together will subsequently be referred to as PKAC1/2 whenever a differentiation by other means is impossible.

Given this high degree of homology between the two isoforms it came as a surprise that different mRNA levels are expressed in the different *T. brucei* life cycle stages. *PKAC1* mRNA is predominantly expressed in blood stream forms and *PKAC2* mRNA in procyclic cells (E. Vassella, unpublished). Furthermore, multiple bands on Western blot indicated possible protein modifications (T. Klöckner, Ph.D. thesis 1996). Life cycle stage dependent differences in expression and structure of PKAC1 and PKAC2 were of interest, since these kinases were candidates to be involved in signaling events triggering differentiation (Vassella *et al.*, 1997).

3.1.1. *Tb*PKAC1/2 is posttranslationally modified in SS and PCF cells

Three PKAC1/2 forms have been distinguished by their different apparent molecular weights on Western blot: one fast running form predominantly present in LS cells, one slow running form mainly found in SS cells and one form that runs only slightly slower than PKAC1/2 from LS cells and is exclusively present in procyclic cells (T. Klöckner, Ph.D. thesis 1996). We conclude from this that PKAC1/2 of SS cells and of PCF cells carries posttranslational modifications that are absent from LS cells. These modifications

will be further referred to as “stumpy specific” or “PCF specific”.

All subsequent biochemical analyses of the PKAC1/2 modifications will be done exclusively with monomorphic trypanosomes, since they are easier to handle and to manipulate than pleomorphic cells. Although these laboratory adapted strains are unable to differentiate into short stumpy cells, they acquire some features of this life cycle stage when grown to high cell densities (Breidbach *et al.*, 2002). Among these is the stumpy specific modification. Monomorphic trypanosomes grown to high cell densities will further be called SP cells, for stationary phase.

A Western blot with PKAC1/2 from the different life cycle stages is shown in figure 6.

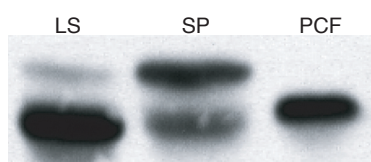


Fig. 6: Life cycle stage dependent changes in *Tb*PKAC1/2 gel mobility:

Western blot with protein lysates from different life cycle stages (LS, SP, PCF) probed with anti-PKAC1/2. Three different PKAC1/2 forms are clearly distinguishable by their different gel mobility. Note that LS cells do always contain a certain percentage of SP-PKAC1/2 and vice versa, since it is difficult to obtain pure cultures of LS or SP cells.

3.1.1.1. The stumpy specific modification

At first, our interest focussed on the biochemical characterization of the stumpy specific modification. It was shown previously with phosphatase treatments that the stumpy specific modification is a Ser/Thr phosphorylation that is probably localized at the protein surface, since it is accessible to phosphatases (S. Schimpf, Diploma thesis 2000). It was further shown with phospho specific antibodies that this phosphorylation is not located at threonine 179 in the kinase activation loop. The activation loop threonine is highly conserved in all PKAs and its constitutive phosphorylation is essential for kinase activity (Shoji *et al.*, 1979; Steinberg *et al.*, 1993; Adams *et al.*, 1995). Likewise to the activation loop threonine in mammalian PKAs, Thr179 of *T. brucei* PKAC1 was found to be constitutively phosphorylated in all analysed life cycle stages (S. Schimpf, Diploma thesis 2000).

3.1.1.1.1. *In silico* search for potential PKAC1/2 phosphorylation sites

The first aim was to map the stumpy specific phosphorylation site. Prior to mass spectrometry, it was tried to predict potential phosphorylation sites of PKAC1 and PKAC2 *in silico*. For this, phosphorylation probabilities of all serine and threonine residues from PKAC1 and PKAC2 were calculated, according to the method of Blom *et al.* (1999)

with the WEB based software Net Phos Prediction (<http://www.cbs.dtu.dk/services/NetPhos>). Only 13 Ser/Thr residues of PKAC1 and 11 Ser/Thr residues of PKAC2 have a phosphorylation probability higher than 0.5 and are thus likely to become phosphorylated (Table 1).

In a second step, each of these putative phosphorylation sites was examined for its probability to be on the protein surface. The surface probability was calculated according to the method of Emini *et al.* (1985) and Janin *et al.* (1978) with the aid of the software Gene Inspector (Textco). Accordingly, eight of the putative PKAC1/2 phosphorylation sites were predicted to be on the protein surface with a surface probability higher than 1¹⁾, and could therefore possibly be the stumpy specific phosphorylation site. They are shadowed in table 1.

PKAC1			PKAC2		
Ser/Thr (position)	probability of phosphorylation	Surface access	Ser/Thr (position)	probability of phosphorylation	Surface access
S18	0.842	1.00	S6	0.989	3.00
S46	0.987	0.35	S20	0.842	1.00
S116	0.701	0.20	S48	0.987	0.35
S302	0.998	1.25	S118	0.701	0.20
S307	0.896	0.50	S304	0.998	1.25
S311	0.938	0.30	S309	0.896	0.50
S320	0.741	1.75	S313	0.938	0.30
T2	0.582	no value	T5	0.763	3.00
T4	0.956	1.50	T181	0.978	0.30
T179	0.978	0.30	T226	0.750	0.25
T224	0.750	0.25	T267	0.961	0.25
T265	0.961	0.25			
T324	0.660	2.25			

Table 1: *In silico* search for phosphorylation sites on the surface of PKAC1 and PKAC2

Potential serine/ threonine phosphorylation sites of *Tb*PKAC1 and *Tb*PKAC2 were predicted according to the method of Blom *et al.* (1999) using the web based software NetPhos (<http://www.cbs.dtu.dk/services/NetPhos/>). Phosphorylation sites having a phosphorylation probability of 0.5 and higher are indicated in the table. Homologous amino acids between PKAC1 and PKAC2 are shown in the same line. The probability to be on the protein surface was calculated for each of these potential phosphorylation sites according to the method of Emini *et al.* (1985), using the data of Janin *et al.* (1978). Thereby a surface probability of 1 is defined as the average surface probability of all amino acids from a given protein.

All predicted phosphorylation sites that are likely to be on the protein surface are shadowed.

Interestingly, only two of these sites are found in both, PKAC1 and PKAC2 (S18/20 and S302/304). Two putative phosphorylation sites are present in PKAC2 only (T5, S6) and four sites are restricted to PKAC1 (T2, T4, S320, T324). Since we knew from previous immunoprecipitation studies with epitope tagged PKAC1 that the stumpy specific phosphorylation site is definitely present in PKAC1 (Schimpf, Diploma thesis 2000), it is unlikely that T5 or S6 of PKAC2 are the stumpy specific phosphorylation sites. This leaves six putative phosphorylation sites as candidates for the stumpy specific PKAC1/2 phosphorylation.

The next aim was the identification of the stumpy specific phosphorylation site using mass spectrometry:

1) According to the used method, 1 is defined as the average surface probability of all amino acids.

3.1.1.1.2. The stumpy specific phosphorylation was mapped to Thr324 via mass spectrometry.

Ty1-epitope tagged PKAC1 (Ty1-PKAC1) from SP cells (MITat1.4 Ty1-PKAC1, provided by P. Hassan) was purified by immunoprecipitation, separated on SDS PAGE and stained with Coomassie Brilliant Blue as described in method 2.2.3.8. Since only around half of PKAC1 is phosphorylated in SP cells, it was possible to isolate both the unphosphorylated (lower) and phosphorylated (upper) Ty1-PKAC1 band from the same lane of the gel.

The phosphorylation pattern of Ty1-PKAC1 from both bands was then compared using mass spectrometry by Eberhard Krause (MDC, Berlin Buch). For this, the proteins were digested with endoproteinases and the molecular weights of the resulting peptides were determined. Several digests with different endoproteinases (trypsin, chymotrypsin, Lys-C and Asp-N) were performed. Masses were determined both in the linear and in the reflectron mode of the mass spectrometer. While measurements in the linear mode are possible even with relatively low amounts of protein, measurements in the reflectron mode result in more accurate masses. A summary of the results from all mass spectrometry experiments is shown in figure 7A and B. The graphic color indicates for each experiment whether a peptide was found unmodified, modified, both unmodified and modified or not detectable.

The peptides that contain the activation loop threonine 179 (T191 in Ty1-PKAC1) were found phosphorylated in both the upper and lower PKAC1 band. These data confirm the results from earlier experiments with phosphospecific antibodies described above (Schimpf, diploma thesis 2000).

Differences in phosphorylation between the upper and lower bands were mainly detected in the PKAC1 C terminus. The corresponding potentially phosphorylated peptides from the Lys-C and Asp-N digest were then sequenced by ESI-QTOF MS (E. Krause, MDC Buch) in order to confirm the identity of the peptides and to determine the exact position of phosphorylation. A phosphorylation site at position Thr324 (which corresponds to Thr336 in Ty1-PKAC1) was detected in the peptides from both the Lys-C and Asp-N digest. The other potentially phosphorylated peptides were either not found with ESI-QTOF or could be unequivocally assigned to non phosphorylated peptides.

One stumpy specific PKAC1 phosphorylation site was therefore identified C-terminal at position Thr324, thus at one of the phosphorylation sites that had been predicted with the *in silico* approach described above. PKAC2 has an alanine at the homologous position

that expressed HA-PKAC2 were easily obtained (clones HA-S2 and HA-S4). PKAC1 and PKAC2 from LS and SP cells of this cell line were detected with anti-PKAC1/2 (Fig. 9A). Subsequently, the antibodies were removed and HA-PKAC2 was detected with anti-HA (Fig. 9B).



Fig. 8: Replacement of WT PKAC2 by HA-PKAC2

A neomycine resistance gene (*NEO*: neomycine phosphotransferase, green) together with the 5'UTR and 3'UTR of *ACTIN* (green, unfilled) was inserted into the 3'UTR of *PKAC2*. The HA-epitope tag (red) was introduced at the N-terminus of *PKAC2* (blue). The *ClaI*/*BstZ171* digested plasmid integrates into the WT locus of *PKAC2* by homologous recombination.

As expected, *PKAC2* is difficult to detect with anti-PKAC1/2 due to its equal molecular weight with *PKAC1* and lower expression level (see chapter 3.1.2.). With anti-HA, however, *PKAC2* is easily detectable as a single band that has equal molecular weight in LS and SP cells. The band is absent in cell lysates from WT cells (data not shown). There is no indication of a band shift and hence no evidence for stage-specific phosphorylation of *PKAC2*.

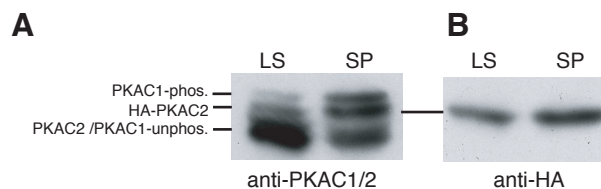


Fig. 9: PKAC2 lacks the stumpy specific phosphorylation

PKAC2 was tagged with an N-terminal HA-epitope tag to enable its distinction from *PKAC1* (cell line: HA-*PKAC2*). Cell extracts of LS and SP cells of this cell line were used for Western blotting.

A) Both *PKAC1* and *PKAC2* were detected with anti-PKAC1/2. Note that *PKAC2* constitutes only a small fraction of PKAC1/2 in BSF cells. The *PKAC2* WT band is hidden behind the abundant *PKAC1* band. *PKAC2* is less abundant in LS cells than in SP cells (see chapter 3.1.2.).

B) After the removal of the antibodies HA-*PKAC2* was detected with anti-HA. No differences in gel mobilities were detectable between HA-*PKAC2* from LS and SP cells.

3.1.1.1.4 The stumpy specific phosphorylation has no influence on kinase activity

After the stumpy specific PKAC phosphorylation was successfully mapped and found to be restricted to *PKAC1*, its functional analysis was now feasible. Before starting reverse genetic analyses it was at first tested whether the phosphorylation influences the activity of *PKAC1* *in vitro*.

For this, Ty1-PKAC1 was immunoprecipitated from LS and SP cells with Ty1-protein G sepharose beads. Equal amounts of the immunoprecipitates were tested for their abilities to phosphorylate the PKA specific peptide substrate kemptide with γ^{32} ATP. To exclude the presence of any non-specific, coprecipitated kinases, an immunoprecipitate from WT cells was used as a control. Further proof for the specificity of the detected kinase activity is provided by the absence of coprecipitated activity with inactive dead mutant (see chapter 3.2.2, not done in this experiment). Each assay was also performed in the presence of the PKA specific inhibitor PKI 5-24 (Kemp *et al.*, 1991). The amount of phosphorylated kemptide was quantified and PKI inhibitable activity directly reflects PKAC1 activity (Fig. 10A). The measured activities were corrected for the slightly different amounts of precipitated Ty1-PKAC1 protein from LS and SP cells, as calculated from a quantitative Western blot (Fig. 10B and C).

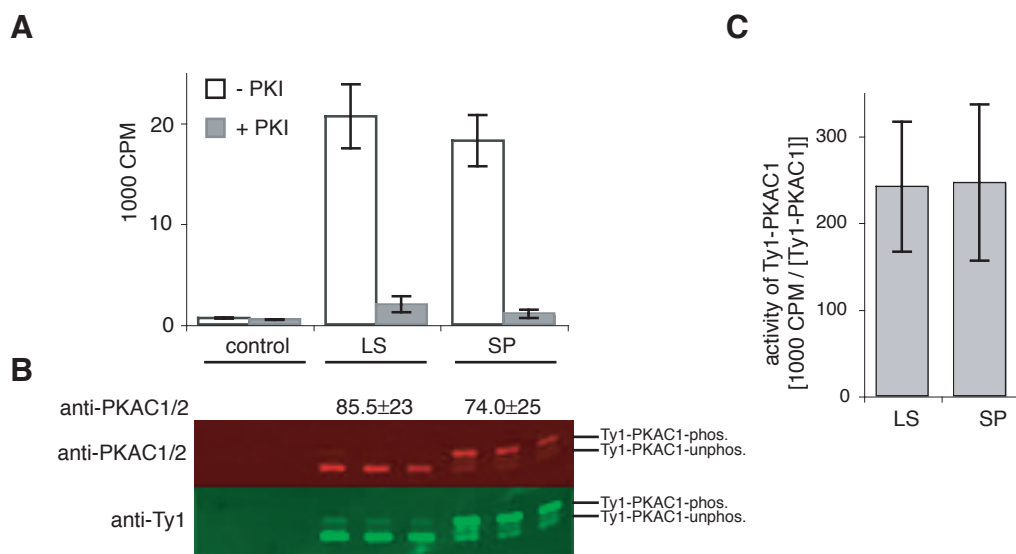


Fig. 10: Comparison of PKAC1 activity in LS and SP cells:

Ty1-PKAC1 was immunoprecipitated from LS and SP cells of the cell line Ty1-PKAC1 with anti-Ty1 protein G sepharose beads, using $5 \cdot 10^7$ cells for each precipitation. To exclude the coprecipitation of an unspecific kinase activity the immunoprecipitate from an equal amount of WT cells (MITat1.2) was used as a control. Equal amounts of the immunoprecipitates were tested for their abilities to phosphorylate the PKA specific peptide substrate kemptide with γ^{32} PATP in the presence and absence of $10 \mu\text{M}$ PKI. Each assay was done in triplicates. The amount of phosphorylated kemptide was quantified using a liquid scintillation counter and the average values of the three assays are shown together with the standard deviations (error bars) (**A**). To ensure that equal amounts of LS and SP PKA were used, the amount of PKAC1 in the immunoprecipitates from LS and SP cells was quantified. Therefore amounts of the precipitate were applied in triplicates to a Western blot and detected with anti-PKAC1/2 (red, secondary antibody Rabbit Alexa 680) and anti-Ty1 (green, secondary antibody Mouse IRDye800). PKAC1 was quantified with the Odyssey Software (Licor) (**B**). The (relative) activity of Ty1-PKAC1 was then calculated as the quotient from the CPM values of the kinase assay and the (relative) amount of Ty1-PKAC1 as quantified from the Western blot (**C**).

No kinase activity was detected in the immunoprecipitate from the control cells (WT cells) that do not contain Ty1-PKAC1. The relative kinase activities from LS and SP cells were 241.3 ± 75 (LS) and 245.9 ± 90 (SP) (CPM / [Ty1-PKAC1]). This means that stumpy specific phosphorylation does not affect *in vitro* activity of PKAC1.

3.1.1.1.5. Site directed mutagenesis at Thr324 of PKAC1 results in the loss of the stumpy specific phosphorylation

In order to confirm that Thr324 was in fact the site of the stumpy specific PKAC1 phosphorylation, mutant cell lines were made that had an alanine or glutamate instead of the threonine at position 324. Two transfection rounds were necessary to generate the mutant cell lines: The first *PKAC1* allele was silenced using the construct $p\Delta PKAC1 BSD$ (provided by Paul Hassan). The second *PKAC1* allele was subsequently replaced by either the mutant *PKAC1* genes or unmutated *PKAC1*, the later serving as a control. This way three stable clonal cell lines were obtained (T, A, E). In order to enable immunoprecipitations, the mutant cell lines were also produced with a N-terminal Ty1-epitope tagged PKAC1 (Ty1-T324, Ty1-A324, Ty1-E324). All cell lines are summarized in figure 11.

Southern blot analyses confirmed that both targeting constructs were correctly integrated into the *PKAC1* genomic locus. The first *PKAC1* WT allele was replaced by the *PKAC1* knockout construct and the second one by the mutated *Ty1-PKAC1*. One of the Southern blots is shown in figure 12.

PKAC1/2 from LS and SP cells of the mutant cell lines was then detected on a Western blot probed with anti-PKAC1/2 (Fig. 13 and B). The Ty1-epitope tagged versions of the mutant PKAC1s were also detected with anti-Ty1. It can be seen that PKAC1 from LS and SP cells have equal molecular weights in the alanine or glutamate mutant cell lines, while PKAC1 of the control cell lines (T324 and Ty1-T324) still had the ability to become phosphorylated in SS cells. Thus, the threonine 324 phosphorylation is in fact the stumpy specific phosphorylation, responsible for the observed gel mobility shift. The experiment does also provide further proof for the absence of the stumpy specific phosphorylation in PKAC2. PKAC1 from the glutamate mutant cell line runs slightly higher on SDS PAGE than unphosphorylated WT PKAC1 which is due to its additional negative charge.

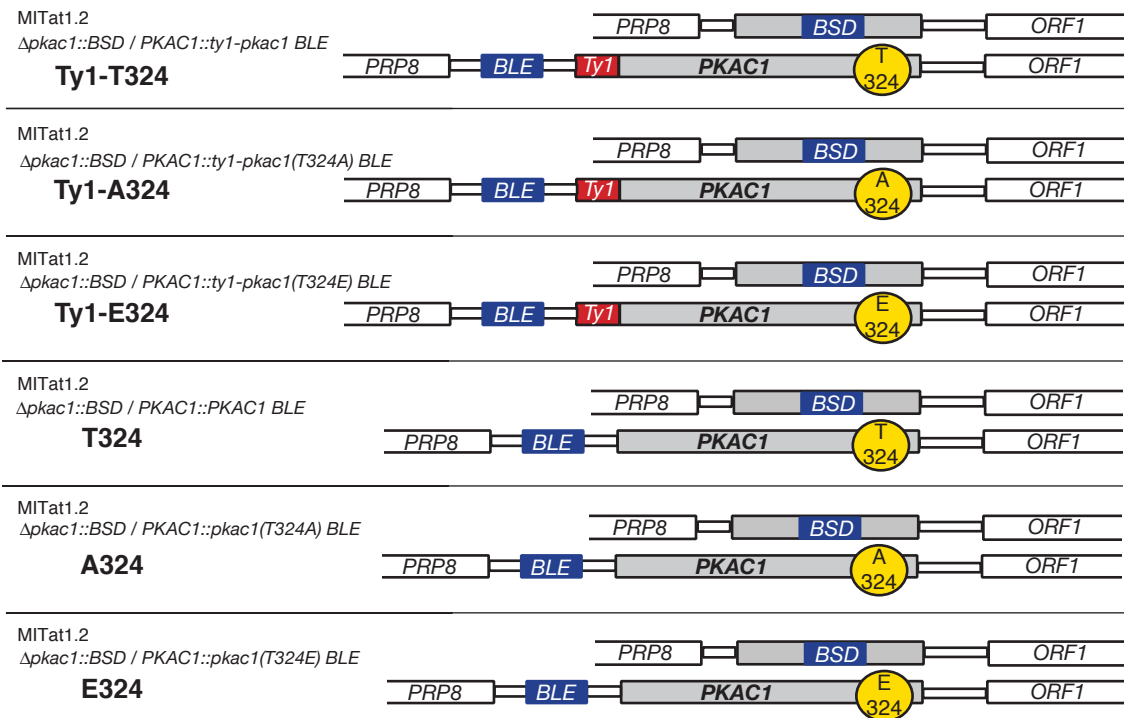


Fig. 11: Site directed mutagenesis at the stumpy specific phosphorylation site of *PKAC1*

Both alleles of the *PKAC1* genomic locus are shown as a not-to-scale drawing, indicating the positions of *PKAC1* (grey), the selection marker (blue), the Ty1-tag (red) and the site of the mutation (yellow circle). The neighboring genes of *PKAC1* (*PRP8* and *ORF1*) are shown as white boxes.

The first *PKAC1* allele was replaced by a blasticidin resistance gene (transfection with $p\Delta PKAC1 BSD$). The second *PKAC1* allele was replaced by the *PKAC1* mutants with and without Ty1-epitope tag, using the constructs $pTy1-PKAC1$, $pTy1-PKAC1-A324$, $pTy1-PKAC1-E324$, $pPKAC1-T324$, $pPKAC1-A324$ and $pPKAC1-E324$. The cell lines will further be referred to as Ty1-T324, Ty1-A324, Ty1-E324, T324, A324 and E324, as indicated in bold letters.

The *PKAC1/2* genomic locus is described in more detail in attachment 1.

3.1.1.1.6. Phenotypic analysis of the Thr324 mutant cell lines

The *PKAC1* mutant cell lines (T324->A, T324->E) were examined in more detail in order to detect potential phenotypes that are due to either the loss of the phosphorylation (T324->A) or the constitutive presence of a (phosphorylation simulating) negative charge (T324->E).

We did observe a slight reduction in growth with a population doubling time ranging from 7 to 9 hours (in comparison to 5.5-6 hours in WT cells) in all cell lines, including the control (Fig. 14A). In order to clarify whether this observed growth phenotype was due to a block in a certain cell cycle phase, both nuclei and kinetoplast were stained with the DNA dye DAPI. With this method three different cell cycle phases are distinguishable in trypanosomes: cells with one kinetoplast and one nucleus (1K1N), cells with two kinetoplasts and one nucleus (2K1N) and cells with two kinetoplasts and two nuclei

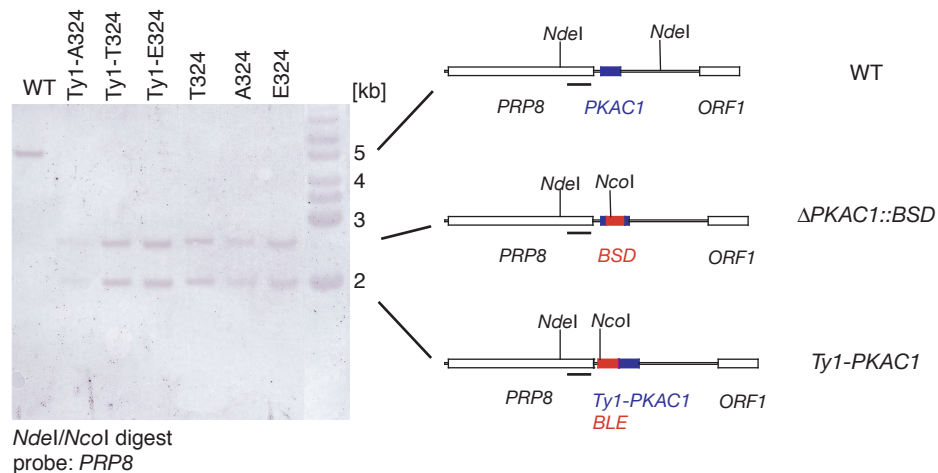


Fig. 12: All mutant cell lines have the correct genotype.

Southernblot: Genomic DNA of the mutant cell lines Ty1-T324, Ty1-A324, Ty1-E324, T324, A324 and E324 (#K6, #A1, #G2, #K2, #A3, #G2-2 respectively) was digested with *NdeI* / *NcoI*, separated on an agarose gel and transferred to a nylon membran. The blot was probed with a *PRP8* specific probe (black line) rather than with a *PKAC1/2* probe to also enable the detection of the deleted *PKAC1* allele.

Maps of the *PKAC1* genomic locus with the integrated constructs are shown for each detected fragment. The position of *PKAC1* (blue), the selection markers (red) and the *PKAC1* neighboring genes *PRP8* and *ORF1* (unfilled) are indicated. The expected sizes of the DNA fragments are 4980 bp (WT), 2516 bp (Δ *PKAC1*) and 1977 bp (*Ty1-PKAC1*, all mutants).

The genomic *PKAC1/2* locus is shown in more detail in attachment 1.

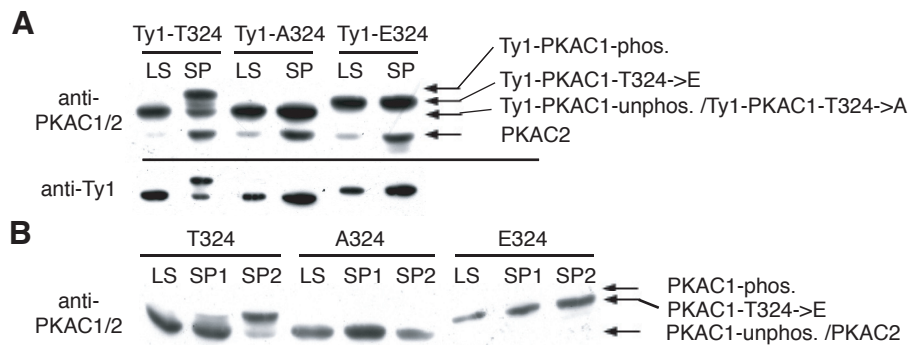


Fig. 13: The stumpy specific phosphorylation is absent in the PKA mutant cell lines A324 and E324

Western blots with protein extract of LS and SP cells (SP, SP1, SP2; SP2 cells were harvested at higher cell densities than SP1) of the cell lines Ty1-T324, Ty1-A324, Ty1-E324 (**A**) and T324, A324, E324 (**B**) were incubated with anti-PKAC1/2 and in the case of the Ty1-cell lines additionally with anti-Ty1 (after the removal of the PKAC1/2 antibodies).

A) In the cells lines that contain Ty1 epitope tagged PKAC1, PKAC1 and PKAC2 are clearly distinguishable with the PKAC1/2 antibody due to the increased molecular weight of Ty1-PKAC1. While Ty1-PKAC1 from the control cell line (Ty1-T324) still has the stumpy specific phosphorylation, it is absent from the mutant cell lines Ty1-A324 and Ty1-E324.

B) In the cell lines with untagged PKAC1, PKAC1 and PKAC2 cannot be distinguished. However, only PKAC1/2 from the control cell line (Ty1-T324) has the stumpy phosphorylation but none of the mutant cell lines. This experiment provides further proof for the absence of the stumpy specific phosphorylation in PKAC2.

(2K2N). However, in all mutant cell lines the distribution of these K/N configurations appeared approximately normal (Fig. 14B). The only exception was the presence of an unusually high percentage of cells with abnormal K/N configurations (distinct from 1K1N, 2K1N and 2K2N) found in all cell lines, including the control cell lines. Since the deletion of one *PKAC1* allele results in the reduction of PKAC1 protein, the observed phenotypes in growth probably result from gene dosage, rather than from the T324 mutations. This gene dosage phenotype of *PKAC1* is investigated in more detail in chapter 3.4.2.2.3.

The next step was to look whether kinase activation was affected in the mutant cell lines. Although no differences in kinase activity were found between PKAC1 from LS and PKAC1 from SP cells (see fig. 10 in chapter 3.1.1.1.4.), we were never able to test whether the kinase activation mechanism was dependent on the stumpy phosphorylation, since PKAC1 from both LS and SP cells is always a mixture of phosphorylated and unphosphorylated protein. With the availability of the PKAC1 mutant cell lines this problem was overcome and we therefore compared the different PKAC1 mutants in respect to their reaction on PKA activating agents. Since activation of *T. brucei* PKA-like kinase was still unsolved, both cAMP and cGMP (Shalaby *et al.*, 2001; compare also chapter 3.3) were tested for kinase activation. Kinase assays were performed with immunoprecipitated Ty1-PKAC1 from all mutant cell lines in the presence of 0.1 mM cAMP or cGMP. The amount of phosphorylated PKA substrate (kemptide) was quantified (Fig. 14C). Since the assay was not corrected for equal amounts of protein from the different cell lines, the absolute values of the activities are not comparable. None of the mutant PKAs was activated by cyclic AMP, while PKA activities were doubled in the presence of cGMP. The significance of cGMP for kinase activation will be discussed later. In this context, it is only important to stress the absence of any differences in activation between the different mutant PKAs and the WT PKA-like kinase (control).

Furthermore, the stumpy specific phosphorylation was examined for any influence on the differentiation process into procyclic cells. Therefore, SP cells of the cell lines Ty1-T324, Ty1-A324, Ty1-E324, T324, A324, E324 were *in vitro* transformed into PCFs. The success of the transformation was controlled morphologically and in addition, the growth was measured (Fig. 14D). All mutant cell lines were equally well able to transform into procyclic cells.

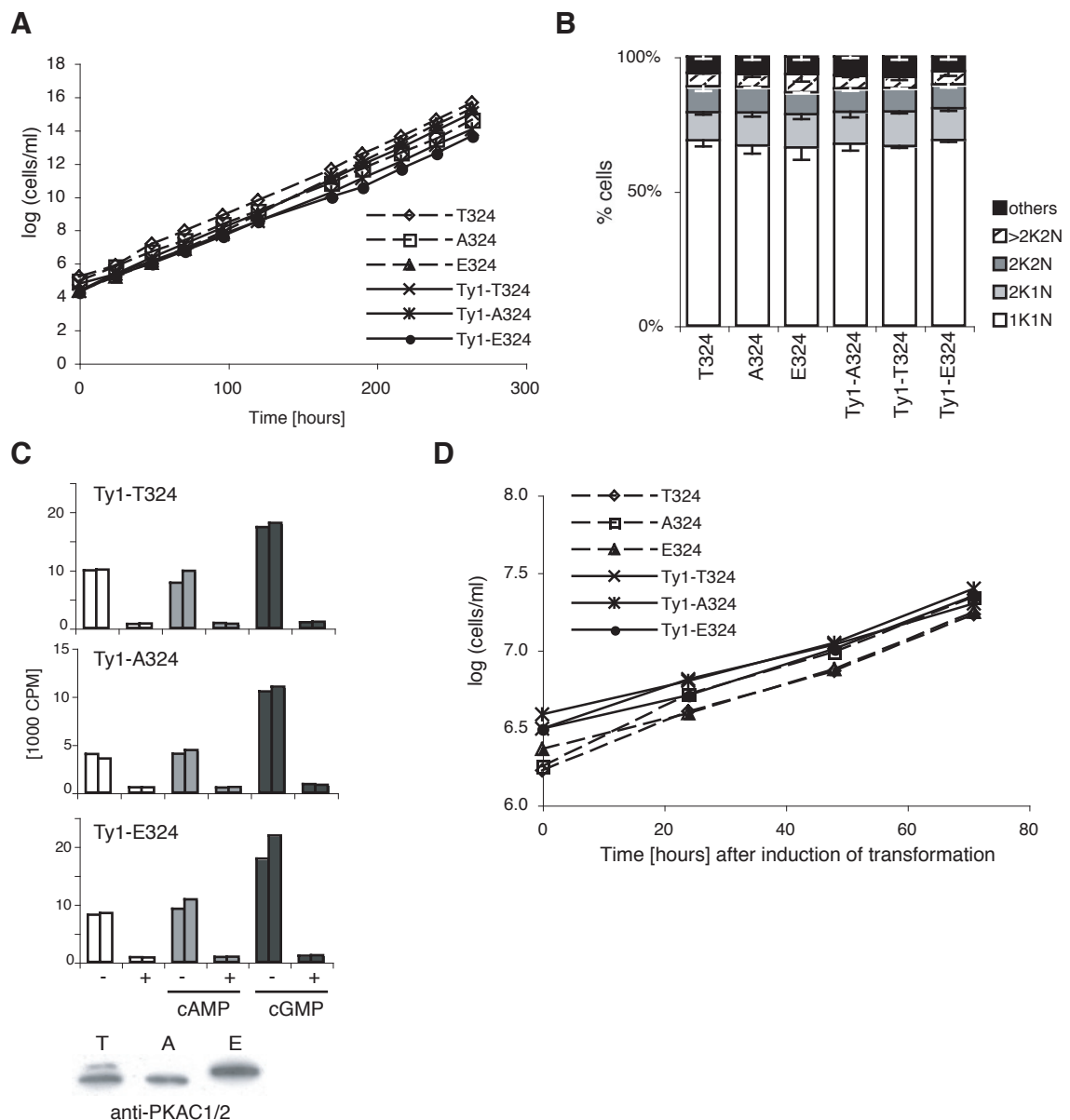


Fig. 14: Phenotypic characterization of the PKAC1 Thr324 mutant cell lines :

A) Growth: Cells of the cell lines Ty1-T324, Ty1-A324, Ty1-E324, T324, A324 and E324 were grown for 264 hours. Cell densities were measured regularly in a Neubauer chamber and cells were kept at cell densities below 8×10^5 cells/ml.

B) K/N configurations: 400 DAPI stained cells from three slides were analyzed for each cell line (T324, A324, E324, Ty1-T324, Ty1-A324, Ty1-E324). The average values of the three analyses are shown and the standard deviations are indicated as error bars.

C) PKA Activation: A kinase assay was performed with immunoprecipitated Ty1-PKAC1 of the cell lines Ty1-T324, Ty1-A324 and Ty1-E324. For activation, 0.1 mM cAMP or cGMP was added. Each assay was done twice (double bars). Note that the absolute activities of the different cell lines are not comparable since the precipitated protein amounts were not corrected. Aliquots of the immunoprecipitates were applied to a Western blot probed with anti-PKAC1/2 to control for the success of the immunoprecipitation (bottom).

D) Transformation into PCFs: The mutant cell lines T324, A324, E324, Ty1-T324, Ty1-A324 and Ty1-E324 were transformed into procyclic cells *in vitro*. The cell density was measured regularly and the cells were kept at cell densities below 1×10^7 cells/ml. In addition, the success of the transformation was controlled morphologically.

Altogether, we were unable to detect any differences between the cell lines with WT PKAC1 and the PKAC1 mutant cell lines. Thus, we did not find a function for the stumpy specific phosphorylation using this reverse genetic approach.

3.1.1.2. The PCF modification

The second PKAC1/2 modification that was identified with the gel mobility shift experiments is exclusively present in procyclic cells. The gel mobility shift is much smaller than the gel mobility shift of the stumpy specific phosphorylation. Previous experiments to determine the nature of the PCF modification failed.

The analysis of the PCF modification in this work was restricted to two questions:

The first was to find out, whether the PCF modification was present in both PKAC1 and PKAC2. It seems present in PKAC2, since PKAC2 is the dominant isoform in PCF cells with PKAC1 hardly being detected on a Western blot (compare chapter 3.1.2.). If the PCF modification would be absent from PKAC2, the gel retardation would not be detectable on a Western blot probed with anti-PKAC1/2. In order to examine whether the PCF modification is also present in PKAC1, we transformed PKAC2 knock-out cells (the cell line is described in chapter 3.4.2.2.1.) into procyclic cells. The gel mobility of PKAC1 during that transformation was monitored by a Western blot (Fig. 15A). It can be seen that PKAC1 also show the gel retardation initiating a PCF specific modification.

Secondly, the time point of the PKAC1/2 modification was determined. For this, monomorphic WT SP cells were *in vitro* transformed into procyclic cells and the gel mobility of PKAC1/2 as well as the growth of the cells was monitored (Fig. 15B). It can be seen that PKA is modified between 12 and 14 hours after the initiation of an *in vitro* transformation, exactly at the time when cells restart proliferating.

No attempt was made to map the PCF-specific phosphorylation site.

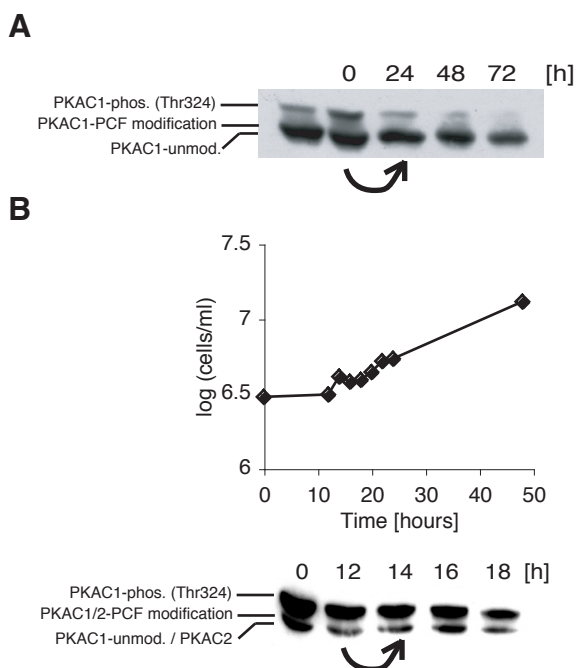


Fig. 15: The PKAC1/2 PCF modification:

A) The PCF modification is present in PKAC1

PKAC2 knock-out cells (described in chapter 3.4.2.2.1.) were *in vitro* transformed into procyclic cells. Cell samples were harvested after the times indicated and analyzed by a Western blot probed with anti-PKAC1/2. The PCF bandshift, in this cell line exclusively due to a PKAC1 modification, is marked with an arrow.

B) The PCF modification is detectable 14 hours after the initiation of transformation

MITat1.2. BSF cells were *in vitro* transformed into procyclic cells. Cells were harvested after the times indicated and PKAC1/2 was detected via a Western blot probed with anti-PKAC1/2. The PKA PCF band shift is marked with an arrow.

3.1.2. Protein expression levels of PKAC1 and PKAC2 in BSF and PCF

PKAC1 and PKAC2 differ not only in their posttranslational modification patterns but also in their life cycle stage dependent changes in mRNA steady state levels. With Northern blots it was previously shown that *PKAC1* mRNA is mainly found in BSF cells, while *PKAC2* mRNA is the abundant transcript in procyclic cells (E. Vassella, unpublished). Thus, it seems that the expression of PKAC1/2 is mainly regulated via mRNA stability, as is the case for most *T. brucei* genes. However, since protein expression in *T. brucei* is also frequently regulated on the translational and posttranslational level, the actual expression of PKAC1 and PKAC2 protein is not predictable from mRNA steady state levels.

We therefore aimed to investigate the protein expression levels of PKAC1 and PKAC2 in the different developmental stages by a Western blot. Since our antibody cannot distinguish between PKAC1 and PKAC2 and both isoforms have nearly identical molecular weights, it was necessary to artificially increase the molecular weight of one isoform. This was achieved by the replacement of one *PKAC1* allele by the (heavier) Ty1-epitope tagged *PKAC1*. The second *PKAC1* allele was silenced with the construct *pΔPKAC1BSD* (provided by P. Hassan). In this way both isoforms are easily distinguishable on a Western blot by their different mobilities, the slower form being Ty1-PKAC1 and the faster form being exclusively PKAC2. The cell line (Ty1-T324) was already available from

the functional analyses of the stumpy specific phosphorylation described above. For the analysis of the life cycle stage specific expressions, this cell line was transformed into SP cells and PCF cells.

PKAC1 and PKAC2 expression of LS, SP and PCF cells was compared via Western blot probed with anti-PKAC1/2 and anti-Ty1. In addition, the blot was incubated with anti-PFR (paraflagellar rod) to control for equal loading. (Fig. 16)

It can be seen that the total amount of PKAC1/2 remains approximately constant throughout the life cycle stages, although the expression of each isoform changes significantly. Thus, PKAC1 is the dominant PKA in BSF cells and is expressed at approximately equal levels in both LS and SP cells but is not detectable in PCF cells. PKAC2 is mainly expressed in procyclic cells, but constitutes a minor proportion of the BSF PKAC1/2 that is slightly higher in SP cells than in LS cells.

These life cycle stage specific differences in PKAC1 and PKAC2 expression correspond roughly to the results from the transcription analyses.

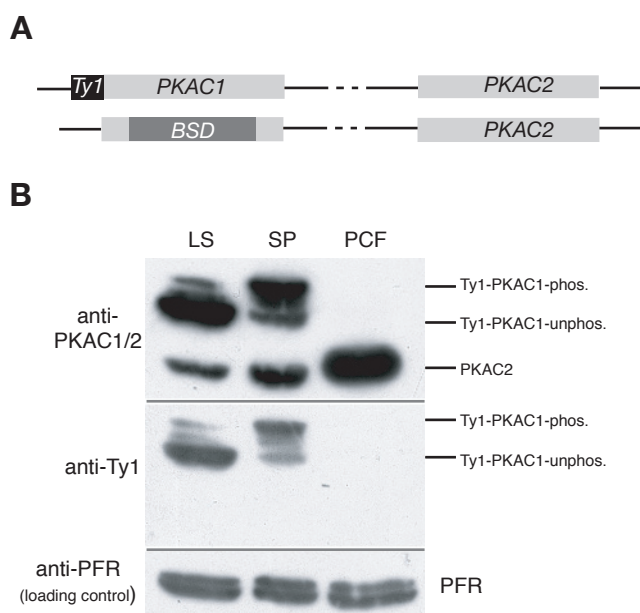


Fig. 16: Expression of PKAC1 and PKAC2 protein in the different life cycle stages of *T. brucei*.

A) Simplified genetic map of the PKAC1/2 genomic locus in the cell line Ty1-T324. Both alleles of the PKAC1/2 locus are shown. One PKAC1 allele was replaced by Ty1-PKAC1, the other by a blasticidine resistance gene using the construct pΔPKAC1BSD (P. Hassan). Both PKAC2 alleles remained unchanged. The PKAC1/2 genomic locus is shown in more detail in attachment 1.

B) Cell extracts from LS, SP and PCF cells of the monomorphic cell line Ty1-T324 (clone 6) were applied to a Western blot. Both Ty1-PKAC1 (upper bands) and PKAC2 (lower bands) were detected with anti-PKAC1/2. Additionally, Ty1-PKAC1 was detected with anti-Ty1 after the PKAC1/2 antibodies had been removed. PFR was used to control for equal loading.

3.2. Composition of the *T. brucei* PKA-like holoenzyme

PKAs from higher eukaryotes are heterotetramers consisting of two regulatory and two catalytic subunits. Whether this classical subunit composition also applies to *T. brucei* PKA-like kinase still remains unknown. Although C. Schulte zu Sodingen could show via coimmunoprecipitation studies that PKAC1/2 and PKAC3 are able to bind to the regulatory subunit (Ph.D. thesis 2000), the question of holoenzyme composition could not be solved with this approach.

To determine the subunit composition of *T. brucei* PKA-like kinase, three different approaches, all based on coimmunoprecipitation studies, have been used. The differences lie in the detection of the coprecipitated proteins.

3.2.1. Coimmunoprecipitation studies with subsequent immunoblotting

Firstly, immunoprecipitations of each subunit were coupled to detect the potentially coprecipitated subunits via a Western blot using specific antibodies. Two problems needed to be solved in advance: Firstly, a coprecipitation of the same subunit (homodimer) is not detectable with this method. Secondly, specific antibodies are only available for PKAR and PKAC3 since anti-PKAC1/2 cannot distinguish between PKAC1 and PKAC2. As a solution, each subunit of *T. brucei* PKA-like kinase was provided with an epitope tag. Epitope tagged subunits run slower on SDS gel and are easily distinguishable from WT subunits. Different epitope tags for PKAC1 and PKAC2 enable a distinction between the two.

3.2.1.1. Generation of cell lines that express epitope tagged subunits

Four different stable cell lines were needed, one for the expression of each epitope tagged subunit of *T. brucei* PKA-like kinase. Therefore, Ty1 epitope tagged versions of *PKAR*, *PKAC3*, *PKAC1* and HA epitope tagged *PKAC2* were (over)expressed either from extragenic sites (*PKAR*, *PKAC3*) or by gene replacement of one WT allele (*PKAC1* and *PKAC2*). All cell lines and constructs are summarized in table 2. Note that in each cell line all four WT subunits are present along with one epitope tagged subunit.

At first, the expression of the different epitope tagged proteins was controlled. For this, Western blots were stained with subunit specific antibodies (red) and the epitope tag antibody (green) (Fig. 17A).

subunit	Name of the cell line	Clone	Construct	Epitope tag	Expression
C1	Ty1-PKAC1	#1	pTy1-PKAC1	Ty1	gene replacement
C2	HA-PKAC2	#S2	pHA-PKAC2	HA	gene replacement
C3	Ty1-PKAC3	pool	pTSArib Ty1-PKAC3	Ty1	overexpression (rDNA locus)
R	Ty1-PKAR (C. Schulte zu Sodingen)	#C2	pLew82 Ty1-PKAR	Ty1	overexpression (rDNA locus)

Table 2: Overview about the cell lines with the epitope tagged subunits of *T. brucei* PKA-like kinase.

Name and clone number is indicated for each cell line together with the name of the construct used for transfection. pTSArib integrates into the ribosomal promoter region (Xong *et al.*, 1998). pLew82 integrates into the non transcribed ribosomal spacer region. Expression is driven by the T7 promoter. (Wirtz *et al.*, 1999) The Ty1-PKAR cell line was already available (C. Schulte zu Sodingen, Ph.D. thesis 2000).

Yellow bands result from color blending and represent the epitope tagged PKA-like subunits (red and green). It can be seen that all epitope tagged proteins are actually expressed (yellow bands). As expected, in the gene replacement cell lines (Ty1-PKAC1 and HA-PKAC2) the expression levels of the epitope tagged and WT subunits were approximately equal. They are easily distinguishable due to the gel mobility shift caused by the epitope tag. However, in the overexpression cell lines (Ty1-PKAC3 and Ty1-PKAR) the amount of epitope tagged subunit was higher than the amount of WT subunit. This complicated the detection of the corresponding WT subunit. In comparison to WT cells, PKAC3 expression was 10 times higher in the Ty1-PKAC3 cells and upon tetracycline induction Ty1-PKAR expression was 2.5 times higher (Fig. 17B). However, the overexpression cell lines are nevertheless suitable for the subsequent coimmunoprecipitation studies, since the interaction between two subunits is always confirmed ‘from both sites’ with two independent precipitations. Any influence of the unnaturally high expression levels of Ty1-PKAR and Ty1-PKAC3 on the result of the coimmunoprecipitation experiment will thus be noticed.

3.2.1.2. Catalytic subunits are only coprecipitated with the regulatory PKA subunit but not with another catalytic subunit

The different epitope tagged subunits from the cell lines described above were immunoprecipitated with anti-Ty1 or anti-HA protein G sepharose beads. The precipitates were applied to four Western blots, each containing samples of each immunoprecipitation. The Western blots were probed with the three different PKA antibodies (red) and additionally with the epitope tag antibodies (green) (Fig. 18). It can be seen that PKAR is

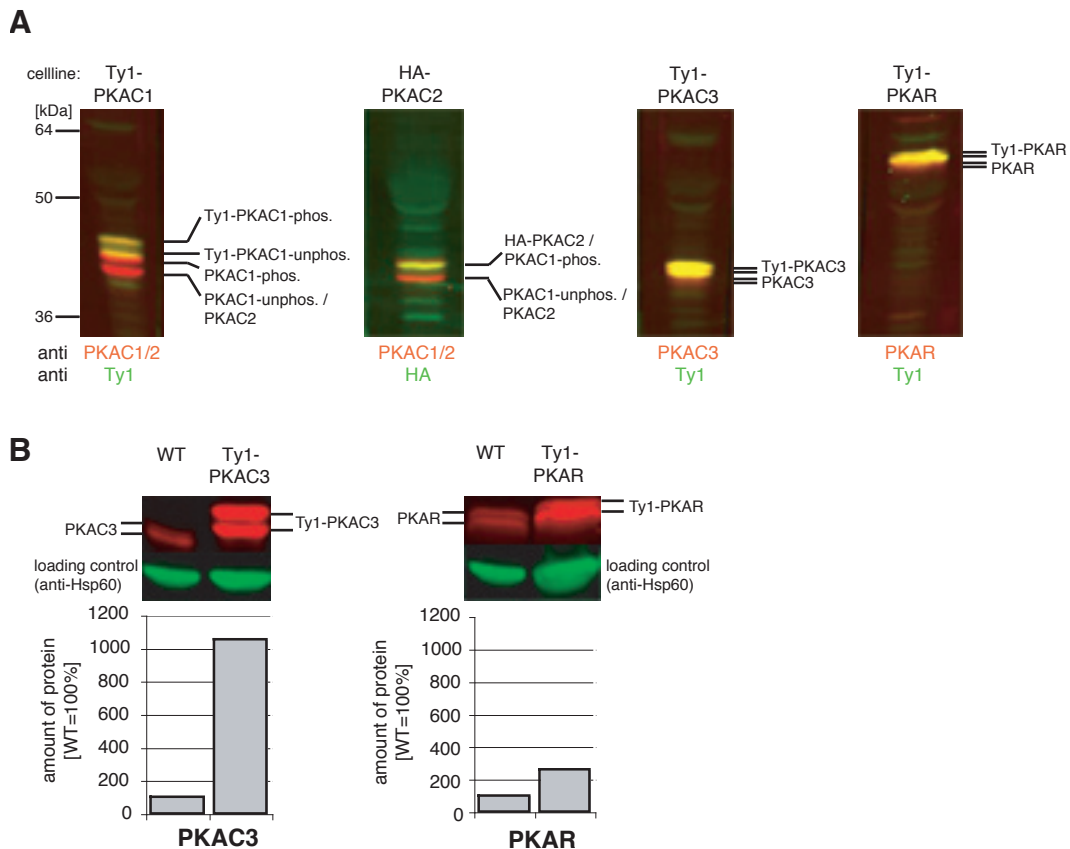


Fig. 17: Expression of the epitope tagged subunits Ty1-PKAC1, HA-PKAC2, Ty1-PKAC3 and Ty1-PKAR.

A) Detection of the epitope tagged subunits of *T. brucei* PKA-like kinase on a Western blot

The expression of the epitope tagged proteins from the cell lines Ty1-PKAC1, HA-PKAC2, Ty1-PKAC3 and Ty1-PKAR was controlled on a Western blot. For this, cell extract from 5×10^6 cells of each cell line was applied to SDS PAGE and the resulting Western blot was incubated with the different PKA antibodies (anti-PKAC1/2, anti-PKAC3, anti-PKAR). In addition, each Western blot was also incubated with anti-Ty1 or anti-HA antibody, as indicated. Rabbit Alexa680 (red) was used for the detection of the PKA antibodies while MouseIRDye800 (green) was used as secondary antibody for the detection of anti-Ty1 and anti-HA. Proteins that are recognized by both antibodies appear yellow.

It can be seen that each epitope tagged subunit is expressed (yellow bands).

B) Expression levels of Ty1-PKAC3 and Ty1-PKAR in comparison to WT cells

Cell lysates from 5×10^6 cells of the Ty1-PKAC3 and Ty1-PKAR cell lines and of WT cells were applied to SDS PAGE and the resulting Western blot was probed with anti-PKAC3 or anti-PKAR and additionally with anti-Hsp60 that served as loading control. The PKA antibodies were detected with Rabbit Alexa680 (red). The Hsp60 antibody was detected with MouseIRDye800 (green). The amount of PKAR and PKAC3 in the overexpression cell lines and in WT cells was quantified using the Odyssey Software (Licor) and is shown in the diagram below (WT=100%). The data were corrected for unequal loading using Hsp60.

Note that both PKAC3 and PKAR are always detected as double bands on Western blots. This is probably due to posttranslational modifications that have not been examined further in this work.

the only subunit that was coprecipitated with Ty1-PKAC1, HA-PKAC2 and Ty1-PKAC3. None of the catalytic subunits were found to coprecipitate with any of the other catalytic subunits or the same (untagged) catalytic subunit. Ty1-PKAR coprecipitates all three catalytic subunits as seen previously. There is no evidence that Ty1-PKAR coprecipitates

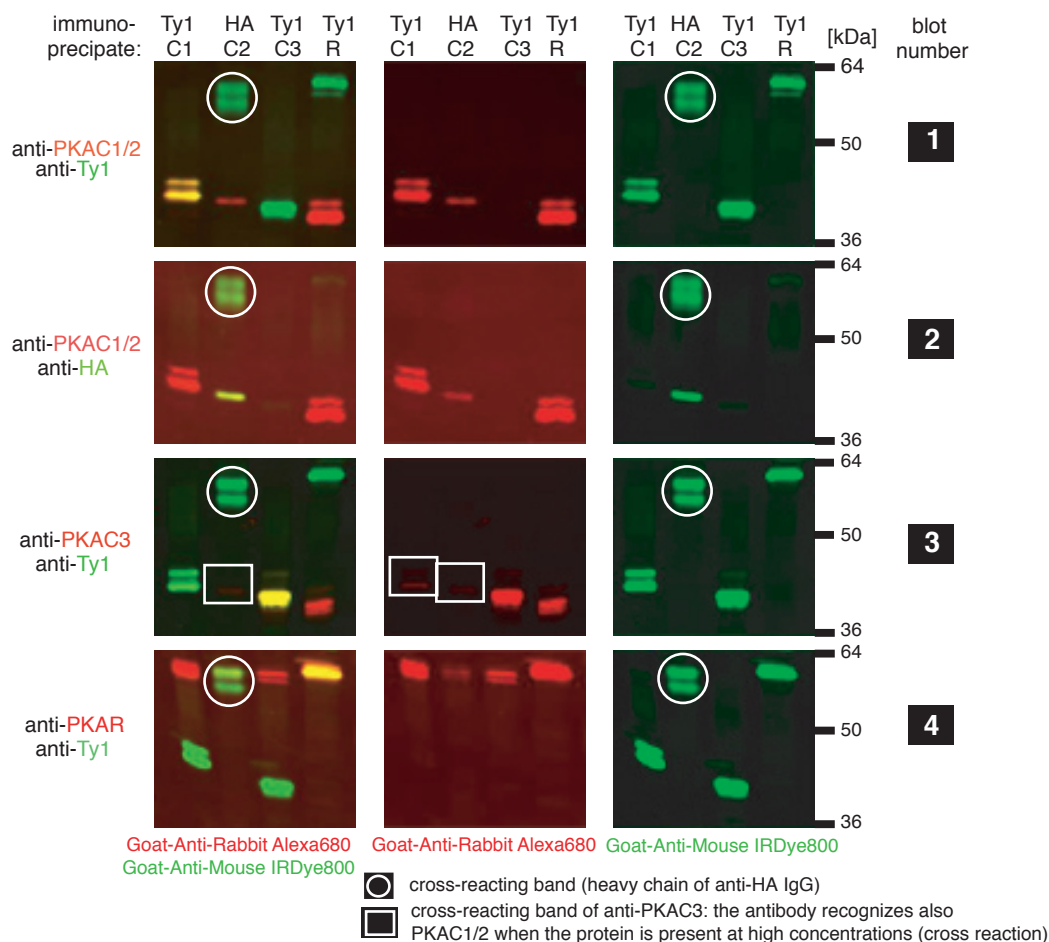


Fig. 18: Coimmunoprecipitation studies with the different epitope tagged subunits

The interactions between the different subunits of *T. brucei* PKA-like kinase were examined using coimmunoprecipitation studies. For this, Ty1-PKAC1, HA-PKAC2, Ty1-PKAC3 and Ty1-PKAR were immunoprecipitated with the epitope tag antibodies anti-Ty1 or anti-HA (4 different precipitations). The precipitates were run on four SDS gels, each precipitate was loaded to each gel. The gels were blotted, and each blot was probed with a different PKA antibody together with the respective anti-tag antibody anti-Ty1 or anti-HA, as indicated. Anti-rabbit Alexa680 (red) was used as secondary antibody for the PKA antibodies while MouseIRDye800 (green) was used as secondary antibody for anti-Ty1 and anti-HA. Note that the HA antibody recognizes one unspecific band at around 50 kDa (white circle). Also, anti-PKAC3 recognizes PKAC1/2 (cross reaction), although to a much lower extent than it recognizes PKAC3 (white square).

Each Western blot is shown three times. On the left side it is shown with both secondary antibodies. PKA that is recognized by both antibodies appears yellow. In the center the same blots are shown with the PKA antibodies only (red) and on the right side with the epitope tag-antibodies only (green).

The first lane of each blot contains immunoprecipitate of the Ty1-PKAC1 cell line. Ty1-PKAC1 was detected with anti-PKAC1/2 (blot 1 and 2) and anti-Ty1 (blot 1,3,4) as expected. The only coprecipitated PKA subunit was PKAR (red band on blot 4). Coprecipitation of WT PKAC1/2 can be excluded since WT PKAC1/2 would have been detectable as a red band in blot 1 with lower molecular weight than Ty1-PKAC1. Furthermore, coprecipitation of PKAC3 is also excluded, since PKAC3 would have been detectable on blot 3. The second lane of each blot contains immunoprecipitate of the HA-PKAC2 cell line. HA-PKAC2 was detected with anti-PKAC1/2 (blot 1 and 2) and anti-HA (blot 2), as expected. Again, the only coprecipitated PKA subunit was PKAR (blot 4). It has the same size than the (stronger) unspecific band of the HA-antibody and is therefore best visible in the absence of that band (center row). Neither WT PKAC1/2 nor PKAC3 were coprecipitated. The third lane of each blot contains immunoprecipitate from the Ty1-PKAC3 cell line. As expected, Ty1-PKAC3 was detected with anti-PKAC3 (blot 3) and anti-Ty1 (blot 1,2,4). Again, only PKAR (blot 4) but none of the other PKA subunits is coprecipitated with Ty1-PKAC3. The fourth lane contains immunoprecipitate of the Ty1-PKAR cell line. Ty1-PKAR was detected with anti-PKAR (blot 4) and anti-Ty1 (blot 1,3,4). PKAC1/2 (blot 1,2) and PKAC3 (blot3) were coprecipitated with Ty1-PKAR.

the WT regulatory subunit, although this cannot be excluded, since Ty1-PKAR is difficult to distinguish from untagged PKAR due to a very slight change in gel mobility.

These results implicate that the *T. brucei* PKA-like holoenzyme is a dimer that consists of one regulatory and one of three catalytic subunits (C₁R₁). It therefore differs from the classical tetrameric PKA subunit composition (C₂R₂).

3.2.2. No further coimmunoprecipitated PKAR subunits were detectable on a Coomassie stained gel

Genes for several putative cNMP binding proteins have in the meantime been found in the *T. brucei* genome database (see also chapter 3.5.1.). Some of these might potentially be additional interacting regulatory subunits.

Therefore, the coimmunoprecipitation experiment was repeated with the Ty1-PKAC1 cell line as described above with the exception that the coprecipitated proteins were detected with the protein dye Coomassie Blue, rather than with PKA specific antibodies. To enable the distinction between unspecific coprecipitated proteins and proteins that bind to Ty1-PKAC1, a control immunoprecipitation was performed with WT cells. 3*10⁸ cells were used for each immunoprecipitation. The Coomassie stained gel with the immunoprecipitates of WT and Ty1-PKAC1 cells is shown in figure 19. As expected, both Ty1-PKAC1 and PKAR were precipitated from Ty1-PKAC1 cells, but not from WT cells. However, no additional proteins selectively coprecipitated with Ty1-PKAC1.

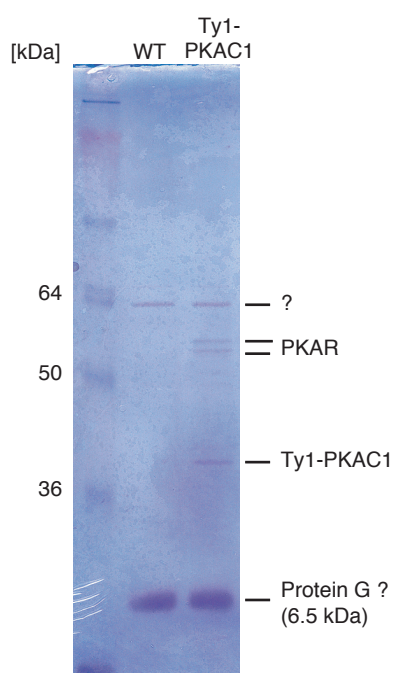


Fig. 19: Detection of coprecipitated proteins of Ty1-PKAC1 on a Coomassie stained gel

Ty1-PKAC1 was immunoprecipitated from 3*10⁸ WT cells (control) and 3*10⁸ Ty1-PKAC1 cells with anti-Ty1-protein G sepharose beads. The protein containing beads were heated in Laemmli buffer and applied to SDS page. The gel was stained with Coomassie Blue. It can be seen that Ty1-PKAC1 and (coprecipitated) PKAR were present in the immunoprecipitate from the Ty1-PKAC1 cell line, but absent from the immunoprecipitate of WT cell, as expected.

In addition, two other proteins were detected in the immunoprecipitates. However, since these proteins were present in the immunoprecipitate of both WT cells and Ty1-PKAC1 cells, they are either unspecifically precipitated or protein components of the anti-Ty1-protein G sepharose. The smaller protein might be identical to Protein G (6.5 kDa).

Two proteins were detected in both the WT and Ty1-PKAC1 precipitate. They can therefore be attributed to proteins that are either unspecifically coprecipitated or to proteins that origin from the Ty1-protein G sepharose beads (e.g. protein G).

Thus, no further PKAC1 binding partners were detected with that method.

3.2.3. No kinase activity was coprecipitated with an inactive PKAC1 (dead mutant)

In order to ensure that no further (yet unknown) catalytic subunits were coprecipitated, we made one additional experiment that was based on the detection of (potential) coprecipitated kinase activity, rather than on the detection of the protein itself. For this, a cell line was produced that had one WT *PKAC1* allele replaced by a dead mutant PKAC1. Dead mutant PKAC1 is catalytically inactive due to an amino acid substitution (N165->A) in its catalytic center. The dead mutant PKAC1 was additionally provided with an Ty1-epitope tag to enable immunoprecipitation. If *T. brucei* PKA-like kinase is a dimer, as suggested from the experiments above, no kinase activity should be coprecipitated.

Ty1-PKAC1-dead from three independent clones of the cell line Ty1-PKAC1-dead (#11, 12, 14) was immunoprecipitated with anti-Ty1. As a positive control, (active) Ty1-PKAC1 from two independent clones (#1,2) of the Ty1-PKAC1 cell line was also precipitated. The immunoprecipitates were assayed for their ability to phosphorylate the PKA specific substrat kemptide, as described earlier. The amount of phosphorylated kemptide was quantified as a measure of kinase activity (Fig. 20).

No activity was precipitated with any of the dead mutant PKAC1 clones, although the immunoprecipitation was successfull (Western blot). In contrast, the positive control, Ty1-PKAC1, showed significant activity that could be inhibited with the PKA specific inhibitor PKI. Conclusively, no additional catalytic subunit or contaminating kinase was coprecipitated with Ty1-PKAC1.

Taken together, all three coimmunoprecipitation experiments revealed that *T. brucei* PKA-like kinase is a dimer consisting of one regulatory subunit and one out of three catalytic subunit isoforms. No evidence for additional interacting proteins or kinase activities was obtained.

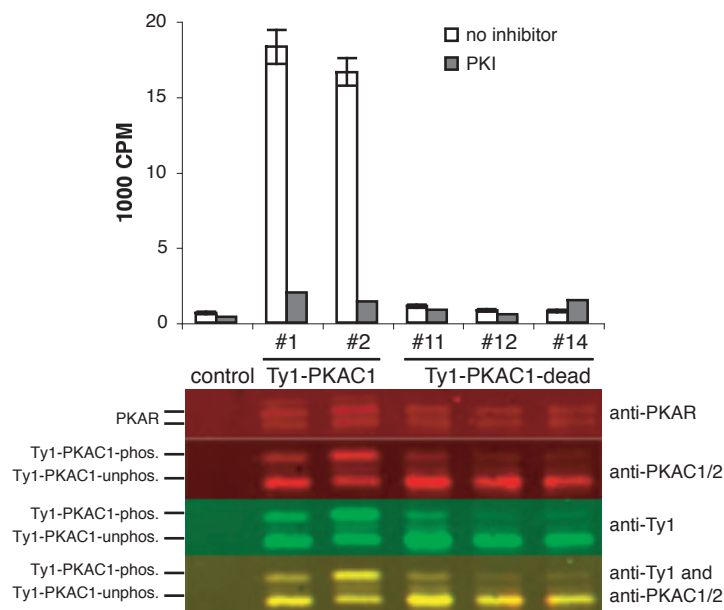


Fig. 20: No kinase activity is coprecipitated with PKAC1 dead mutants:

Ty1-PKAC1-dead from three independent clonal cell lines (#11,12,14) and Ty1-PKAC1 from two independent clonal cell lines (#1,2; positive control) was immunoprecipitated with anti-Ty1 protein G sepharose beads. To control for the specificity of the precipitation, an additional immunoprecipitation was performed using WT cells (control). Equal amounts of the precipitates were assayed for kinase activity as described in 2.2.3.9.. Each reaction was done three times and in addition once in the presence of the PKA specific inhibitor PKI (Kemp *et al.*, 1991). The graphic (top) shows the kinase activities (in 1000 CPM) for each clone. Mean values of the three reactions are shown and the standard deviations are indicated by error bars.

Parts of the immunoprecipitates were used for Western blotting (bottom) to control for the success of the precipitation and to ensure that equal amounts of the proteins were used for the kinase assays. PKAC1 was detected with anti-PKAC1/2 and anti-Ty1. Coimmunoprecipitated PKAR was detected with anti-PKAR. The secondary antibodies Rabbit Alexa680 (red) and MouseIRDye800 (green) were used for the detection of anti-PKAC1 / anti-PKAR and anti-Ty1, respectively.

It can be seen that no kinase activity is coprecipitated with the dead mutant of PKAC1.

3.3. Activation of *T. brucei* PKA-like kinase

3.3.1. cGMP, not cAMP causes *in vitro* dissociation of the holoenzyme

The dissociation of the holoenzyme of PKA-like kinase by cyclic nucleotides was studied using the following *in vitro* assay: The holoenzyme complex of catalytic and regulatory subunit was immunoprecipitated via Ty1-PKAC1 and remained coupled to the protein G sepharose beads. Upon addition of cAMP or cGMP, release of PKAR into the supernatant was monitored. All reactions were performed in the presence of PKI 5-24, a PKA specific peptide inhibitor that binds to the catalytic center of all characterized PKAs (Kemp *et al.*, 1991). This way the reassociation of the holoenzyme complex was prevented with the aim to drive the reaction towards holoenzyme dissociation. After 60 minutes of incubation at 30 °C, beads and supernatant were separated by filtration and the amount of PKAC1 and PKAR in each fraction was analyzed by a Western blot (Fig. 21).

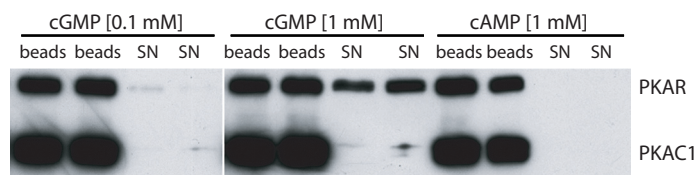


Fig. 21: The holoenzyme of PKA-like kinase partially dissociates in the presence of mM concentrations of cGMP, but not of cAMP.

Holoenzyme of PKA-like kinase was coupled to anti-Ty1 protein G sepharose beads via the Ty1-PKAC1 subunit. The beads were incubated with cAMP [1 mM] or cGMP ([0.1 mM] and [1 mM]) in the presence of PKI [5 μ M] for 60 minutes at 30°C on a shaker. Each reaction was performed in duplicates.

In case of holoenzyme dissociation, PKAR would be released from the beads into the supernatant. The supernatant was separated from the beads by filtration. Ty1-PKAC1 and PKAR coupled to the beads (beads) and free PKAR released into the supernatant (SN) were detected via a Western blot probed with anti-PKAC1/2 and anti-PKAR. It can be seen that both Ty1-PKAC1 and PKAR are always detected in the beads fraction. A partial release of the regulatory subunit into the supernatant was only observed in the presence of 1 mM cGMP, but not with cAMP. Note that the film was overexposed on purpose to stress the absence of any PKAR in the supernatant without cAMP.

Upon incubation with cAMP, both PKAC1 and PKAR were detected in the “beads fraction” but completely absent from the supernatant, thus, cAMP was unable to dissociate the PKA-like kinase holoenzyme. These results were consistent with the inability of cAMP to activate PKA-like kinase as observed previously (Schulte zu Sodingen, Ph.D. thesis 2000). In contrast, incubation with >0.1 mM cGMP led to the partial release of PKAR into the supernatant. No holoenzyme dissociation was detected in the absence of PKI (data not shown).

3.3.2. cGMP, but not cAMP can activate PKA-like kinase *in vitro*

The holoenzyme dissociation experiments described above already implicate that the activation of *T. brucei* PKA-like kinase differs from the classical PKA activation mechanism that involves cAMP.

Therefore, the influence of both cAMP and cGMP on the activity of PKA-like kinase was tested. In addition the effects of the lipophilic derivatives pCPT-cAMP and pCPT-cGMP on kinase activity were examined in order to enable a comparison of these *in vitro* data with subsequent *in vivo* experiments. The holoenzyme of PKA-like kinase was purified by immunoprecipitation via Ty1-PKAC1. Equal amounts of the immunoprecipitate were incubated with the different cyclic nucleotides at different concentrations and tested for their ability to phosphorylate the PKA substrate RRRRSIIFI¹⁾ with γ^{32} P-ATP. As a control for the specificity of the measured activity we used catalytically inactive PKAC1 dead mutant (N165->A) (described in chapter 3.2.3.).

As can be seen in figure 22A, an increase in kinase activity was only detected in the presence of cGMP or pCPT-cGMP, but not with cAMP or its derivatives. Kinase activity was found to increase 5 fold in the presence of 1 mM cGMP and 1.5 fold in the presence of 0.1 mM cGMP. Interestingly, 10 times more pCPT-cGMP was needed to give the same activating effect as cGMP.

We next examined whether there were any differences in activation between the holoenzymes isoforms RC1, RC2 and RC3. Therefore, kinase assays were performed with activity precipitated via HA-PKAC2, Ty1-PKAR or Ty1-PKAC3 (Fig. 22B-D).

None of the holoenzyme isoforms was activated by cAMP. When the holoenzyme was precipitated via HA-PKAC2 or Ty1-PKAR a five fold activation was achieved with 1 mM cGMP and an 1.5 to 2 fold activation was observed with 0.1 mM cGMP. These results are consistent with the activation of the holoenzyme observed after precipitation with Ty1-PKAC1. In contrast, Ty1-PKAC3 precipitated holoenzyme was not activated by cGMP. It should be noted that Ty1-PKAC3 has a ten times higher expression level than PKAC3 in WT cells (see Fig. 17B in chapter 3.2.1.1.). It is therefore possible that only a fraction of PKAC3 is bound to the regulatory subunit. Most of the enzyme might be already active and hence no activation results from addition of cyclic GMP.

1) RRRRSIIFI is a small peptide that was identified as the best PKA substrate with the aid of an oriented peptide library (Songyang *et al.*, 1994). For *T. brucei* PKA-like kinase it works equally well as the classical PKA peptide substrate kemptide (LRRASLG) (data not shown).

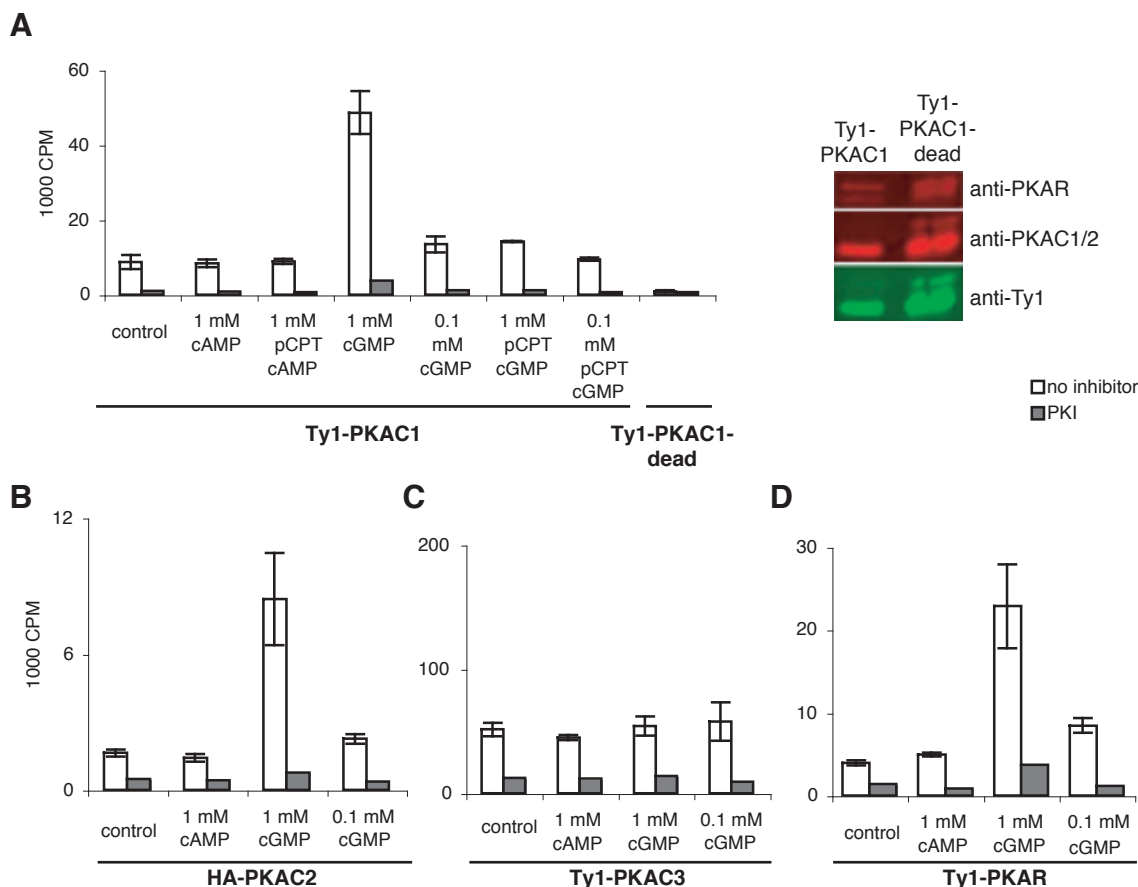


Fig 22: PKA-like kinase is activated with cGMP and pCPT-cGMP, but not with cAMP

Holoenzyme of *T. brucei* PKA-like kinase was immunoprecipitated via Ty1-PKAC1 (A), HA-PKAC2 (B), Ty1-PKAC3 (C) or Ty1-PKAR (D). The immunoprecipitated PKA-like kinases were tested on their abilities to phosphorylate the PKA specific substrate RRRRSIIIFI (Songyang *et al.*, 1994) with $\gamma^{32}\text{P}$ -ATP in the absence (control) and presence of different cyclic nucleotides or cyclic nucleotide derivatives. The amount of phosphorylated PKA substrate was quantified with a liquid scintillation counter as a measure of kinase activity. Each reaction was done in triplicates. Average values are shown (white bars) and the standard deviation is indicated by error bars. Additionally, each reaction was done once in the presence of the PKA specific inhibitor PKI (grey bars).

For experiment A) two additional controls were performed:

First, the specificity of the measured activity was controlled using an inactive mutant kinase (Ty1-PKAC1-dead). It can be seen that no contaminating kinase activity was coprecipitated with the dead mutant Ty1-PKAC1. Secondly, the success of the immunoprecipitations was controlled on a Western blot with samples of the immunoprecipitates. The Western blot was probed with anti-PKAC1/2, anti-PKAR and anti-Ty1, using anti-rabbit Alexa680 (red) and anti-MouseIRDye800 (green) as secondary antibodies. It can be seen that both immunoprecipitations were successful. PKAR was coprecipitated with Ty1-PKAC1 and Ty1-PKAC1-dead.

3.3.3. *T. brucei* PKA-like kinase is not activated by cXMP, cIMP, cUMP or cCMP

The cGMP concentration necessary for activation of the *T. brucei* PKA-like kinase of 1 mM is between 1 to 3 orders of magnitudes higher than cGMP concentrations needed to activate cGMP dependent kinases (PKGs) in other organisms (compare table 8 in 4.1.2.1.). Furthermore, neither guanylyl cyclases nor cGMP specific phosphodiesterases

have yet been described in trypanosomes and it is still unclear whether cGMP is present at all. Therefore, it remains doubtful whether cGMP is in fact the physiological PKA activator in *T. brucei*. Alternatively, PKA-like kinase could be activated by other cyclic nucleotides that are distinct from both cAMP and cGMP. One might expect the activating cyclic nucleotide to be structurally more similar to cGMP than to cAMP. We therefore tested the purine based cyclic nucleotides cyclic Xanthosine monophosphate (cXMP) and cyclic Inosine monophosphate (cIMP) for their abilities to activate PKA-like kinase. Both, cXMP and cIMP differ only at position C2 of the guanine nucleobase from cGMP. In addition, we tested two pyrimidine based cyclic nucleotides (cUMP and cCMP). (Fig. 23A) The results of the kinase assay are shown in figure 23B. It can be seen that none of the tested cyclic nucleotides was able to activate *T. brucei* PKA-like kinase, although there was a very slight increase in kinase activity after incubation with the purine based cyclic nucleotides cIMP and cXMP. Thus, none of the tested cyclic nucleotides was any better than cGMP.

3.3.4. Detection of *in vivo* kinase activity with the PKA reporter substrate VASP

The unusually high cGMP concentrations needed for kinase activation could also be an artefact of the *in vitro* conditions of the kinase assay. Activation might depend on conditions, cofactors or on a specific intracellular localization not available *in vitro*. An *in vivo* approach was therefore chosen to further investigate the kinase activation.

3.3.4.1. Transgenic expression of the PKA reporter substrate VASP in *T. brucei*

The mammalian vasodilator-stimulated phosphoprotein (VASP) plays an important role in actin filament assembly and cell motility in a variety of organisms and cell types (Krause *et al.*, 2003). In addition, it is a substrate for PKA and PKG making it a useful reporter for cyclic nucleotide signaling (Smolenski *et al.*, 1998; Aktas *et al.*, 2003; Hou *et al.*, 2003; Deguchi *et al.*, 2002 and others). VASP has three phosphorylation sites that are specific for either PKA or PKG. In this context only the PKA specific phosphorylation site at Ser157 is of interest. Phosphorylation at this site results in an apparent shift of molecular mass from 46 to 50 kDa (Smolenski *et al.*, 1998) and can thus be detected on a Western blot. We aimed to use VASP as a reporter substrate to analyze *in vivo* PKA activity in *T. brucei*. Since trypanosomes have no genes that are homologous to VASP, it was

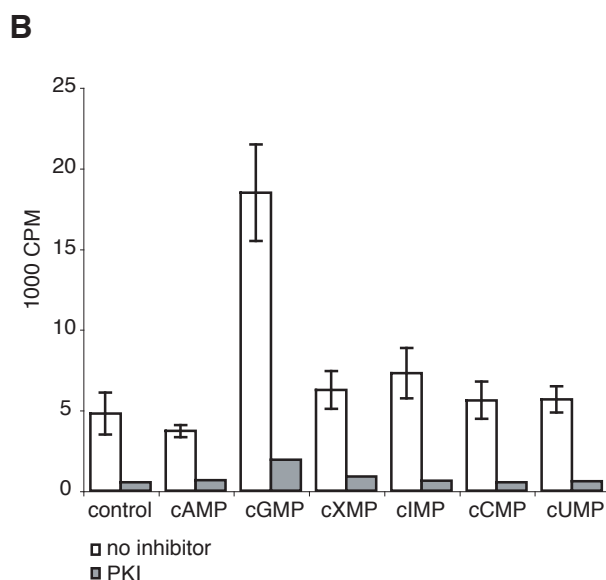
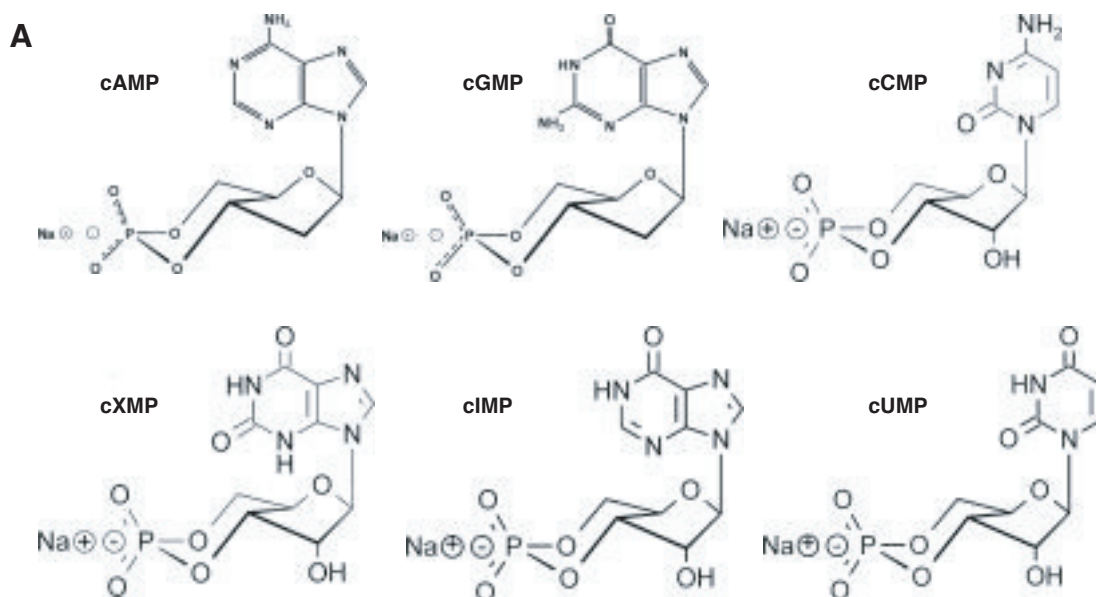


Fig 23: PKA-like kinase is not activated with cXMP, cIMP, cCMP or cUMP.

A) Structures of the different cyclic nucleotides that were tested on their ability to activate *T. brucei* PKA-like kinase (pictures taken from www.biolog.de).

B) Kinase assay: The holoenzyme of PKA-like kinase was immunopurified via Ty1-PKAC1. Equal amounts of the immunoprecipitate were tested on their ability to phosphorylate the PKA specific substrate RRRRSIIFI (Songyang *et al.*, 1994) with ³²P-ATP in the absence (control) and presence of different cyclic nucleotides (1 mM), as indicated. The amount of phosphorylated PKA substrate was quantified with a liquid scintillation counter and directly reflects kinase activity. Each reaction was done in triplicate. Mean values are shown (white bars) and the standard deviation is indicated by error bars. Additionally each reaction was done once in the presence of the PKA specific inhibitor PKI (grey bars).

necessary to express *VASP* transgenically. For this, *VASP* cDNA from human HL-60 cells (Haffner *et al.*, 1995; kindly provided by the laboratory of Ulrich Walter, Würzburg) was cloned into the overexpression vector pTSArib (Xong *et al.*, 1998) and transfected into trypanosomes (MITat1.2). Only one hygromycin resistant clone was obtained showing a slight growth phenotype. Cells adapted to normal growth after one week in culture. The expression of *VASP* was controlled by a Western blot. *VASP* from 5*10⁵ cells was easily detectable with the polyclonal antibody AB19728 (kind gift from Thomas Renné and Ulrich Walter, Würzburg; Halbrügge *et al.*, 1990) (Fig. 24) and equally well with anti-*VASP* M4 (Immunoglobulin) (data not shown). Two *VASP* bands could be distinguished

by their different apparent molecular weight representing phosphorylated (50 kDa) and unphosphorylated VASP (46 kDa). Thus, VASP is in fact phosphorylated by a *T. brucei* kinase with a PKA-like substrate specificity.

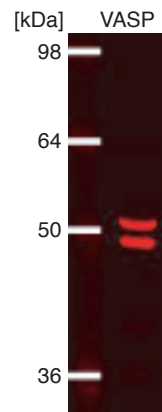


Fig. 24: Western blot: Detection of the transgenically expressed PKA reporter substrate VASP in *T. brucei*
 VASP cDNA from human HL60-cells (Haffner *et al.*, 1995) was cloned into the overexpression vector pTSArif (Xong *et al.*, 1998) and the resulting plasmid (pTSArifVASP) was transfected into MITat1.2 cells. One hygromycine resistant clone was obtained that was controlled for VASP expression on a Western blot with the polyclonal antibody AB197228 (kind gift from Ulrich Walter, Würzburg), using cell extract of $5 \cdot 10^5$ cells. The antibody recognized two bands of approximately 46 and 50 kDa. These bands represent the phosphorylated and unphosphorylated VASP form (at Ser157). No further proteins were detected with the VASP antibody.

We did, however, observe differences in the extent of basal VASP phosphorylation between different experiments. The reason remained unclear until it became apparent that temperature influences VASP phosphorylation (compare chapter 3.4.1.2.). The variations in basal VASP phosphorylation between the different experiments described in this chapter can thus be attributed to slightly different cell harvesting procedures. However, the samples of one assay were always treated equally and conclusions were only drawn from comparisons among different samples of the same assay.

3.3.4.2. VASP phosphorylation increases in the presence of the PDE inhibitors dipyridamole and etazolate

At first it was tested whether changes in VASP phosphorylation were detectable with the new reporter cell line. To test for activation by cyclic nucleotides of the VASP phosphorylating kinase, we used the PDE inhibitors dipyridamole and etazolate. Both are inhibitors of all known *T. brucei* PDEs (Rascón *et al.*, 2002; Zoraghi *et al.*, 2001; Kunz *et al.*, 2004; Zoraghi *et al.*, 2002) that were shown to increase intracellular cAMP and possibly cGMP.

Cells of the VASP expressing cell line were incubated in the presence of 100 μ M dipyridamole (dissolved in DMSO at 200 mM) or etazolate (dissolved in PBS at 5 mM) and as a control with equal concentrations of the respective solvents. Samples of the cells were harvested after 0, 1, 2, 5 and 10 minutes and applied to a Western blot,

subsequently probed with anti-VASP M4 (Fig. 25A). VASP phosphorylation at Ser157 was monitored via the gel retardation of the phosphorylated VASP form (band shift), using the Odyssey Software (Licor) for the quantification of the protein bands (Fig. 25B).

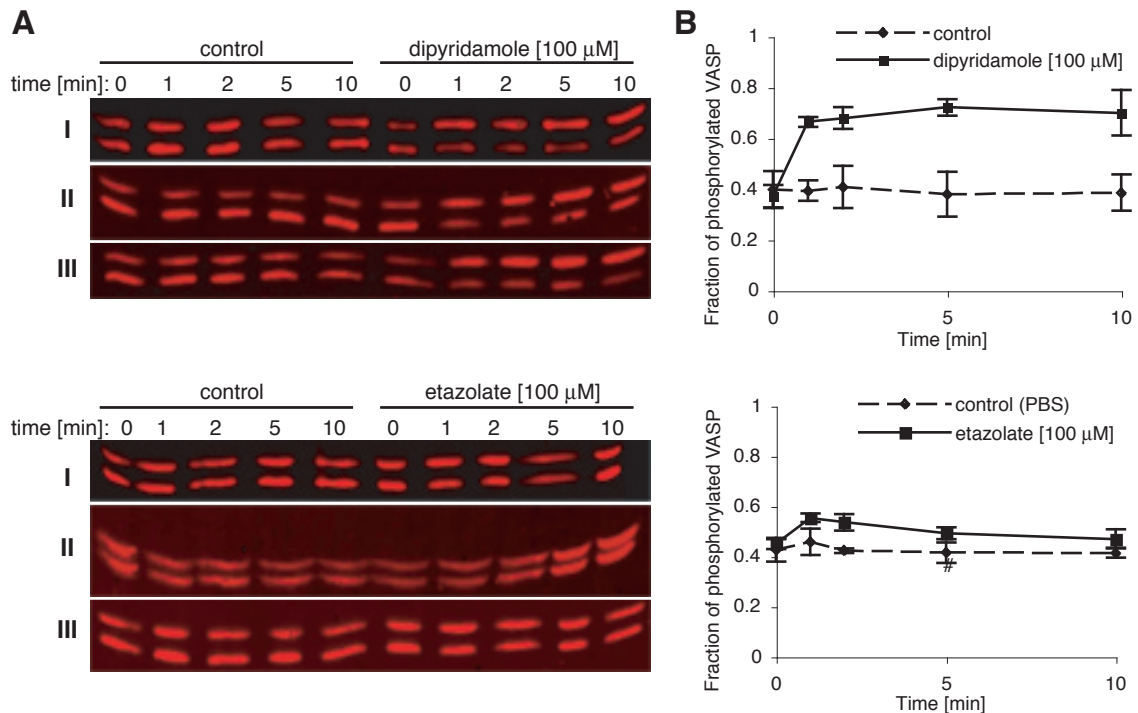


Fig. 25: VASP phosphorylation increases in the presence of the PDE inhibitors dipyridamole and etazolate

$5 \cdot 10^5$ cells from the VASP reporter cell line were incubated in the presence of 100 μ M dipyridamole (desolved in DMSO at 200 mM) or 100 μ M etazolate (desolved in PBS at 5 mM) at 37°C on a shaker for the times indicated. Control cells were incubated with an equal volume of either DMSO or PBS. Cells were harvested (30", 10000g, 37°C) and heated with 6 x Laemmli buffer for 5 minutes at 99°C. VASP was detected on a Western blot incubated with anti-VASP M4 (compare also method 2.2.3.10.).

A) Western Blots of three independent experiments (I,II,III) for dipyridamole (top) and etazolate (bottom).

B) VASP phosphorylation (VASP-phos. / (VASP-phos + VASP-unphos.)) was quantified using the Odyssey Software (Licor). Mean values of the three experiments (I-III) are shown for dipyridamole (top) and etazolate (bottom). The standard deviations are indicated by error bars.

A significant increase of VASP phosphorylation was detected after only one minute incubation with either dipyridamole or etazolate. When incubated with dipyridamole, VASP phosphorylation was increased from 40% to 70% and did not decrease during the time of observation (10 minutes). Etazolate induced a lower increase of VASP phosphorylation from 40% to only around 50%. Furthermore, etazolate induced VASP phosphorylation slightly decreased after 10 minutes. The observed differences in the induction of VASP phosphorylation between dipyridamole and etazolate might be due

to the different affinities of the inhibitors towards *T. brucei* PDEs (compare table 10 in 4.3.1.1.).

The obtained data clearly show that the VASP based *in vivo* kinase assay works in *T. brucei* and is suitable for the detection of fast changes in the activity of a *T. brucei* kinase. This kinase is probably a PKA orthologous protein, since on the one hand VASP Ser157 is a PKA specific phosphorylation site and, on the other hand, PDE inhibitors are bound to increase cNMP levels.

3.3.4.3. VASP phosphorylation decreases in the presence of the PKA specific inhibitor KT5720

Whether VASP phosphorylation really reflects PKA activity and not the activity of some other kinase was further examined with the aid of the cell permeable PKA specific inhibitor KT5720. KT5720 belongs to the group of isoquinolinesulfonamide (K252 group) that were identified as highly potent inhibitors of cNMP dependent kinases and PKC (Hidaka *et al.*, 1984). Although structurally unrelated to ATP, the inhibitors compete with ATP for the ATP binding sites of these kinases. KT5720 was found to be highly specific for PKA with an IC₅₀ value of 0.056 μ M for mammalian PKAs (Kase *et al.*, 1987).

If VASP is a PKA substrate, it should become dephosphorylated in the presence of the PKA inhibitor and remain so even when dipyridamole is added.

VASP expressing cells were incubated in the presence of KT5720 for 12 minutes and protein samples were taken every two minutes. During the last two minutes dipyridamole was added. VASP phosphorylation was monitored via a Western blot. As can be seen in figure 26A, VASP phosphorylation decreased in the presence of the PKA inhibitor. It is thus very likely that VASP is in fact phosphorylated by a PKA activity.

However, most surprisingly, dipyridamole was still able to initiate VASP phosphorylation even in the presence of KT5720. This can only be explained by the presence of a cNMP dependent kinase that is not affected by KT5720. We therefore examined the inhibitory effect of KT5720 on *T. brucei* PKAC1, PKAC2 and PKAC3 with an *in vitro* kinase assay (Fig. 26C). Ty1-PKAC1, HA-PKAC2 and Ty1-PKAC3 were purified by immunoprecipitation and tested for their abilities to phosphorylate the PKA peptide substrate RRRRSIIFI with ³²P-ATP as described above (chapter 3.3.2.). KT5720 was added in different concentrations. The activity of both PKAC1 and PKAC2 was decreased

with 10 μM KT5720 to 15-17%. Higher concentrations of KT5720 did not cause a further decrease. In contrast, the activity of PKAC3 was not affected even at 100 μM KT5720. Thus, it seems that PKAC3 is not inhibited by KT5720. The remaining dipyridamole stimulated activity in the presence of KT5720 can therefore be attributed to PKAC3. These experiments do not prove that PKAC1/2/3 are the cNMP regulated kinase(s) detected in the VASP phosphorylation assay, but the results are still compatible with that interpretation.

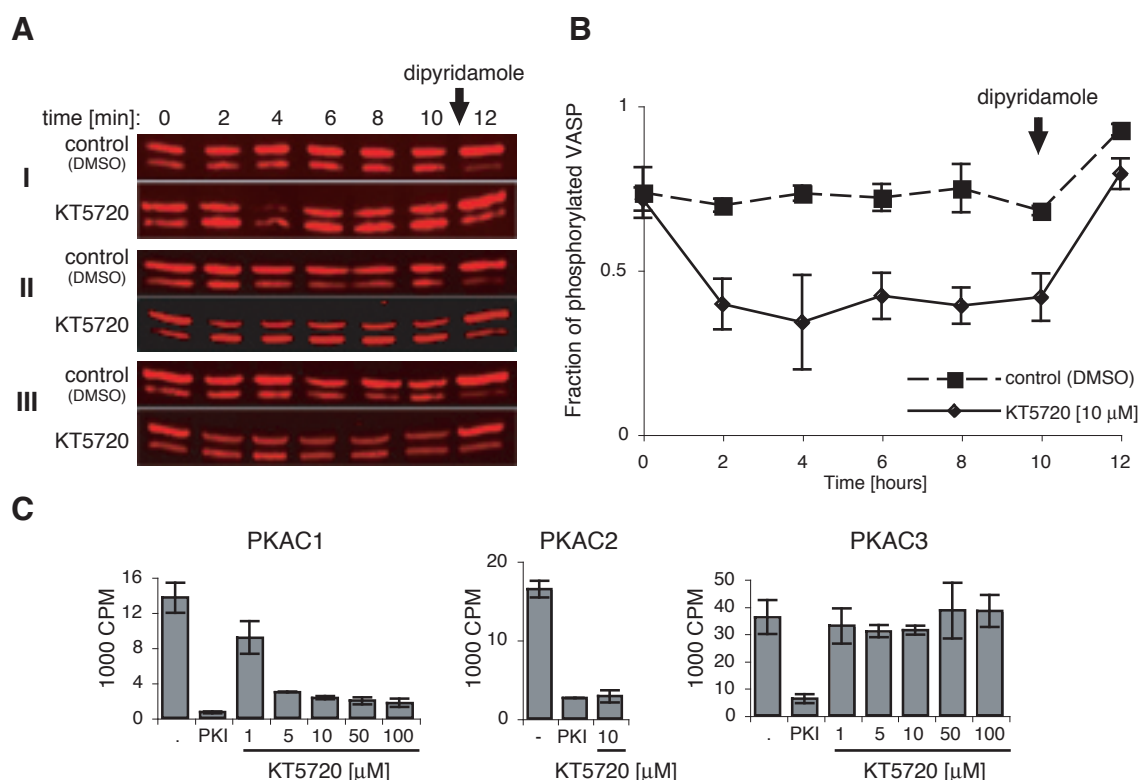


Fig. 26: KT5720 inhibits VASP phosphorylation

A) 5×10^5 cells of the VASP reporter cell line were incubated with 10 μM of the PKA specific inhibitor KT5720 (desolved in DMSO at 2 mM) for 12 minutes. Control cells were incubated with an equal volume of DMSO. After 10 minutes, 100 μM dipyridamole (desolved in DMSO at 200 mM) was added. Cells were harvested (1', 10,000 g, 4°C) and VASP was detected on a Western blot probed with anti-VASP. The experiment was repeated three times (I, II, III).

B) VASP phosphorylation (VASP-phos. / (VASP-phos. + VASP-unphos.)) was quantified using the Odyssey Software (Licor). Mean values from the three experiments (A I,II,III) are shown and the standard deviations are indicated by error bars.

C) KT5720 selectively inhibits PKAC1 and PKAC2, but not PKAC3

The effects of KT5720 on the activities of the different catalytic subunits of *T.brucei* PKA-like kinase were assayed *in vitro*. For this, immunoprecipitated Ty1-PKAC1, Ty1-PKAC2 and Ty1-PKAC3 were tested on their abilities to phosphorylate the PKA specific substrate RRRRSIIIFI (Songyang *et al.*, 1994) with $\gamma^{32}\text{P}$ -ATP in the presence of different concentrations of KT5720 (1-100 μM). PKI (5 μM), that had been shown previously to inhibit all three *T.brucei* PKAs, was used as a positive control. Each assay was repeated three times. Average values are shown and the standard deviations are indicated by error bars. It can be seen that PKAC1 and PKAC2 are inhibited by 10 μM KT5720, while PKAC3 is still active in the presence of even 100 μM KT5720.

3.3.4.4. VASP phosphorylation increases with pCPT-cGMP and decreases with pCPT-cAMP

The *in vivo* kinase assay was therefore used to address the question of which cyclic nucleotide was responsible for PKA activation. However, no changes in VASP phosphorylation were detected with 250 μ M of the membrane permeable cNMP derivatives pCPT-cAMP or pCPT-cGMP (data not shown), although these concentrations of pCPT-cAMP were sufficient to induce LS to SS differentiation in pleomorphic trypanosomes (Vassella *et al.*, 1997) or to arrest growth in monomorphic cells (Reuner, Ph.D. thesis 1997; Schimpf, Diploma thesis 2000).

Given the limited cell permeability, VASP expressing cells were incubated with higher concentrations of these cNMP derivatives. Incubation of VASP expressing cells with 5 mM pCPT-cGMP increased VASP phosphorylation (Fig. 27A/B, left), compatible with the *in vitro* data. The unusually high concentration of pCPT-cGMP needed to increase VASP phosphorylation *in vivo* corresponded to the results from the *in vitro* kinase assays (compare Fig. 22A in chapter 3.3.2.) that clearly showed that pCPT-cGMP is less suitable for activation of PKAC1 than cGMP.

Surprising results were obtained with pCPT-cAMP (Fig. 27A/B, right): VASP phosphorylation decreased in the presence of pCPT-cAMP suggesting that this analogue in fact acts as a kinase inhibitor instead of an activator. Kinetic analyses revealed that one minute of incubation with 1 mM pCPT-cAMP was already sufficient to significantly decrease VASP phosphorylation that then remained decreased for at least 30 minutes (Fig. 28).

3.3.5. cAMP inhibits PKA *in vitro*

The observed inhibitory effect of pCPT-cAMP on VASP phosphorylation (that most likely reflects activity of the PKA-like kinases) was unexpected. Two mechanisms could account for this inhibition. Firstly, cAMP could interfere with proteins from other signaling pathways and thus indirectly cause inhibition via a cross talk mechanism. Cross talk between cAMP and cGMP signaling has been proposed to exist in higher eukaryotes (reviewed by Abdel-Latif, 2001). Alternatively, cAMP could bind to the cNMP binding sites of PKAR but then fail to provoke the structural changes that are necessary for kinase activation. cAMP would therefore compete with the physiological activator.

Since cross talk between different signaling pathways is highly complex and for this reason

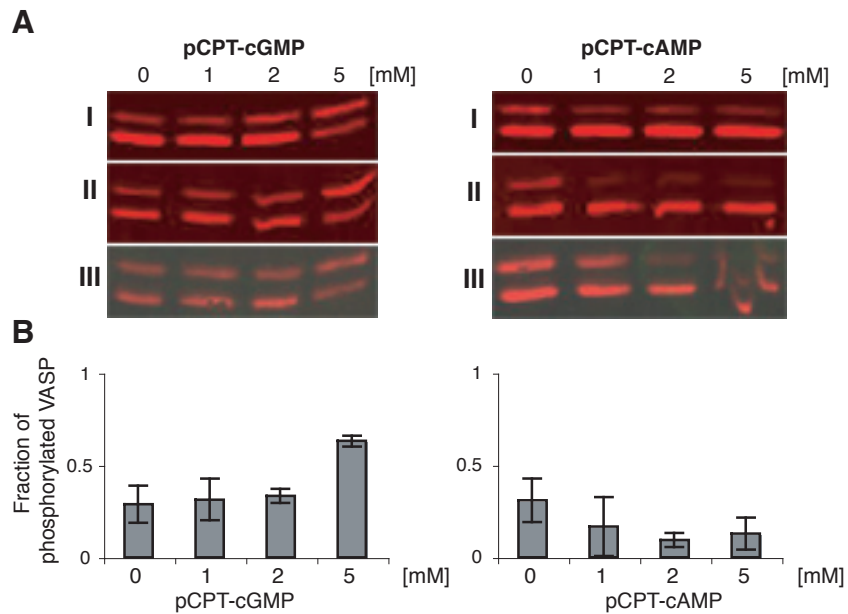


Fig. 27: VASP phosphorylation in the presence of the cyclic nucleotide derivatives pCPT-cGMP and pCPT-cAMP

VASP expressing cells were harvested (10', 1400g, 4°C) and resuspended in HMI9 at $2.5 \cdot 10^7$ cells/ml. 20 μ l of these cells (corresponding to $5 \cdot 10^5$ cells) were incubated in the presence of 0, 1, 2, or 5 mM pCPT-cGMP or pCPT-cAMP (from a 10 mM stock desolved in PBS) for 5 minutes at 37°C on a shaker. The reactions were stopped with 4 μ l 6x Laemmli buffer (5', 99°C). Samples were applied to SDS gels and VASP was detected with anti-VASP on the resulting Western blots.

A) Western blots of three independent experiments (I, II, III).

B) VASP phosphorylation (VASP-phos. / (VASP-phos + VASP-unphos.)) from A) was quantified using the Odyssey Software (Licor). Mean values from the three experiments are shown and the standard deviations are indicated by error bars.

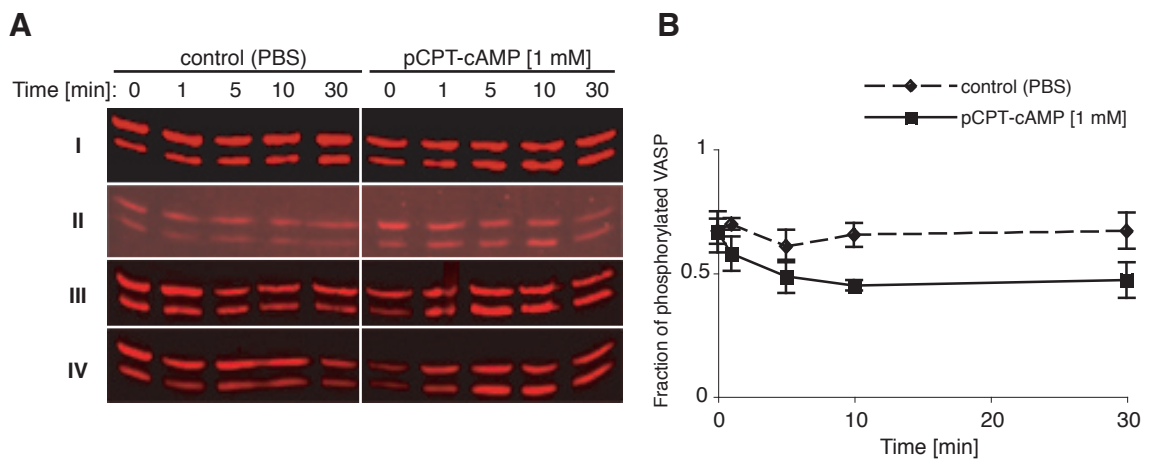


Fig. 28: VASP phosphorylation remains decreased in the presence of 1 mM pCPT-cAMP for at least 30 minutes

A) VASP expressing cells at $5 \cdot 10^5$ cells/ml were incubated in the presence of 1 mM pCPT-cAMP (desolved in PBS as 10 mM stock) or equal volumes of PBS (control) for 0, 1, 5, 10 or 30 minutes at 37°C on a shaker. Cells were harvested (30', 10000g, 4°C), incubated in Laemmli buffer (5', 99°C) and applied to SDS PAGE. VASP was detected on a Western blot probed with anti-VASP. Western blots of four independent experiments (I, II, III, IV) are shown.

B) VASP phosphorylation (VASP-phos. / (VASP-phos + VASP-unphos.)) from the Western blots I, II, III, and IV from (A) was quantified using the Odyssey Software (Licor). Mean values are shown together with the standard deviations indicated by error bars.

difficult to investigate, analyses were in this work restricted to the second hypothesis that can easily be tested with an *in vitro* kinase assay. For this, immunopurified holoenzyme of PKA-like kinase (precipitated via Ty1-PKAR) was incubated with different concentrations of cAMP, ranging from 0-10 mM, in addition to 1 mM cGMP. Kinase activities (measured as the amount of phosphorylated PKA peptide substrate as described in chapter 3.3.2.) in the presence of cGMP and cAMP are shown in figure 29A. As previously observed, kinase activity increased five fold in the presence of 1 mM cGMP, while cAMP alone had no effect. However, in the presence of both cyclic nucleotides kinase activity was significantly reduced. With equimolar concentrations of cAMP kinase activity was decreased by one third and with a ten fold excess of cAMP, kinase activity was found to be near basal activity. Similar (slightly weaker) inhibitory effects of cAMP on PKA activity were observed when the holoenzyme was precipitated via the Ty1-epitope tagged PKAC1 (Fig. 29B).

Conclusively, cAMP inhibits PKA activity directly, probably by competing with cGMP.

In order to control the specificity of cAMP as a PKA inhibitor, other cyclic nucleotides were tested on their ability to also decrease PKA activity. However, none of the tested cyclic nucleotides (cUMP, cCMP, cIMP) had an inhibitory effect on PKA activity, suggesting that cAMP does inhibit PKA specifically (data not shown).

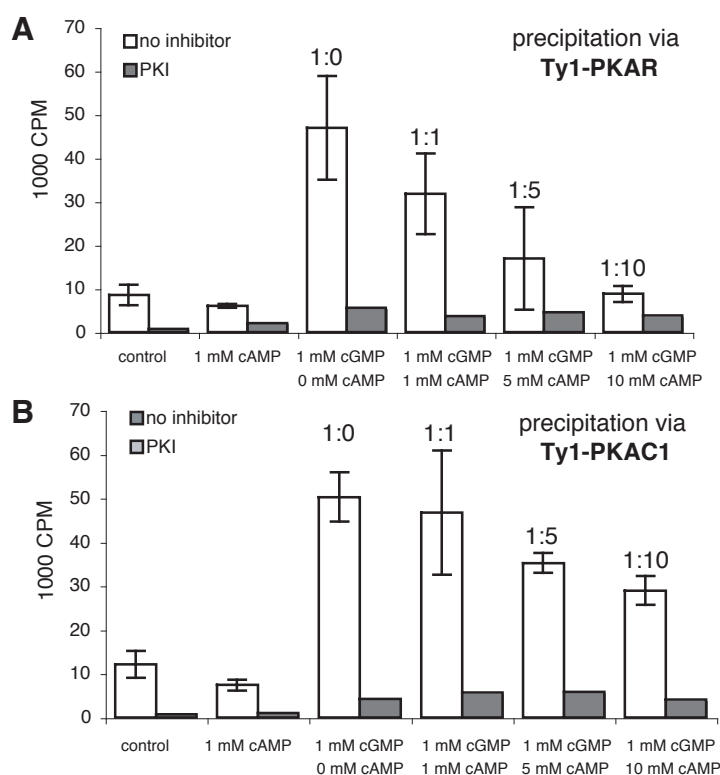


Fig. 29: cAMP inhibits PKA-like kinase *in vitro*

The holoenzyme of *T. brucei* PKA-like kinase was immunoprecipitated via Ty1-PKAR (**A**) or Ty1-PKAC1 (**B**). Equal amounts of the immunoprecipitates were tested on their abilities to phosphorylate the PKA specific substrate RRRRSIIFI (Songyang *et al.*, 1994) with $\gamma^{32}\text{P}$ -ATP in the absence (control) and presence of different concentrations of cAMP and/or cGMP. Each reaction was done in triplicates. Mean values are shown (white bars) together with the standard deviations (error bars). In addition, each reaction was performed once in the presence of PKI [5 μM] (grey bars).

3.4. Role of *T. brucei* PKA-like kinase *in vivo*

Two completely different approaches have been used to obtain information about the function of the kinase in question. The phenotypic consequences of altered expression of the PKA-like kinase were examined using several reverse genetic approaches. The second approach concentrated on the identification of extracellular signals that may affect the VASP phosphorylating activity. Although it seems likely that this activity is identical with the PKA-like kinases, this is not considered an established fact for the following section.

3.4.1. Changes in VASP phosphorylation due to different extracellular stresses

During their complex life cycle trypanosomes are confronted with dramatic changes in their environment, especially when they shuttle between their different hosts. Trypanosomes must be able to sense these changes that might on the one hand provide differentiation signals and on the other hand require quick adaptations in order to ensure survival. The underlying signaling pathways for environmental sensing are still unknown (reviewed in Parsons and Ruben, 2000).

3.4.1.1. Effects of increased cell density on VASP phosphorylation

Some of the subsequent experiments addressing the activity of the VASP phosphorylating kinase(s) in response to different stresses needed to be performed with cells at increased cell densities. In this way, reactions could be stopped directly by the addition of Laemmli buffer without the need of a potentially interfering harvesting procedure.

Thus, the first test was to see whether an increase in cell density had any effect on VASP-phosphorylation. For this, cells were concentrated at a cell density of 5×10^7 cells/ml and diluted in fresh medium to obtain cell densities of 5×10^5 , 1×10^6 , 2×10^6 , 5×10^6 , 1×10^7 or 5×10^7 cells/ml. The cells were then incubated on a shaker at 37 °C for 2, 10 or 30 minutes, harvested and VASP phosphorylation was quantified via a Western blot (Fig. 30). We did not observe significant differences in VASP phosphorylation between the samples of different cell densities for any of the incubation times.

Conclusively, VASP phosphorylation is not affected by an increase in cell density, at least not within the first 30 minutes. The VASP-based *in vivo* kinase assay can therefore be used with samples.

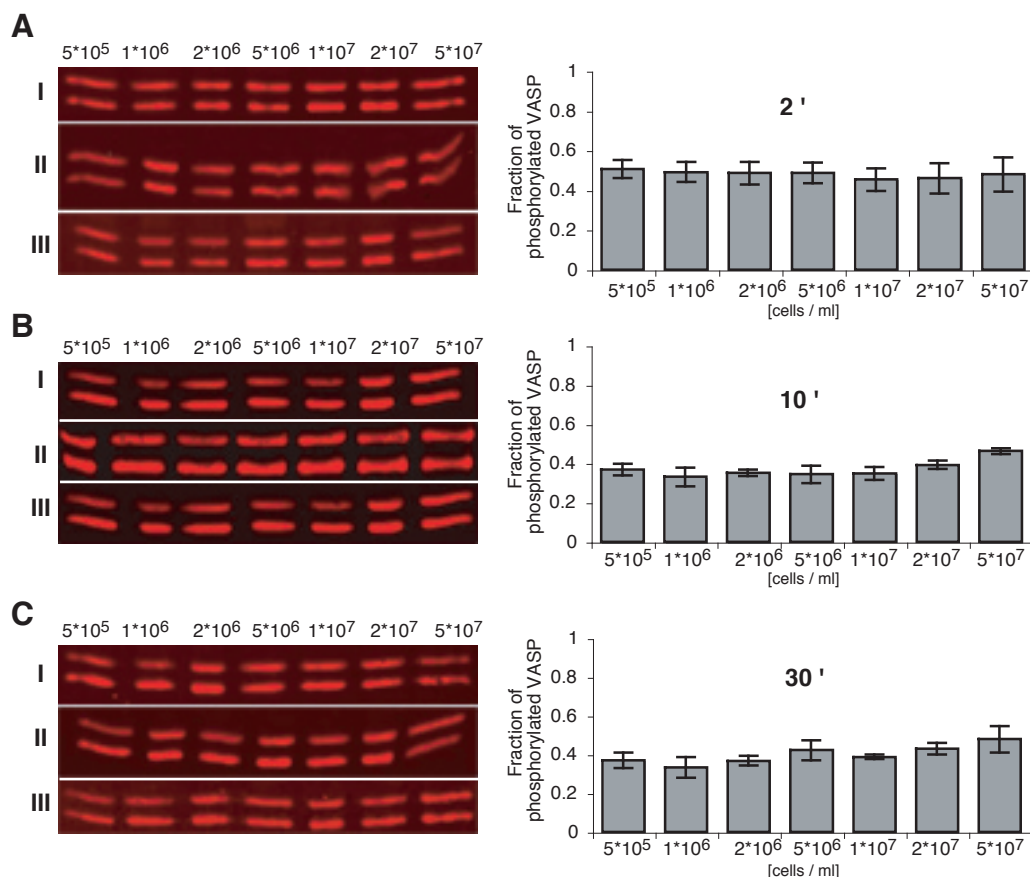


Fig. 30: Effects of cell densities on VASP phosphorylation

VASP expressing cells were harvested (10', 1400g, 37°C) and resuspended in HMI9 at 5×10^7 cells/ml. 10 μ l of these cells were added to 990, 490, 240, 90, 40, 15 and 0 μ l HMI9 (pipetting time maximal 1'), to obtain cell densities of 5×10^5 , 1×10^6 , 2×10^6 , 5×10^6 , 1×10^7 , 2×10^7 and 5×10^7 cells/ml, respectively. Cells were incubated at 37°C on a shaker for 2 minutes (A), 10 minutes (B) or 30 minutes (C). Afterwards cells were harvested (30", 10000g, 37°C), incubated with 5 μ l 6x Laemmli buffer (5', 99°C) and applied to SDS PAGE. VASP phosphorylation (VASP-phos. / (VASP-phos + VASP-unphos.)) was quantified from a Western blot probed with anti-VASP using the Odyssey Software (Licor).

Each experiment was done three times (I, II, III). The Western blots of the three experiments are shown on the left site and the corresponding diagrams reflecting VASP phosphorylation are shown on the right site. Standard deviations are indicated by error bars.

3.4.1.2. VASP phosphorylation increases at low temperatures

The influence of different temperatures on VASP phosphorylation was examined. VASP expressing cells (at cell densities of 5×10^7 cells/ml) were incubated at 0 °C (ice), 4°C, 12°C, 20°C, 30°C or 37°C for two minutes. The reaction was stopped by the addition of 6x Laemmli buffer (5', 99 °C) and VASP phosphorylation was determined by a Western blot (Fig. 31). A decrease in temperature resulted in an increase in VASP phosphorylation. A significant increase in VASP phosphorylation was already observed at 30°C. VASP phosphorylation further increased at 20°C and reached its maximum at 12°C. No further increase was observed at 4°C or 0°C. The observed increase in VASP phosphorylation

was reversible: When cells were transferred back to 37°C VASP phosphorylation decreased back to normal.

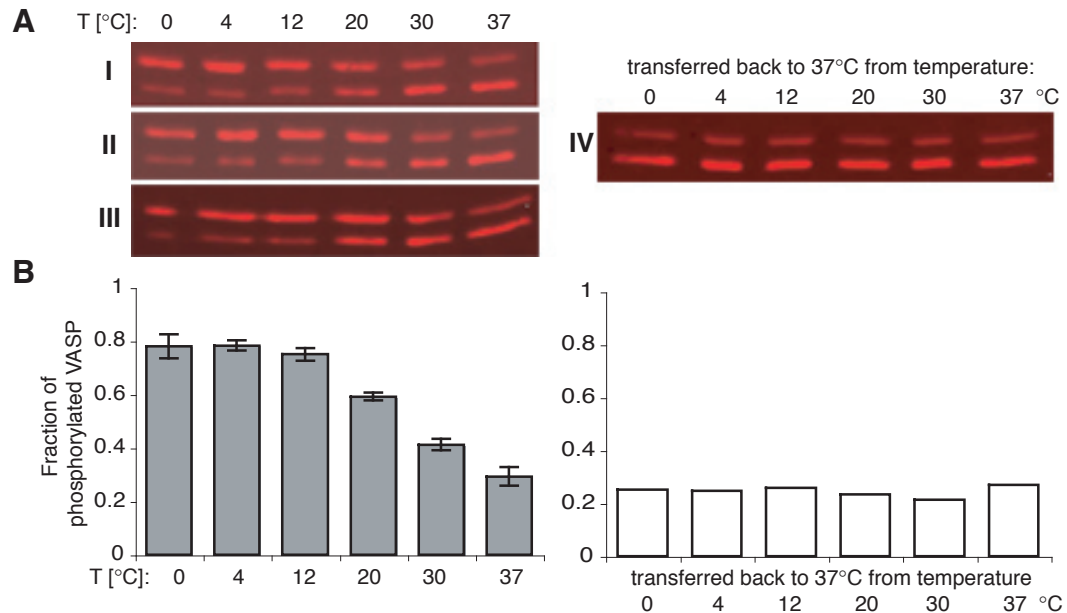


Fig. 31: VASP phosphorylation increases at low temperatures

VASP expressing cells were harvested (10', 1400g, 37°C) and resuspended in HMI9 at 5×10^7 cells/ml. 10 μ l of these cells were incubated at 37°C for one minute and subsequently at 0, 4, 12, 20, 30 or 37°C for two minutes (without shaking). The reaction was stopped by directly adding 2 μ l 6x Laemmli buffer to the cells without removing them from their particular temperatures and subsequently heating them to 99°C for 5 minutes. Samples were subsequently applied to SDS PAGE and VASP was detected with anti-VASP on a Western blot. The experiment was done three times.

A) I-III) Western blots of three independent experiments. **IV)** To control for the reversibility of temperature dependent changes in VASP phosphorylation, cells were treated as described above but incubated for an additional two minutes at 37°C.

B) VASP phosphorylation (VASP-phos. / (VASP-phos + VASP-unphos.)) was quantified using the Odyssey software (Licor). Data from the three experiments (I, II, III) are summarized and the standard deviations are shown as error bars (left, grey bars). The data from experiments IV are shown on the right site (white bars).

In theory the observed changes in VASP phosphorylation could also be due to a reaction of the responsible kinase on cell lysis, rather than to a direct influence of the temperature change on kinase activity. At different temperatures the reaction of kinase on cell lysis could vary, leading to the observed temperature dependent differences in VASP phosphorylation. Therefore, a control experiment was performed in order to examine whether cell lysis itself had any effect on VASP phosphorylation.

Cells were incubated for 5 minutes at 37 °C, for one minute at either -196 °C (shock frozen in liquid N₂), 0 °C (ice) or 37 °C, then for one minute in 6x Laemmli buffer at the same temperatures and finally for 5 minutes at 99 °C. VASP phosphorylation was quantified via a Western blot (Fig. 32). No difference in VASP phosphorylation was

observed between cells that were lysed at 37 °C or -196 °C, while kinase activity was increased when cells were incubated on ice. This proves that cell lysis does not affect the extent of VASP phosphorylation and that the increase in VASP phosphorylation is in fact due to the temperature drop.

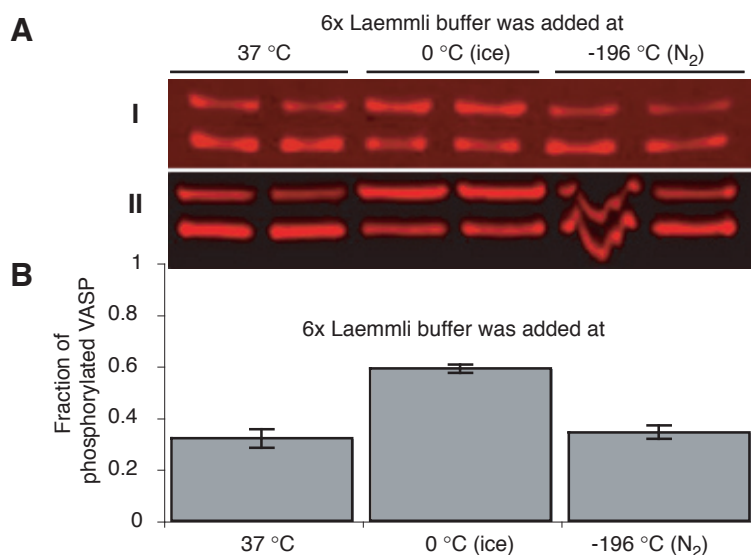


Fig.32: Cell lysis has no effect on VASP phosphorylation

VASP expressing cells were harvested (10', 1400g, 37°C) and resuspended in HMI9 at 5×10^7 cells/ml. 10 μ l of these cells (5×10^5 cells) were incubated at 37°C for 5 minutes on a shaker. Subsequently, cells were incubated for one minute either at 37 °C (two samples), or on ice (two samples) or in liquid nitrogen (two samples). Afterwards, 2 μ l 6x Laemmli buffer was added and the cells were incubated first for one additional minute at their particular temperatures and then at 99°C for 5 minutes. Samples were applied to SDS PAGE and VASP was detected with anti-VASP on a Western blot.

A) Western blots of two independent experiments (I, II).

B) VASP phosphorylation (VASP-phos. / (VASP-phos. + VASP-unphos.)) was quantified using the Odyssey software (Licor). Data from experiment I and II are summarized (thus each bar represents data from altogether 4 samples) and mean values are shown. Standard deviations are indicated by error bars.

3.4.1.3. VASP phosphorylation depends on osmolarity

In order to examine whether the VASP phosphorylating kinase activity depends on osmolarity, cells were incubated in TDB (5 mM KCl, 1 mM MgSO₄, 20 mM Na₂HPO₄, 2 mM NaH₂PO₄, 20 mM glucose, pH 7.7) complemented with different concentrations of NaCl. Hypotonic conditions were achieved with NaCl concentrations of 20, 40 and 60 mM, isotonic conditions with 80 mM NaCl and hypertonic conditions with 100, 120, 140 and 160 mM NaCl. After 5 minutes incubation, cells were harvested, applied to a Western blot and the extent of phosphorylated VASP was determined (Fig. 33, left). VASP phosphorylation increased at hypotonic conditions and decreased at hypertonic

conditions.

Two controls were performed to verify that cells were still viable in the different buffers. Using phase contrast microscopy we found no changes in morphology or motility after 10 minutes incubation in each of the buffers (data not shown). Furthermore, the changes in VASP phosphorylation were reversible when cells were transferred back into isotonic TDB (Fig. 33, right).

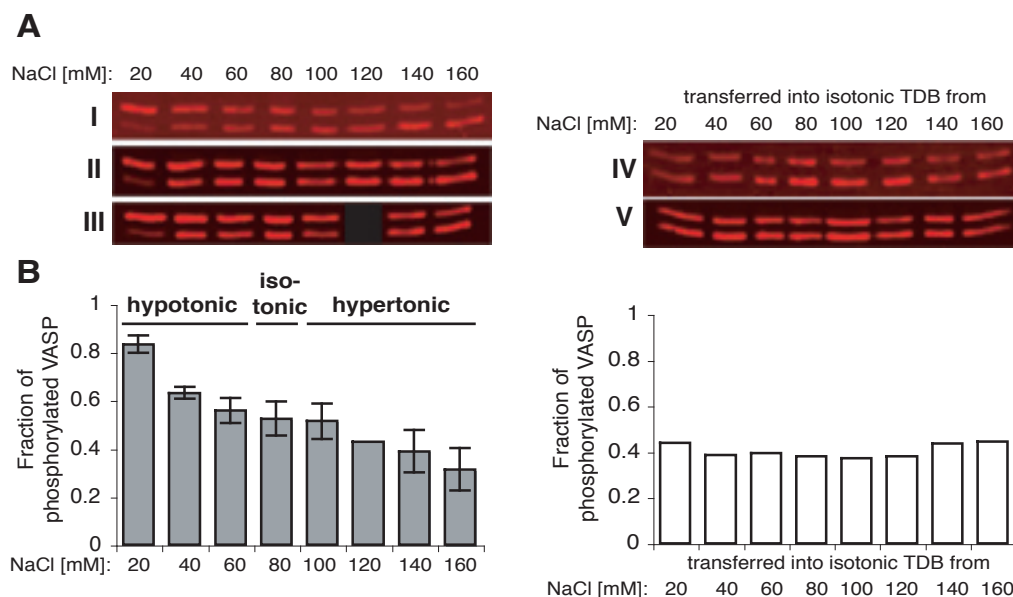


Fig. 33: VASP phosphorylation depends on the osmolarity of the medium

VASP expressing cells were harvested (10', 1400g, 37°C) and resuspended in HMI9 at 5×10^7 cells/ml. 10 μ l of these cells were added to 1 ml TDB buffer containing 20, 40, 60, 80, 100, 120, 140 or 160 mM NaCl. Cells were incubated at 37°C on a shaker for 5 minutes, harvested (30", 10000g, 37°C), incubated in 6x Laemmli buffer for 5 minutes at 99°C and applied to SDS Page. VASP phosphorylation was quantified from a Western blot probed with anti-VASP using the Odyssey Software (Licor).

A) Western blots of three independent experiments (I, II, III). To control for the reversibility of the salt dependent changes in VASP phosphorylation, cells from experiment II and III were retransferred into isotonic TDB (80 mM NaCl), incubated for 5 minutes and harvested (IV,V).

B) VASP phosphorylation (VASP-phos. / (VASP-phos + VASP-unphos.)) was quantified using the Odyssey Software (Licor). The data from experiments I to III are summarized and the standard deviations are indicated by error bars (grey bars, left). The data from the experiments IV and V are also summarized (white bars, right).

3.4.1.4. VASP phosphorylation depends on pH

To investigate whether VASP phosphorylation was dependent on the pH value of the medium, cells were transferred into HMI9 (pH 7.35) and into HMI9 titrated to different pH values (5.5, 6.5, 8.5, 9.5). After 5 minutes incubation, cells were harvested and applied to SDS PAGE. VASP phosphorylation was determined from a Western blot (Fig. 34). It can be seen that the activity of the VASP phosphorylating kinase(s) is increased at low pH

values and decreased at high pH values. VASP phosphorylation was restored to normal when cells were transferred back into HMI9 (pH 7.35).

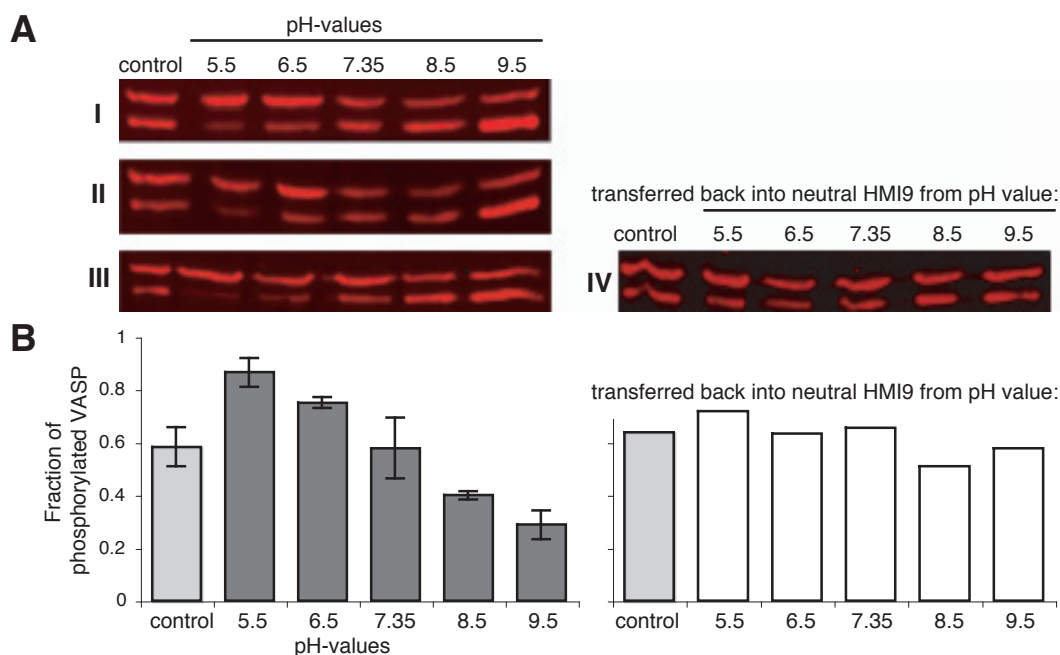


Fig. 34: VASP phosphorylation at different pH-values

VASP expressing cells ($5 \cdot 10^5$) were harvested (10', 1400g, 4°C) and resuspended either in neutral HMI9 (pH 7.35) or in HMI9 adapted to different pH values (pH 5.5, 6.5, 8.5 and 9.5). To exclude any influence of the harvesting procedure on PKA activity, control cells (control) were not transferred to new medium. Cells in their particular media were then incubated for 5 minutes at 37°C on a shaker, harvested (30", 10000 g, 4°C), incubated in Laemmli buffer at 99°C for 5 minutes and applied to SDS PAGE. VASP was detected on a Western blot probed with anti-VASP.

A) Western blots from three independent experiments (I, II, III). An additional control was performed in parallel to experiment III to control for the reversibility of pH dependent changes in VASP phosphorylation (IV). For this, cells from the different media were transferred back into neutral HMI9 (pH 7.35), incubated for 5 minutes (37°C, slightly shaking) and harvested (30", 10000 g, 4°C).

B) VASP phosphorylation (VASP-phos. / (VASP-phos. + VASP-unphos.)) was quantified using the Odyssey software (Licor). The average values from experiment I to III are shown in the left diagram (grey bars) and the data from experiment IV are shown in the diagram on the right site (white bars). Standard deviations for experiments I to III are shown as error bars.

The changes in VASP phosphorylation in reaction to the different environmental stimuli is summarized in table 3:

Stimuli		Change in VASP phosphorylation
Cell density	increase	none
Temperature	decrease	increase
Osmolarity	hypotonic	increase
	hypertonic	decrease
pH-value	acidic	increase
	basic	decrease

Table 3: Overview about the changes in VASP phosphorylation upon different stimuli.
The data from chapter 3.4.1. are summarized.

3.4.2. Revers genetic analyses of *T. brucei* PKA-like kinase

Several reverse genetic approaches were applied in order to obtain further information about the function of *T. brucei* PKA-like kinase. Thereby each subunit was examined individually. To enable an easy comparison between the different subunits, a table was inserted at the end of each chapter summarizing all phenotypes described so far. The first subunit addressed was the regulatory PKA subunit:

3.4.2.1. Depletion of PKAR with RNA interference

There is evidence that *T. brucei* PKAR is an important, probably essential protein, since overexpression of PKAR caused a growth phenotype (C. Schulte zu Sodingen, Ph.D. thesis 2000). For this reason PKAR function was analyzed with inducible RNA interference rather than using a gene deletion strategy.

A 500 bp fragment of the *PKAR* N-terminus was cloned into the p2T7 vector (LaCount *et al.*, 2000) and transfected into the tetracycline inducible 13-90 cell line (Wirtz *et al.*, 1999). Several independent clonal transfectants were incubated with tetracycline. Four clones (#1, #4, #6, #8) showed a strong growth phenotype. From these two were chosen for further analyses (#1, #4). Immunoblotting revealed that the amount of PKAR was decreased to less than 10% (Fig. 35A). Interestingly, the amounts of the catalytic subunits PKAC1 and PKAC2 were equally reduced and the amount of PKAC3 protein was decreased to approximately 50%. The reason for this is probably the loss of stability of the uncomplexed C subunits. Similar co-depletions had been previously observed by Estévez *et al.* (2003) when targeting RNAi against components of the proteasome complex.

3.4.2.1.1 Repression of PKAR blocks cellular proliferation

After 8 hours of tetracycline incubation, the cell number of both clones did not increase further (Fig. 35B). In order to examine whether this growth arrest can be attributed to a certain cell cycle phase, tetracycline induced and non-induced cells of both clones were stained with the DNA dye DAPI. In trypanosomes, DAPI stains both the nuclear DNA and the DNA of the single mitochondrion (kinetoplast), thus, allowing the distinction of three cell cycle phases: Cells with one kinetoplast (K) and one nucleus (N) (1K1N), cells with two kinetoplasts and one nucleus (2K1N) and cells with two kinetoplasts and two nuclei (2K2N). Since the kinetoplast always divides prior to the nucleus, 1K2N cells do not

normally occur. A logarithmically growing trypanosome population contains around 70% 1K1N cells and around 15% of each 2K1N and 2K2N cells.

The K/N configurations of tetracycline induced and non-induced PKAR RNAi cells are shown in figure 35C. The fraction of 2K2N cells increased from 15% to about 50% within 10 hours of incubation with tetracycline, while the number of 1K1N cells decreased. Additionally, the amount of multinucleated cells ($xKyN$; $x,y>2$) rose. There were no changes in the number of 2K1N cells. After 8 to 10 hours of tetracycline incubation we observed a slight increase in 1K2N cells. Such an increase in 1K2N cells (1 to 4% of the total cells) was also observed with other clones (data not shown). Altogether these data indicate that the observed growth arrest of the cells is due to a postmitotic cell cycle arrest. Cells are able to separate their nuclei and kinetoplasts but are prevented from cytokinesis. Instead, they start another round of nuclear and kinetoplast DNA replication and become multinucleated.

3.4.2.1.2. Repression of PKAR still allows the complete partition of the nuclei

BSF cells cannot undergo cytokinesis when mitosis is inhibited (mitotic exit checkpoint) (Hammarton *et al.*, 2003a). Therefore, it was at first examined whether an uncompleted mitosis was the reason for the cytokinesis block. Although neither nuclear division nor separation appeared to be inhibited, the 2K2N cells might still be arrested in the very last phase of mitosis, in the partition of the nuclear envelope. During mitosis, the nuclear envelope surrounds both nuclei and is only divided upon successful division and separation of the nuclei. It can be stained with an antibody against a nuclear pore protein (NUP1) anti-Nup (kindly provided by K. Ersfeld; Ogbadoyi *et al.*, 2000). Examples of 2K2N cells that have their nuclei completely separated are shown in Fig. 36A and B, 2K2N cells with their nuclear envelopes still connected are shown in Fig 36C and D. The nuclear envelopes of 100 tetracycline induced and 100 non-induced 2K2N cells were examined. 81% of the tetracycline induced cells and 74% of the control cells had their nuclei completely separated (Fig. 36E). This shows that cells can still separate their nuclei upon PKAR depletion and are therefore not arrested at the mitotic exit checkpoint.

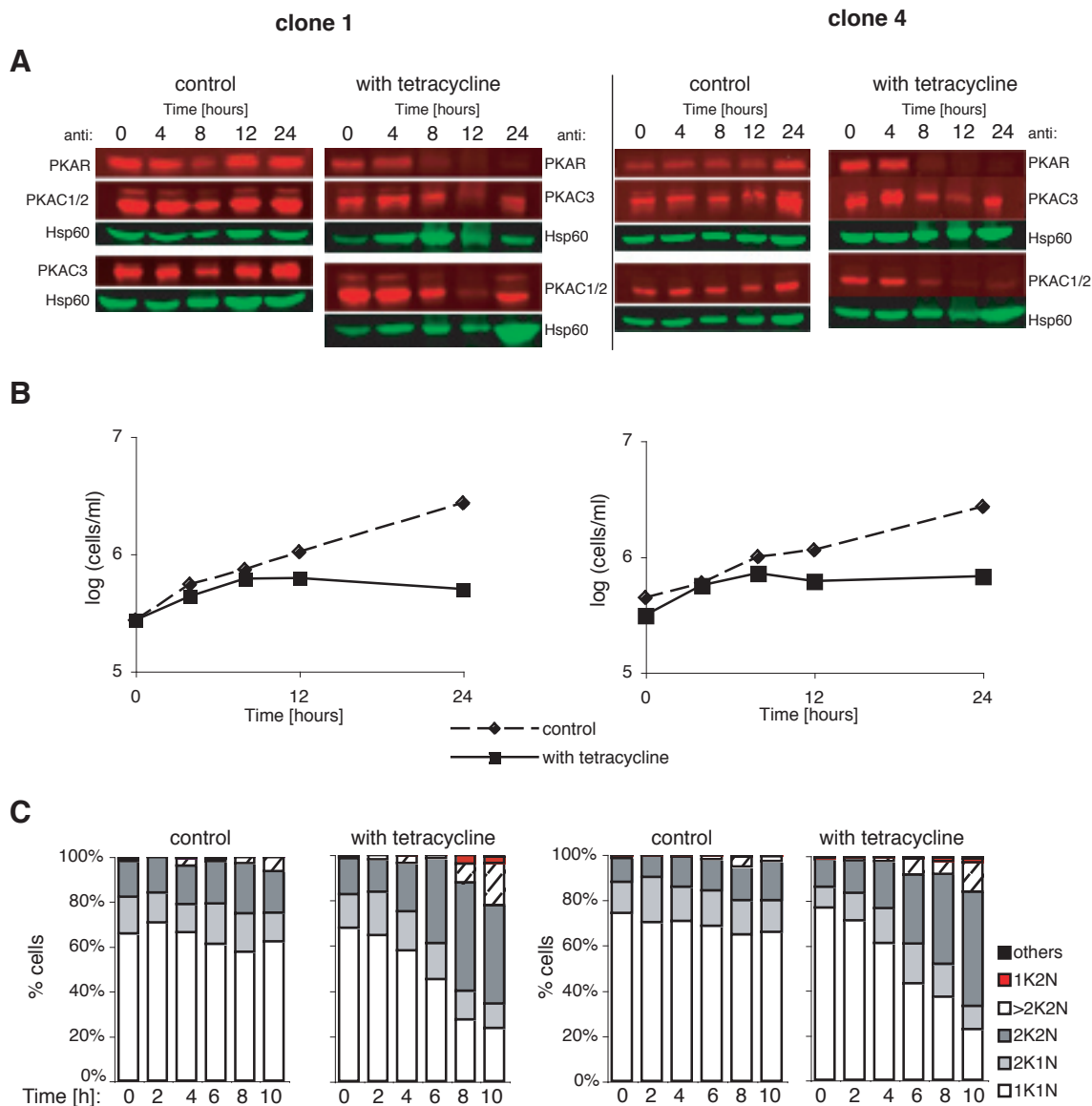


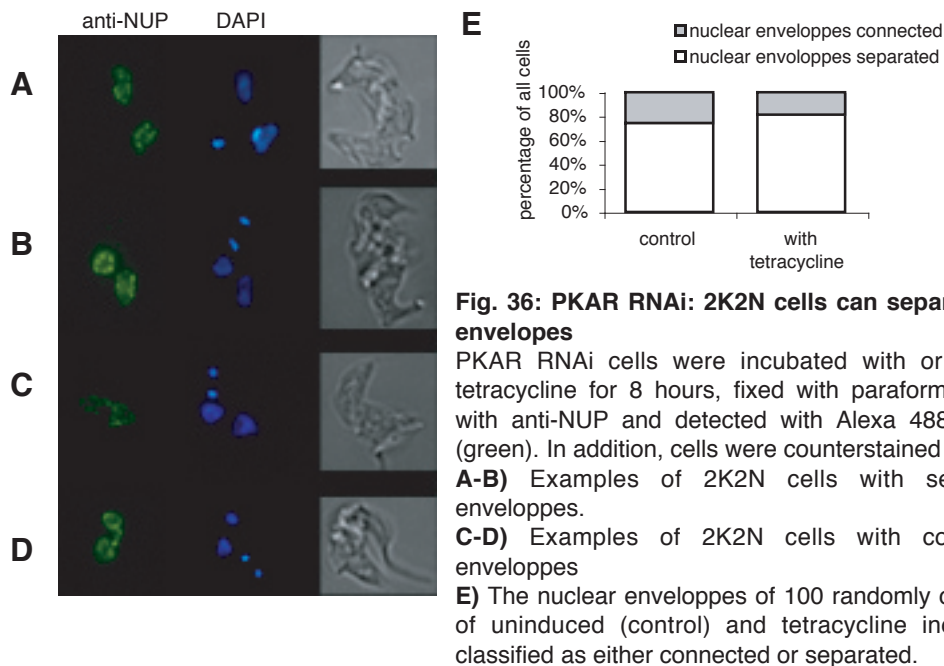
Fig. 35: PKAR depletion by RNA interference:

Cells were incubated in the presence or absence (control) of tetracycline [$10\mu\text{g/ml}$] for 24 hours. Data from two independent clonal cell lines (#1 and #4) are shown.

A) Western blots: Protein samples were collected 0,4,8,12 and 24 hours after incubation with and without tetracycline (control) and applied to SDS PAGE. The resulting Western blots were incubated with anti-PKAR, anti-PKAC1/2, anti-PKAC3 and anti-Hsp60, the latter serving as a control for equal loading. Since PKAC3 and PKAC1/2 have equal molecular weights, two Western blots (loaded with the same samples) were performed for each time course and incubated with either anti-PKAC1/2 or anti-PKAC3, as indicated. Rabbit Alexa680 (red) and Mouse IRDye800 (green) were used for the detection of anti-PKAR/anti-PKAC3/anti-PKAC1/2 and anti-Hsp60, respectively, using the Odyssey IR scanner (Licor).

B) Growth curves: Growth curves of induced and uninduced PKAR RNAi cells. Cell densities were kept below 7×10^5 cells/ml.

C) K/N configurations: Cells were fixed in methanol after 0, 2, 4, 6, 8, 10 and 12 hours of incubation with or without tetracycline and subsequently stained with DAPI. K/N configurations of 400 cells were determined for each time point.



3.4.2.1.3 Cells can initiate cytokinesis but are unable to complete it

The stage of the division furrow of 2K2N cells was determined in tetracycline induced and non-induced cells (Fig. 37). Without tetracycline, most cells (55-70%) had no division furrow, between 10 to 20% had a division furrow and around 25% of the cells had nearly finished cytokinesis and were only attached at their most posterior cell ends.

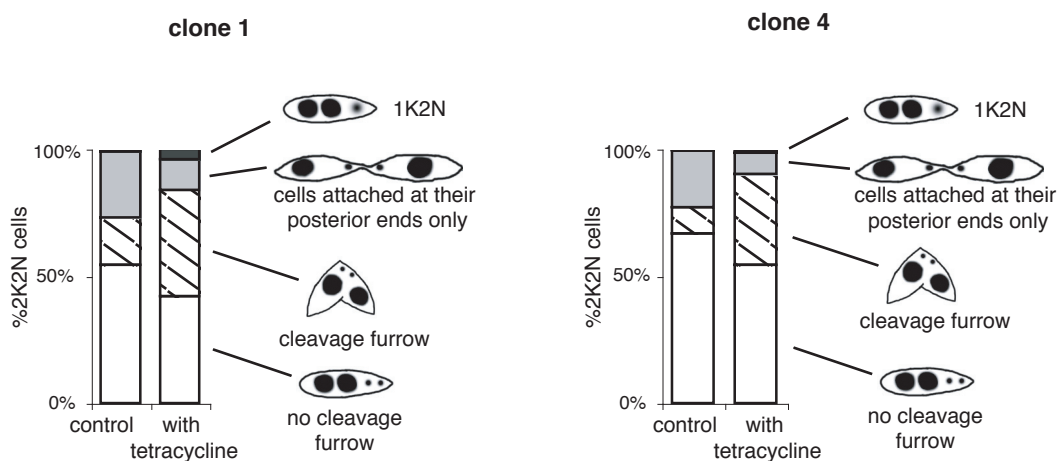


Fig. 37: Division furrow stage of 2K2N cells upon PKAR RNAi:

2K2N cells and 1K2N cells of tetracycline induced and uninduced cultures were classified according to the stage of their division furrow. 200 2K2N cells were analysed that were incubated with or without tetracycline for 8 hours.

In the tetracycline induced cells the amount of cells with division furrow was significantly increased to 35 to 40%, while the fraction of cells without division furrow or cells that had nearly finished cytokinesis was found decreased. Interestingly, the division furrow appeared to always be at approximately the same position, at half of the cell length. This accumulation of cells with division furrow suggests that PKAR RNAi cells are able to initiate cytokinesis but are unable to carry it through to completion.

3.4.2.1.4. 2K2N cells have increased kinetoplast distances

A marked difference between the 2K2N cells of tetracycline induced and non-induced cells was the position of their kinetoplasts.

In BSF trypanosomes, kinetoplasts are always located posterior of the posterior nucleus. Upon kinetoplast division, the old (mother) and the new (daughter) kinetoplast segregate. The mother kinetoplast (that is attached to the basal body with the old flagellum) moves towards the anterior cell end, but does not normally reach the posterior nucleus. The daughter kinetoplast (that is attached to the basal body that nucleates the new flagellum) moves towards the posterior cell end (M. Engstler, unpublished).

In many induced PKAR RNAi cells the mother kinetoplast was located very close to the posterior nucleus and sometimes even between the nuclei. Thus, the distances between the mother and the daughter kinetoplast were increased. These unusual kinetoplast positions were found both in 2K2N cells without a division furrow as well as in cells that had already started dividing (Fig. 38A). The kinetoplast distances of 400 randomly chosen tetracycline induced and non-induced 2K2N cells were measured and are shown in figure 38B. The average kinetoplast distance was $2.72 \pm 0.61 \mu\text{m}$ in non-induced cells and increased to $3.85 \pm 1.92 \mu\text{m}$ upon PKAR depletion. 35.3% of the induced cells had kinetoplast distances higher than $4 \mu\text{m}$, compared to only 2.5% of the control cells. The difference between the kinetoplast distances of induced and non-induced cells is highly significant with a t-test P-value (1 tail, unpaired) of 1.21×10^{-26} .

3.4.2.1.5. The increased kinetoplast distances are not a consequence of cytokinesis block

Two mechanisms could account for the observed increase in kinetoplast distance in response to PKAR RNAi. Either PKAR is directly involved in the regulation of kinetoplast movement or the increase in kinetoplast distance is a secondary effect that results from

the cytokinesis block.

In order to distinguish between these two possibilities, kinetoplast positions needed to be studied with cytokinesis being blocked using method unrelated to PKA-like kinase. In *T. cruzi*, cytokinesis but not kinetoplast movement was found to be blocked with 100 μM of the microtubules inhibitor vincristine (Grellier *et al.*, 1999). In *T. brucei*, similar effects were obtained with 0.2 μM vincristine. Cells were completely growth arrested within 4 hours. The number of 2K2N cells was significantly increased after 6 hours and nearly two thirds of these 2K2N cells ($62\pm 3\%$ compared to only 11% of the control cells) possessed a cleavage furrow. 2K2N cells were perfectly able to further divide and segregate their kinetoplasts, resulting in 4K2N cells. The data are shown in attachment 2.

However, the kinetoplast positions in the vincristine treated cells appeared to be normal. The mother kinetoplast was never found to be near the posterior nucleus. The average kinetoplast distance for vincristine treated cells was with $2.26\pm 0.52 \mu\text{m}$ even smaller than the kinetoplast distance of untreated control cells ($2.83\pm 0.57 \mu\text{m}$) (Fig. 38C). The slight reduction in kinetoplast distance in response to vincristine incubation is due to the unusually high amount of cells (2/3 of all 2K2N cells) that were blocked in the process of cell division. When measuring the direct distance, the kinetoplasts move closer towards each other during this stage of cytokinesis.

To summarize, cytokinesis inhibition with vincristine did not result in increased kinetoplast distances. Conclusively, the observed increase in kinetoplast distance upon PKAR RNAi is probably not a consequence of the cell cycle arrest in cytokinesis. Instead, evidence is that *T. brucei* PKA-like kinase directly regulates basal body segregation.

	WT	PKAR RNAi					
Growth	PDT: 5.5-6 h	growth arrest [8 h]					
[2K2N]	10-15%	40-48% [8 h]					
[1K2N]	0%	1.7 -3.9% [8 h]					
[2K2N cells with division furrow]	8-12%	35-40% [8 h]					
increase in kinetoplast distance	NO	YES					

The table summarizes all PKA phenotypes describes so far.

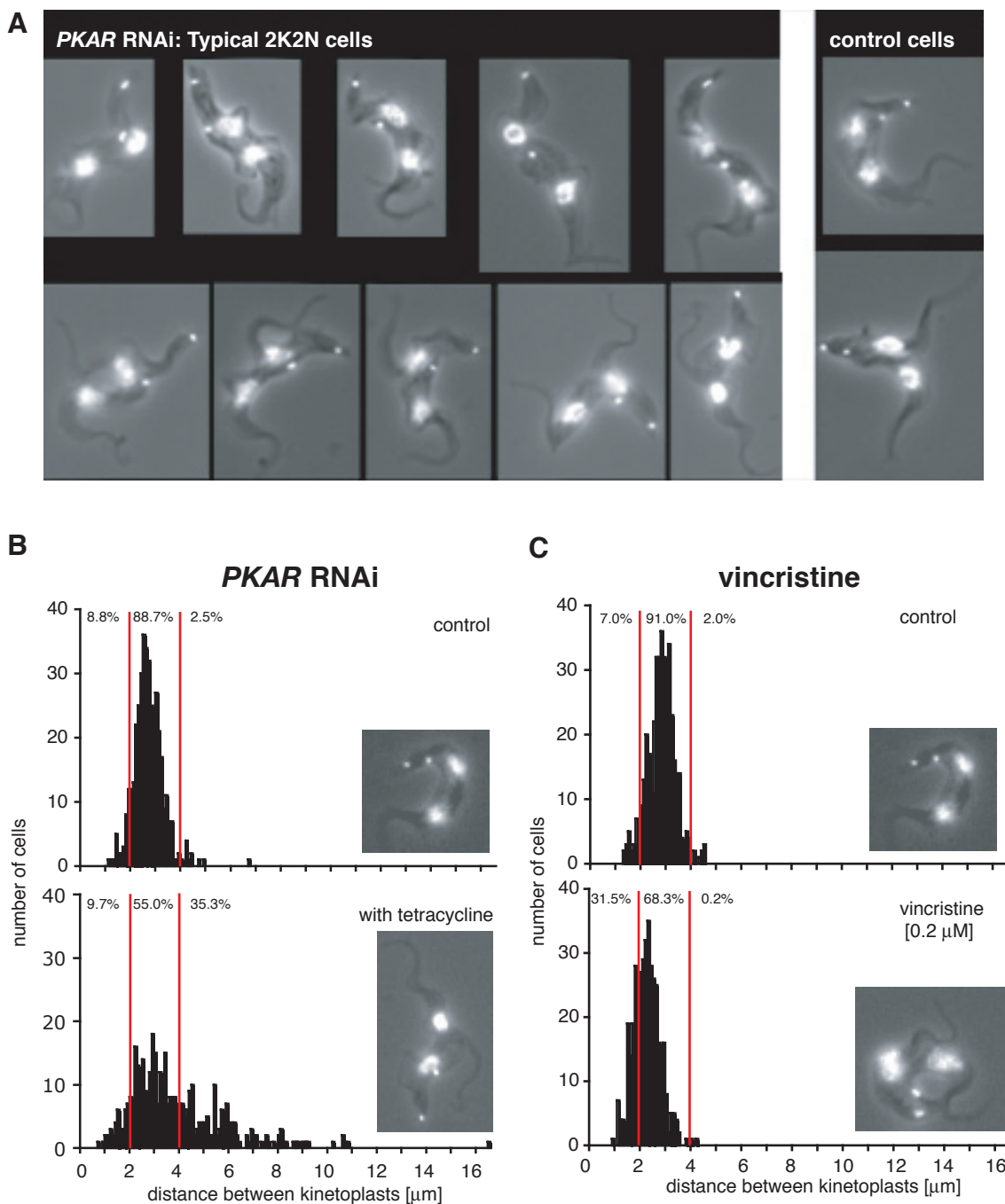


Fig. 38: Increase in kinetoplast distances after *PKAR* depletion

A) Photographs of DAPI stained 2K2N cells of tetracycline induced and uninduced (control) *PKAR* RNAi cells.

B) Distances between mother and daughter kinetoplast in induced and uninduced *PKAR* RNAi cells. Photographs of 400 2K2N cells were randomly taken and the distance between the two kinetoplasts was determined using the software IP-lab. When the cell was bended, kinetoplast distances were measured according to cell shape rather than in direct line. Cells with kinetoplast distances varying within $0.1 \mu\text{m}$ were pooled. The histogram plots the kinetoplast distance (with a $0.1 \mu\text{m}$ resolution) to the number of cells. In addition, the percentage of cells with kinetoplast distances below $2 \mu\text{m}$, between 2 and $4 \mu\text{m}$ and above $4 \mu\text{m}$ is indicated for both uninduced and induced cells. A photograph of a typical 2K2N cell of tetracycline induced and uninduced *PKAR* RNAi cells is shown together with each histogram

C) Distances between kinetoplasts in the presence of vincristine:

Cytokinesis was inhibited with $0.2 \mu\text{M}$ vincristine to examine whether the observed increase in kinetoplast distance upon *PKAR* RNAi is due to cytokinesis inhibition. The quantification of the kinetoplast distances was performed as described in B).

3.4.2.2. Reverse genetic interference with PKAC1/2

It was shown that the PKA regulatory subunit is involved in the regulation of cytokinesis and kinetoplast movement. However, the data described above did not reveal whether this phenotype is due to the loss or gain of kinase activity and if there are functional differences between the three catalytic subunits of PKA-like kinase. Therefore, in a second approach, the functions of the two very homologous subunits, PKAC1 and PKAC2, were investigated reverse genetically by gene deletion (knock-out and hemizygous knock-out) and inducible RNA interference.

3.4.2.2.1. Deletion of *PKAC2* led to reduced growth and block in cytokinesis

Given that *PKAC2* is hardly present in LS cells (compare chapter 3.1.2.) and therefore possibly not essential, it was aimed to generate *PKAC2* null mutants for the reverse genetic investigation of *PKAC2* function. The strategy for the deletion of *PKAC2* is shown in figure 39. At first, one *PKAC2* allele of the monomorphic trypanosoma strain MITat1.2 was replaced by a hygromycin resistance gene upon transfection with the *PKAC2* targeting construct p Δ *PKAC2**HYG* (provided by P. Hassan). Several hygromycin resistant clones were obtained that had no obvious phenotypes. For the deletion of the second *PKAC2* allele one of these clones (clone 2) was further transfected with p Δ *PKAC2**NEO* (provided by P. Hassan), aiming to replace the remaining *PKAC2* allele with a neomycin resistance gene.

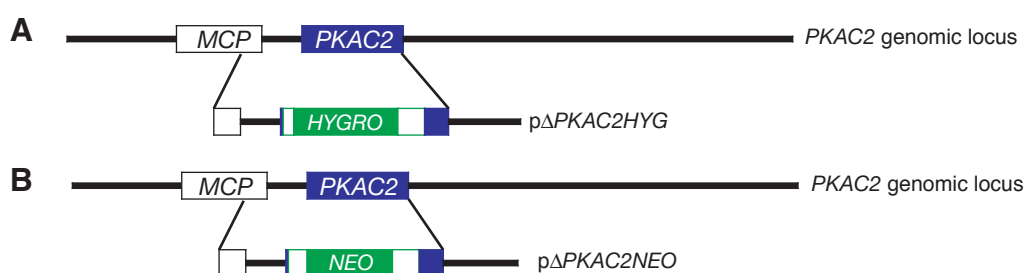


Fig. 39: Deletion of *PKAC2*

PKAC2 is shown in a scaled drawing on its genomic locus together with its upstream gene *MCP* (putative mitochondrial carrier protein, Tb09.211.2370).

A) Deletion of the first *PKAC2* allele: WT *PKAC2* was replaced by a hygromycin resistance gene (green) together with the 5'UTR and 3'UTR of *ACTIN* (green, unfilled).

B) Deletion of the second *PKAC2* allele: WT *PKAC2* was replaced by a neomycin resistance gene (green) together with the 5'UTR and 3'UTR of *ACTIN* (green, unfilled).

The genomic locus of *PKAC1/2* is shown in more detail in attachment 1.

After the second transfection only one double resistant clone (clone 2-1) was obtained. Southern analyses confirmed that it had both *PKAC2* alleles correctly replaced by the targeting constructs (Fig. 40A) and did not possess any further WT *PKAC2* genes (Fig. 40B). The *PKAC2* knock-out cells did grow unusually slowly. During the first week after transfection the population doubling time was about 8.5 hours. It increased slightly during the time cells were kept in culture. The very low clone recovery efficiency together with the decreased growth rate indicated that PKAC2 is important for normal growth in BSF cells, despite of its low abundance in these cell forms.

The *PKAC2* knock-out cells were examined in more detail together with hemizygous *PKAC2* knock-out cells and WT cells. The later two served as controls. At the time of the analysis the population doubling times were 6.8 hours for the knock-out and 6.3 and 5.6 hours for the hemizygous knock-out and WT, respectively (Fig. 41A). An analysis of the K/N configurations revealed that the percentage of 2K2N cells and multinucleated cells (xKyN; x,y>2) was slightly increased in the hemizygous *PKAC2* knock-out (22±3% 2K2N) and significantly higher in the knock-out (31±4% 2K2N) (Fig. 41B). A more detailed investigation of the 2K2N cells further showed that an unusually high amount of these cells had a division furrow reaching to approximately half of the cell body (Fig. 41C).

To summarize, PKAC2 depletion resulted in block in cytokinesis, similar to what was observed after PKAR depletion. In contrast to the PKAR RNAi phenotype we did not find changes in kinetoplast positions in the *PKAC2* knock-out cells. Surprisingly, the deletion of only one *PKAC2* allele was already sufficient to achieve the observed phenotype, despite of the low PKAC2 expression in blood stream forms.

	WT	PKAR RNAi	PKAC2 k.o.					
Growth	PDT: 5.5-6 h	growth arrest [8 h]	PDT: 6.82 h					
[2K2N]	10-15%	40-48% [8 h]	31%					
[1K2N]	0%	1.7 -3.9% [8 h]	not sign.					
[2K2N cells with division furrow]	8-12%	35-40% [8 h]	25%					
increase in kinetoplast distance	NO	YES	NO					

The table summarizes all PKA phenotypes describes so far.

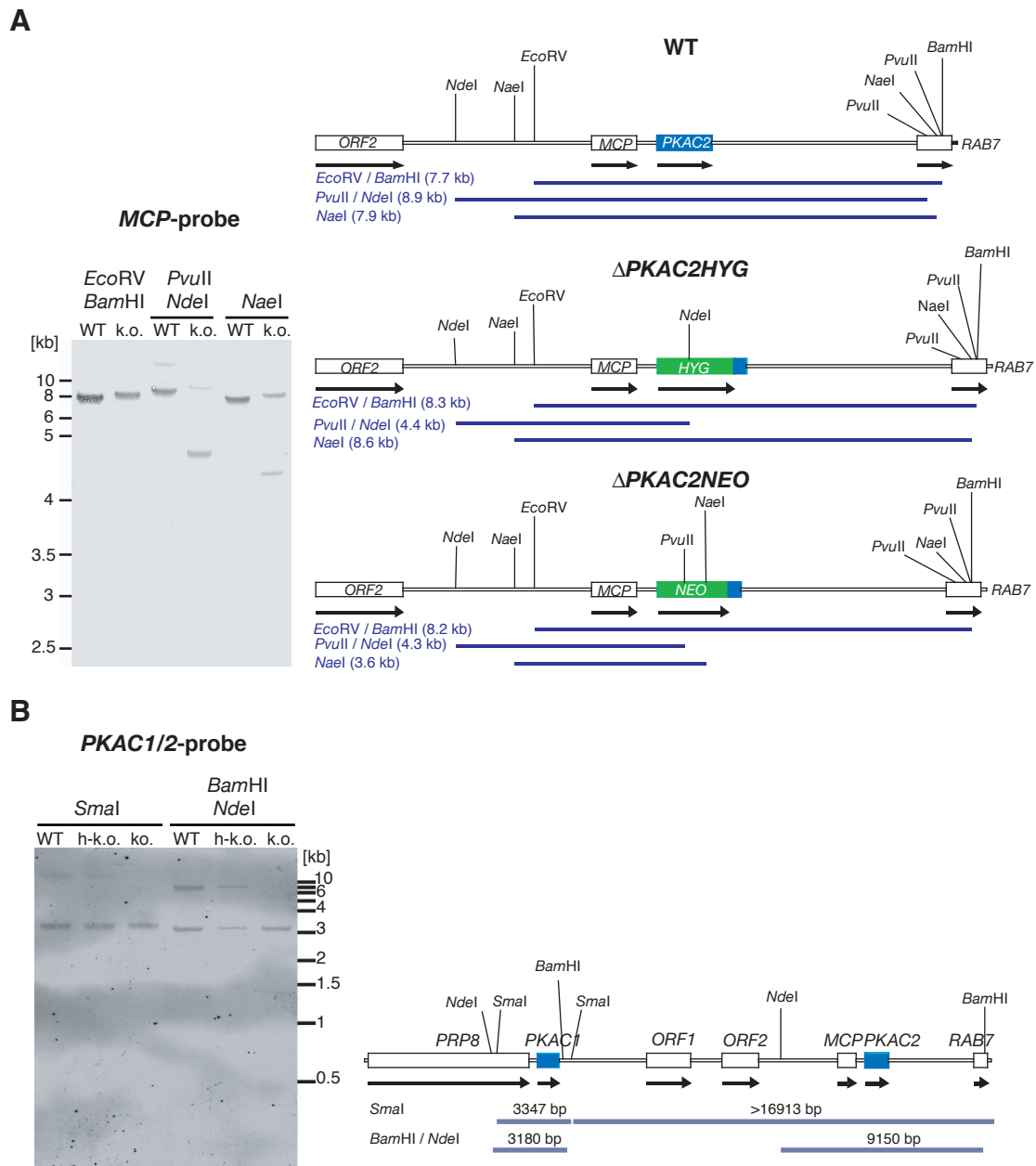


Fig. 40: Southern analyses of PKAC2 knock-out and PKAC2 hemizygous knock-out cells

A) Both PKAC2 knock-out constructs are integrated at the correct positions

Genomic DNA of WT cells and PKAC2 knock-out cells (k.o.) was digested with the indicated enzymes, separated on an agarose gel and blotted to a nylon membrane. The blot was probed with digoxigenine labeled MCP. MCP (Tb09.211.2370) is the gene upstream of PKAC2. It was used instead of a PKAC1/2 probe to enable the detection of the PKAC2 knock-out fragments. Restriction maps are shown for the WT, Δ PKAC2HYG and Δ PKAC2NEO locus. Sizes of the expected DNA fragments are indicated.

B) No PKAC2 WT alleles are present

Genomic DNA of WT cells, hemizygous PKAC2 knock-out (h-k.o.) and PKAC2 knock-out (k.o.) cells was digested with the indicated enzymes, separated on an agarose gel and blotted to a nylon membrane. The blot was probed with digoxigenine labeled PKAC1/2 probe. A restriction map of the WT locus is shown on the right site. Note that the PKAC1/2 probe detects both PKAC1 and PKAC2 but not the deleted PKAC2 allele. The correct integration of the PKAC2 knock-out construct is thus proven by the absence of PKAC2 detection in the PKAC2 knock-out cell line.

The PKAC1/2 genomic locus, including the positions of the PKAC1/2 and MCP probe, is shown in attachment 1.

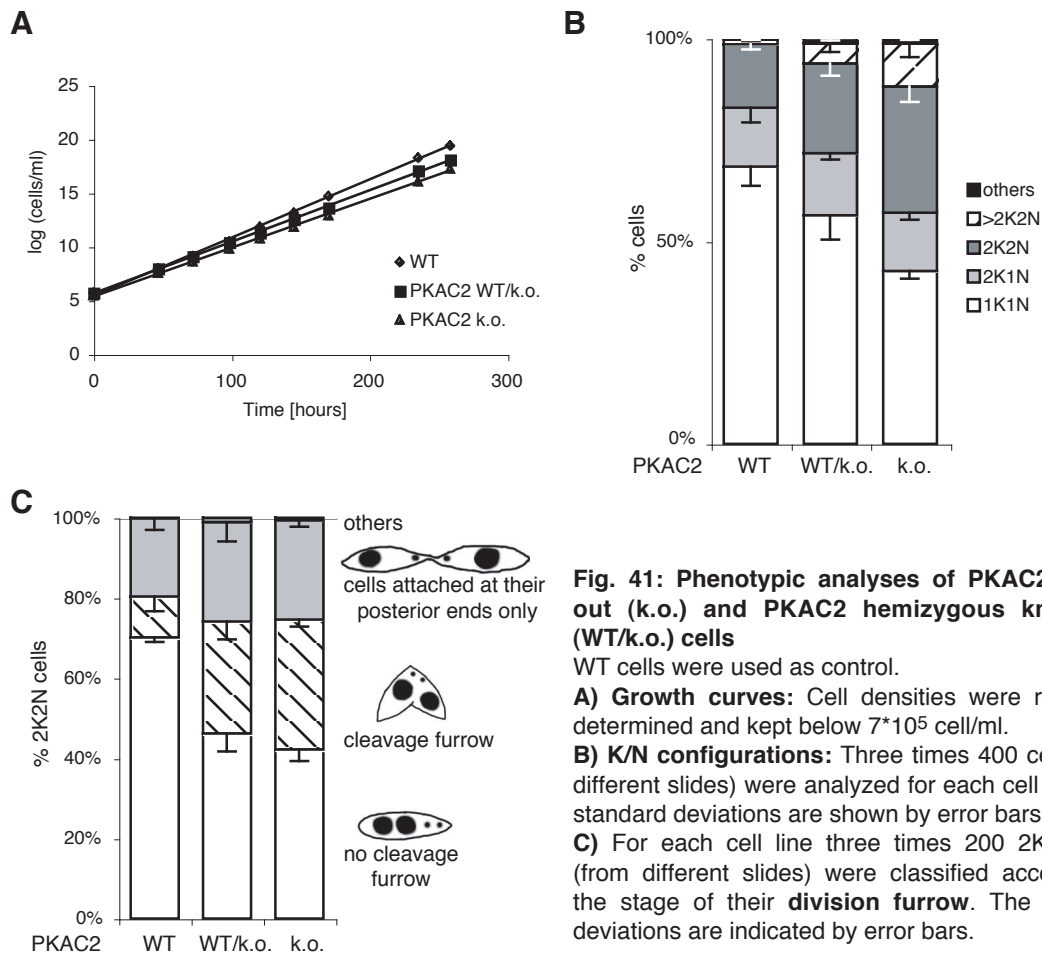


Fig. 41: Phenotypic analyses of PKAC2 knock-out (k.o.) and PKAC2 hemizygous knock-out (WT/k.o.) cells

WT cells were used as control.

A) Growth curves: Cell densities were regularly determined and kept below $7 \cdot 10^5$ cell/ml.

B) K/N configurations: Three times 400 cells (from different slides) were analyzed for each cell line. The standard deviations are shown by error bars.

C) For each cell line three times 200 2K2N cells (from different slides) were classified according to the stage of their **division furrow**. The standard deviations are indicated by error bars.

3.4.2.2.2. PKAC2 is not essential for differentiation into procyclic cells

PKAC2 expression depends on the life cycle stage showing low expression levels in LS cells. These levels increase in SS cells and are at their highest in procyclic cells (compare chapter 3.1.2.). Thus, although *PKAC2* knock-out cells had only a slight growth phenotype in the long slender stage, they might have a stronger phenotype in later developmental stages. Therefore, *PKAC2* null mutant cells were tested for their ability to transform into procyclic cells. An *in vitro* transformation was performed with *PKAC2* knock-out cells, *PKAC2* hemizygous knock-out cells and WT cells. Growth and morphology was monitored simultaneously.

All cells were able to successfully transform into procyclic cells, judged by morphology. During the transformation, no significant differences in growth were observed between knock-out, hemizygous knock-out and WT cell (Fig. 42). Thus, PKAC2 is not essential for the differentiation into procyclic cells.

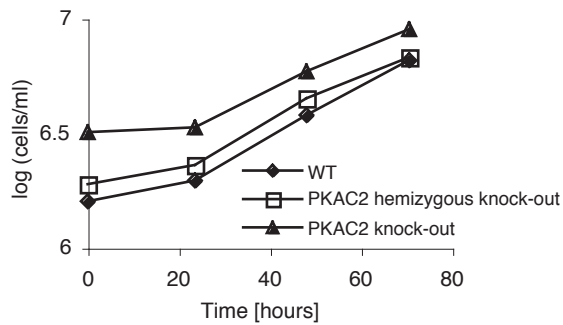


Fig. 42: Growth during transformation of PKAC2 knock-out cells into PCFs

PKAC2 knock-out cells, PKAC2 hemizygous knock-out cells and WT cells, the latter serving as control, were *in vitro* transformed into procyclic cells. The cell density was measured every 24 hours. The success of the transformation was additionally controlled morphologically.

3.4.2.2.3. Deletion or mutation of one *PKAC1* allele results in reduced growth and block in cytokinesis

Two different strategies were chosen for the functional analysis of PKAC1, the predominant PKAC1/2 isoform in BSF cells.

At first, one *PKAC1* allele was replaced by a blasticidin resistance gene (*BSD*) with the aim to reduce the PKAC1 expression level. Therefore, the targeting construct $p\Delta PKAC1 BSD$ (P. Hassan) was transfected into the monomorphic cell line MITat1.2. Several blasticidin resistant clonal populations were obtained and one clone (clone 5) was chosen for further analysis (*PKAC1* hemizygous knock-out).

Alternatively, *PKAC1* was not deleted but replaced by a mutated *PKAC1* gene (N165->A) resulting in the expression of catalytically inactive PKAC1 (dead mutant). In order to enable immunoprecipitations, this dead mutant PKAC1 was further equipped with an N-terminal Ty1-tag. Several independent Ty1-PKAC1-dead clones were obtained and clone 11,12 and 14 were chosen for further analysis of PKAC1 function. Immunoprecipitated Ty1-PKAC1-dead was catalytically inactive (see Fig. 20, chapter 3.2.3.).

A summary of the cell lines that were used for the functional PKAC1 analysis is shown in figure 43. In addition to the cell lines mentioned above, WT cells and two different clones of Ty1-PKAC1 cells (without the dead mutation) were used as controls. Southern analyses confirmed that all cell lines had the expected genotype (Fig. 44A). Furthermore, all clones (except of course the *PKAC1* hemizygous knock-out) expressed Ty1 epitope tagged PKAC1 (Fig. 44B).

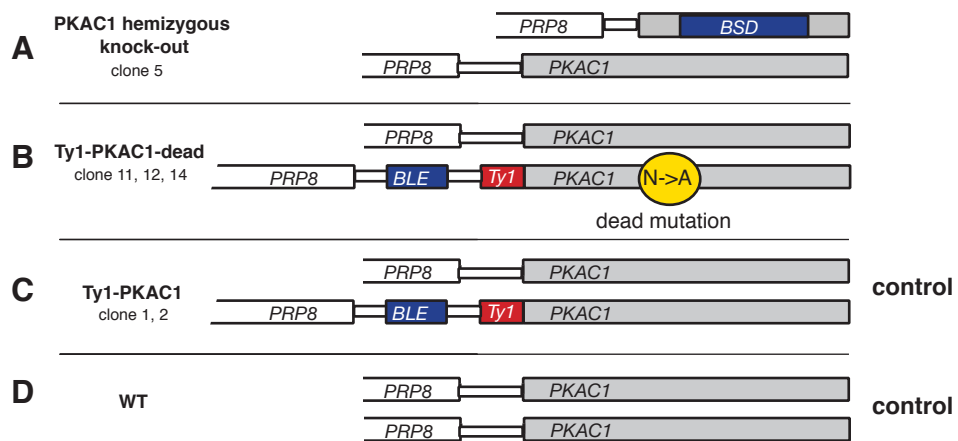


Fig. 43: Overview about the cell lines used to examine PKAC1 function

Schematic non-to-scale drawing of the cell lines that were used for the functional analysis of PKAC1. Both alleles of the *PKAC1* genomic locus (together with the 3' part of its upstream gene *PRP8*) are shown. The positions of the blasticidin resistance genes (*BSD*, blue), the phleomycin resistance genes (*BLE*, blue), the Ty1-epitope tags (red) and the dead mutation (N->A, yellow) are indicated. Further information about the *PKAC1/2* genomic locus is available in attachment 1.

A) One WT *PKAC1* allele was exchanged by a blasticidin resistance gene using the construct p Δ *PKAC1**BSD* (P.Hassan). Clone 5 was used for subsequent phenotypic analysis.

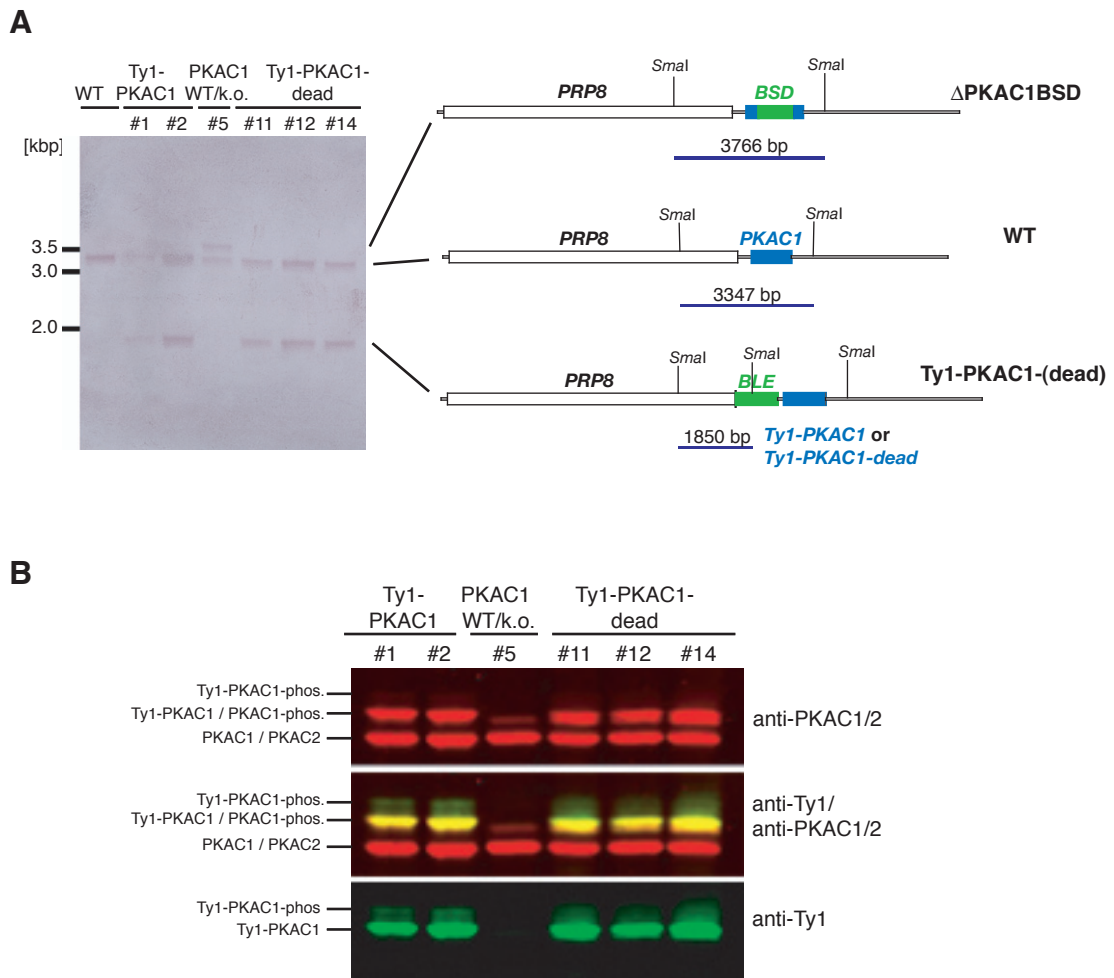
B) One WT *PKAC1* allele was replaced by a Ty1-epitope tagged PKAC1 dead mutant using the construct p*Ty1-PKAC1-dead*. Three clonal transfectants were used for subsequent phenotypic analyses (clones 11,12,14). Ty1-PKAC1-dead is catalytically inactive (Fig. 20, chapter 3.2.3.).

C) One WT *PKAC1* allele was replaced by a Ty1-epitope tagged PKAC1. Two clonal transfectants (clone 1 and 2) were used for phenotypic analyses. This cell line served as a control.

D) WT cells (MITat1.2) were used as further control.

All cell lines were now applied to phenotypic characterization. Both Ty1-PKAC1-dead and *PKAC1* hemizygous knock-out cells had a reduced growth rate (Fig. 45A). Population doubling times were 7.9 for Ty1-PKAC1-dead (average value of #11,12,14) and 6.5 hours for *PKAC1* hemizygous knock-out cells, compared to 5.5 hours in WT cells. K/N configuration analyses revealed that the amount of 2K2N cells was doubled in both the Ty1-PKAC1-dead and *PKAC1* hemizygous knock-out cells (Fig. 45B). Additionally, one quarter of the cells was multinucleated. A more detailed analysis of the 2K2N cells showed that 50% of these cells had a division furrow and were halfway through cytokinesis, compared to only 12% of the 2K2N cells from the control cell lines (Fig. 45C). Photographs of typical 2K2N and multinucleated cells are shown in figure 45D. Usually, the multinucleated cells consisted of several cell bodies attached to each other instead of having a single cell body.

The observed phenotype was thus very similar to the phenotype that had been observed in the *PKAC2* null mutant cell lines and with PKAR RNAi. Cells were unable to successfully progress through cytokinesis resulting in an increase in 2K2N cells with a division furrow



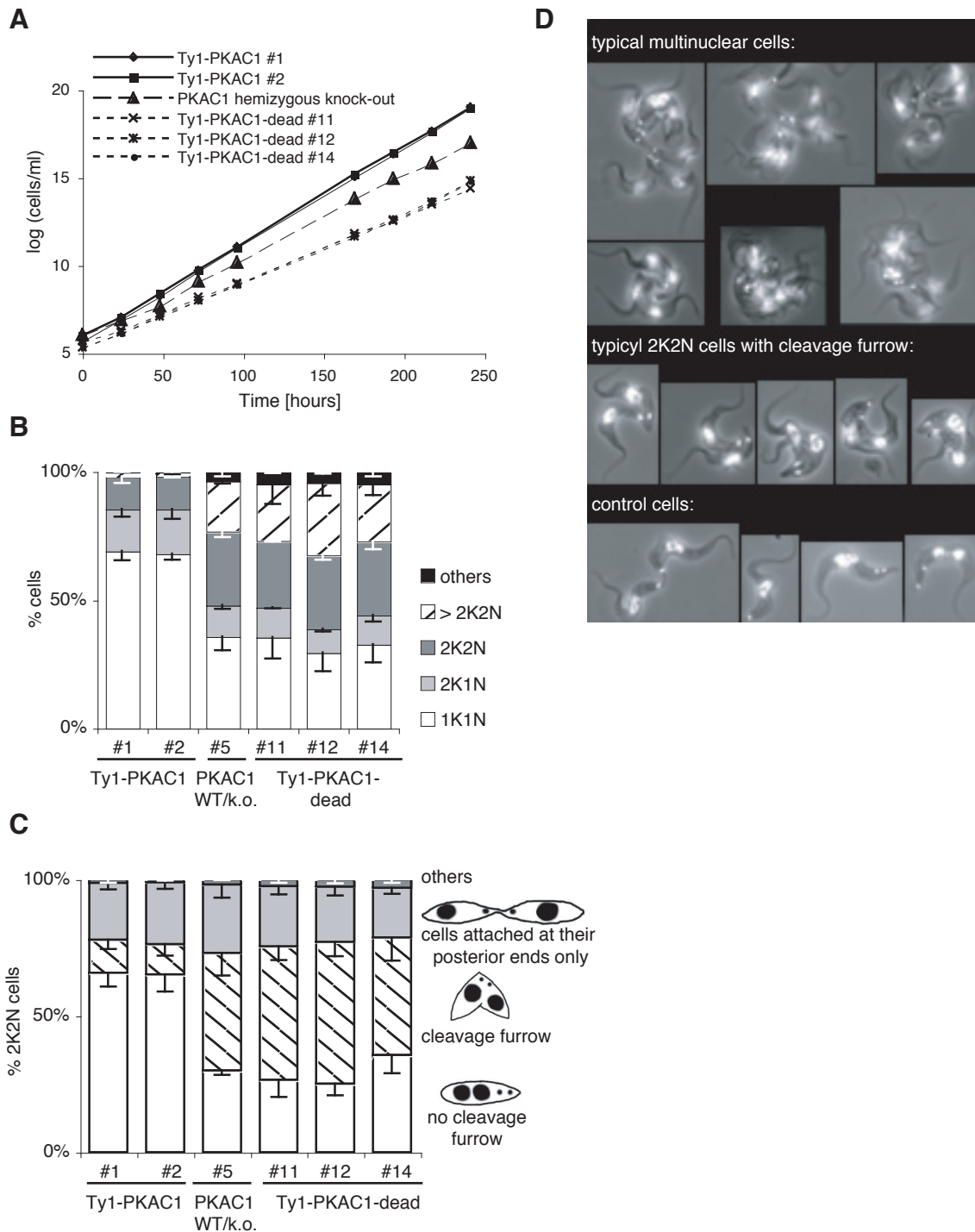


Fig. 45: Deletion or inactivation of one *PKAC1* allele prevents cells from cytokinesis progression

The subsequently described analyses were performed with the cell lines introduced in figure 43.

A) Growth curves: Cell densities were measured regularly and kept below $7 \cdot 10^5$ cells/ml.

B) K/N configuration: Cells were methanol fixed on a slide and K/N configurations of 400 DAPI stained cells were determined. Three different slides were analyzed from each cell line. Average values from these three slides are shown in the diagram and standard deviations are indicated as error bars.

C) Stage of the division furrow: 2K2N cells of the slides from (B) were grouped according to the stage of their division furrows. 200 cells were analyzed from each slide, thus 600 for each cell line. Standard deviations are indicated by error bars.

D) Photographs of typical multinucleated and 2K2N cells of the PKA dead mutant cell line (#12) are shown. Cells of the other clones as well as of the PKAC1 hemizygous knock-out cell line look similar.

reaching to approximately half of the cell body.

The PKAC1 dead mutant cells showed a stronger growth phenotype compared to the hemizygous *PKAC1* knock-out cells. While both cell lines lack one functional *PKAC1* allele (gene doses effect), in the PKAC1 dead mutants an additional dominant negative effect might occur due to the binding of inactive PKAC1 to the regulatory subunit.

	WT	PKAR	PKAC2	PKAC1				
		RNAi	k.o.	hemizyg. k.o.	dead mutant			
Growth	PDT: 5.5-6 h	growth arrest [8 h]	PDT: 6.82 h	PDT: 6.5 h	PDT: 7.9 h			
[2K2N]	10-15%	40-48% [8 h]	31%	29%	28%			
[1K2N]	0%	1.7 -3.9% [8 h]	not sign.	not sign.	not sign.			
[2K2N cells with division furrow]	8-12%	35-40% [8 h]	25%	43-52%	43%			
increase in kinetoplast distance	NO	YES	NO	NO	NO			

The table summarizes all PKA phenotypes describes so far.

3.4.2.2.4. Gene conversion of the WT *PKAC1* allele in hemizygous PKAC1 dead mutants

Further evidence for the essentiality of PKAC1 in BSF trypanosomes was found during the generation of the PKAC1 dead mutant cell lines described above. Phleomycin resistant clonal transfectants that contained active Ty1-PKAC1 instead of the dead mutant Ty1-PKAC1 were frequently obtained (data not shown). This interesting phenomenon was further examined by a systematic screening of the genomic DNA of 30 clonal transfectants for the presence or absence of the dead mutation in Ty1-PKAC1 (done by Anne Marinière). It turned out that 18 of these transfectants had WT Ty1-PKAC1 instead of the dead mutant Ty1-PKAC1. One example of such a screen is shown in figure 46. Thus, it seems that the replacement of one *PKAC1* allele by a gene coding for inactive PKAC1 favours the selection of cells that repair this gene. This probably occurs by a gene conversion event with the aid of the intact WT *PKAC1* allele.

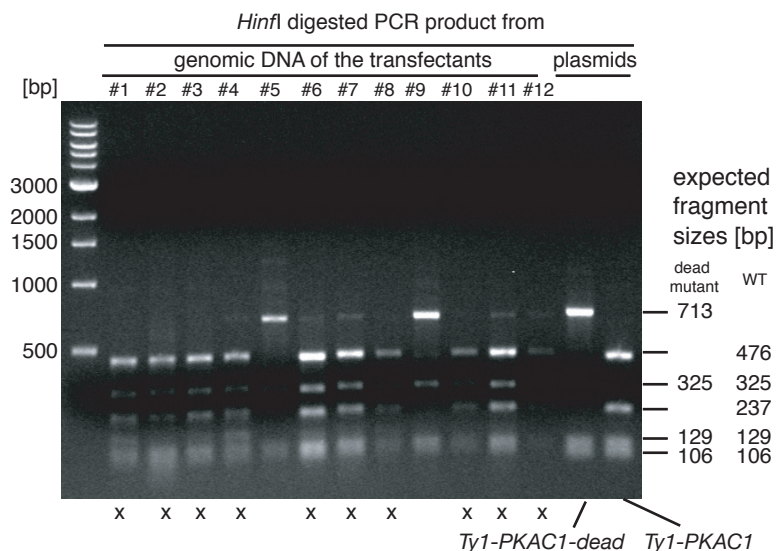


Fig. 46: Screen for gene conversion in hemizygote PKAC1-dead mutants

MITat1.2 WT cells were transfected with the construct *pTy1-PKAC1-dead*. Genomic DNA was prepared from 12 clonal transfectants after approximately 25 cell divisions (thus as soon as 50 ml cells were available). *Ty1-PKAC1* was amplified from the genomic DNA (using the oligos 19.11.01 ty1/upper and *PKAC1.seq.l.19/7/01*) and screened for the dead mutation (N165->A). This was possible with a *HinfI* restriction digest because WT *PKAC1* contained one *HinfI* site more than dead-mutant *PKAC1*.

The agarose gel with the *HinfI* digests is shown. The expected fragment sizes for the *HinfI* digestion of dead mutant *PKAC1* and WT *PKAC1* are indicated on the right site. Out of the 12 clones that were examined in this experiment, 10 had lost their dead mutant *PKAC1*, these clones are marked with an x. The experiment was done by Anne Marinière (lab student).

3.4.2.2.5. Depletion of PKAC1/2 with RNAi results in cytokinesis block and cell death

The gene deletion experiments described above for PKAC1 and PKAC2 were exclusively performed using stable transfected cell lines. Thus, it may be that these cell lines had adapted to compensate for the loss of one PKAC allele before we were able to analyze them. For this, an additional experiment based on PKAC1 and PKAC2 reduction by inducible RNA interference was performed.

However, these RNAi experiments proved to be particularly difficult. Although several different parts of the *PKAC1/2* sequence were used as a template for RNAi (including the 5'UTRs of *PKAC1* and *PKAC2*) all transfectants did either show no reaction to tetracycline or had already a phenotype without tetracycline (data not shown). The most likely reason for this is the relatively low concentration of tet repressor in the 13-90 cell line. It allows a weak transcription of the target sequence in the p2T7 vector even in the absence of tetracycline (leakiness). In the 13-90 cell line the tet repressor is cotranscribed

with a hygromycin resistance gene (*hygromycin phosphotransferase*). Hygromycin is inactivated by phosphorylation (thus, a catalytic process), enabling relatively few proteins of hygromycin phosphotransferase to sufficiently inactivate many hygromycin molecules. Therefore there is low selective pressure on expression level of the tet repressor. To overcome this problem, a different tetracycline inducible cell line was used. In this cell line (1313-514, C. Clayton, unpublished) the tet repressor is transcribed together with a phleomycin resistance gene (*BLE*). The BLE protein inactivates phleomycin by binding to it. It is therefore needed in at least equimolar concentrations to phleomycin, resulting in a selection pressure towards cells with a high transcription rate of the *BLE* gene and therefore also the tet repressor. Additionally, it was necessary to use a different RNAi vector (p2T7TAbblue, Alibu *et al.*, in press) carrying hygromycin resistance instead of phleomycin resistance.

The PKAC1 N-terminal fragment (corresponding to the amino acids 10 to 216) was cloned into the p2T7TAbblue vector and transfected into 1313-514 BSF cells (cell line and vector kindly provided by C. Clayton, Heidelberg).

Out of 12 hygromycin resistant clonal populations two were selected showing no or little phenotype in the absence of tetracycline but a strong growth phenotype after overnight induction (clone 2 and 3). Further analyses revealed that cells stopped growing within four hours after tetracycline was added and died within two days (Fig. 47A). Cells looked abnormal (fat, shapeless, multiple cell bodies) after 4 to 6 hours. A decrease of PKAC1/2 protein was observed after 4 to 8 hours (80-90%) accompanied by a slight decrease in PKAR protein (20-35%) (Fig. 47B). Considering the high homologies between PKAC1 and PKAC2 it is probable that both isoforms are affected by RNA interference, although they cannot be distinguished on a Western blot. The RNAi phenotype was investigated in more detail by a K/N configuration analysis with DAPI stained cells (Fig 47C). A significant increase in 2K2N cells and multinucleated cells was already found four hours after induction with tetracycline. Within 8 hours nearly 100% of the population consisted of 2K2N and multinucleated cells. After 10 hours more than two thirds of the cells were multinucleated. Note that an unusually high fraction of multinucleated cells was also found in the non-induced control cells, suggesting that there is still a certain degree of T7 polymerase dependent transcription in the absence of tetracycline even with the 1313-514 cell line. A very slight increase in 1K2N cells was found after 10 hours (1.2 to 3-5%).

A more detailed examination of the 2K2N cells revealed that an unusually high number

of these cells had a division furrow reaching to approximately half of the cell body (Fig. 47D). Multinucleated cells usually consisted of multiple cell bodies. Typical 2K2N and multinucleated cells are shown in figure 47E.

To summarize, the PKAC1/2 RNAi phenotype is qualitatively identical to the phenotypes observed after reducing the levels of PKAC1 or PKAC2 by gene deletion. Cells are unable to complete cytokinesis and instead proceed to the next M phase. However, the RNAi phenotype is stronger than the gene deletion phenotypes.

	WT	PKAR	PKAC2	PKAC1		PKAC1/2		
		RNAi	k.o.	hemizyg. k.o.	dead mutant	RNAi		
Growth	PDT: 5.5-6 h	growth arrest [8 h]	PDT: 6.82 h	PDT: 6.5 h	PDT: 7.9 h	growth arrest [4 h] dead [2 d]		
[2K2N]	10-15%	40-48% [8 h]	31%	29%	28%	58% [6 h]		
[1K2N]	0%	1.7 -3.9% [8 h]	not sign.	not sign.	not sign.	1.2-3.5% [10 h]		
[2K2N cells with division furrow]	8-12%	35-40% [8 h]	25%	43-52%	43%	32-40% [6 h]		
increase in kinetoplast distance	NO	YES	NO	NO	NO	NO		

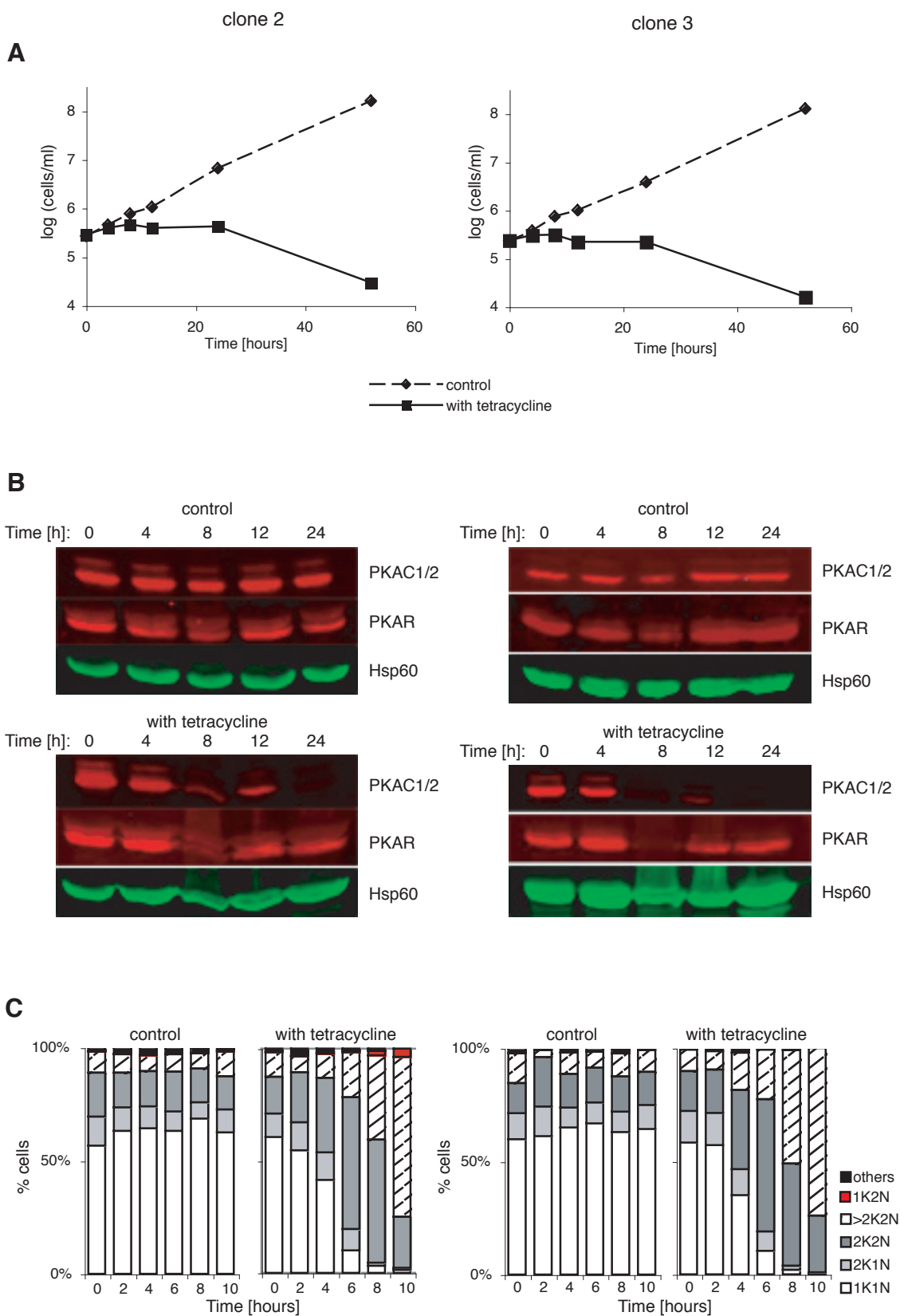
The table summarizes all PKA phenotypes describes so far.

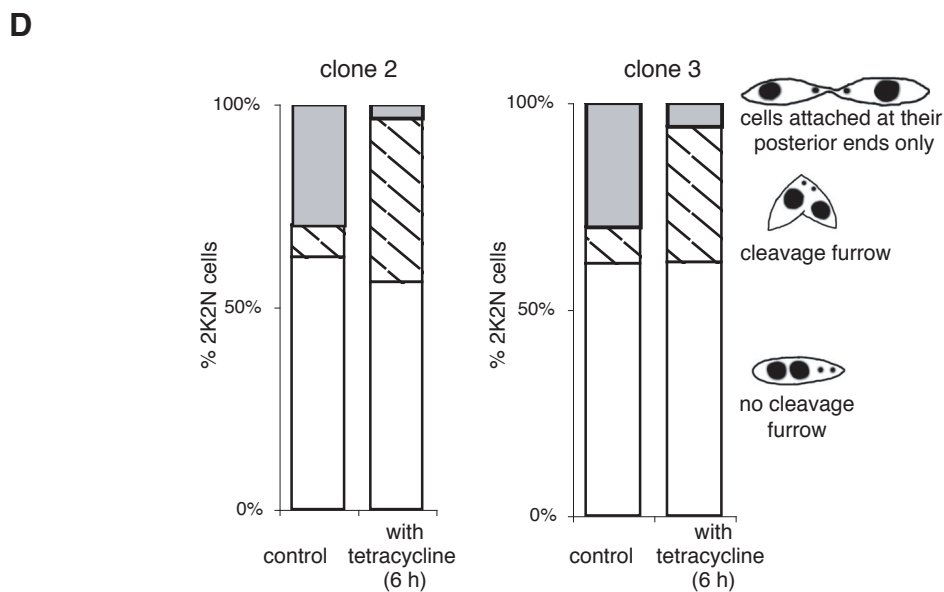
3.4.2.2.6. The PKAC1/2 specific inhibitor KT5720 led to block in cytokinesis and accumulation of 1K2N cells

KT5720 is a specific inhibitor for PKAC1/2 with much less inhibition of PKAC3 (see Fig. 26C in chapter 3.3.4.3.). For this reason it was used to further examine PKAC1/2 function.

Cells (MITat1.2) were incubated in the presence of KT5720 dissolved in DMSO. The optimal inhibitor concentration for the experiments was found to be 4 μ M. Higher concentrations killed the cells within 3 hours and lower concentrations showed no effect. Growth and K/N configurations of cells treated either with KT5720 or with DMSO (control) were analyzed after 3 and 6 hours.

Within the first 3 hours, KT5720 treated cells grew very slowly and after 6 hours the number of cells decreased (Fig. 48A). After 3 hours of incubation with KT5720 the number of 2K2N cells was significantly increased to more than 40%, while the number of multinucleated cells and 1K2N cells only increased slightly (Fig. 48B). The number





E

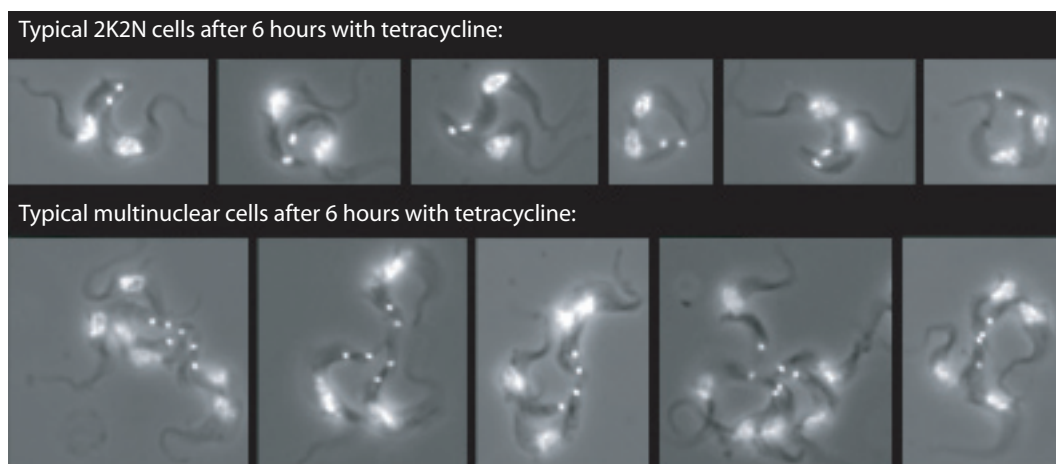


Fig. 47: Depletion of PKAC1/2 using inducible RNA interference

PKAC1/2 RNAi cells were incubated in the presence or absence (control) of tetracycline for 52 hours. Data from two independent clonal cell lines (#2 and #3) are shown.

A) Growth curves of induced and uninduced PKAC1/2 RNAi cells. Cell densities were kept below 7×10^5 cells/ml.

B) Western blots. Protein samples of uninduced and induced cells were collected at the times indicated and applied to SDS PAGE. The resulting Western blots were incubated with anti-PKAR, anti-PKAC1/2 and anti-Hsp60, the latter serving as control for equal loading. Rabbit Alexa680 (red) and Mouse IRDye800 (green) were used for the detection of anti-PKAR/anti-PKAC3/anti-PKAC1/2 and anti-Hsp60, respectively, using the Odyssey IR scanner (Licor).

C) K/N configurations: Cells were fixed in methanol after 0, 2, 4, 6, 8 and 10 hours of incubation with or without tetracycline and subsequently stained with DAPI. K/N configurations of 400 cells were determined for each time point.

D) 2K2N cells and 1K2N cells were classified according to the stage of their **division furrows**. 200 cells were analyzed for each clone. Cells had been incubated with or without tetracycline for 6 hours.

E) Photographs of typical multinucleated cells observed after RNAi depletion of PKAC1/2 (6 hours induction). Nuclei and kinetoplasts are stained with DAPI.

of 2K2N cells with a division furrow slightly increased in the presence of KT5720 (Fig. 48C).

After 6 hours of incubation with KT5720 one forth of the cells had the unusual 1K2N K/N configuration (Fig. 48D), many of these cells had a division furrow.

	WT	PKAR	PKAC2	PKAC1		PKAC1/2		
		RNAi	k.o.	hemizyg. k.o.	dead mutant	RNAi	KT5720	
Growth	PDT: 5.5-6 h	growth arrest [8 h]	PDT: 6.82 h	PDT: 6.5 h	PDT: 7.9 h	growth arrest [4 h] dead [2 d]	growth arrest [3 h]	
[2K2N]	10-15%	40-48% [8 h]	31%	29%	28%	58% [6 h]	41% [3 h]	
[1K2N]	0%	1.7 -3.9% [8 h]	not sign.	not sign.	not sign.	1.2-3.5% [10 h]	1.7% [3 h] 26.3% [6 h]	
[2K2N cells with division furrow]	8-12%	35-40% [8 h]	25%	43-52%	43%	32-40% [6 h]	16% [3h]	
increase in kinetoplast distance	NO	YES	NO	NO	NO	NO	NO	

The table summarizes all PKA phenotypes describes so far.

3.4.2.3. Depletion of PKAC3 results in cytokinesis block and accumulation of 1K2N cells, but not in decreased kinetoplast distances

An increase in 1K2N cells, such as was found upon inhibition of PKAC1/2 with KT5720, has already been described for the third catalytic PKA subunit (PKAC3) by Thorsten Riek (Diploma thesis 2001). The function of PKAC3 was investigated using inducible RNA interference, since it was not possible to obtain BSF knock-out cells. Upon PKAC3 depletion cells were cell cycle arrested in cytokinesis and around 10% of the cells had the unusual 1K2N K/N configuration with a single large kinetoplast.

Together with the observed increase in kinetoplast distance during PKAR knock-down, these results led to the hypothesis that *T. brucei* PKA-like kinase might play a role in kinetoplast segregation during cytokinesis. Depletion of PKAC3 by RNAi should then result in the opposite phenotype, thus in decreased kinetoplast distances in 2K2N cells. The observed 1K2N cells would be the extreme example for no kinetoplast movement. In order to test this hypothesis, the RNAi experiment of Thorsten Riek was repeated with the aim to quantify kinetoplast distances in 2K2N cells. This time the p2T7TAbblue vector and the 1313-514 cell line (cell line and vector kindly provided by C. Clayton, Heidelberg) were used to obtain higher levels of tet repressor (see above chapter 3.4.2.2.5.). As RNAi target served the N-terminal *PKAC3* fragment (467 bp).

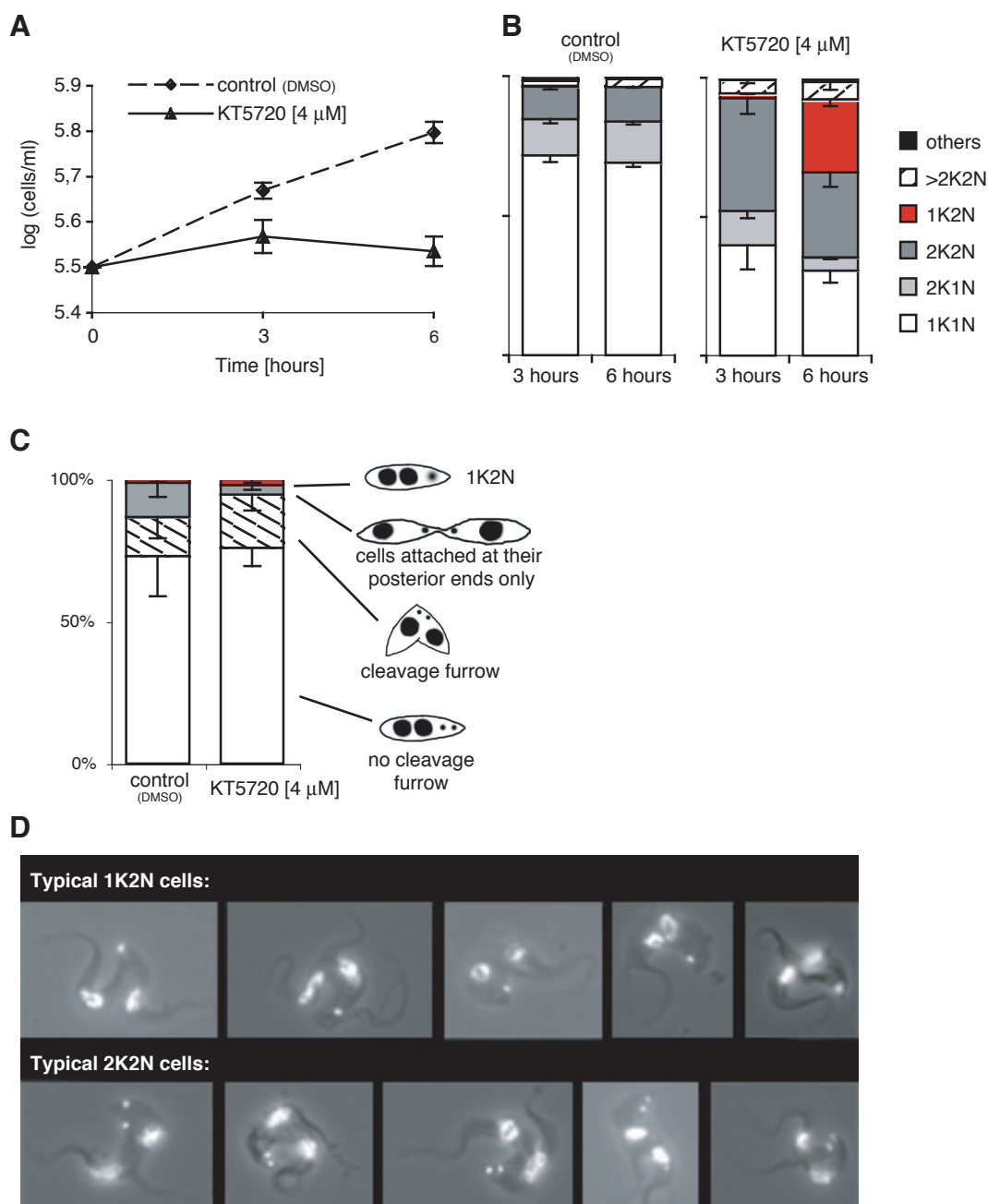


Fig. 48: Effects of the PKAC1/2 specific PKA inhibitor KT5720 on WT cells

WT cells (MITat1.2) were incubated with 4 μM KT5720 (stock: 2 mM desolved in DMSO) or with an equal volume of DMSO (control). Cell densities were determined regularly and cells were fixed in methanol and stained with DAPI to enable K/N analyses. Average data from three independent experiments are shown. Standard deviations are indicated by error bars.

A) Growth curves: Cell densities (cells/ml) were measured 0, 3 and 6 hours after addition of KT5720 or DMSO.

B) K/N configurations: 400 DAPI stained cells were analyzed for each experiment. Cells had been incubated with KT5720 for either 3 or 6 hours.

C) Division furrow stage: 2K2N cells and 1K2N cells were classified according to the stage of their division furrow. 200 cells were analyzed for each experiment. Cells had been incubated with KT5720 or DMSO for 3 hours.

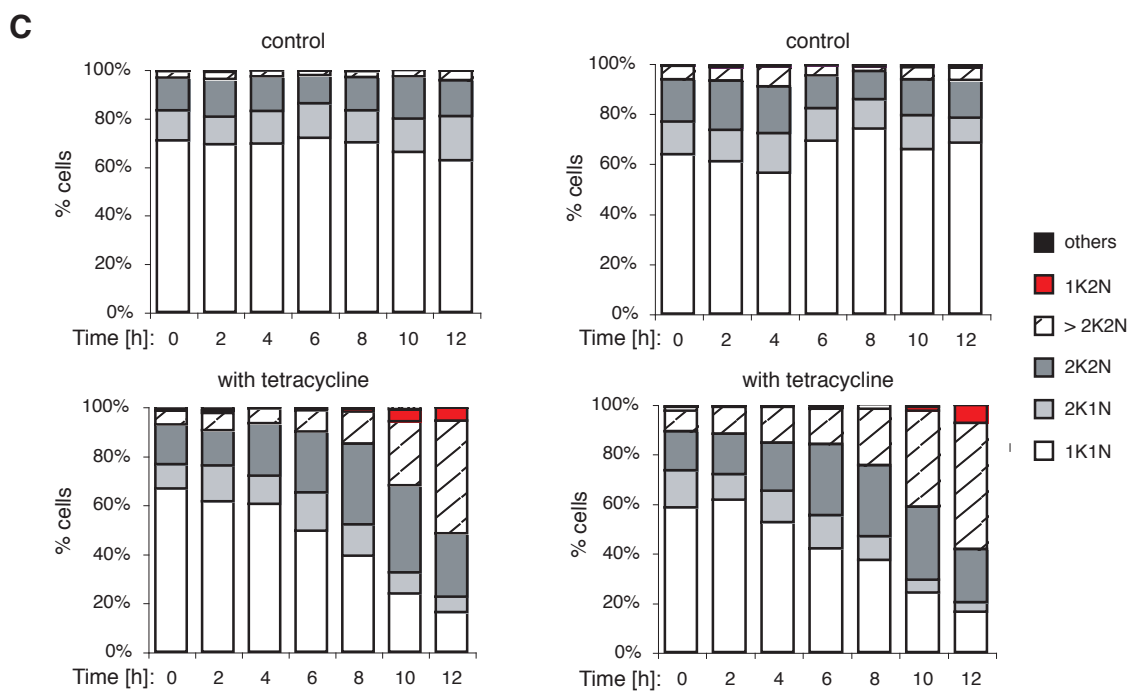
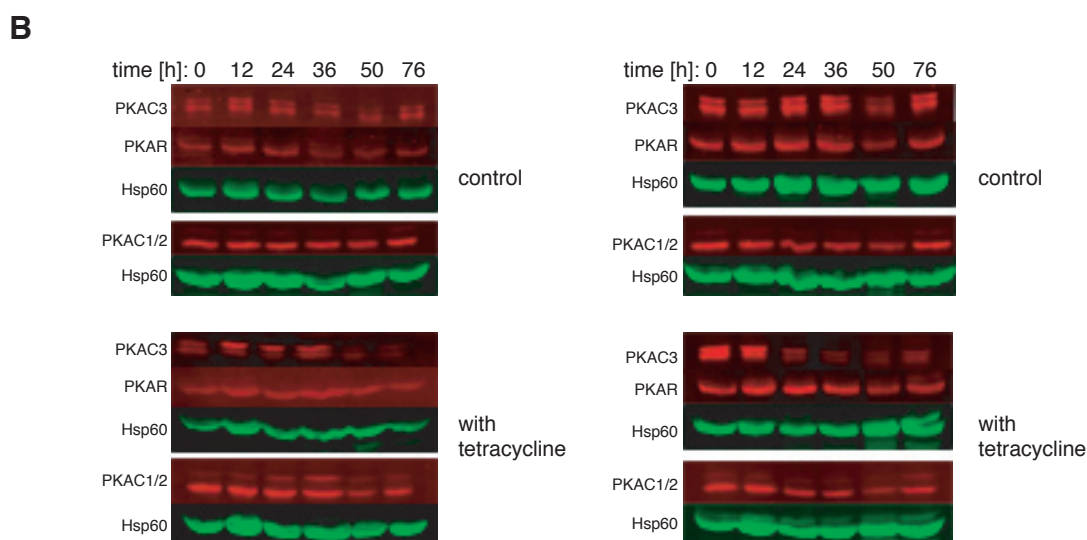
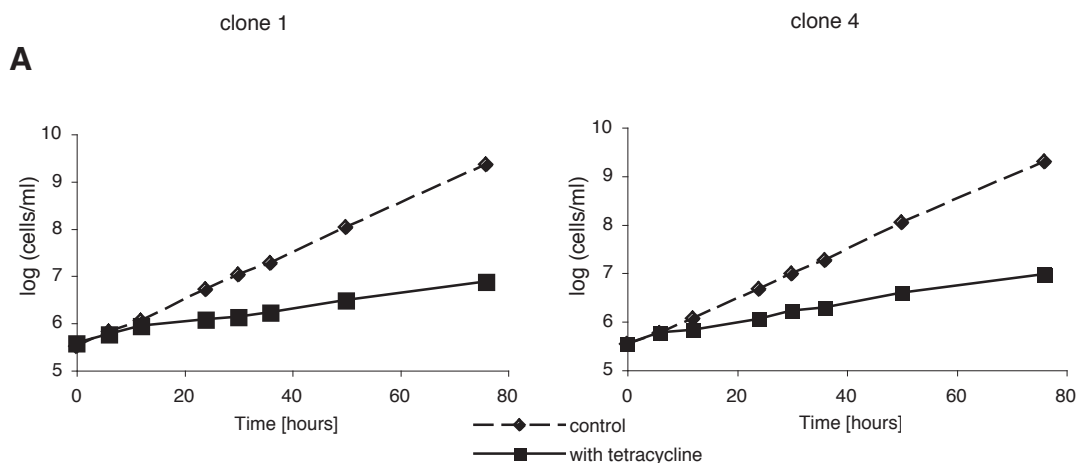
D) Photographs of typical 1K2N and 2K2N cells after 6 hours of incubation with KT5720. The cells were stained with DAPI.

Out of 11 hygromycin resistant clones four clearly reacted to tetracycline (growth decrease, abnormal morphology) after incubation overnight. The others either showed no reaction or already had phenotypes in the absence of tetracycline. Two out of these four clones were further analyzed (clone 1 and clone 4). After incubation with tetracycline, cells reduced their growth rate (Fig. 49A). The population doubling times increased from 6 hours (non-induced) to 16.2 /18.6 hours (clone 1/ clone 4). An 80 to 90% reduction in PKAC3 protein was detectable on a Western blot 36 to 50 hours after tetracycline induction for clone 1 and after 12 to 24 hours for clone 4 (Fig. 49B). None of the other PKA-like subunits were affected. The number of 2K2N cells and the number of multinucleated cells increased with time. The number of 1K2N cells slightly increased up to 9% after 10 to 12 hours incubation with tetracycline, but no 1K2N cells were found at earlier time points (Fig. 49C). The amount of 2K2N cells with a division furrow slightly increased (Fig. 49D) suggesting that the cell cycle arrest was caused by a problem in progression through cytokinesis, as observed for the other subunits. This hypothesis was further confirmed by the appearance of the multinucleated cells mostly consisting of several cell bodies (Fig. 49E).

However, when 2K2N cells were examined in more detail, we could not detect any decrease in kinetoplast distances. This already became clear from qualitative microscopy. Conclusively, we could not confirm the hypothesis stated above that PKAC3 depletion inhibits kinetoplast segregation. The reason for the occurrence of 1K2N cells at late time points remains unclear.

	WT	PKAR	PKAC2	PKAC1		PKAC1/2		PKAC3
		RNAi	k.o.	hemizyg. k.o.	dead mutant	RNAi	KT5720	RNAi
Growth	PDT: 5.5-6 h	growth arrest [8 h]	PDT: 6.82 h	PDT: 6.5 h	PDT: 7.9 h	growth arrest [4 h] dead [2 d]	growth arrest [3 h]	reduced growth PDT: 16.2-18.6 h
[2K2N]	10-15%	40-48% [8 h]	31%	29%	28%	58% [6 h]	41% [3 h]	36-45% [10 h]
[1K2N]	0%	1.7 -3.9% [8 h]	not sign.	not sign.	not sign.	1.2-3.5% [10 h]	1.7% [3 h] 26.3% [6 h]	7.1 to 9.5% [12 h]
[2K2N cells with division furrow]	8-12%	35-40% [8 h]	25%	43-52%	43%	32-40% [6 h]	16% [3h]	22-24% [10 h]
increase in kinetoplast distance	NO	YES	NO	NO	NO	NO	NO	NO

The table summarizes all PKA phenotypes describes so far.



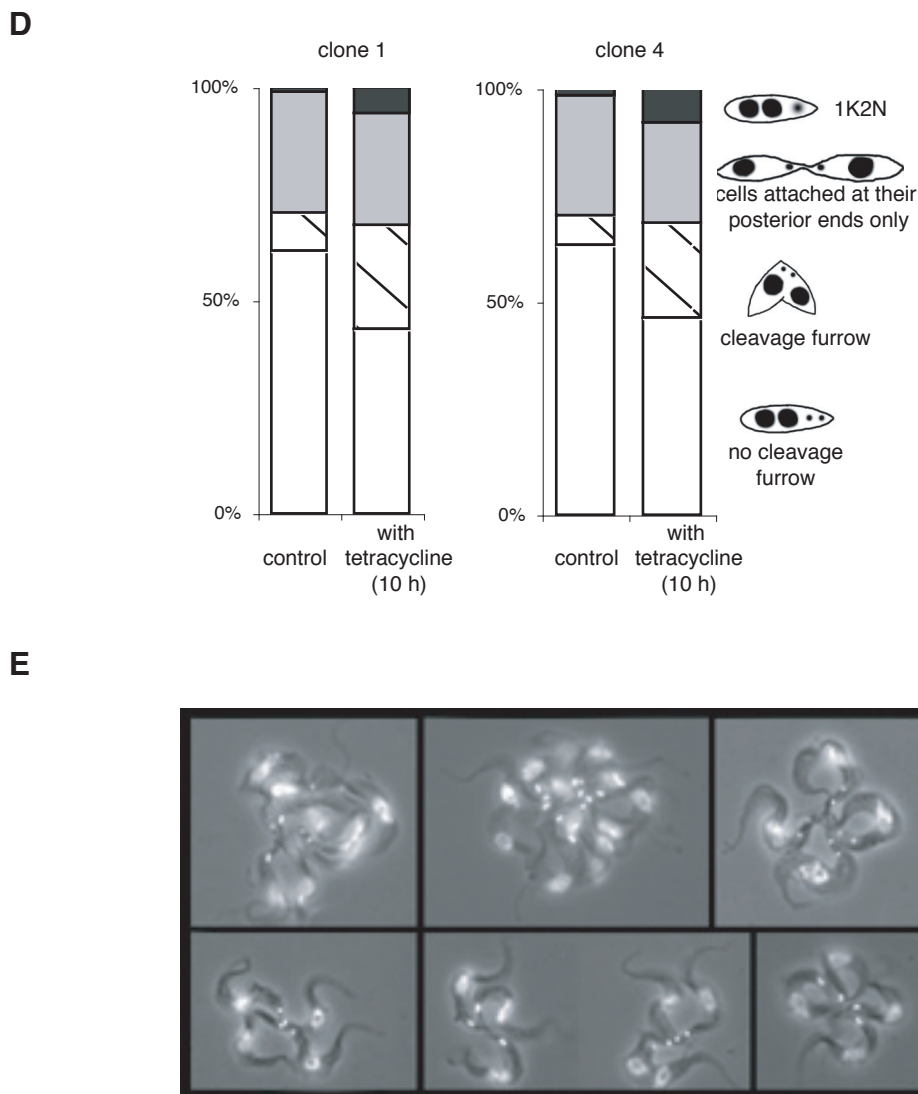


Fig. 49: Depletion of PKAC3 using inducible RNA interference

PKAC3 RNAi cells were incubated in the presence or absence (control) of tetracycline for 76 hours. Data from two independent clonal cell lines (#1 and #4) are shown.

A) Growth curves of induced and uninduced PKAC3 RNAi cells. Cell densities were kept below 7×10^5 .

B) Western blots. Protein samples of uninduced and induced cells were collected at the times indicated and applied to SDS PAGE. The resulting Western blots were incubated with anti-PKAC3, anti-PKAR, anti-PKAC1/2 and anti-Hsp60, the latter serving as control for equal loading. Since PKAC3 and PKAC1/2 have equal molecular weights, two Western blots (containing the same samples) were performed for each time course, one was incubated with anti-PKAR and anti-PKAC3, the other with anti-PKAC1/2. Rabbit Alexa680 (red) and Mouse IRDye800 (green) were used for the detection of anti-PKAR/anti-PKAC3/anti-PKAC1/2 and anti-Hsp60, respectively, using the Odyssey IR scanner (Licor).

C) K/N configurations: Cells were fixed in methanol after 0, 2, 4, 6, 8, 10 and 12 hours of incubation with or without tetracycline and subsequently stained with DAPI. K/N configurations of 400 cells were determined for each time point.

D) 2K2N cells and 1K2N cells were classified according to the stage of their **division furrows**. 200 cells were analyzed for each clone. Cells had been incubated with or without tetracycline for 10 hours.

E) Photographs of typical multinucleated cells observed after RNAi depletion of PKAC3 (10 hours induction). Nuclei and kinetoplasts are stained with DAPI.

3.5. *In silico* search for further putative subunits of PKA-like kinases

Experiments of this Ph.D. project were so far focussed on the isoforms/subunits PKAC1, PKAC2, PKAC3 and PKAR. The *T. brucei* genome sequencing project has only recently been finished and might now contain sequences not available at the beginning of this work. If the PKA-like kinase characterized in this work doesn't transmit the cAMP signal thought to stimulate differentiation processes, is there another regulatory PKA subunit that actually becomes activated by cAMP?

3.5.1. Hidden regulatory subunits?

Regulatory PKA subunits of most organisms have two conserved sequence motifs. The most prominent features are the two cNMP binding sites that are arranged in tandem, usually at the C-terminus of the protein. In addition, type II PKARs have an RIIa domain at their N-termini mediating the dimerization between the two regulatory subunits and the binding to A-kinase anchoring proteins (AKAPs).

The *T. brucei* genome database was screened for proteins with these characteristic PKAR motifs with the aid of a computational algorithm based on the hidden Markov model (HMM) (reviewed by Eddy 2004). In contrast to BLAST searches, HMM based searches offer the ability to perform model-based searches against a multiple sequence alignment rather than against one single target sequence. This enables a broader "space" to be searched.

3.5.1.1. Search for cNMP binding proteins in the *T. brucei* genome database

The multiple sequence alignments of cNMP binding domains as provided by Pfam (<http://www.sanger.ac.uk/cgi-bin/Pfam/>; version 10.0; Bateman *et al.*, 2004) and by SMART (<http://smart.embl-heidelberg.de/>; version 4.0, Schultz *et al.*, 1998; Letunic *et al.*, 2004) were used as templates for HMM based searches (HMMER version 2.3.2. downloaded from <http://hmmer.wustl.edu/>; default parameters with an e-value threshold of 10) against the local copy of the *T. brucei* genome database (<http://www.genedb.org/genedb/tryp/index.jsp>, release 3, the HMM search was performed by M. Kador (this lab)). 14 *T. brucei* proteins were identified with the SMART alignment, 18 with the Pfam alignment and 11 proteins were found with both alignments. These proteins are shown in the table in figure 50A (left columns) together with the e-values of the HMMER searches. They were

subsequently examined for cNMP binding domains with the web services of Pfam and SMART using default parameters as set by the servers. 14 proteins had predicted Pfam cNMP domains out of which 10 had also predicted SMART cNMP domains (Fig. 50A, right columns).

The results from the HMMER search were controlled with a BLAST search using cNMP binding domains of PKARs from five different organisms as targets (attachment 3). With this alternative approach, we did identify all proteins that had high HMMER e-values (marked with an “x” in figure 50A), but none in addition.

It is therefore likely that all *T. brucei* proteins with cNMP domains were identified.

3.5.1.1.1. Three *T. brucei* proteins have two cNMP binding domains in tandem

Most of the putative cNMP binding proteins identified above have only one predicted cNMP binding site, often with low significance (compare e-values). However, three *T. brucei* proteins (Tb10.70.1860, Tb03.48K5.800, Tb11.01.7890) were found that had two predicted cNMP domains with sufficiently high significance (Pfam e-value below 7.2E-3). They are therefore possible candidates for new regulatory PKA subunits. The domain structures of these three proteins are shown in figure 50B, in comparison with the domain structures of the known *T. brucei* PKAR and bovine PKAR. The cNMP domains of all three proteins are arranged in tandem as is the case in regulatory PKAR subunits.

Interestingly, all three PKAR candidates have unusually long C-termini absent from both the known *T. brucei* PKAR and bovine PKAR. In addition, they possess an N-terminal extension. Such an N-terminal elongation is also present in the known *T. brucei* PKAR, but we could not identify any homology between the PKAR N-terminus and the N-termini of the identified cNMP binding proteins. With the exception of a C2 domain (a Ca²⁺-dependent membrane-targeting module) in Tb10.70.1860 no further domains were found in any of the PKAR candidates, not even an RIIa domain.

3.5.1.1.2. Two of the *T. brucei* PKAR candidates have highest homologies to PKARs

The most related proteins were identified for each of the three putative *T. brucei* PKAR proteins using a BLAST search in EMBL nr. For this, the protein database nr at NCBI (GenBank (<http://www.ncbi.nlm.nih.gov/BLAST/>), blastp, default parameters as set by the NCBI server; Altschul *et al.*, 1997) was searched with the sequences of the *T. brucei*

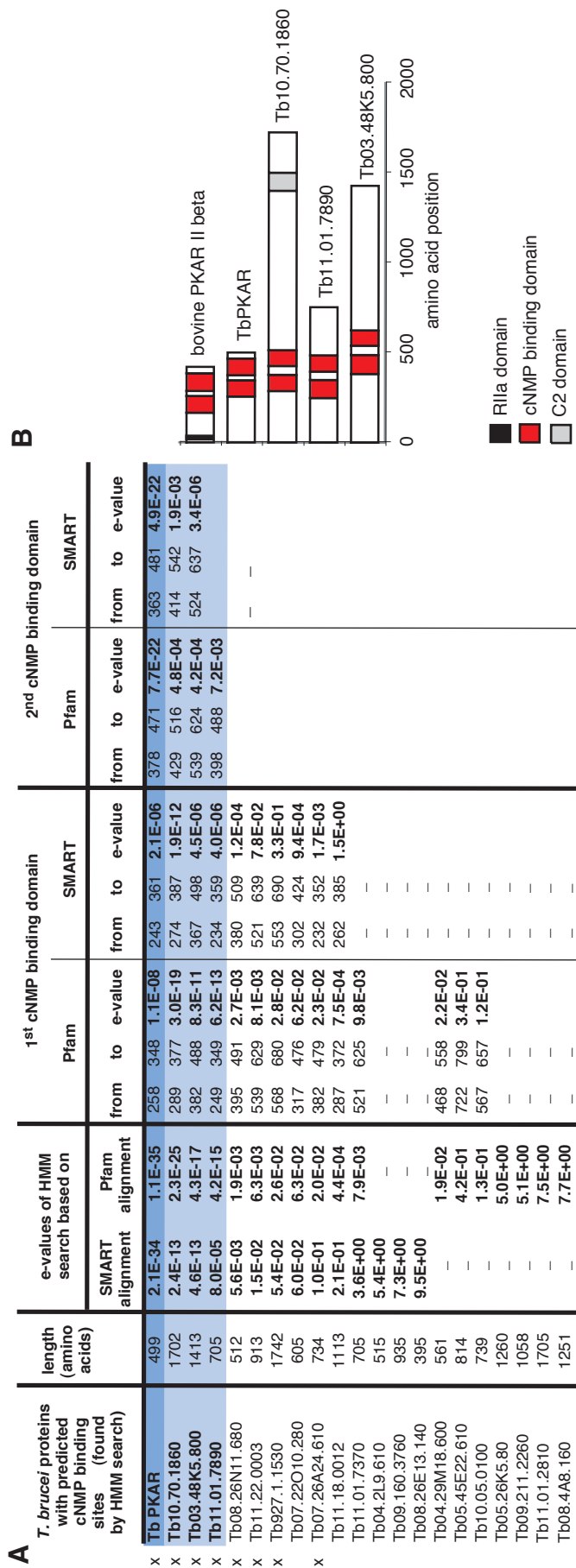


Fig. 50: Putative cNMP binding proteins of *T. brucei* proteins
A) HMMER search for *T. brucei* cNMP binding proteins

The multiple sequence alignments of cNMP binding domains as provided by Pfam (<http://www.sanger.ac.uk/cgi-bin/Pfam/>; version 10.0; Bateman *et al.*, 2004) and by SMART (<http://smart.embl-heidelberg.de/>; version 4.0, Schultz *et al.*, 1998; Letunic *et al.*, 2004) were used as templates for HMM based searches (HMMER version 2.3.2, downloaded from <http://hmmer.wustl.edu/>; Durbin *et al.*, 1998; default parameters) against the *T. brucei* genome database (<http://www.genedb.org/genedb/try/index.jsp>, release 3). All *T. brucei* proteins that were found with these approaches are indicated (column 1) together with their size (number of amino acids, column 2) and the e-value(s) from the HMMER searches (column 3 and 4). Subsequently, the web services of SMART and Pfam were used to screen the resulting *T. brucei* proteins for conserved domains. The position (from, to) and the e-value as provided by SMART or Pfam are indicated for each predicted cNMP binding domain. In addition to the known *T. brucei* PKAR (dark shadowed), three further *T. brucei* proteins were identified that had two cNMP binding sites (light shadowed) and are thus possible candidates for regulatory PKA subunits. Alternatively, a BLAST based approach was performed to identify cNMP binding proteins that is described in more detail in attachment 3. The proteins that have been also identified with this BLAST search are marked with a "x".

B) Domain structure of *T. brucei* proteins with two predicted cNMP binding sites

The domain structure of all *T. brucei* proteins from A) that have two predicted cNMP binding domains is shown graphically. For comparison, the domain structure of bovine PKAR II beta (type II β , Acc No.: NP_777074) and of the known *T. brucei* PKAR are also shown. With the exception of the C2 domain (Tb10.70.1860) none of the putative PKAR subunits of *T. brucei* has any known conserved protein domains. Note that no RIIa domain has been detected in any of the *T. brucei* PKAR candidates.

PKAR candidates. The results are listed in table 4.

putative <i>T. brucei</i> PKAR	highest homology to				
	protein	organism	e-value	% identity	sequence overlap
Tb10.70.1860	Regulatory subunit of the cyclic AMP-dependent protein kinase	<i>Saccharomyces cerevisiae</i>	5.0E-10	21	192
	cAMP-dependent protein kinase regulatory subunit	<i>Yarrowia lipolytica</i>	1.0E-7	25	188
	KAPR_EMENI CAMP-DEPENDENT PROTEIN KINASE REGULATORY CHAIN	<i>Aspergillus nidulans FGSC A4</i>	8.0E-6	22	301
Tb11.01.7890	cyclic nucleotide-gated K+	<i>Bdellovibrio bacteriovirus</i>	6.0E-7	32	123
	cyclic GMP-dependent protein kinase	<i>Hydra oligactis</i>	2.0E-5	23	269
	cGMP-dependent protein kinase foraging	<i>Apis mellifera</i>	2.0E-5	24	169
Tb03.48K5.800	PREDICTED: similar to cAMP-dependent protein kinase type I-beta regulatory chain	<i>Homo sapiens</i>	4.0E-3	33	62
	protein kinase (EC 2.7.1.37), cAMP-dependent, type I-beta regulatory chain - human	<i>Homo sapiens</i>	6.0E-3	22	167
	cAMP-dependent protein kinase type I-beta regulatory chain	<i>Mus musculus</i>	3.2E-2	22	167

Table 4: Blast searches with the three *T. brucei* PKAR candidates

The protein database nr at NCBI (GenBank (<http://www.ncbi.nlm.nih.gov/BLAST/>), blastp, default parameters as set by the NCBI server; Altschul *et al.*, 1997) was searched with each of the three *T. brucei* PKAR candidates (Tb10.70.1860, Tb11.01.7890, Tb03.48K5.800). The three proteins with the highest homologies (others than putative proteins) as judged by the e-value are indicated for each *T. brucei* PKAR candidate together with the e-value and the identity and sequence overlap to the target sequence.

Tb10.70.1860 and Tb03.48K5.800 had highest homologies to PKARs from various organisms (21-33% ID), while Tb11.01.7890 had highest homology to a cyclic nucleotide gated ion channel and to PKGs (23-32% ID).

3.5.1.1.3. Substrate or pseudosubstrate sequences in the new *T. brucei* PKAR candidates

The substrate or pseudosubstrate sequence RRX [A,T,S]_y (y=hydrophobic) is a further characteristic feature of regulatory PKA subunits. It is located N-terminal of the cNMP binding domain and mediates the binding to the catalytic subunit.

The N-termini of the three PKAR candidates, corresponding to the region upstream of the first cNMP binding site, were searched for such a substrate or pseudosubstrate sequence. In Table 5 the substrate or pseudosubstrate sequence is shown for each of the putative PKARs together with its position in relation to the first cNMP binding site. For comparison, the substrate or pseudosubstrate sequences of bovine PKAR and of the

known *T. brucei* PKAR are also shown.

	Substrate or Pseudosubstrate Sequence		
	Sequence	Position	Distance to 1 st cNMP binding site
bovine PKAR	RRASV	112-116	38
<i>Tb</i> PKAR	RRTTV	206-210	33
Tb10.70.1860	LRMTV	250-254	20
Tb11.01.7890	RRLAV	200-204	30
Tb03.48K5.800	none		

Table 5: The N-terminal sequences of the PKAR candidate proteins were searched for a substrate or pseudosubstrate sequence RRX [A,T,S]y (y=hydrophobic). The position and the distance to the first cNMP binding site (as predicted by SMART) is shown. Variations to the classical substrate or pseudosubstrate sequence are shown in italic/bold (Tb10.70.1860). For comparison, the substrate/pseudosubstrate sequences are also shown for bovine PKAR (type II, β , Acc No.: NP_777074) and the known *Tb* PKAR.

Only one of the three new PKAR candidates (Tb11.01.7890) has a classical pseudosubstrate sequence (RRLAV). It is located 30 amino acids upstream of the first cNMP binding site, thus in a similar relative position as in bovine or the known *T. brucei* PKAR. Tb10.70.1860 has a substrate sequence that varies in the first amino acid (L / Y instead of R) from the classical substrate sequence and is located 20 amino acids upstream of the first cNMP binding site. Variations in that position were already described for *Paramecium tetraurelia* (Carlson and Nelson, 1996). Tb03.48K5.800 has no substrate or pseudosubstrate sequence.

3.5.1.1.4. All new PKAR candidates have significant homology to a PKA specific conserved 14 amino acid stretch in the cNMP binding sites

cNMP binding domains are also present in several other proteins such as the catabolite activator protein (CAP) (Eron *et al.*, 1971; Weber and Steitz 1987), cyclic nucleotide-gated ion channels (Nakamura and Gold 1987; Ludwig *et al.*, 1990) and guanine nucleotide exchange factors (Kawasaki *et al.*, 1998).

A method for the univocal identification of regulatory PKA subunits was developed by Canavas *et al.* (2002). They identified a degenerative 14 amino acid stretch in the cNMP binding domain of regulatory PKA subunits that is highly conserved between PKARs from various species, but absent from cNMP binding domains of other proteins: F-G-E-[LIF]-A-L-[LIMV]-X(3)-[PV]-R-[ANVQ]-A.

The sequences of the three putative PKAR subunits of *T. brucei* were aligned to this PKAR specific 14 amino acid stretch (Fig. 51). Bovine PKAR and the known *T. brucei* PKAR

served as positive controls. Two of the *T. brucei* proteins with only one predicted cNMP binding domain (Tb08.26N11.680, Tb07.26A24.610) were used as negative controls. The known *T. brucei* PKAR has already several amino acid substitutions to the consensus sequence, three in domain A and four in domain B. Four of these substitutions are non-conservative. Similar or only slightly higher numbers of amino acid substitutions were found for all three *T. brucei* PKAR candidates (Tb10.70.1860, Tb11.01.7890 and Tb03.48K5.800). In contrast, *T. brucei* proteins with only one cNMP domain, that are unlikely to be regulatory PKAR subunits, have 11 (Tb08.26N11.680) or 9 (Tb07.26A24.610) amino acid substitutions to the consensus sequence.

	1st cNMP binding domain													2nd cNMP binding domain														
	F	G	E	[LIF]	A	L	[LIMV]	X	X	X	[PV]	R	[ANVQ]	A	F	G	E	[LIF]	A	L	[LIMV]	X	X	X	[PV]	R	[ANVQ]	A
consensus	F	G	E	[LIF]	A	L	[LIMV]	X	X	X	[PV]	R	[ANVQ]	A	F	G	E	[LIF]	A	L	[LIMV]	X	X	X	[PV]	R	[ANVQ]	A
+ bovine PKAR	F	G	E	L	A	L	M	Y	N	T	P	R	A	A	F	G	E	L	A	L	V	T	N	K	P	R	A	A
+ <i>T. brucei</i> PKAR	V	G	E	L	E	L	M	Y	Q	T	P	T	V	A	V	G	E	L	E	F	L	N	N	H	A	N	V	A
* Tb10.70.1860	F	G	E	V	S	V	I	F	D	E	P	R	C	C	V	G	E	L	F	L	H	P	H	L	W	P	T	D
* Tb11.01.7890	V	G	E	F	A	L	V	C	K	E	P	R	S	A	V	G	I	F	E	C	A	C	S	V	N	E	R	K
* Tb03.48K5.800	F	G	E	L	S	V	L	F	G	E	P	R	Q	F	I	G	E	P	T	I	I	L	H	R	W	P	L	G
- Tb07.26A24.610	F	T	P	T	E	L	A	S	S	L	Q	E	K	H														
- Tb08.26N11.680	A	V	D	V	W	T	R	L	R	T	C	C	C	S														

Fig. 51: The conserved PKA specific sequence in the *T. brucei* PKAR candidates

The homologous sequence to the conserved sequence stretch in the cNMP binding sites of PKAs as defined by Canaves *et al.* (2002) is shown for each of the three putative *T. brucei* PKARs (Tb10.70.1860, Tb11.01.7890, Tb03.48K5.800) (*). As positive controls, both bovine PKAR (type II β , Acc No.: NP_777074) and the known *T. brucei* PKAR are shown (+). As negative controls we used two *T. brucei* proteins with only one predicted cNMP domain (Tb08.26N11.680, Tb07.26A24.610) (-) that are unlikely to be regulatory PKA subunits. All amino acids that are identical to the consensus sequence are uncolored, conservative amino acid substitutions to the consensus sequence are shadowed light yellow and non-conservative amino acid substitutions yellow.

3.5.1.2. Search for *T. brucei* proteins with RIIa domains

In a second approach, the RIIa domain, present in all type II PKARs, was used as a template to identify further related proteins in *T. brucei*. The multiple sequence alignment of RIIa domains provided by Pfam (<http://www.sanger.ac.uk/cgi-bin/Pfam/>; version 10.0; Bateman *et al.*, 2004) was used for an HMM based search (HMMER version 2.3.2. downloaded from <http://hmmer.wustl.edu/>; Durbin *et al.*, 1998; default parameters) against the *T. brucei* genome database (<http://www.genedb.org/genedb/tryp/index.jsp>, release 3). Nine *T. brucei* proteins were identified that had HMMER e-values below 1.0. They are listed in the left column of figure 52A. These proteins were subsequently screened for RIIa domains and cNMP binding domains with the web services of SMART and Pfam. The positions of the RIIa domains together with the e-value as provided by SMART or Pfam are indicated (Fig. 52A, right columns). Surprisingly, none of the proteins

with predicted RIIa domains had a cNMP domain. In fact, the two proteins with the highest probability to have a RIIa domain (Tb09.211.2250 and Tb11.01.5260) are very small and did not possess additional known domains (Fig. 52B). It is therefore unlikely that any of the identified proteins are regulatory PKAR subunits.

A

<i>T. brucei</i> proteins with predicted RIIa domains	length [amino acids]	HMMER search [e-value]	RIIa domain identified by					
			SMART			Pfam		
			from	to	e-value	from	to	e-value
Tb09.211.2250	268	6.6E-10	21	58	1.7E-08	21	58	3.7E-10
Tb11.01.5260	196	3.2E-03	41	78	3.3E-01	41	78	1.6E-03
Tb09.160.1660	81	3.8E-02	18	56	2.7E+00	18	56	1.9E-02
Tb10.70.7640	324	6.0E-02	31	130	3.9E+00	31	130	2.9E-02
Tb11.02.0990	1017	1.4E-01	–	–	–	975	1009	6.8E-02
Tb10.70.3330	155	1.8E-01	83	119	9.9E+00	83	119	8.7E-02
Tb09.160.1690	76	2.2E-01	23	60	1.2E+01	23	60	1.1E-01
Tb927.1.1530	1742	3.4E-01	–	–	–	23	56	1.6E-01
Tb05.6E7.1020	260	7.4E-01	17	51	3.3E+01	17	51	3.4E-01

B

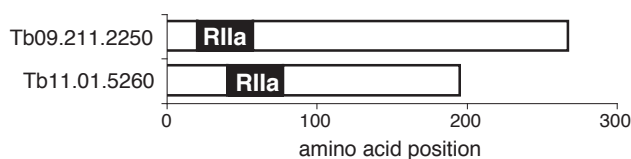


Fig. 52: *T. brucei* proteins with predicted RIIa domains

A) HMMER search for *T. brucei* proteins with RIIa domains

The multiple sequence alignment of RIIa domains as provided by Pfam (<http://www.sanger.ac.uk/cgi-bin/Pfam/>; version 10.0; Bateman *et al.*, 2004) was used as template for a HMM based search (HMMER version 2.3.2. downloaded from <http://hmmer.wustl.edu/>; Durbin *et al.*, 1998; default parameters) against the *T. brucei* genome database (<http://www.genedb.org/genedb/tryp/index.jsp>, release 3). All *T. brucei* proteins with an e-value lower than 1.0 are indicated (column 1) together with their size (number of amino acids, column 2) and the e-value of the HMMER search (column 3). Subsequently, the web services of SMART (<http://smart.embl-heidelberg.de/>; version 4.0, Schultz *et al.*, 1998; Letunic *et al.*, 2004) and Pfam (<http://www.sanger.ac.uk/cgi-bin/Pfam/>; version 10.0; Bateman *et al.*, 2004) were used to screen the resulting *T. brucei* proteins for RIIa domains. The position (from, to) and the corresponding e-value as provided by SMART and Pfam are indicated for each predicted RIIa domain.

B) Domain structure of *T. brucei* proteins with predicted RII domains

The domain structure of the two *T. brucei* proteins with highest probability to contain a RIIa domain (Tb09.211.2250, Tb11.01.5260) is shown in the graphics. Both proteins are small and do not possess additional known domains.

3.5.1.3. *T. brucei* might contain up to three further PKAR subunits

Altogether, three further proteins with homologies to regulatory PKA subunits were identified in *T. brucei* in addition to the known *T. brucei* PKAR. They have several PKA

specific characteristics that are summarized in table 6. For comparison, the respective features are also indicated for the bovine PKAR and the known *T. brucei* PKAR (first two rows).

	cNMP binding site (e-value)		Conserved Amino acids in the PKA specific amino acid sequence (F-G-E-[LIF]-A-L-[LIMV]-X(3)-[PV]-R-[ANVQ]-A) in the cNMP binding sites		substrate / pseudosubstrate sequence			highest homology to
	domain A	domain B	domain A	domain B	classical	one mismatch	no match	
bovine PKAR	3.1E-26	9.8E-30	11	11	x			PKAR
Tb PKAR	5.6E-10	4.0E-23	8	6	x			PKAR
Tb10.70.1860	3.0E-19	4.8E-4	6	4		x		PKAR
Tb03.48K5.800	8,3E-11	4.2E-4	8	3			x	PKAR
Tb11.01.7890	6.2E-13	7.2E-3	9	2	x			K+ ion channel, PKG

Table 6: PKAR-characteristic features of the three *T. brucei* PKAR homologous proteins

The characteristics of the three *T. brucei* PKAR homologous proteins (Tb10.70.1860, Tb11.01.7890, Tb03.48K5.800) identified in the chapter above are summarized. The first column shows the e-values of the predicted cNMP binding sites as calculated by Pfam (<http://www.sanger.ac.uk/Software/Pfam/>) (see also Fig. 51). The second column shows the number of conserved amino acid residues to the 14 amino acid PKAR specific sequence stretch. Since three of the 14 amino acids are flexible, 100% homology is achieved with 11 conserved amino acids (see chapter 3.5.1.1.4.). The third column indicates whether the PKAR has a classical substrate/pseudosubstrate sequence, a non-classical (one mismatch) or no match (chapter 3.5.1.1.3.). The fourth column shows the protein with the highest homology to the *T. brucei* PKAR homologous proteins as determined by searching GeneDB EMBL nr (see table 4 for more details). For comparison, the respective features of bovine PKAR (type II, β , Acc No.: NP_777074) and the known *Tb*PKAR are also indicated (first two rows).

All three PKAR candidates have two cNMP binding domains in tandem (with Pfam e-values between 7.1E-3 and 3E-19) and sufficient homology to the PKA specific 14 amino acid stretch (F-G-E-[LIF]-A-L-[LIMV]-X(3)-[PV]-R-[ANVQ]-A). At least two of the PKAR candidates have highest homology to a PKAR. Tb11.01.7890 possess a classical PKA pseudosubstrate sequence at the correct position and Tb10.70.1860 has a putative substrate sequence that differs in one amino acid.

These candidates should be tested for cNMP binding and association with catalytic subunits.

3.5.2. *T. brucei* has no further proteins with homologies to catalytic PKA subunits

Due to the lack of a PKAC specific domain, the *in silico* search for additional catalytic PKA subunits proved to be more difficult than the search for PKAR homologous proteins. Catalytic PKA subunits mainly consist of a kinase domain, and kinase domains are highly

conserved among all existing kinases. Only small segments of PKA sequences, 6-8 amino acids in length, differ significantly from other kinases (Hanks and Quinn, 1991). They are too small to be used as templates for a HMMER motif search.

We therefore used a BLAST approach to screen the *T. brucei* genome database (<http://www.genedb.org/genedb/tryp/blast.jsp>) for PKAC homologous proteins. PKAC sequences of *T. brucei* (PKAC3), *H. sapiens* (PKA β), *C. elegans*, *D. melanogaster* and *S. cerevisiae* were used as targets (blastp, matrix blossom 62). From the resulting proteins only *T. brucei* proteins with at least 270 amino acids sequence overlap to the target PKA were considered as potential PKAC candidates. The number of 270 was arbitrary chosen. It is slightly higher than the length of a kinase domain (256-258) and should therefore reduce the amount of false positive results due to other protein kinases. Also, it is smaller than the conserved sequence stretch of PKAs (308-312 amino acids) and should still allow the identification of unconventional PKAs. (For an overview about conserved regions of PKAs compare PKAC alignment in attachment 4) This way, 35 *T. brucei* proteins with homologies to PKAs were identified, including the three known PKAC subunits, serving as positive controls (Table 7, left column).

In the next step, GenBank (<http://www.ncbi.nlm.nih.gov/BLAST/>, blastp) was searched with each of these 35 *T. brucei* proteins and the protein with the highest homology (according to the e-value as defined by Karlin and Altschul, 1990) was determined (Table 7, right columns).

It can be seen that all new hits have highest homologies to a kinase other than PKA, while the three known *T. brucei* PKACs (positive controls) have highest homologies to PKAs. To summarize, there is no evidence for additional PKA-related kinase catalytic subunits in the *T. brucei* genome.

The *T. brucei* genome data base was searched with PKAs from:

T. brucei (C3) **S. cerevisiae** **C. elegans** **H. sapiens** **D. melanogaster**

Genbank was searched with the resulting *T. brucei* PKA homologous proteins and the protein with the highest homology is shown:

<i>T. brucei</i> proteins with homology to PKAs:	% ID	overlap [amino acids]	S. cerevisiae % ID	overlap [amino acids]	C. elegans % ID	overlap [amino acids]	H. sapiens % ID	overlap [amino acids]	D. melanogaster % ID	overlap [amino acids]	Protein	Organismus	% ID	overlap [amino acids]
TbPKAC3	100	363	50	296	48	295	52	293	48	301	CAMP-dependent protein kinase catalytic subunit	<i>E. gracilis</i>	68	329
TbPKAC1	61	327	51	312	55	293	53	300	52	293	protein kinase-A catalytic subunit	<i>T. cruzi</i>	75	323
TbPKAC2	60	322	52	300	55	293	54	300	53	293	CAMP-dependent protein kinase catalytic subunit	<i>E. gracilis</i>	62	319
Tb06.4M18.630	40	328	44	293	39	305	41	303	39	306	rac serine-threonine kinase homolog	<i>T. cruzi</i>	55	427
Tb11.01.1030	34	312	35	281	35	278	35	277	35	278	RAC-family serine/threonine-protein kinase homolog	<i>D. discoideum</i>	43	300
Tb03.4808.470	32	289	33	339	28	333	32	305	31	301	RAC-family serine/threonine-protein kinase homolog	<i>D. discoideum</i>	37	353
Tb08.12016.490	31	270									CBL-interacting protein kinase 8	<i>A. thaliana</i>	53	266
Tb07.2F2.540	33	276	32	300							putative mitogen-activated protein kinase kinase 3	<i>L. mexicana</i>	47	471
Tb10.05.0200	30	275	32	272			31	271			NAF specific protein kinase family	<i>A. thaliana</i>	45	269
Tb09.160.0570	29	281	29	311							Aurkc protein	<i>M. musculus</i>	38	276
Tb07.28B13.300	31	274	30	291							MAP kinase	<i>L. major</i>	38	340
Tb10.70.1800	26	301	27	293							mitogen-activated protein kinase kinase	<i>S. maritima</i>	36	353
Tb10.70.0960	27	295									NIMA-related kinase	<i>C. fasciculata</i>	36	496
Tb927.2.2120	26	307									Nek3 protein	<i>M. musculus</i>	35	294
Tb10.70.0970	27	295									NIMA-related kinase	<i>C. fasciculata</i>	36	496
Tb11.46.0003	30	276									MEK kinase alpha	<i>D. discoideum</i>	36	267
Tb03.48K5.570	26	319	26	325			23	316			putative mitogen-activated protein kinase kinase	<i>L. aethiopica</i>	64	367
Tb03.1J15.60	29	283	26	271	26	271	26	289	26	271	Protein kinase, interferon-inducible ds RNA dependent	<i>R. norvegicus</i>	29	329
Tb08.30K1.240	25	280	25	283			23	272			Serine/threonine-protein kinase-like protein	<i>A. thaliana</i>	36	279
Tb07.13M20.90	25	272	33	293							CBL-interacting protein kinase 24	<i>A. thaliana</i>	27	275
Tb11.01.0330			29	307			26	303			putative aurora/ipl1p-like protein kinase	<i>L. major</i>	79	299
Tb927.2.1820			31	281			30	280			OspK4-like protein	<i>O. sativa</i>	42	277
Tb10.70.7860			29	294							Serine/threonine-protein kinase Nek1	<i>M. musculus</i>	36	420
Tb04.30O21.210			27	271							Myosin light chain kinase	<i>D. discoideum</i>	37	275
Tb11.01.2900			28	275							NIMA-related kinase 3	<i>D. reinhardtii</i>	32	261
Tb06.4M18.220			28	313							MEK kinase alpha	<i>D. discoideum</i>	42	257
Tb07.13M20.690			26	273	25	277	25	271			SNF1	<i>L. esculentum</i>	35	298
Tb07.15M23.380			25	319							MEK kinase alpha	<i>D. discoideum</i>	39	298
Tb06.28P18.710			25	273							mitogen-activated protein kinase 1 homolog	<i>A. sativa</i>	39	381
Tb10.70.3410					27	274	27	273	25	274	calcium-dependent protein kinase	<i>B. rodhaini</i>	28	483
Tb11.01.0670					27	320					putative protein kinase 1	<i>L. mexicana</i>	46	299
Tb03.26J7.970							30	307			Snf1-related protein kinase	<i>A. thaliana</i>	51	343
Tb08.10K10.710							28	306			NIMA-related kinase	<i>C. fasciculata</i>	39	370
Tb927.1.3130							26	283			NIMA-related kinase 3	<i>C. reinhardtii</i>	33	287
Tb927.1.1530									25	275	MEK kinase	<i>L. esculentum</i>	35	276

Table 7: *T. brucei* PKAC homologues

The *T. brucei* genome data base (<http://www.genedb.org/genedb/trypan/blast.jsp>, *T. brucei* predicted proteins, default parameters as set by the genedb server) was searched against PKA protein sequences from *T. brucei* (PKAC3), *H.sapiens* (PKA β , Acc No.:P22694), *C.elegans* (Acc No.: P21137), *D.melanogaster* (Acc No.: P12370) and *S.cerivisiae* (PKA1, Acc No.:P06244) (blastp, matrix blossom62). All *T. brucei* proteins with at least 270 amino acids sequence overlap to any of these PKAs are indicated (left column) together with the percentage of identical amino acids (% ID) and the number of overlapping amino acids (overlap) (left part of the table). In addition each of these *T. brucei* proteins was used to search the protein database nr at NCBI (GenBank (<http://www.ncbi.nlm.nih.gov/BLAST/>), blastp) with default parameters as set by the NCBI server (right part of the table).

The protein with the highest homology according to the stochastic model of Karlin and Altschul (1990) (e-value) is shown together with its organism and the number of identical residues and sequence overlap to the *T. brucei* homologue PKAC proteins. If possible, characterized proteins were chosen, rather than putative ones, thus in some cases the protein with the second or third highest e-value is shown rather than a putative protein with the highest e-value.

4. Discussion

The aim of this project has been the characterization of a family of *T. brucei* PKA-like kinases, that were originally cloned in search for components of the cAMP signaling pathway associated with LS to SS differentiation (Vassella *et al.*, 1997). We found, however, that these kinases significantly differs from classical PKAs and are in fact not activated, but rather inhibited by cyclic AMP. *T. brucei* PKA-like kinases play an important role for progress through cytokinesis. Their activity seems regulated by external stress conditions as evidenced by an *in vivo* kinase assay developed in this work.

4.1. The catalytic subunits of *T. brucei* PKA-like kinase

Three different isoforms of catalytic PKA-like subunits have been previously cloned from *T. brucei* (T. Klöckner, Ph.D. thesis 1996). We did not find other closely related kinases in the now nearly complete *T. brucei* genome database. This suggests that these three isoforms are the full complement of PKAC subunits in *T. brucei*.

Biochemical characteristics of the *T. brucei* PKAC-like subunits have been studied in this and previous work either using immunopurified epitope tagged versions of the kinases or a recombinant GST-fusionprotein expressed in the baculovirus system. (N. Wild, unpublished results; C. Schulte zu Sodingen, Ph.D. thesis 2000; T. Klöckner, Ph.D. thesis 1996; this work). Thereby it was found that all three subunits phosphorylate the classical PKA substrate kemptide and are inhibitable with 5 μ M of the PKA specific peptide inhibitor PKI 5-24. K_i values for inhibition of recombinant PKAC3 with either PKI 5-24 or full length PKI were one order of magnitude higher than for mammalian PKAs, but still in the nanomolar range (N. Wild, unpublished). Here we also tested the effects of the PKA specific inhibitor KT5720 on the different immunopurified *T. brucei* PKAC-like subunits. We found an inhibition of PKAC1 and PKAC2 with an IC_{50} value between 1 and 5 μ M (compare Figure 28 in chapter 3.3.4.3.). This is 20 to 100 times higher than the IC_{50} values of KT5720 for mammalian PKAs (56 nM, Kase *et al.*, 1987). PKAC3 activity, however, was not affected even with 100 μ M KT5720. The different sensitivities of PKAC1/2 and PKAC3 towards KT5720 provide a useful tool for the discrimination between the isoforms.

Activity of recombinant PKAC3 was inhibited by purified bovine regulatory PKA subunit (N. Wild, unpublished). This inhibition was readily reversed with cAMP in nanomolar concentrations.

We conclude that the three catalytic PKA-like subunits from *T. brucei* possess all essential features in terms of sequence, substrate and inhibitor specificities and interaction with a heterologous R subunit that characterize a classical PKA. In comparison to mammalian PKAs, binding affinities of inhibitors are lowered for the *T. brucei* kinases. This is not surprising, given the evolutionary distance between *T. brucei* PKA-like kinase and mammalian PKA for which these inhibitors were optimized.

4.2. The regulatory subunit of *T. brucei* PKA-like kinase

In addition to the three catalytic PKA-like subunits, one protein with homologies to regulatory PKA subunits has been previously identified in *T. brucei* (C. Schulte zu Sodingen, Ph.D. thesis 2000). *TbPKAR* has two predicted cNMP binding domains and possess 38% identity to mammalian PKAR subunits. Unlike the catalytic *T. brucei* PKA-like subunits, *T. brucei* PKAR has several features that clearly distinguish it from PKARs of most other organisms.

4.2.1. Holoenzyme formation

An important feature of regulatory PKA subunits is their ability to bind to catalytic PKA subunits. This binding is mainly mediated by a conserved inhibitory sequence R R X [A/S/T] Ψ (Ψ =hydrophobic amino acid), located N-terminal of the cNMP binding sites. *T. brucei* PKAR, that possess such a classical inhibitor sequence (RRTTV), is in fact able to bind each of the three catalytic *T. brucei* PKA-like subunits PKAC1, PKAC2 and PKAC3. This was shown with different coimmunoprecipitation studies in this and previous work and provided the first proof for the role of *TbPKAR* as regulatory subunit of the PKA-like kinase.

In addition to their binding to catalytic subunits, most regulatory PKA subunits studied so far dimerize to enable the formation of a tetrameric PKA holoenzyme (R₂C₂). Responsible for dimerization is an N-terminal dimerization/docking domain. *T. brucei* PKAR lacks such a dimerization/docking domain in its N-terminus that is unusually

long. Coimmunoprecipitation studies revealed that *Tb*PKAR is unable to form R dimers, resulting in a dimeric (RC) rather than tetrameric PKA holoenzyme (compare chapter 3.2.). Dimeric PKAs were also found in several other lower eukaryotes, such as *Dictyostelium discoideum* (Mutzel *et al.*, 1987), *Paramecium tetraurelia* (Hochstrasser and Nelson, 1989) or the dinoflagellate *Amphidinium operculatum* (Leighfield *et al.*, 2002). This suggests that the development of the tetrameric PKA structure has occurred rather late in evolution. PKARs from *Paramecium* (Carlson and Nelson *et al.*, 1996) and *Dictyostelium* have unusually short N-termini that lack the dimerization domain (Fig. 53).

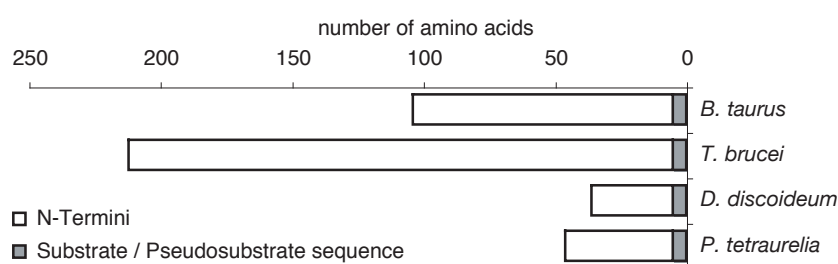


Fig. 53: Length differences in the N-termini of regulatory PKA subunits

The N-termini (here defined as the region N-terminal of the Substrate/Pseudosubstrate sequence) of PKAR subunits of *B. taurus* (PKAR1 α , Acc No. P00514), *T. brucei*, *D. discoideum* (Acc No. P05987) and *P. tetraurelia* (Acc No. AAC47268) are shown. PKARs from *D. discoideum* and *P. tetraurelia* have shorter N-termini than *B. taurus* PKAR and lack dimerization domains. In contrast, *T. brucei* PKAR has an unusually long N-terminus that is nevertheless devoid of a dimerization domain.

If the N-terminus of *T. brucei* PKAR does not mediate the binding to another regulatory subunit, what is its possible function? Interestingly, similar long N-termini are also present in the PKARs of the related organisms *Leishmania* and *T. cruzi* and are even highly conserved among these trypanosomatidae (Fig. 54). This high degree in conservation suggests that they fulfill an important function different from dimerization. Furthermore, the PKAR N-termini of kinetoplastida show no significant homologies to proteins from any other organisms (<http://www.ncbi.nlm.nih.gov/BLAST/>, default parameters as set by the ncbi server), suggesting that their function might be unique to trypanosomatidae. The most obvious function of these unusual N-termini would be the binding to a (yet undefined) A kinase anchoring protein (AKAP) to mediate subcellular PKA localization.

4.2.2. Activation of the *T. brucei* PKA-like kinase

Upon cAMP binding, structural changes of the regulatory PKA subunit lead to the release of the catalytic subunit from the holoenzyme complex and thus to PKA activation. This, however, turned out not to be true for *T. brucei* PKA-like kinase:

4.2.2.1. *T. brucei* PKA-like kinase is activated with cGMP in unphysiologically high concentrations only

Several different cyclic nucleotides were tested for their abilities to activate *T. brucei* PKA-like kinase *in vitro*. We could not detect any increase in kinase activity neither with the classical PKA activator cAMP nor with cIMP, cUMP, cXMP or cCMP, not even in mM concentrations. The only cyclic nucleotide that activated *T. brucei* PKA-like kinase was cGMP. Although this observation was also reported by a different laboratory (Shalaby *et al.*, 2001), the role of cGMP as the physiological activator of *T. brucei* PKA-like kinase remains highly doubtful for two main reasons:

Firstly, the cGMP concentrations needed for activation of the PKA-like kinase were unusually high. In fact, the concentration necessary for half maximal kinase activation ($K_{a(cGMP)}$) was higher than 100 μM (compare Fig. 22 in chapter 3.3.2.), which lies at least two orders of magnitudes above the K_a values of other cGMP dependent protein kinases (see table 8).

Kinase	$K_{a(cGMP)}$	Reference
<i>T. brucei</i> PKA-like kinase	>100 μM	this work
<i>T. brucei</i> PKA-like kinase	< 20 μM	Shalaby <i>et al.</i>, 2001
<i>Plasmodium</i> PKG	0.17 μM	Deng <i>et al.</i> , 2003
<i>C. elegans</i> CGK-1C	0.190 μM	Stansberry <i>et al.</i> , 2001
<i>E. tenella</i> PKG	2.3 μM	Gurnett <i>et al.</i> , 2002
<i>D. melanogaster</i> PKG	0.19 μM	Foster <i>et al.</i> , 1996
<i>T. gondii</i> PKG	1.7 μM	Donald <i>et al.</i> , 2002
PKG from bovine aorta, type alpha	0.29 μM	Wolfe <i>et al.</i> , 1989
Human PKG1beta	0.691 μM	Richie-Jannetta <i>et al.</i> 2003
Mouse brain CGKII	0.3 μM	Uhler, 1993
<i>Dictyostelium</i> PKG	0.001 μM	Wanner and Wurster, 1990

Table 8: cGMP concentrations needed for half maximal activation of cGMP dependent kinases from different organisms in comparison to *T. brucei* PKA-like kinase.

The cGMP dependent kinases were chosen arbitrarily. In the first two rows (bold) the corresponding values are shown for *T. brucei* PKA-like kinase as determined in this work and by Shalaby *et al.*, respectively.

Shalaby *et al.* claimed maximal activation of *T. brucei* PKA-like with only 20 μM cGMP, but even this concentration is unusually high and the authors did not actually show these data.

The second argument against cGMP as the physiological activator of *T. brucei* PKA-like kinase is the absence of any components of cGMP signaling in *T. brucei*. Neither cGMP, nor guanylyl cyclases have yet been found in *T. brucei* and all *T. brucei* PDEs that have been cloned and characterized so far, were found to be highly specific for cAMP (Zoraghi *et al.*, 2001; Zoraghi *et al.*, 2002; Gong *et al.*, 2001; Kunz *et al.*, 2004; Rascon *et al.*, 2002).

Whether the observed activation of *T. brucei* PKA-like kinase with cGMP is accompanied by a dissociation of the holoenzyme complex, remains unclear. In fact, we did observe a partial dissociation of the *T. brucei* PKA-like holoenzyme when incubated with 1 mM cGMP for 30 min (Fig. 21 in 3.3.1.), but only in the presence of the PKA specific inhibitor PKI 5-24. This peptide inhibitor binds to the catalytic center of PKA and this way probably inhibits the reassociation of the holoenzyme. Without PKI, the holoenzyme remains associated, even when cGMP is added. It therefore remains unlikely that the observed holoenzyme dissociation reflects the physiological mechanism of kinase activation. Alternatively, the binding of cGMP could cause a structural change in the holoenzyme complex which only decreases rather than abolishes the binding affinity between regulatory and catalytic subunit. In the presence of PKI, the dissociated subunits would accumulate, since the reassociation of the holoenzyme is prevented.

A dimeric PKA that does not dissociate in the presence of cyclic nucleotides has been purified from mouse liver cytosol (Nikolokaki *et al.*, 1999). The authors obtained half maximal activity of the kinase with either 0.1 μM cAMP, 0.8 μM cGMP or 2 μM of either cGMP or cUMP but could not dissociate the holoenzyme with even 1 μM cAMP, although they could show that regulatory and catalytic units of the kinase were on different polypeptide chains.

4.2.2.2. *T. brucei* PKA-like kinase is inhibited by cAMP

cAMP was not only unable to activate *T. brucei* PKA-like kinase, it even inhibited cGMP stimulated kinase activity. A similar effect has also been observed by Shalaby *et al.* (2001) in some, but not all of their kinase assays. These results were unexpected. There are some reports about kinases that are activated with both cAMP and cGMP (Vardanis

et al., 1980; Lin and Volcani *et al.*, 1989), but to our knowledge no kinase has yet been shown to be actually inhibited by a cyclic nucleotide.

The most likely mechanism for the inhibition of *T. brucei* PKA-like kinase by cAMP is a competition of cAMP with cGMP (or another yet unknown PKA activating cyclic nucleotide) for the cNMP binding pockets of PKAR. Cyclic AMP would bind to the cNMP binding sites but fail to cause the structural changes necessary for kinase activation.

At first sight such a competition between cAMP and cGMP for the cNMP binding sites appears contradictory to results from Shalaby *et al.* (2001). The authors examined the binding capabilities of recombinantly expressed cNMP binding domains of *T. brucei* PKAR towards cGMP in the presence of cAMP. According to their data, a 100-fold excess of cAMP does not interfere with the cGMP binding to either of the two cGMP domains.

However, Shalaby and coauthors only worked with single cNMP binding domains, instead of the entire protein. Their data might therefore not reflect the physiological binding parameters of the cNMP binding sites in their “native environment”. At least for mammalian PKAs it has been shown that the binding of cyclic nucleotides to one cNMP binding site allosterically influences structure and binding abilities of the second cNMP binding site (Ogreid and Doskeland 1981a; Ogreid and Doskeland, 1981b).

Therefore, competitive binding assays with cAMP and cGMP should be repeated using the complete PKAR subunit.

4.2.2.3. Establishment of an *in vivo* kinase assay for *T. brucei* PKA-like kinase

In order to exclude that the failure to activate *T. brucei* PKA-like kinase with cyclic nucleotides was not simply due to an *in vitro* artefact, an *in vivo* PKA kinase assay was established in this work. It is based on the immunological detection of phosphorylated VASP protein, a reporter substrate for PKA activity (Smolenski *et al.*, 1998; compare 3.3.4.). For this, VASP was transgenically expressed in trypanosomes. From a decrease in VASP phosphorylation with the PKA inhibitor KT5720 and from the consistence of the results from all *in vitro* and *in vivo* kinase assays we conclude that VASP phosphorylation does most likely reflect the activity of *T. brucei* PKA-like kinase. However, KT5720, a specific inhibitor of mammalian PKAs that has lower affinities towards *T. brucei* PKAs (compare 4.1) might also inhibit other *T. brucei* kinases. Therefore, we cannot fully exclude that VASP is phosphorylated by another *T. brucei* kinase.

With the aid of this *in vivo* kinase assay we observed an increase in kinase activity with the membrane permeable cGMP derivative pCPT-cGMP in high concentrations and a decrease with the cAMP derivative pCPT-cAMP. Thus, the *in vitro* data were confirmed.

4.2.2.4. The cNMP binding sites of *T. brucei* PKAR

The reason for the observed unusual reactions of *T. brucei* PKAR towards cyclic nucleotides must lie in its cNMP binding sites. In fact, three amino acids are absent in *T. brucei* PKAR that are highly conserved between PKARs of most species and have been shown to contribute synergistically to the binding of cAMP and presumably also cGMP (Su *et al.*, 1995).

First of all, a conserved arginine (218 and 347 in the 1st respectively 2nd cNMP binding sites of human PKAR type II alpha) is not present in *T. brucei* PKAR. This arginine normally interacts with the equatorial exocyclic oxygen of the cAMP or cGMP phosphate and therefore plays a major role in cNMP binding. A replacement of that arginine with the very similar lysine in mammalian PKA already significantly decreases PKA affinity towards cAMP (Herberg *et al.*, 1996).

The second sequence difference affects a conserved alanine (211 and 340 in the 1st respectively 2nd cNMP binding sites of human PKAR type II alpha) that is replaced by glutamate in both cNMP binding domains of *Tb*PKAR. The alpha amino group of that alanine normally forms hydrogen bonds to the equatorial oxygen of the cAMP phosphate. The negative charged glutamate of *T. brucei* PKAR might be unable to fulfill a similar function next to the (negatively charged) phosphate group.

The third difference between *T. brucei* PKAR and other cyclic nucleotide dependent kinases was found at a position that is responsible for the selectivity of the domain towards either cGMP or cAMP (219 and 348 in the 1st respectively 2nd cNMP binding sites of human PKAR type II alpha). Usually, an alanine is found in PKAs and a serine or threonine in PKGs. The hydroxyl group of the serine or threonine forms a hydrogen bond with the C2 amino group of the guanine as shown in figure 55. It was shown with site directed mutagenesis that this serine or threonine residue is essential for high affinity binding of cGMP but does not affect cAMP binding (Shabb *et al.*, 1991; Kaupp *et al.*, 1992; Reed *et al.*, 1996; Reed *et al.*, 1997). Surprisingly, *T. brucei* PKAR has neither

alanine nor serine/threonine, but valine at this position that cannot form any hydrogen bond. The significance for this remains unclear.

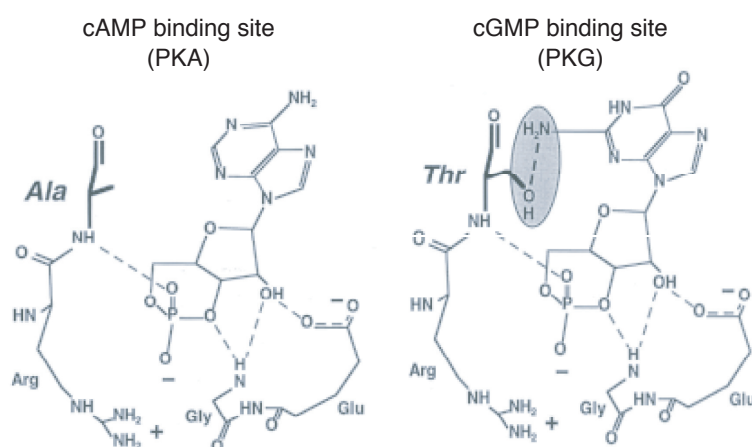


Fig. 55: cAMP and cGMP binding to the binding pockets of cA and cG kinases: Specificity towards cAMP or cGMP of cNMP binding sites is mediated by a very conserved amino acid (219 and 348 in human PKAR type II alpha) that is alanine in PKAs and serine or threonine in PKGs. In PKGs forms the hydroxyl group of the serine or threonine a hydrogen bond with the C2 amino group of the guanine. No such hydrogen bond is present in PKAs. The picture is taken from Francis *et al.*, 1999.

Similar amino acid substitutions are also found in the cNMP binding sites of PKAR orthologous proteins from the related kinetoplastida *T. cruzi* and *L. major*. In fact, two of the three substituted amino acids have been replaced by identical amino acids in *T. brucei*, *L. major* and *T. cruzi* (E and V) and are thus conserved between kinetoplastida (Table 9).

Unusual amino acids in the cNMP binding domains of kinetoplastida PKAR orthologues							
position relative to human PKAR type II alpha (domain A/ domain B)	human PKAR (both domains)	Kinetoplastida PKAR orthologues					
		domain A			domain B		
		<i>Tb</i>	<i>Tc</i>	<i>Lm</i>	<i>Tb</i>	<i>Tc</i>	<i>Lm</i>
218 / 347	R	T	V	A	N	T	T
211 / 340	A	E	E	E	E	E	E
219 / 348	A	V	V	V	V	V	V

Table 9: Unusual amino acids in the cNMP binding domains of kinetoplastida PKAR orthologues Three very conserved amino acids present in the cAMP binding pockets of most PKARs are absent in all kinetoplastida PKAR orthologues. The amino acids at the homologous positions in kinetoplastida PKAR orthologues (A and B) are shown. *Tb*=*T. brucei*; *Tc*=*T. cruzi*; *Lm*=*L. major*

This suggests that PKAR orthologous proteins from other kinetoplastida have similar binding properties to cyclic nucleotides compared to *T. brucei* PKAR. In fact, a kinase activity has been purified from *L. donovani* that has several characteristics of a classical PKA, but shows no reaction on either 0.05 mM cAMP or cGMP (Banerjee *et al.*, 1992). It might become activated with cGMP in higher concentrations, similar to *T. brucei* PKAR. In contrast, a kinase activity has been purified from *T. cruzi* that is activated with only

nanomolar concentrations of cAMP (Ulloa *et al.*, 1988). There are, however, doubts on the reproducibility of these data.

The observed amino acid substitutions appear to be unique to PKAR orthologues from Trypanosomatidae. An alignment of the cNMP binding domains from kinetoplastida PKAR orthologues with the corresponding domains of PKAs and PKGs from various other organisms is shown in figure 56. Of the examined organisms, only *Plasmodium* PKGs have different amino acids at the position of the conserved arginine 218/347. A negatively charged amino acid at the position of the highly conserved alanine 211/340 was not found in any of the examined organisms, only *Plasmodium* and some fungi have a serine or tyrosine at the homologous positions. Alanine 219/348 was only absent in domain A of *Plasmodium* PKGs (F) and in domain B of some fungi/yeasts (N,V,Q).

Altogether, the observed differences in primary sequence in kinetoplastida PKAR orthologues are likely to influence the affinities of the cNMP binding sites towards cyclic nucleotides and thus affect the kinase activation mechanism.

4.2.3. Are there further PKAR homologous proteins in *T. brucei*?

With HMMER based searches against the nearly completed *T. brucei* genome database three further PKAR related proteins were identified (compare chapter 3.5.1.). All of them have two predicted cNMP binding domains in tandem, one has a classical inhibitor sequence that might mediate the binding to a catalytic PKA subunit. The new *T. brucei* PKAR homologous proteins are unusually large.

Whether any of these proteins is in fact able to bind to catalytic PKA subunits is currently investigated. When the PKA-like holoenzyme is immunoprecipitated via Ty1-PKAC1, the only coprecipitated protein that is detectable on a Coomassie stained gel is the *Tb*PKAR protein investigated in this work (compare figure 19 in chapter 3.2.2.). Thus, potential PKAR subunits should be present in lower amounts than *Tb*PKAR or exclusively bind to either PKAC2 or PKAC3; otherwise they would have been detected most likely.

	domain A	domain B
PKA <i>T. brucei</i>	EGTAVGEL EL MYQTP TV ATVKVCTP	KGDHVGEL EL FNH ANV ADVVAKT-
PKA <i>T. cruzi</i>	EGTAVGEL EL MYDTP W ATVKVCTD	QGDHIGEL EL FNH RTV ADVVAKT-
PKA <i>L. major</i>	EGTAVGEL EL LYDTP AV ATVKVSTE	SGDHIGEL EL FNKH RTV ADIVAVT-
PKA <i>A. fumigatus</i>	PGGSFGELALMYNAPRAATIVSADP	RGDFFGELALLDDK P RAASVVAKT-
PKA <i>A. niger</i>	PGGSFGELALMYNAPRAATVSVDP	RGDYFGELALLDDK P RAASIVAKT-
PKA <i>E. nidulans</i>	PGGSFGELALMYNAPRAATIVSTEP	RGDYFGELALLDDK P RAASVRAKT-
PKA <i>N. crassa</i>	EGGSFGELALMYNAPRAATVSAEP	KGDFFGELALLND P RAASVISQT-
PKA <i>M. grisea</i>	AGGSFGELALMYNAPRAATVMSAEP	KGDFFGELALLND P RAASVVSKT-
PKA <i>T. atroviride</i>	AGGSFGELALMYNAPRAATIIISAEG	KGDFFGELALLND P RAASVIATS-
PKA <i>C. lagenarium</i>	AGGSFGELALMYNAPRAATVISAEP	KGDFFGELALLND P RAASIVATT-
PKA <i>C. trifolii</i>	AGGSFGELALMYNAPRAATVISAEP	KGDFFGELALLND P RAASIVATT-
PKA <i>B. emersonii</i>	AGGSFGELALMYNAPRAATVVATAE	KGNYFGELALLSD K PR V ATIRAKG-
PKA <i>M. racemosus</i>	AGGSFGELALMYNAPRAATIIITSD	RGSYFGELALLND P RAATVVAHG-
PKA <i>C. neoformans</i>	EGSFGELALMHNAPRAASIIISLTP	QGDFFGELALLNR R TRAA T IRAEGP
PKA <i>S. pombe</i>	PGEYFGELALMYNAPRAASVVS K TP	KGDFFGELAL I HETV R NA T VQAKT-
PKA <i>C. albicans</i>	EGSFGELALMYNSPRAATAVAATD	KGDFFGELALIKDL P RA T VEALD-
PKA <i>bovine (RIIbeta)</i>	NRGSFGELALMYNTPRAATITATSP	RGQYFGELALV T N K PRAASAHATG-
PKA <i>rat (RIIbeta)</i>	NRGSFGELALMYNTPRAATITATSP	RGQYFGELALV T N K PRAASAHATG-
PKA <i>mouse (RIIalpha)</i>	NRGSFGELALMYNTPRAATIIATSE	KGQYFGELALV T N K PRAASAYGVG-
PKA <i>rat (RIIalpha)</i>	NRGSFGELALMYNTPRAATIVATSD	KGQYFGELALV T N K PRAASAYAVG-
PKA <i>human (RIIalpha)</i>	NRGSFGELALMYNTPRAATIVATSE	KGQYFGELALV T H R PRAASVYATGG
PKA <i>D. melanogaster (RII)</i>	HTGLFGELALLY N PRAATVQAETS	SSDYFG E IALLLDR P RAATVIAKT-
PKA <i>O. volvulus</i>	EGGSFGELAL I YGT P RAATVAKSD	MSDYFG E IALLLDR P RAATVIAKT-
PKA <i>C. elegans</i>	EGGSFGELAL I YGT P RAATVIAKID	PSDYFG E IALLLDR P RAATVIAKG-
PKA <i>California sea hare</i>	EGGSFGELAL I YGT P RAATVIAKID	PSDYFG E IALLLDR P RAATVIAKG-
PKA <i>A. Californica</i>	EGGSFGELAL I YGT P RAATVIAKID	PSDYFG E IALLLDR P RAATVIAKG-
PKA <i>bovine (RIalpha)</i>	EGGSFGELAL I YGT P RAATVIAKTN	PSDYFG E IALLLDR P RAATVIAKG-
PKA <i>rat (RIalpha)</i>	EGGSFGELAL I YGT P RAATVIAKTN	PSDYFG E IALLLDR P RAATVIAKG-
PKA <i>human (RIalpha)</i>	EGGSFGELAL I YGT P RAATVIAKTN	PSDYFG E IALLLDR P RAATVIAKG-
PKA <i>mouse (RIbeta)</i>	EGGSFGELAL I YGT P RAATVIAKTD	SSDYFG E IALLLDR P RAATVIAKG-
PKA <i>D. melanogaster (RI)</i>	EGGSFGELAL I YGT P RAATVIAKTD	PSDYFG E IALLLDR P RAATVIAKG-
PKA <i>E. octocoidium</i>	EGGSFGELAL I YGS P RAATVIAKTD	PSDYFG E IALLLDR P RAATVIAKG-
PKA <i>P. falciparum</i>	SKDVF G ELALLY N S K RAATATATLTK	KGDFFGELALL K N K PRAAT I KAQN-
PKA <i>P. yoelii yoelii</i>	SKDVF G ELALLY N S K RAATATATLTK	KGDFFGELALL K D Q PRAATVIAES-
PKA <i>T. gondii</i>	PGDAFGELALMYNAPRAATVIAADD	KGDFFGELALL K D Q PRAATVIAES-
PKA <i>E. octocarinatus</i>	PGDAFGELALLY N APRAAT I KA K TE	YGDYFG E IALLL K NE P RAASVIAKT-
PKA <i>P. tetraurelia</i>	PGESFGELALLY N V P RAAT I KA K TD	VGDYFGELAL I K H E P RAAN I VIAKS-
PKG <i>E. tenella</i>	TGQAF G E I SL I HNSARTATIKTLSE	RGEYFG E RALLY D E P RSAT I AE E P
PKG <i>E. maxima</i>	QGQAF G E I SL I HNSARTATIKTLSD	KGDFFGELALLY D E P RSAT I AE E E
PKG <i>T. gondii</i>	KGKAF G E I AL I HNT E RSATVVASST	KGDFFGELALLY K E P RSAT I AE E F
PKG <i>P. falciparum</i>	KGSSFG E AAL I HNT Q RSAT I IA E T-	KGDFFGELALLY D E P RSAT I IA E K E P
PKG <i>C. parvum</i>	EGTAF G ELAL I HNT P RSAT I L V IE-	EGDAFG E RS L MF D E P RSAT I AN A T
PKG <i>A. mellifera</i>	PGKVL G ELAILY N CKRTAT I TA A TD	KGDFFG E KAL Q GD L RTAN I IA D DD
PKG <i>B. mori (typeII)</i>	PGKVF G ELAILY N CKRTAT I KA A TD	KGDFFG E KAL Q GD L RTAN I V C D S P
PKG <i>bovine (I alpha)</i>	PGKVF G ELAILY N CTRTAT V K L V N	KGDFFG E KAL Q G E D V RTAN V IA-- A
PKG <i>human (type I)</i>	PGKVF G ELAILY N CTRTAT V K L V N	KGDFFG E KAL Q G E D V RTAN V IA-- A
PKG <i>rabbit (typeI alpha)</i>	PGKVF G ELAILY N CTRTAT V K L V N	KGDFFG E KAL Q G E D V RTAN V IA-- A
PKG <i>rat</i>	MWTT F GELAILY N CTRTAS V KA I T N	KGDFFG E KAL I S D D V RSAN I IA E - E
PKG <i>human (type II)</i>	MWTT F GELAILY N CTRTAS V KA I T N	KGDFFG E KAL I S D D V RSAN I IA E - E
PKG <i>mouse (type II)</i>	MWTT F GELAILY N CTRTAS V KA I T N	KGDFFG E KAL I S D D V RSAN I IA E - E
PKG <i>H. oligactis</i>	PGEL F GELAILY N CTRTAS V KA I DD	KGDFFG E KAL I S D D V RSAN I IA E - E
PKG <i>P. yoelii yoelii</i>	RGK S FGD Q Y V LN Q K Q K F K H T L K S L E	KGDFFG E KAL I S D D V RSAN I IA E - E
PKG <i>P. falciparum</i>	RGMS F GD Q Y V LN Q K Q P F K H T I K S L E	KGDFFG E KAL I S D D V RSAN I IA E - E
	.*: ::	.** : *

Figure 56: Conserved sequences in PKA and PKG cNMP binding pockets

The cNMP binding domains of PKAs and PKGs of the indicated organisms were aligned with the WEB based services of ClustalW (<http://www.ebi.ac.uk/clustalw/>) using default parameters as provided by the EBI server. Only a 25 amino acid sequence of each domain (domain A and domain B) is shown (amino acids 202-227 and 332-357 referring to human PKA type II alpha). The unusual amino acids of kinetoplastida PKA-like kinases are colored red/bold. Any unusual amino acids at this position in other organisms are colored blue/bold.

4.3. Functions of *T. brucei* PKA-like kinase

Results from several reverse genetic experiments suggest that *T. brucei* PKA-like kinase regulates cell cycle progression and basal body segregation. In addition, we provide evidence for a role of the kinase in the regulation of differentiation processes. This is suggested from an increase in (*in vivo*) kinase activity caused by several environmental stresses that have been shown to participate in either LS to SS or SS to PCF differentiation.

4.3.1. *T. brucei* PKA-like kinase: a transmitter of environmental stress?

4.3.1.1. Kinase activity in the presence of the PDE inhibitors dipyridamole and etazolate

The PDE inhibitor etazolate induces differentiation from LS to SS cells (Vassella *et al.*, 1997). Dipyridamole, another potent PDE inhibitor, inhibits major *T. brucei* PDEs with higher affinity than etazolate (table 10) but has never been tested on its ability to stimulate differentiation.

	IC ₅₀ [μ M]	
	dipyridamole	etazolate
<i>Tb</i> PDE1	13.0	25.0
<i>Tb</i> PDE2A	5.9	30.3
<i>Tb</i> PDE2B	27.0	127.0
<i>Tb</i> PDE2C	14.6	30.6

Table 10: Inhibition of the known *T. brucei* PDEs by the PDE inhibitors dipyridamole and etazolate. IC₅₀ values are indicated for *Tb*PDE1, *Tb*PDE2A, *Tb*PDE2B, *Tb*PDE2C as determined by Kunz *et al.*, 2004; Zoraghi *et al.*, 2000; Rascón *et al.*, 2002 and Zoraghi *et al.*, 2002, respectively.

We measured *in vivo* kinase activity in the presence of etazolate or dipyridamole. With both PDE inhibitors we observed an increase in kinase activity. With dipyridamole the increase in kinase activity was higher than with (equimolar concentrations) of etazolate. This might be explained by the different affinities of the two inhibitors towards *T. brucei* PDEs, but could also be due to several other factors, such as differences in membrane passing abilities.

The reason for the observed activation of *T. brucei* PKA-like kinase in the presence of PDE inhibitors remains unclear. In fact, assuming that the kinase activity derived from cloned kinases is cNMP stimulated at all, one would expect an inhibition of kinase activity rather than an activation, since all *T. brucei* PDEs studied so far are highly specific

for cAMP (Kunz *et al.*, 2004; Zoraghi *et al.*, 2000; Rascón *et al.*, 2002 and Zoraghi *et al.*, 2002). PDE inhibition should therefore result in an increase in cAMP, which has in fact been shown for dipyridamole (Zoraghi *et al.*, 2001) and cAMP inhibits PKA-like kinase. We cannot, however, exclude that the PDE inhibitors also activate a yet unknown *T. brucei* PDE. This PDE might even be specific for another cyclic nucleotide, given that in mammals dipyridamole does not only inhibit cAMP specific PDEs but also the cGMP specific PDEs, PDE5 and PDE6, with IC₅₀ values of 0.9 and 0.4 μ M respectively (reviewed in Essayan *et al.*, 2001). Two further PDEs have already been identified in *T. brucei* but not yet characterized (PDE2D, PDE2E, Seebeck *et al.*, 2001).

To identify the mechanism of kinase activation by PDE inhibitors it is essential to measure both cAMP and cGMP levels in parallel to *in vivo* kinase activity.

4.3.1.2. Temperature

A drop in temperature has long been known to play a role in differentiation from short stumpy to procyclic cells. For this reason it is frequently used to induce differentiation *in vitro*, together with citrate / cis-aconitate (Ziegelbauer *et al.*, 1990; Rolin *et al.*, 1993; Matthews and Gull, 1994; Vassella and Boshart, 1996). The mechanism of cold shock sensing in trypanosomes was established by recent studies from this lab. Engstler and Boshart (2004) could show that cold shock (37°C→20°C) induces the expression of the insect stage specific procyclin in BSF cells by a postranscriptional mechanism. Furthermore, although cold shock alone is not sufficient to induce differentiation, it dramatically increases the sensitivity of the cells towards the differentiation stimuli cis-aconitate / citrate. Thus, there is strong evidence for the participation of cold shock in the differentiation from short stumpy to procyclic cells.

We measured *in vivo* activity of *T. brucei* PKA-like kinase at different temperatures with the aid of the VASP reporter substrate and found a significant increase in activity at all temperatures below 37°C. Thereby the increase in kinase activity was nearly proportional to the decrease in temperature. Kinase activity reached its maximum at 12°C and then remained equally high at lower temperatures. Conclusively, the activity of *T. brucei* PKA like kinase is temperature dependent.

To our knowledge, *T. brucei* PKA-like kinase is the first PKA homologue that has been shown to be activated by changes in temperature. Although temperature sensing has been described for many organisms and a large body of information is available on cold shock induced (mainly prokaryotic) genes (reviewed in Yamanaka *et al.*, 1999; Los *et al.*, 1999), surprisingly little is known about the upstream factors of a temperature sensing signaling pathway.

In bacteria it was shown that membranes can sense temperature changes (reviewed in Rock and Cronan, 1996) and transmit signals as a consequence of changes in their membrane phase state and microdomain organization (Vigh *et al.*, 1998; Hoppe *et al.*, 2000; Suzuki *et al.*, 2000). A two component-signal transduction pathway, consisting of a sensor kinase and a response regulator, has been shown to transmit cold shock signals across the bacterial plasma membrane (Aguilar *et al.*, 2001). For plants, a similar cold shock sensing mechanism has been proposed. There is evidence that membrane structures of plants change after cold shock and that these membrane changes cause an influx in Ca²⁺ and subsequent activation of cold shock dependent MAP kinases (Sangwan *et al.*, 2002a; Gimalov *et al.*, 2003; Jonak *et al.*, 1996). Using cell free extracts it was shown that a heat shock activated MAP kinase is even able to sense temperature shifts directly (Sangwan *et al.*, 2002b). The involvement of MAP kinases in cold and heat shock response is not restricted to plants but has also been shown in yeast (Soto *et al.*, 2002). Most interestingly, heat shock response in *Leishmania* was found to be accompanied by an Ca²⁺ influx, both from internal pools and from the outside milieu (Sarkar *et al.*, 1995).

It is tempting to speculate that *T. brucei* PKA-like kinase participates in the upstream signaling events in response to cold shock. It has already been shown that a temperature drop below 26°C results in major changes in the *T. brucei* plasma membrane (Ter Kuile *et al.*, 1992).

4.3.1.3. pH value

Similar to cold shock, mild acid stress also induces differentiation. This was not only shown for *T. brucei* (Rolin *et al.*, 1998) but also for the related kinetoplastida *T. cruzi* (Kanbara *et al.*, 1990; Tomlinson *et al.*, 1995) and *Leishmania* (Zilberstein *et al.*, 1991; Bates *et al.*, 1992; Zilberstein *et al.*, 1994). In *T. brucei*, mild acid stress can induce the

transformation of short stumpy cells into the insect stage form even in the absence of citrate/cis-aconitate, although very inefficiently (Rolin *et al.*, 1998). It still remains unclear whether mild acid stress has any relevance for *in vivo* differentiation, since the pH value in the alimentary tracts of the tsetse fly is alkaline rather than acid (J. Van Den Abbeele, unpublished). However, mild acid stress might occur at some stage on the way from the mammalian blood to the intestine of the insect vector and there act as differentiation stimulus.

We measured *in vivo* activity of *T. brucei* PKA-like kinase of cells in both acid and alkaline medium and found a linear dependency between kinase activity and the extracellular pH values. Low pH values resulted in kinase activation and high pH values in kinase inhibition. The tested pH values ranged from 5.5 to 9.5 and had no effect on the viability and motility of the cells during the time of observation, as judged by phase microscopy. Furthermore, changes in kinase activity were reversible. Conclusively, the activity of *T. brucei* PKA-like kinase is depending on the pH value of the environment.

The signaling events that underlie mild acid stress response in *T. brucei* were studied by Rolin *et al.* (1996). The authors found an increase in adenylate cyclase activity at pH 5.5. With an artificial acidification of the cytosol by a protonophore they observed the same effect even at neutral extracellular pH. This suggests that adenylate cyclase is activated due to a slight acidification of the cytosol. Interestingly, the activation of adenylate cyclase after mild acid stress was restricted to LS trypanosomes, but absent from the insect stage (Rolin *et al.*, 1996) and the cell cycle arrested fly-preadapted short stumpy stage (Nolan *et al.*, 2000).

Whether the observed activation of PKA-like kinase at mild acid stress is dependent on the activation of adenylate cyclases remains to be shown. Like the observed activation of PKA-like kinase with PDE inhibitors, this would be contradictory to the fact that *T. brucei* PKA-like kinase is inhibited by cAMP.

4.3.1.4. Life cycle stage dependent differences in expression and posttranslational modification of PKAC1 and PKAC2

In search of a putative function for *T. brucei* PKA-like kinase in differentiation, two of the catalytic PKA-like subunits were studied in more detail. These isoforms, that have nearly

identical sequences, are of particular interest in this context, since both their expression and posttranslational modification had been shown to be developmentally regulated.

We found that PKAC1 and PKAC2 protein levels are inversely regulated, with PKAC1 being mainly expressed in blood stream form cells and PKAC2 in the insect stage form. Thereby the overall protein level of PKAC1/2 remained constant. mRNA levels (E. Vassella, unpublished) roughly corresponded to protein levels, suggesting that expression of PKAC1 and PKAC2 is mainly regulated by mRNA abundance. *T. brucei* PKAC1 and PKAC2 thus belong to the 2% of all *T. brucei* genes that are currently thought to be regulated in a life cycle stage dependent manner (number estimated from transcriptome analysis, Diehl *et al.*, 2002).

The second difference between the two PKAC isoforms was a life cycle stage dependent phosphorylation found in PKAC1 of SS cells, but not in PKAC2 (T. Klöckner, Ph.D. thesis 1996; S. Schimpf, Diploma thesis 2000, this work). In this work the phosphorylation site was mapped to the C-terminal Thr324 of PKAC1 using mass spectrometry. We could not, however, identify any function of this phosphorylation with reverse genetics. Thus, PKAC1 might simply be “accidentally” phosphorylated by a kinase that is expressed or active in the short stumpy stage only. NetPhosK, a neural network based phosphorylation prediction software (Blom *et al.*, 1999; Sicheritz-Ponten *et al.*, in preparation; NetPhosK, <http://www.cbs.dtu.dk/services/NetPhosK/>) predicts Thr324 of PKAC1 to be phosphorylated by a cyclin dependent kinase (Cdk5, probability 0.7). In fact, several cyclin dependent kinases of kinetoplastida have been shown to be activated in a life cycle stage dependent way (Mottram *et al.*, 1993; Grant *et al.*, 1998; Wang *et al.*, 1998). An experimental confirmation of these *in silico* predictions was, however, out of the focus of this work, given the negative functional data.

The stumpy specific PKAC1 phosphorylation nevertheless constitutes a new marker for the still insufficiently characterized short stumpy stage of *T. brucei*. Most known stumpy markers are rather unspecific, such as morphological changes (Vickerman, 1965) or cell cycle arrest in G1 (Shapiro *et al.*, 1984). They do not allow the unequivocal classification of a certain cell population. Specific stumpy markers are confined to the detection of metabolic changes (e.g. NADH diaphorase activity and dihydrolipoamide dehydrogenase (Tyler *et al.*, 1997)), changes in biosynthesis (e.g. ribonucleotide reductase (Breibach

et al., 2000)) and changes in protein trafficking and processing (Kelley *et al.*, 1995). The PKAC1 phosphorylation, easily detectable as band shift on a Western blot, constitutes the first stumpy marker that is based on stumpy specific changes in signaling pathways.

We were unable to identify any functional differences between PKAC1 and PKAC2 that could explain the observed life cycle stage specific differences between the isoforms. Any reverse genetic interference with either PKAC1 or PKAC2 always resulted in the same cytokinesis block phenotypes. In fact, it seems that the two isoforms can even complement each other. PKAC2 null mutants were perfectly able to transform into procyclic cells, that normally exclusively express PKAC2. Thus, the reason for the differential expression and modification of PKAC1 and PKAC2 remains unknown.

4.3.2. Role for *T. brucei* PKA-like kinase in cell cycle regulation

4.3.2.1. *T. brucei* PKA-like kinase is essential for cytokinesis progression

Evidence for a function of *T. brucei* PKA-like kinase during cytokinesis progression is provided by results from several reverse genetic experiments targeted against the different PKA-like subunits. Every interference with the abundance of either subunit prevented cells from completing cell division, while S-phase, mitosis and cytokinesis entry were not affected. It thereby appears that cytokinesis is blocked at a distinct point, since division furrows of cytokinesis blocked cells were of approximately equal sizes.

Two observations might help to evaluate the role of *T. brucei* PKA-like kinase in cell cycle regulation. The first was that minor changes in kinase protein level were already sufficient to severely interfere with cell cycle progression. The best example for this was the deletion of one PKAC2 allele that led to significantly reduced growth. This was a surprising result, given that PKAC2 is hardly expressed in LS trypanosomes. The second observation was that RNAi experiments targeted against PKAR not only led to PKAR depletion but also to a decrease of all three catalytic subunits. Obviously, cells keep the ratio of regulatory and catalytic subunit, and thus, the „net“ kinase activity constant. We conclude from this that a constant activity of PKA-like kinase, strictly kept within a very narrow range, is essential for accurate cell cycle progression.

Interestingly, we could not detect any qualitative differences between the phenotypes of the different PKA-like subunits, with the exception of the basal body phenotype discussed

below. In theory, depletion of the regulatory subunit should result in increased kinase activity, while depletion of the catalytic subunit should decrease kinase activity. One would therefore expect opposite phenotypes upon RNAi with PKAR and PKAC. However, due to the co-depletion of the PKAC-like subunits by RNAi targeted against PKAR, the change in net kinase activity for each particular RNAi experiment is unpredictable. Furthermore, depletion of catalytic and regulatory PKA-like subunits might at first result in opposite (non-visible) phenotypes that then both subsequently lead to the same cytokinesis block phenotypes.

4.3.2.2. Role for *T. brucei* PKA-like kinase in basal body movement

Data from RNA interference experiments targeted against PKAR also suggests the involvement of *T. brucei* PKA-like kinase in another major cell cycle event: the basal body segregation.

Basal bodies are the key regulators of the trypanosomal cell cycle. They are responsible for the nucleation of the new flagellum and mediate the segregation of the mitochondrial genome (Robinson *et al.*, 1991; Ogbadoyi *et al.*, 2003). At the end of their segregation, they adapt particular, highly conserved positions (Woodward and Gull 1990; Robinson *et al.*, 1995) that are thought to determine the position of the division furrow later on. Nothing is yet known about the underlying signaling pathways that regulate basal body movement, but evidence for an involvement of protein kinases in this complex process has been provided by Das *et al.* (1994). The authors treated cells with the phosphatase inhibitor ocadaic acid, which probably increases net kinase activity, and found basal body segregation inhibited.

Data from this work provide evidence that one of these basal body regulating kinases is identical to PKA-like kinase. When the regulatory PKA subunit was depleted by RNA interference we found enhanced basal body movement, thus the opposite phenotype described by Das *et al.* In fact, basal bodies were obviously incapable in recognizing their normal stop positions, but instead continued to segregate until they reached most unusual, far too anterior positions.

We at first thought that this observed extension in basal body movement was simply a secondary effect of the cytokinesis inhibition that occurred in parallel (see above). In theory, the process of cytokinesis itself could cease basal body segregation. Thus, in

the absence of cytokinesis basal bodies would continue to move. However, we could not confirm this hypothesis, since basal body movement was not affected when cytokinesis (but not basal body movement) was inhibited with the microtubules inhibitor vincristine. We therefore suggest that the *T. brucei* PKA-like kinase is directly involved in the control of basal body segregation.

So far, the only study that approaches the regulation of basal body segregation was performed by Kohl *et al.* (2003) using RNAi targeted against components of intraflagellar transport. The authors found decreased basal body distances in the absence of intraflagellar transport and conclude that the flagellum plays an essential role in the regulation of basal body movement. In addition, they also provide indirect evidence for a function of the flagellum in the regulation of cytokinesis, since cells without flagella fail to divide.

Given that 1) PKA-like kinase is localized in the trypanosomal flagellum (C. Krumbholz, this lab) and 2) both the flagellum and PKA-like kinase have been shown to be important for basal body movement and cytokinesis, is there any connection between the flagellar localization of the PKA-like kinase and its function as a cell cycle regulator?

4.3.2.3. The trypanosomal flagellum: a signaling compartment for cell cycle regulation?

The flagellum of *T. brucei* consists of the classical axoneme and an additional lattice-like structure called the paraflagellar rod (PFR) (reviewed in Gull, 1999). With the exception of its distal tip, it is attached along the length of the cell body. This attachment is mediated by cytoskeletal structures that lie underneath the plasma membrane and follow the path of the flagellum, the flagellum attachment zone (FAZ).

Increasing evidence suggests that the function of trypanosomal flagella is not restricted to motility. They probably also play an important role in cell cycle regulation, control of basal body movement, the positioning of the FAZ and the positioning of the division furrow (Kohl *et al.*, 1999; Kohl *et al.*, 2003, reviewed in McKean 2003). The outgrowth of the daughter flagellum can thus be seen as a pivotal event in trypanosomal morphogenesis. These complex processes require strict regulations mediated by signaling pathways. It is therefore not surprising that several proteins have been identified in flagella that

have (predicted) functions distinct from motility. Examples are adenylate kinase in trypanosomal flagella (Pullen *et al.*, 2004; D'Angelo *et al.*, 2002) and a MAP kinase in the flagellum of *Leishmania* (Wiese *et al.*, 2003).

With PKA-like kinase we have now identified a further flagellar protein that is involved in cell cycle regulation, to be more precise, in cytokinesis progression and basal body segregation. In this chapter we will concentrate on the discussion of possible mechanisms for the role of the flagellar localized PKA-like kinase in basal body movement. We can think of two mechanism that could explain the observed elongated basal body movement upon PKAR RNAi:

The first is that the kinase regulates the outgrowth of the daughter flagellum. The depletion of PKAR by RNAi would then result in uncontrolled growth of the daughter flagellum. Since the daughter flagellum is essential for basal body segregation (Kohl *et al.*, 2003), its uncontrolled growth could result in the observed changes in basal body positions.

Alternatively, PKA-like kinase could act as a sensor of flagellum length. One could speculate that both the mother and the daughter flagellum send signals to the basal body at the origin of each flagellum. As long as the flagella have different lengths, the basal bodies obtain signals of different strength and move. If both flagella reach equal lengths, both basal bodies obtain equally strong signals and stop moving. This way PKA-like kinase would ensure that basal body movement stops as soon as the daughter flagellum has reached its full length. It has been shown that both basal body movement and flagella growth are correlated in a nearly linear way and that both events are completed simultaneously (Robinson *et al.*, 1995; BSF cells: M. Engstler, unpublished).

4.4. *T. brucei* PKA-like kinase: current view and outlook

The aim of this last chapter is to highlight the remaining unsolved questions and possible experimental approaches.

The current view is that *T. brucei* has one regulatory PKA-like subunit and three isoforms for catalytic PKA subunits. The catalytic subunits PKAC1, PKAC2 and PKAC3 appear to be conventional PKAs as judged from substrate and inhibitor specificities and the fact that

PKAC3 forms a heterologous holoenzyme complex with bovine PKARs that dissociates in the presence of cAMP (T. Klöckner, Ph.D. thesis 1996; N. Wild unpublished, this work). The regulatory subunit has several features that distinguish it from a classical regulatory PKA subunit, such as its unusually long N-terminus that lacks a dimerization domain and several substitutions of conserved amino acids in its cNMP binding pockets. It has, however, a classical inhibitor sequence (substrate sequence) and is able to bind each of the catalytic subunits to form a dimeric holoenzyme.

With the exception of PKAC3, all PKA subunits are expressed and, in the case of PKAC1, also phosphorylated in a life cycle stage dependent manner (C. Schulte zu Sodingen, Ph.D. thesis 2000; T. Klöckner, Ph.D. thesis 1996; this work). The reason for this remains unknown. Data from several reverse genetic experiments provide evidence for a function of *T. brucei* PKA-like kinase in cell cycle regulation, especially in basal body segregation and cytokinesis progression. *T. brucei* PKA-like kinase is localized in the flagellum, in a subdomain of the paraflagellar rod proximal to the axoneme (C. Krumbholz, this lab).

So far, *T. brucei* PKA-like kinase possess all features that characterize a classical PKA. Problems start, however, when it comes to the question of kinase activation:

It has been shown, both *in vitro* and *in vivo*, that *T. brucei* PKA-like kinase is activated by cGMP, but in unphysiologically high concentrations only. In fact, cGMP concentrations needed for activation of *T. brucei* PKA-like kinase were 2-5 orders of magnitudes higher than cGMP concentrations needed for activation of other cGMP dependent kinases. The role of cGMP as the physiological activator of PKA-like kinase thus remains highly doubtful, even more so, since neither guanylyl cyclases, nor cGMP dependent phosphodiesterases or cGMP itself have yet been found in *T. brucei*.

Even more surprising with the finding, that cAMP not only failed to activate *T. brucei* PKA-like kinase but instead inhibited it. Again, this was shown both *in vitro* and *in vivo*. These results are in contradiction to other observations: If PKA is inhibited with cAMP, why is it activated with several stimuli that have been shown to activate adenylate cyclases or increase intracellular cAMP concentrations, such as PDE inhibitors and mild acid stress? We were so far unable to solve these contradictions.

What are the next important steps on the way to further understanding of the *T. brucei* PKA-like kinase ?

A major aim will be to finally solve the activation mechanism of the kinase. Correlations between *in vivo* activity of the PKA-like kinase and cyclic nucleotides are so far either based on indirect observations only or on the use of membrane permeable cNMP derivatives. None of these methods allows to directly correlate *in vivo* activity of PKA-like kinase with a certain cyclic nucleotide. It is therefore important to extend the *in vivo* kinase assay and measure not only phosphorylation of the PKA reporter substrate VASP but in parallel also changes in intracellular cGMP and cAMP concentrations. Also, instead of using membrane permeable cNMP derivatives that might differ in their affinities towards PKA compared to cNMPs, cAMP and cGMP should be added directly using living, permeabilized cells. In order to understand if and how cAMP acts as a PKA inhibitor, biochemical data about the binding affinities of *T. brucei* PKAR towards different cyclic nucleotides would be most useful.

The second major aim will be to use the VASP based *in vivo* kinase assay established in this work to study the role of *T. brucei* PKA in both LS to SS and SS to PCF differentiation. For this, VASP needs to be expressed in pleomorphic *T. brucei* cell lines, since the laboratory adapted monomorphic cell lines are unable to differentiate into SS cells. Kinase activity can then be directly monitored during the whole differentiation processes and correlated to other events that characterize differentiation.

AKAP	A kinase anchoring protein
APS	ammonium persulfate
ATP	adenosine 3' phosphate
BCIP	5-Bromo-4-chloro-3-indolyl-phosphate, 4-toluidine salt
BSD	blastidicin S deaminase
BLE	bleomycin resistance protein
bp	base pair
BSA	bovine serume albumine
BSF	blood stream form
cAMP	cyclic adanosine monophosphate
cCMP	Cytidine- 3', 5'- cyclic monophosphate
cGMP	cyclic guanosine monophosphate
cIMP	Inosine- 3', 5'- cyclic monophosphate
CPM	counts per minute
cUMP	Uridine- 3', 5'- cyclic monophosphate
cXMP	Xanthosine- 3', 5'- cyclic monophosphate
Da	dalton
DAPI	4,6-Diamidino-2-phenylindole
dCTP	2'-deoxycytidine 5'-triphosphate
dNTP	2'-deoxynucleosid 5'-triphosphate
dsRNA	double stranded RNA
DTT	dithiothreitol
EDTA	ethylenediaminetetraacetic acid
EGTA	tetra(acetoxymethyl ester)
ESAG	expression site associated gene
FCS	fetal calf serume
GAF	cGMP-specific and -stimulated phosphodiesterases, Anabaena adenylate cyclases and E.coli FhtA
HMM	Hidden Markov Model
HYG	hygromycin phosphotransferase
IP	immunoprecipitate / immunoprecipitation
IPTG	isopropyl thio-b-D-galactoside
LAR	Leukocyte antigen related
LB	Luria Bertani
LS	long slender
MCP	mitochondrial carrier protein
mRNA	messenger RNA
NBT	nitro blue tetrazolium chloride
NEO	neomycin phosphotransferase
ORF	open reading frame
PARP	procyclic acidic repetitive protein
PBS	phosphate-buffered saline
PCF	procyclic form
PDT	population doubling time
PFR	paraflagellar rod
PKA	cAMP dependent protein kinase

PKI	protein kinase inhibitor (PKA specific)
PVDF	polyvinylidene fluoride
RNAi	RNA interference
RT	room temperature
SDM	semi defined medium
SDS	sodium dodecyl sulfate
SIF	stumpy induction factor
SN	supernatant
SP	stationary phase (monomorphic SS-like cells)
SS	short stumpy
T7POL	T7 polymerase
TBS	Tris-buffered saline
TDB	trypanosome dilution buffer
TEMED	N,N,N',N'-Tetramethylethylen-diamin
Tet	tetracycline
TETR	tetracycline repressor
Tris	hydroxymethyl aminomethane
UTR	untranslated region
UV	ultra violett
VASP	vasidolator stimulated phosphoprotein
VSG	variant surface glycoprotein

- Abdel-Latif A. A. (2001) Cross talk between cyclic nucleotides and polyphosphoinositide hydrolysis, protein kinases, and contraction in smooth muscle. *Exp Biol Med* (Maywood) **226**, 153-63.
- Aboagye-Kwarteng T., ole-MoiYoi O. K. and Lonsdale-Eccles J. D. (1991) Phosphorylation differences among proteins of bloodstream developmental stages of *Trypanosoma brucei brucei*. *Biochem J* **275** (Pt 1), 7-14.
- Adams J. A., McGlone M. L., Gibson R. and Taylor S. S. (1995) Phosphorylation modulates catalytic function and regulation in the cAMP-dependent protein kinase. *Biochemistry* **34**, 2447-54.
- Aguilar P. S., Hernandez-Arriaga A. M., Cybulski L. E., Erazo A. C. and de Mendoza D. (2001) Molecular basis of thermosensing: a two-component signal transduction thermometer in *Bacillus subtilis*. *Embo J* **20**, 1681-91.
- Aktas B., Utz A., Hoenig-Liedl P., Walter U. and Geiger J. (2003) Dipyridamole enhances NO/cGMP-mediated vasodilator-stimulated phosphoprotein phosphorylation and signaling in human platelets: in vitro and in vivo/ex vivo studies. *Stroke* **34**, 764-9.
- Alexandre S., Paindavoine P., Tebabi P., Pays A., Halleux S., Steinert M. and Pays E. (1990) Differential expression of a family of putative adenylate/guanylate cyclase genes in *Trypanosoma brucei*. *Mol Biochem Parasitol* **43**, 279-88.
- Alibu V. P. , Storm L., Haile S., Clayton C. and Horn D. (2004) A doubly inducible system for RNA interference and rapid RNAi plasmid construction in *Trypanosoma brucei*, **in press** *Molecular and Biochemical Parasitology*.
- Altschul S. F., Madden T. L., Schaffer A. A., Zhang J., Zhang Z., Miller W. and Lipman D. J. (1997) Gapped BLAST and PSI-BLAST: a new generation of protein database search programs. *Nucleic Acids Res* **25**, 3389-402.
- Ashcroft M. T. (1960) A comparison between a syringe-passaged and a tsetse-fly-transmitted line of a strain of *Trypanosoma rhodesiense*. *Ann Trop Med Parasitol* **54**, 44-53.
- Banerjee C. and Sarkar D. (1992) Isolation and characterization of a cyclic nucleotide-independent protein kinase from *Leishmania donovani*. *Mol Biochem Parasitol* **52**, 195-205.
- Bastin P., Ellis K., Kohl L. and Gull K. (2000) Flagellum ontogeny in trypanosomes studied via an inherited and regulated RNA interference system. *J Cell Sci* **113** (Pt 18), 3321-8.
- Bateman A., Coin L., Durbin R., Finn R. D., Hollich V., Griffiths-Jones S., Khanna A., Marshall M., Moxon S., Sonnhammer E. L., Studholme D. J., Yeats C. and Eddy S. R. (2004) The Pfam protein families database. *Nucleic Acids Res* **32 Database issue**, D138-41.

- Bates P. A., Robertson C. D., Tetley L. and Coombs G. H. (1992) Axenic cultivation and characterization of *Leishmania mexicana* amastigote-like forms. *Parasitology* **105** (Pt 2), 193-202.
- Biebinger S., Wirtz L. E., Lorenz P. and Clayton C. (1997) Vectors for inducible expression of toxic gene products in bloodstream and procyclic *Trypanosoma brucei*. *Mol Biochem Parasitol* **85**, 99-112.
- Bieger B. and Essen L. O. (2001) Structural analysis of adenylate cyclases from *Trypanosoma brucei* in their monomeric state. *Embo J* **20**, 433-45.
- Blom N., Gammeltoft S. and Brunak S. (1999) Sequence and structure-based prediction of eukaryotic protein phosphorylation sites. *J Mol Biol* **294**, 1351-62.
- Borst P. (2002) Antigenic variation and allelic exclusion. *Cell* **109**, 5-8.
- Breidbach T., Krauth-Siegel R. L. and Steverding D. (2000) Ribonucleotide reductase is regulated via the R2 subunit during the life cycle of *Trypanosoma brucei*. *FEBS Lett* **473**, 212-6.
- Breidbach T., Ngazoa E. and Steverding D. (2002) *Trypanosoma brucei*: in vitro slender-to-stumpy differentiation of culture-adapted, monomorphic bloodstream forms. *Exp Parasitol* **101**, 223-30.
- Brun R. and Schonenberger. (1979) Cultivation and in vitro cloning or procyclic culture forms of *Trypanosoma brucei* in a semi-defined medium. Short communication. *Acta Trop* **36**, 289-92.
- Brun R. and Schonenberger M. (1981) Stimulating effect of citrate and cis-Aconitate on the transformation of *Trypanosoma brucei* bloodstream forms to procyclic forms in vitro. *Z Parasitenkd* **66**, 17-24.
- Canaves J. M. and Taylor S. S. (2002) Classification and phylogenetic analysis of the cAMP-dependent protein kinase regulatory subunit family. *J Mol Evol* **54**, 17-29.
- Carlson G. L. and Nelson D. L. (1996) The 44-kDa regulatory subunit of the *Paramecium* cAMP-dependent protein kinase lacks a dimerization domain and may have a unique autophosphorylation site sequence. *J Eukaryot Microbiol* **43**, 347-56.
- Clayton C., Adams M., Almeida R., Baltz T., Barrett M., Bastien P., Belli S., Beverley S., Biteau N., Blackwell J., Blaineau C., Boshart M., Bringaud F., Cross G., Cruz A., Degrave W., Donelson J., El-Sayed N., Fu G., Ersfeld K., Gibson W., Gull K., Ivens A., Kelly J., Vanhamme L. and *et al.* (1998) Genetic nomenclature for *Trypanosoma* and *Leishmania*. *Mol Biochem Parasitol* **97**, 221-4.
- Clayton C. E. (2002) Life without transcriptional control? From fly to man and back again. *Embo J* **21**, 1881-8.
- Cross G. A. (1975) Identification, purification and properties of clone-specific glycoprotein antigens constituting the surface coat of *Trypanosoma brucei*. *Parasitology* **71**, 393-417.

- Cross G. A. and Manning J. C. (1973) Cultivation of *Trypanosoma brucei* ssp. in semi-defined and defined media. *Parasitology* **67**, 315-31.
- Cross G. A., Wirtz L. E. and Navarro M. (1998) Regulation of vsg expression site transcription and switching in *Trypanosoma brucei*. *Mol Biochem Parasitol* **91**, 77-91.
- D'Angelo M. A., Montagna A. E., Sanguineti S., Torres H. N. and Flawia M. M. (2002) A novel calcium-stimulated adenylyl cyclase from *Trypanosoma cruzi*, which interacts with the structural flagellar protein paraflagellar rod. *J Biol Chem* **277**, 35025-34.
- D'Angelo M. A., Sanguineti S., Reece J. M., Birnbaumer L., Torres H. N. and Flawia M. M. (2004) Identification, characterization and subcellular localization of TcPDE1, a novel cAMP-specific phosphodiesterase from *Trypanosoma cruzi*. *Biochem J* **378**, 63-72.
- Das A., Gale M., Jr., Carter V. and Parsons M. (1994) The protein phosphatase inhibitor okadaic acid induces defects in cytokinesis and organellar genome segregation in *Trypanosoma brucei*. *J Cell Sci* **107** (Pt 12), 3477-83.
- Deguchi A., Soh J. W., Li H., Pamukcu R., Thompson W. J. and Weinstein I. B. (2002) Vasodilator-stimulated phosphoprotein (VASP) phosphorylation provides a biomarker for the action of exisulind and related agents that activate protein kinase G. *Mol Cancer Ther* **1**, 803-9.
- Delauw M. F., Pays E., Steinert M., Aerts D., Van Meirvenne N. and Le Ray D. (1985) Inactivation and reactivation of a variant-specific antigen gene in cyclically transmitted *Trypanosoma brucei*. *Embo J* **4**, 989-93.
- Deng W., Parbhu-Patel A., Meyer D. J. and Baker D. A. (2003) The role of two novel regulatory sites in the activation of the cGMP-dependent protein kinase from *Plasmodium falciparum*. *Biochem J* **374**, 559-65.
- Dey R., Mitra S. and Datta S. C. (1995) Cyclic AMP mediates change in superoxide dismutase activity to monitor host-parasite interaction in *Leishmania donovani*. *J Parasitol* **81**, 683-6.
- Diehl S., Diehl F., El-Sayed N. M., Clayton C. and Hoheisel J. D. (2002) Analysis of stage-specific gene expression in the bloodstream and the procyclic form of *Trypanosoma brucei* using a genomic DNA-microarray. *Mol Biochem Parasitol* **123**, 115-23.
- Donald R. G., Allocco J., Singh S. B., Nare B., Salowe S. P., Wiltsie J. and Liberator P. A. (2002) *Toxoplasma gondii* cyclic GMP-dependent kinase: chemotherapeutic targeting of an essential parasite protein kinase. *Eukaryot Cell* **1**, 317-28.
- Dower W. J., Miller J. F. and Ragsdale C. W. (1988) High efficiency transformation of *E. coli* by high voltage electroporation. *Nucleic Acids Res* **16**, 6127-45.
- Durbin R. (1998) Biological sequence analysis: probabilistic models of proteins and nucleic acids. *Cambridge University Press*.

- Eddy S. R. (2004) What is a hidden Markov model? *Nat Biotechnol* **22**, 1315-6.
- El-Sayed N. M., Hegde P., Quackenbush J., Melville S. E. and Donelson J. E. (2000) The African trypanosome genome. *Int J Parasitol* **30**, 329-45.
- Emini E. A., Hughes J. V., Perlow D. S. and Boger J. (1985) Induction of hepatitis A virus-neutralizing antibody by a virus-specific synthetic peptide. *J Virol* **55**, 836-9.
- Engstler and Boshart. (2004) Cold shock and regulation of surface protein trafficking convey sensitization to inducers of stage differentiation in *Trypanosoma brucei*. *GENES & DEVELOPMENT* **18**, 2798-2811.
- Eron L., Arditti R., Zubay G., Connaway S. and Beckwith J. R. (1971) An adenosine 3': 5'-cyclic monophosphate-binding protein that acts on the transcription process. *Proc Natl Acad Sci U S A* **68**, 215-8.
- Essayan D. M. (2001) Cyclic nucleotide phosphodiesterases. *J Allergy Clin Immunol* **108**, 671-80.
- Fire A., Xu S., Montgomery M. K., Kostas S. A., Driver S. E. and Mello C. C. (1998) Potent and specific genetic interference by double-stranded RNA in *Caenorhabditis elegans*. *Nature* **391**, 806-11.
- Flynn I. W. and Bowman I. B. (1973) The metabolism of carbohydrate by pleomorphic African trypanosomes. *Comp Biochem Physiol B* **45**, 25-42.
- Foster J. L., Higgins G. C. and Jackson F. R. (1996) Biochemical properties and cellular localization of the *Drosophila* DG1 cGMP-dependent protein kinase. *J Biol Chem* **271**, 23322-8.
- Francis S. H. and Corbin J. D. (1999) Cyclic nucleotide-dependent protein kinases: intracellular receptors for cAMP and cGMP action. *Crit Rev Clin Lab Sci* **36**, 275-328.
- Geigy R., Jenni L., Kauffmann M., Onyango R. J. and Weiss N. (1975) Identification of *T. brucei*-subgroup strains isolated from game. *Acta Trop* **32**, 190-205.
- Goncalves M. F., Zingales B. and Colli W. (1980) cAMP phosphodiesterase and activator protein of mammalian cAMP phosphodiesterase from *Trypanosoma cruzi*. *Mol Biochem Parasitol* **1**, 107-18.
- Gong K. W., Kunz S., Zoraghi R., Kunz Renggli C., Brun R. and Seebeck T. (2001) cAMP-specific phosphodiesterase TbPDE1 is not essential in *Trypanosoma brucei* in culture or during midgut infection of tsetse flies. *Mol Biochem Parasitol* **116**, 229-32.
- Gonzales-Perdomo M., Romero P. and Goldenberg S. (1988) Cyclic AMP and adenylate cyclase activators stimulate *Trypanosoma cruzi* differentiation. *Exp Parasitol* **66**, 205-12.

- Grant K. M., Hassan P., Anderson J. S. and Mottram J. C. (1998) The *crk3* gene of *Leishmania mexicana* encodes a stage-regulated *cdc2*-related histone H1 kinase that associates with p12. *J Biol Chem* **273**, 10153-9.
- Gull K. (1999) The cytoskeleton of trypanosomatid parasites. *Annu Rev Microbiol* **53**, 629-55.
- Gull K., Alsford S. and Ersfeld K. (1998) Segregation of minichromosomes in trypanosomes: implications for mitotic mechanisms. *Trends Microbiol* **6**, 319-23.
- Gurnett A. M., Liberator P. A., Dulski P. M., Salowe S. P., Donald R. G., Anderson J. W., Wiltsie J., Diaz C. A., Harris G., Chang B., Darkin-Rattray S. J., Nare B., Crumley T., Blum P. S., Misura A. S., Tamas T., Sardana M. K., Yuan J., Biftu T. and Schmatz D. M. (2002) Purification and molecular characterization of cGMP-dependent protein kinase from Apicomplexan parasites. A novel chemotherapeutic target. *J Biol Chem* **277**, 15913-22.
- Haffner C., Jarchau T., Reinhard M., Hoppe J., Lohmann S. M. and Walter U. (1995) Molecular cloning, structural analysis and functional expression of the proline-rich focal adhesion and microfilament-associated protein VASP. *Embo J* **14**, 19-27.
- Halbrugge M., Friedrich C., Eigenthaler M., Schanzenbacher P. and Walter U. (1990) Stoichiometric and reversible phosphorylation of a 46-kDa protein in human platelets in response to cGMP- and cAMP-elevating vasodilators. *J Biol Chem* **265**, 3088-93.
- Hammarton T. C., Clark J., Douglas F., Boshart M. and Mottram J. C. (2003a) Stage-specific differences in cell cycle control in *Trypanosoma brucei* revealed by RNA interference of a mitotic cyclin. *J Biol Chem* **278**, 22877-86.
- Hammarton T. C., Mottram J. C. and Doerig C. (2003b) The cell cycle of parasitic protozoa: potential for chemotherapeutic exploitation. *Prog Cell Cycle Res* **5**, 91-101.
- Hanks S. K. and Quinn A. M. (1991) Protein kinase catalytic domain sequence database: identification of conserved features of primary structure and classification of family members. *Methods Enzymol* **200**, 38-62.
- Hannaert V., Saavedra E., Duffieux F., Szikora J. P., Rigden D. J., Michels P. A. and Opperdoes F. R. (2003) Plant-like traits associated with metabolism of *Trypanosoma* parasites. *Proc Natl Acad Sci U S A* **100**, 1067-71.
- Hannon G. J. (2002) RNA interference. *Nature* **418**, 244-51.
- Herberg F. W., Taylor S. S. and Dostmann W. R. (1996) Active site mutations define the pathway for the cooperative activation of cAMP-dependent protein kinase. *Biochemistry* **35**, 2934-42.
- Hidaka H., Inagaki M., Kawamoto S. and Sasaki Y. (1984) Isoquinolinesulfonamides, novel and potent inhibitors of cyclic nucleotide dependent protein kinase and protein kinase C. *Biochemistry* **23**, 5036-41.

- Higgins D. G. (1994) CLUSTAL V: multiple alignment of DNA and protein sequences. *Methods Mol Biol* **25**, 307-18.
- Hirumi H. and Hirumi K. (1989) Continuous cultivation of *Trypanosoma brucei* blood stream forms in a medium containing a low concentration of serum protein without feeder cell layers. *J Parasitol* **75**, 985-9.
- Hochstrasser M. and Nelson D. L. (1989) Cyclic AMP-dependent protein kinase in *Paramecium tetraurelia*. Its purification and the production of monoclonal antibodies against both subunits. *J Biol Chem* **264**, 14510-8.
- Hoppe T., Matuschewski K., Rape M., Schlenker S., Ulrich H. D. and Jentsch S. (2000) Activation of a membrane-bound transcription factor by regulated ubiquitin/proteasome-dependent processing. *Cell* **102**, 577-86.
- Hou Y., Lascola J., Dulin N. O., Ye R. D. and Browning D. D. (2003) Activation of cGMP-dependent protein kinase by protein kinase C. *J Biol Chem* **278**, 16706-12.
- Huang H., Werner C., Weiss L. M., Wittner M. and Orr G. A. (2002) Molecular cloning and expression of the catalytic subunit of protein kinase A from *Trypanosoma cruzi*. *Int J Parasitol* **32**, 1107-15.
- Janin J. and Wodak S. (1978) Conformation of amino acid side-chains in proteins. *J Mol Biol* **125**, 357-86.
- Kanbara H., Uemura H., Nakazawa S. and Fukuma T. (1990) Effect of low pH on transformation of *Trypanosoma cruzi* trypomastigotes to amastigote. *Jpn J Parasitology* **39**, 226-8.
- Karlin S. and Altschul S. F. (1990) Methods for assessing the statistical significance of molecular sequence features by using general scoring schemes. *Proc Natl Acad Sci U S A* **87**, 2264-8.
- Kase H., Iwahashi K., Nakanishi S., Matsuda Y., Yamada K., Takahashi M., Murakata C., Sato A. and Kaneko M. (1987) K-252 compounds, novel and potent inhibitors of protein kinase C and cyclic nucleotide-dependent protein kinases. *Biochem Biophys Res Commun* **142**, 436-40.
- Kaupp U. B. and Koch K. W. (1992) Role of cGMP and Ca²⁺ in vertebrate photoreceptor excitation and adaptation. *Annu Rev Physiol* **54**, 153-75.
- Kawasaki H., Springett G. M., Toki S., Canales J. J., Harlan P., Blumenstiel J. P., Chen E. J., Bany I. A., Mochizuki N., Ashbacher A., Matsuda M., Housman D. E. and Graybiel A. M. (1998) A Rap guanine nucleotide exchange factor enriched highly in the basal ganglia. *Proc Natl Acad Sci U S A* **95**, 13278-83.
- Kelley R. J., Brickman M. J. and Balber A. E. (1995) Processing and transport of a lysosomal membrane glycoprotein is developmentally regulated in African trypanosomes. *Mol Biochem Parasitol* **74**, 167-78.

- Kemp B. E., Benjamini E. and Krebs E. G. (1976) Synthetic hexapeptide substrates and inhibitors of 3':5'-cyclic AMP-dependent protein kinase. *Proc Natl Acad Sci U S A* **73**, 1038-42.
- Kemp B. E., Graves D. J., Benjamini E. and Krebs E. G. (1977) Role of multiple basic residues in determining the substrate specificity of cyclic AMP-dependent protein kinase. *J Biol Chem* **252**, 4888-94.
- Kemp B. E., Pearson R. B. and House C. M. (1991) Pseudosubstrate-based peptide inhibitors. *Methods Enzymol* **201**, 287-304.
- Klößner, T. (1996) cAMP Signaltransduktion in *Trypanosoma brucei*: Klonierung und Charakterisierung von Proteinkinase A- und Phosphodiesterase-Homologen. Dissertation. Ludwig-Maximilians-Universität München.
- Kohl L., Robinson D. and Bastin P. (2003) Novel roles for the flagellum in cell morphogenesis and cytokinesis of trypanosomes. *Embo J* **22**, 5336-46.
- Kohl L., Sherwin T. and Gull K. (1999) Assembly of the paraflagellar rod and the flagellum attachment zone complex during the *Trypanosoma brucei* cell cycle. *J Eukaryot Microbiol* **46**, 105-9.
- Krause M., Dent E. W., Bear J. E., Loureiro J. J. and Gertler F. B. (2003) Ena/VASP proteins: regulators of the actin cytoskeleton and cell migration. *Annu Rev Cell Dev Biol* **19**, 541-64.
- Kunz S., Kloeckner T., Essen L. O., Seebeck T. and Boshart M. (2004) TbPDE1, a novel class I phosphodiesterase of *Trypanosoma brucei*. *Eur J Biochem* **271**, 637-47.
- Kyhse-Andersen J. (1984) Electrophoretic transfer of proteins from polyacrylamide to nitrocellulose: a simple apparatus without buffer tank for rapid transfer of proteins from polyacrylamide to nitrocellulose. *J Biochem Biophys Methods* **10**, 203-9.
- LaCount D. J., Bruse S., Hill K. L. and Donelson J. E. (2000) Double-stranded RNA interference in *Trypanosoma brucei* using head-to-head promoters. *Mol Biochem Parasitol* **111**, 67-76.
- Laemmli U. K. (1970) Cleavage of structural proteins during the assembly of the head of bacteriophage T4. *Nature* **227**, 680-5.
- Lammel E. M., Barbieri M. A., Wilkowsky S. E., Bertini F. and Isola E. L. (1996) *Trypanosoma cruzi*: involvement of intracellular calcium in multiplication and differentiation. *Exp Parasitol* **83**, 240-9.
- Leighfield T. A., Barbier M. and Van Dolah F. M. (2002) Evidence for cAMP-dependent protein kinase in the dinoflagellate, *Amphidinium operculatum*. *Comp Biochem Physiol B Biochem Mol Biol* **133**, 317-24.
- Letunic I., Copley R. R., Schmidt S., Ciccarelli F. D., Doerks T., Schultz J., Ponting C. P. and Bork P. (2004) SMART 4.0: towards genomic data integration. *Nucleic Acids Res* **32 Database issue**, D142-4.

- Li Z. and Wang C. C. (2003) A PHO80-like cyclin and a B-type cyclin control the cell cycle of the procyclic form of *Trypanosoma brucei*. *J Biol Chem* **278**, 20652-8.
- Lin PP-C V. B. (1989) Novel adenosine 3',5'-cyclic monophosphate dependent protein kinases in a marine diatom. *Biochemistry* **28**, 6624-6631.
- Los D. A. and Murata N. (1999) Responses to cold shock in cyanobacteria. *J Mol Microbiol Biotechnol* **1**, 221-30.
- Lucke S., Klockner T., Palfi Z., Boshart M. and Bindereif A. (1997) Trans mRNA splicing in trypanosomes: cloning and analysis of a PRP8-homologous gene from *Trypanosoma brucei* provides evidence for a U5-analogous RNP. *Embo J* **16**, 4433-40.
- Ludwig J., Margalit T., Eismann E., Lancet D. and Kaupp U. B. (1990) Primary structure of cAMP-gated channel from bovine olfactory epithelium. *FEBS Lett* **270**, 24-9.
- Matthews K. R. and Gull K. (1994) Evidence for an interplay between cell cycle progression and the initiation of differentiation between life cycle forms of African trypanosomes. *J Cell Biol* **125**, 1147-56.
- McCulloch R., Vassella E., Burton P., Boshart M. and Barry J. D. (2004) Transformation of monomorphic and pleomorphic *Trypanosoma brucei*. *Methods Mol Biol* **262**, 53-86.
- McKean P. G. (2003) Coordination of cell cycle and cytokinesis in *Trypanosoma brucei*. *Curr Opin Microbiol* **6**, 600-7.
- Mottram J. C., Kinnaid J. H., Shiels B. R., Tait A. and Barry J. D. (1993) A novel CDC2-related protein kinase from *Leishmania mexicana*, LmmCRK1, is post-translationally regulated during the life cycle. *J Biol Chem* **268**, 21044-52.
- Muller I. B., Domenicali-Pfister D., Roditi I. and Vassella E. (2002) Stage-specific requirement of a mitogen-activated protein kinase by *Trypanosoma brucei*. *Mol Biol Cell* **13**, 3787-99.
- Mutzel R., Lacombe M. L., Simon M. N., de Gunzburg J. and Veron M. (1987) Cloning and cDNA sequence of the regulatory subunit of cAMP-dependent protein kinase from *Dictyostelium discoideum*. *Proc Natl Acad Sci U S A* **84**, 6-10.
- Nakamura T. and Gold G. H. (1987) A cyclic nucleotide-gated conductance in olfactory receptor cilia. *Nature* **325**, 442-4.
- Ngo H., Tschudi C., Gull K. and Ullu E. (1998) Double-stranded RNA induces mRNA degradation in *Trypanosoma brucei*. *Proc Natl Acad Sci U S A* **95**, 14687-92.
- Nikolakaki E., Fissentzidis A., Giannakouros T. and Georgatsos J. G. (1999) Purification and characterization of a dimer form of the cAMP-dependent protein kinase from mouse liver cytosol. *Mol Cell Biochem* **197**, 117-28.

- Nolan D. P., Rolin S., Rodriguez J. R., Van Den Abbeele J. and Pays E. (2000) Slender and stumpy bloodstream forms of *Trypanosoma brucei* display a differential response to extracellular acidic and proteolytic stress. *Eur J Biochem* **267**, 18-27.
- Ogbadoyi E. (2003) A high-order trans-membrane structural linkage is responsible for mitochondrial genome positioning and segregation by flagellar basal bodies in trypanosomes. *Mol Biol Cell*. **14**, 1769-79.
- Ogbadoyi E., Ersfeld K., Robinson D., Sherwin T. and Gull K. (2000) Architecture of the *Trypanosoma brucei* nucleus during interphase and mitosis. *Chromosoma* **108**, 501-13.
- Ogreid D. and Doskeland S. O. (1981a) The kinetics of association of cyclic AMP to the two types of binding sites associated with protein kinase II from bovine myocardium. *FEBS Lett* **129**, 287-92.
- Ogreid D. and Doskeland S. O. (1981b) The kinetics of the interaction between cyclic AMP and the regulatory moiety of protein kinase II. Evidence for interaction between the binding sites for cyclic AMP. *FEBS Lett* **129**, 282-6.
- Overath P., Czichos J. and Haas C. (1986) The effect of citrate/cis-aconitate on oxidative metabolism during transformation of *Trypanosoma brucei*. *Eur J Biochem* **160**, 175-82.
- Paques F. and Haber J. E. (1999) Multiple pathways of recombination induced by double-strand breaks in *Saccharomyces cerevisiae*. *Microbiol Mol Biol Rev* **63**, 349-404.
- Parsons M. and Ruben L. (2000) Pathways involved in environmental sensing in trypanosomatids. *Parasitol Today* **16**, 56-62.
- Parsons M., Valentine M. and Carter V. (1993) Protein kinases in divergent eukaryotes: identification of protein kinase activities regulated during trypanosome development. *Proc Natl Acad Sci U S A* **90**, 2656-60.
- Parsons M., Valentine M., Deans J., Schieven G. L. and Ledbetter J. A. (1991) Distinct patterns of tyrosine phosphorylation during the life cycle of *Trypanosoma brucei*. *Mol Biochem Parasitol* **45**, 241-8.
- Pays E., Lips S., Nolan D., Vanhamme L. and Perez-Morga D. (2001) The VSG expression sites of *Trypanosoma brucei*: multipurpose tools for the adaptation of the parasite to mammalian hosts. *Mol Biochem Parasitol* **114**, 1-16.
- Ploubidou A., Robinson D. R., Docherty R. C., Ogbadoyi E. O. and Gull K. (1999) Evidence for novel cell cycle checkpoints in trypanosomes: kinetoplast segregation and cytokinesis in the absence of mitosis. *J Cell Sci* **112** (Pt 24), 4641-50.
- Priest J. W. and Hajduk S. L. (1994) Developmental regulation of mitochondrial biogenesis in *Trypanosoma brucei*. *J Bioenerg Biomembr* **26**, 179-91.

- Pullen T. J., Ginger M. L., Gaskell S. J. and Gull K. (2004) Protein targeting of an unusual, evolutionarily conserved adenylate kinase to a eukaryotic flagellum. *Mol Biol Cell* **15**, 3257-65.
- Rall T. W., Sutherland E. W. and Wosilait W. D. (1956) The relationship of epinephrine and glucagon to liver phosphorylase. III. Reactivation of liver phosphorylase in slices and in extracts. *J Biol Chem* **218**, 483-95.
- Rangel-Aldao R., Allende O., Triana F., Piras R., Henriquez D. and Piras M. (1987) Possible role of cAMP in the differentiation of *Trypanosoma cruzi*. *Mol Biochem Parasitol* **22**, 39-43.
- Rascon A., Soderling S. H., Schaefer J. B. and Beavo J. A. (2002) Cloning and characterization of a cAMP-specific phosphodiesterase (TbPDE2B) from *Trypanosoma brucei*. *Proc Natl Acad Sci U S A* **99**, 4714-9.
- Reed R. B., Sandberg M., Jahnsen T., Lohmann S. M., Francis S. H. and Corbin J. D. (1996) Fast and slow cyclic nucleotide-dissociation sites in cAMP-dependent protein kinase are transposed in type I beta cGMP-dependent protein kinase. *J Biol Chem* **271**, 17570-5.
- Reed R. B., Sandberg M., Jahnsen T., Lohmann S. M., Francis S. H. and Corbin J. D. (1997) Structural order of the slow and fast intrasubunit cGMP-binding sites of type I alpha cGMP-dependent protein kinase. *Adv Second Messenger Phosphoprotein Res* **31**, 205-17.
- Reuner B., Vassella E., Yutzy B. and Boshart M. (1997) Cell density triggers slender to stumpy differentiation of *Trypanosoma brucei* bloodstream forms in culture. *Mol Biochem Parasitol* **90**, 269-80.
- Richie-Jannetta R., Francis S. H. and Corbin J. D. (2003) Dimerization of cGMP-dependent protein kinase I beta is mediated by an extensive amino-terminal leucine zipper motif, and dimerization modulates enzyme function. *J Biol Chem* **278**, 50070-9.
- Riviere L., van Weelden S. W., Glass P., Vegh P., Coustou V., Biran M., van Hellemond J. J., Bringaud F., Tielens A. G. and Boshart M. (2004) Acetyl :succinate CoA-transferase in procyclic *Trypanosoma brucei*. Gene identification and role in carbohydrate metabolism. *J Biol Chem* **279**, 45337-46.
- Robinson D. R. and Gull K. (1991) Basal body movements as a mechanism for mitochondrial genome segregation in the trypanosome cell cycle. *Nature* **352**, 731-3.
- Robinson D. R., Sherwin T., Ploubidou A., Byard E. H. and Gull K. (1995) Microtubule polarity and dynamics in the control of organelle positioning, segregation, and cytokinesis in the trypanosome cell cycle. *J Cell Biol* **128**, 1163-72.
- Rock C. O. and Cronan J. E. (1996) *Escherichia coli* as a model for the regulation of dissociable (type II) fatty acid biosynthesis. *Biochim Biophys Acta* **1302**, 1-16.

- Roditi I., Schwarz H., Pearson T. W., Beecroft R. P., Liu M. K., Richardson J. P., Buhning H. J., Pleiss J., Bulow R., Williams R. O. and *et al.* (1989) Procyclin gene expression and loss of the variant surface glycoprotein during differentiation of *Trypanosoma brucei*. *J Cell Biol* **108**, 737-46.
- Rolin S., Halleux S., Van Sande J., Dumont J., Pays E. and Steinert M. (1990) Stage-specific adenylate cyclase activity in *Trypanosoma brucei*. *Exp Parasitol* **71**, 350-2.
- Rolin S., Hancocq-Quertier J., Paturiaux-Hanocq F., Nolan D. P. and Pays E. (1998) Mild acid stress as a differentiation trigger in *Trypanosoma brucei*. *Mol Biochem Parasitol* **93**, 251-62.
- Rolin S., Hanocq-Quertier J., Paturiaux-Hanocq F., Nolan D., Salmon D., Webb H., Carrington M., Voorheis P. and Pays E. (1996) Simultaneous but independent activation of adenylate cyclase and glycosylphosphatidylinositol-phospholipase C under stress conditions in *Trypanosoma brucei*. *J Biol Chem* **271**, 10844-52.
- Rolin S., Paindavoine P., Hanocq-Quertier J., Hanocq F., Claes Y., Le Ray D., Overath P. and Pays E. (1993) Transient adenylate cyclase activation accompanies differentiation of *Trypanosoma brucei* from bloodstream to procyclic forms. *Mol Biochem Parasitol* **61**, 115-25.
- Ruan J. P., Arhin G. K., Ullu E. and Tschudi C. (2004) Functional characterization of a *Trypanosoma brucei* TATA-binding protein-related factor points to a universal regulator of transcription in trypanosomes. *Mol Cell Biol* **24**, 9610-8.
- Salto M. L., Bertello L. E., Vieira M., Docampo R., Moreno S. N. and de Lederkremer R. M. (2003) Formation and remodeling of inositolphosphoceramide during differentiation of *Trypanosoma cruzi* from trypomastigote to amastigote. *Eukaryot Cell* **2**, 756-68.
- Sambrook J., Fritsch, E.F. and Maniatis, T. (1989) Molecular cloning: a laboratory manual. *Cold Spring Harbor Laboratory Press*, Plainview, NY, USA.
- Sanchez M. A., Zeoli D., Klamo E. M., Kavanaugh M. P. and Landfear S. M. (1995) A family of putative receptor-adenylate cyclases from *Leishmania donovani*. *J Biol Chem* **270**, 17551-8.
- Sangwan V. and Dhindsa R. S. (2002) In vivo and in vitro activation of temperature-responsive plant map kinases. *FEBS Lett* **531**, 561-4.
- Sangwan V., Orvar B. L., Beyerly J., Hirt H. and Dhindsa R. S. (2002) Opposite changes in membrane fluidity mimic cold and heat stress activation of distinct plant MAP kinase pathways. *Plant J* **31**, 629-38.
- Saran S., Meima M. E., Alvarez-Curto E., Weening K. E., Rozen D. E. and Schaap P. (2002) cAMP signaling in *Dictyostelium*. Complexity of cAMP synthesis, degradation and detection. *J Muscle Res Cell Motil* **23**, 793-802.
- Sarkar D. and Bhaduri A. (1995) Temperature-induced rapid increase in cytoplasmic free Ca²⁺ in pathogenic *Leishmania donovani* promastigotes. *FEBS Lett* **375**, 83-6.

- Schimpf, S. (2000) Differentielle Phosphorylierung der katalytischen Untereinheit der Proteinkinase A bei der Differenzierung von *Trypanosoma brucei*. Diplomarbeit. Freie Universität Berlin.
- Schulte zu Sodingen, C. (2000) Molekulargenetische Untersuchungen zur Differenzierung von *Trypanosoma brucei*. Dissertation. Universität Konstanz.
- Schultz J., Milpetz F., Bork P. and Ponting C. P. (1998) SMART, a simple modular architecture research tool: identification of signaling domains. *Proc Natl Acad Sci U S A* **95**, 5857-64.
- Seebeck T., Gong K., Kunz S., Schaub R., Shalaby T. and Zoraghi R. (2001) cAMP signalling in *Trypanosoma brucei*. *Int J Parasitol* **31**, 491-8.
- Shabb J. B. (2001) Physiological substrates of cAMP-dependent protein kinase. *Chem Rev* **101**, 2381-411.
- Shabb J. B., Buzzeo B. D., Ng L. and Corbin J. D. (1991) Mutating protein kinase cAMP-binding sites into cGMP-binding sites. Mechanism of cGMP selectivity. *J Biol Chem* **266**, 24320-6.
- Shalaby T., Liniger M. and Seebeck T. (2001) The regulatory subunit of a cGMP-regulated protein kinase A of *Trypanosoma brucei*. *Eur J Biochem* **268**, 6197-206.
- Shapiro S. Z., Naessens J., Liesegang B., Moloo S. K. and Magondi J. (1984) Analysis by flow cytometry of DNA synthesis during the life cycle of African trypanosomes. *Acta Trop* **41**, 313-23.
- Shi H., Djikeng A., Mark T., Wirtz E., Tschudi C. and Ullu E. (2000) Genetic interference in *Trypanosoma brucei* by heritable and inducible double-stranded RNA. *Rna* **6**, 1069-76.
- Shoji S., Titani K., Demaille J. G. and Fischer E. H. (1979) Sequence of two phosphorylated sites in the catalytic subunit of bovine cardiac muscle adenosine 3':5'-monophosphate-dependent protein kinase. *J Biol Chem* **254**, 6211-4.
- Sicheritz-Ponten T., Blom N., Gammeltoft S. and Brunak S. The Phosphoproteome Predicted: Using Neural Networks for Predicting Kinase Substrate Sites in preparation
- Siman-Tov M. M., Aly R., Shapira M. and Jaffe C. L. (1996) Cloning from *Leishmania major* of a developmentally regulated gene, c-lpk2, for the catalytic subunit of the cAMP-dependent protein kinase. *Mol Biochem Parasitol* **77**, 201-15.
- Siman-Tov M. M., Ivens A. C. and Jaffe C. L. (2002) Molecular cloning and characterization of two new isoforms of the protein kinase A catalytic subunit from the human parasite *Leishmania*. *Gene* **288**, 65-75.
- Simpson A. M., Hughes D. and Simpson L. (1985) *Trypanosoma brucei*: differentiation of in vitro-grown bloodstream trypomastigotes into procyclic forms. *J Protozool* **32**, 672-7.

- Skalhegg B. S. and Tasken K. (2000) Specificity in the cAMP/PKA signaling pathway. Differential expression, regulation, and subcellular localization of subunits of PKA. *Front Biosci* **5**, D678-93.
- Smolenski A., Bachmann C., Reinhard K., Honig-Liedl P., Jarchau T., Hoschuetzky H. and Walter U. (1998) Analysis and regulation of vasodilator-stimulated phosphoprotein serine 239 phosphorylation in vitro and in intact cells using a phosphospecific monoclonal antibody. *J Biol Chem* **273**, 20029-35.
- Songyang Z., Blechner S., Hoagland N., Hoekstra M. F., Piwnicka-Worms H. and Cantley L. C. (1994) Use of an oriented peptide library to determine the optimal substrates of protein kinases. *Curr Biol* **4**, 973-82.
- Soto T., Beltran F. F., Paredes V., Madrid M., Millar J. B., Vicente-Soler J., Cansado J. and Gacto M. (2002) Cold induces stress-activated protein kinase-mediated response in the fission yeast *Schizosaccharomyces pombe*. *Eur J Biochem* **269**, 5056-65.
- Souza G. M., da Silva A. M. and Kuspa A. (1999) Starvation promotes *Dictyostelium* development by relieving PufA inhibition of PKA translation through the Yaka kinase pathway. *Development* **126**, 3263-74.
- Stansberry J., Baude E. J., Taylor M. K., Chen P. J., Jin S. W., Ellis R. E. and Uhler M. D. (2001) A cGMP-dependent protein kinase is implicated in wild-type motility in *C. elegans*. *J Neurochem* **76**, 1177-87.
- Steinberg R. A., Cauthron R. D., Symcox M. M. and Shuntoh H. (1993) Autoactivation of catalytic (C alpha) subunit of cyclic AMP-dependent protein kinase by phosphorylation of threonine 197. *Mol Cell Biol* **13**, 2332-41.
- Stojdl D. F. and Clarke M. W. (1996) *Trypanosoma brucei*: analysis of cytoplasmic Ca²⁺ during differentiation of bloodstream stages in vitro. *Exp Parasitol* **83**, 134-46.
- Strickler J. E. and Patton C. L. (1975) Adenosine 3',5'-monophosphate in reproducing and differentiated trypanosomes. *Science* **190**, 1110-2.
- Su Y., Dostmann W. R., Herberg F. W., Durick K., Xuong N. H., Ten Eyck L., Taylor S. S. and Varughese K. I. (1995) Regulatory subunit of protein kinase A: structure of deletion mutant with cAMP binding domains. *Science* **269**, 807-13.
- Suzuki I., Los D. A., Kanesaki Y., Mikami K. and Murata N. (2000) The pathway for perception and transduction of low-temperature signals in *Synechocystis*. *Embo J* **19**, 1327-34.
- Symington L. S. (2002) Role of RAD52 epistasis group genes in homologous recombination and double-strand break repair. *Microbiol Mol Biol Rev* **66**, 630-70, table of contents.
- Ter Kuile B. H., Wiemer E. A., Michels P. A. and Opperdoes F. R. (1992) The electrochemical proton gradient in the bloodstream form of *Trypanosoma brucei* is dependent on the temperature. *Mol Biochem Parasitol* **55**, 21-7.

- Tomlinson S., Vandekerckhove F., Frevert U. and Nussenzweig V. (1995) The induction of *Trypanosoma cruzi* trypomastigote to amastigote transformation by low pH. *Parasitology* **110** (Pt 5), 547-54.
- Tschudi C., Djikeng A., Shi H. and Ullu E. (2003) In vivo analysis of the RNA interference mechanism in *Trypanosoma brucei*. *Methods* **30**, 304-12.
- Tschudi C. and Ullu E. (2002) Unconventional rules of small nuclear RNA transcription and cap modification in trypanosomatids. *Gene Expr* **10**, 3-16.
- Turner C. M. and Barry J. D. (1989) High frequency of antigenic variation in *Trypanosoma brucei* rhodesiense infections. *Parasitology* **99** Pt 1, 67-75.
- Tyler K. M., Matthews K. R. and Gull K. (1997) The bloodstream differentiation-division of *Trypanosoma brucei* studied using mitochondrial markers. *Proc R Soc Lond B Biol Sci* **264**, 1481-90.
- Uhler M. D. (1993) Cloning and expression of a novel cyclic GMP-dependent protein kinase from mouse brain. *J Biol Chem* **268**, 13586-91.
- Ulloa R. M., Mesri E., Esteva M., Torres H. N. and Tellez-Inon M. T. (1988) Cyclic AMP-dependent protein kinase activity in *Trypanosoma cruzi*. *Biochem J* **255**, 319-26.
- Ullu E., Tschudi C. and Chakraborty T. (2004) RNA interference in protozoan parasites. *Cell Microbiol* **6**, 509-19.
- Vanhamme L. and Pays E. (1995) Control of gene expression in trypanosomes. *Microbiol Rev* **59**, 223-40.
- van Weelden S. W., Fast B., Vogt A., van der Meer P., Saas J., van Hellemond J. J., Tielens A. G. and Boshart M. (2003) Procyclic *Trypanosoma brucei* do not use Krebs cycle activity for energy generation. *J Biol Chem* **278**, 12854-63.
- Vardanis A. (1980) A unique cyclic nucleotide-dependent protein kinase. *J Biol Chem* **255**, 7238-43.
- Vassella E. and Boshart M. (1996) High molecular mass agarose matrix supports growth of bloodstream forms of pleomorphic *Trypanosoma brucei* strains in axenic culture. *Mol Biochem Parasitol* **82**, 91-105.
- Vassella E., Kramer R., Turner C. M., Wankell M., Modes C., van den Bogaard M. and Boshart M. (2001) Deletion of a novel protein kinase with PX and FYVE-related domains increases the rate of differentiation of *Trypanosoma brucei*. *Mol Microbiol* **41**, 33-46.
- Vassella E., Reuner B., Yutzy B. and Boshart M. (1997) Differentiation of African trypanosomes is controlled by a density sensing mechanism which signals cell cycle arrest via the cAMP pathway. *J Cell Sci* **110** (Pt 21), 2661-71.
- Vaughan S. and Gull K. (2003) The trypanosome flagellum. *J Cell Sci* **116**, 757-9.

- Vickerman K. (1965) Polymorphism and mitochondrial activity in sleeping sickness trypanosomes. *Nature* **208**, 762-6.
- Vigh L., Maresca B. and Harwood J. L. (1998) Does the membrane's physical state control the expression of heat shock and other genes? *Trends Biochem Sci* **23**, 369-74.
- Von Kreuter B. F., Walton B. L. and Santos-Buch C. A. (1995) Attenuation of parasite cAMP levels in *T. cruzi*-host cell membrane interactions in vitro. *J Eukaryot Microbiol* **42**, 20-6.
- Wainszelbaum M. J., Belaunzaran M. L., Lammel E. M., Florin-Christensen M., Florin-Christensen J. and Isola E. L. (2003) Free fatty acids induce cell differentiation to infective forms in *Trypanosoma cruzi*. *Biochem J* **375**, 705-12.
- Walter R. D. (1974) 3':5'-cyclic-AMP phosphodiesterase from *Trypanosoma gambiense*. *Hoppe Seylers Z Physiol Chem* **355**, 1443-50.
- Walter R. D. (1978) Adenosine 3', 5'-cyclic monophosphate-binding proteins from *Trypanosoma gambiense*. *Hoppe Seylers Z Physiol Chem* **359**, 607-12.
- Walter R. D., Nordmeyer J. P. and Konigk E. (1974) Adenylate cyclase from *Trypanosoma gambiense*. *Hoppe Seylers Z Physiol Chem* **355**, 427-30.
- Wang Y., Dimitrov K., Garrity L. K., Sazer S. and Beverley S. M. (1998) Stage-specific activity of the *Leishmania major* CRK3 kinase and functional rescue of a *Schizosaccharomyces pombe* cdc2 mutant. *Mol Biochem Parasitol* **96**, 139-50.
- Wanner R. and Wurster B. (1990) Cyclic GMP-activated protein kinase from *Dictyostelium discoideum*. *Biochim Biophys Acta* **1053**, 179-84.
- Weber I. T. and Steitz T. A. (1987) Structure of a complex of catabolite gene activator protein and cyclic AMP refined at 2.5 Å resolution. *J Mol Biol* **198**, 311-26.
- Wiese M., Kuhn D. and Grunfelder C. G. (2003) Protein kinase involved in flagellar-length control. *Eukaryot Cell* **2**, 769-77.
- Wirtz E. and Clayton C. (1995) Inducible gene expression in trypanosomes mediated by a prokaryotic repressor. *Science* **268**, 1179-83.
- Wirtz E., Leal S., Ochatt C. and Cross G. A. (1999) A tightly regulated inducible expression system for conditional gene knock-outs and dominant-negative genetics in *Trypanosoma brucei*. *Mol Biochem Parasitol* **99**, 89-101.
- Wolfe L., Corbin J. D. and Francis S. H. (1989) Characterization of a novel isozyme of cGMP-dependent protein kinase from bovine aorta. *J Biol Chem* **264**, 7734-41.
- Woodward R. and Gull K. (1990) Timing of nuclear and kinetoplast DNA replication and early morphological events in the cell cycle of *Trypanosoma brucei*. *J Cell Sci* **95** (Pt 1), 49-57.

- Xong H. V., Vanhamme L., Chamekh M., Chimfwembe C. E., Van Den Abbeele J., Pays A., Van Meirvenne N., Hamers R., De Baetselier P. and Pays E. (1998) A VSG expression site-associated gene confers resistance to human serum in *Trypanosoma rhodesiense*. *Cell* **95**, 839-46.
- Yamanaka K. (1999) Cold shock response in *Escherichia coli*. *J Mol Microbiol Biotechnol* **1**, 193-202.
- Ziegelbauer K., Quinten M., Schwarz H., Pearson T. W. and Overath P. (1990) Synchronous differentiation of *Trypanosoma brucei* from bloodstream to procyclic forms in vitro. *Eur J Biochem* **192**, 373-8.
- Zilberstein D., Blumenfeld N., Liveanu V., Gepstein A. and Jaffe C. L. (1991) Growth at acidic pH induces an amastigote stage-specific protein in *Leishmania* promastigotes. *Mol Biochem Parasitol* **45**, 175-8.
- Zilberstein D. and Shapira M. (1994) The role of pH and temperature in the development of *Leishmania* parasites. *Annu Rev Microbiol* **48**, 449-70.
- Zoraghi R., Kunz S., Gong K. and Seebeck T. (2001) Characterization of TbPDE2A, a novel cyclic nucleotide-specific phosphodiesterase from the protozoan parasite *Trypanosoma brucei*. *J Biol Chem* **276**, 11559-66.
- Zoraghi R. and Seebeck T. (2002) The cAMP-specific phosphodiesterase TbPDE2C is an essential enzyme in bloodstream form *Trypanosoma brucei*. *Proc Natl Acad Sci U S A* **99**, 4343-8.

Danksagung

Ich möchte mich bedanken bei Herrn Professor Dr. Boshart für die Betreuung dieser Arbeit, die Bereitstellung des interessanten Themas, die stete Diskussionsbereitschaft und dafür, dass er mir auch die Möglichkeit gab, auf internationale Kongresse bzw. in andere Labore zu fahren.

Frau Professor Dr. Jung danke ich für die Erstellung des Zweitgutachtens.

Bei Dr. Markus Engstler bedanke ich mich für seine Interpretation von Wissenschaft, von der ich viel lernen konnte, für seine Hilfe bei der Korrektur dieser Arbeit und für manches aufmunternde Wort.

Bedanken möchte ich mich

bei Klaus Ersfeld (University of Hull) für den anti-NUP Antikörper,

bei Thomas Renné und Ulrich Walter (Universität Würzburg) für die VASP cDNA und den VASP Antikörper

bei Eberhard Krause (MDC, Berlin Buch) für die MALDI Experimente

bei Christine Clayton (ZMBH, Heidelberg) für die 1313-514 cell line und den p2T7TAbblue Vektor

bei G.A.M. Cross (New York) für die 13-90 Zelllinie (Wirtz *et al.*, 1999)

Bei allen übrigen Labormitgliedern (aus Berlin und München), vor allem

bei Carsten Krumbholz und Mark Günzel: einfach für alles !!! und beim Carsten für seine Hilfe bei der Korrektur dieser Arbeit. Wien 2005 ?

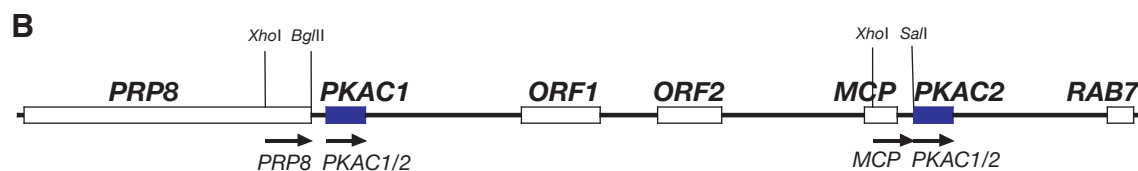
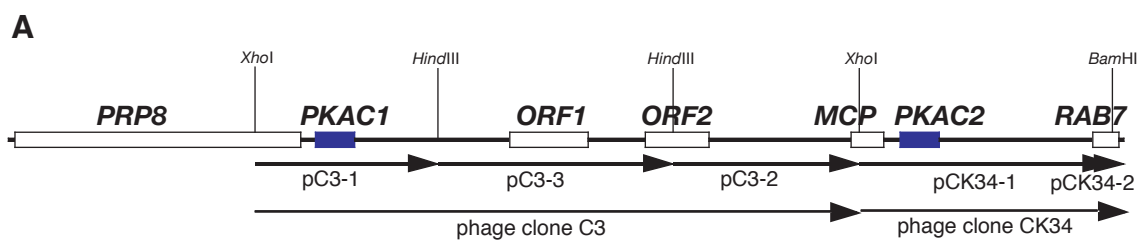
bei Larissa Iwanova für ihre stete Hilfsbereitschaft und jede Praline (einzeln).

bei Katrina Bayer, für die Übersetzung dieser Arbeit in lesbares Englisch.

bei Martin Brenndörfer für das bereitwillige Leihen seiner Scheere und die gute Nachbarschaft an der Bench

bei Susanne Dwars für unzählige Proteingele und Westernblotpuffer

bei Markus Kador für die HMMER search Analysen, seine schnellen Hilfen bei allen Computerproblemen und seine Kochkünste



C

gene	Acc No.	ORF [bp]	amino acids	molecular mass [kDa]	predicted isoelectric point
<i>PRP8</i>	Tb09.211.2420	7209	2403	276.9	8.3
<i>PKAC1</i>	Tb09.211.2410	1002	334	38.0	9.1
<i>ORF1</i>	Tb09.211.2400	1983	661	72.2	6.23
<i>ORF2</i>	Tb09.211.2380	1635	545	58.6	9.3
<i>MCP</i>	Tb09.211.2370	888	296	52.2	9.2
<i>PKAC2</i>	Tb09.211.2360	1008	336	38.6	9.3
<i>RAB7</i>	Tb09.211.2330	660	220	23.8	5.2

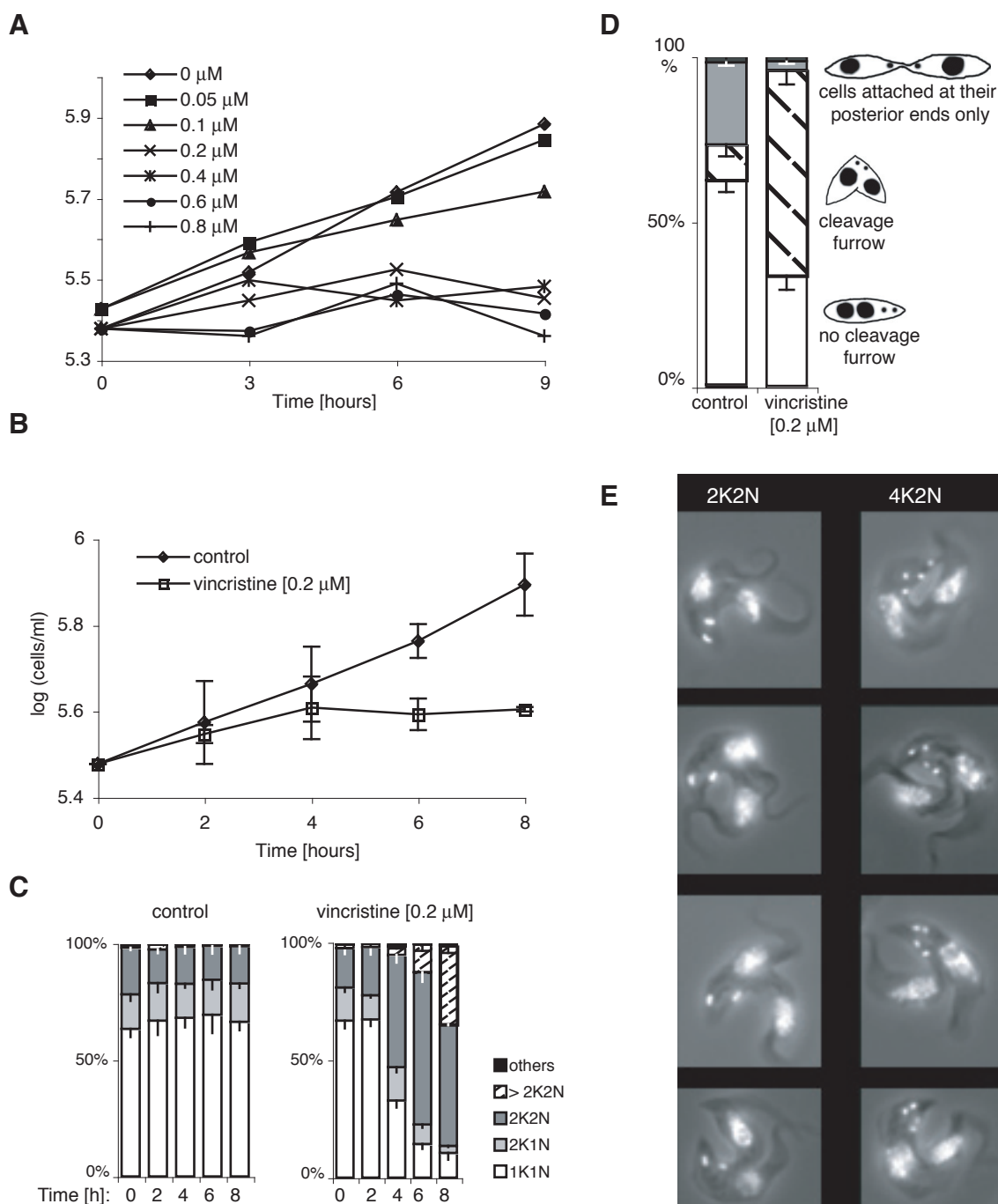
Attachment 1: The genomic locus of *PKAC1* and *PKAC2*

The complete sequence of the *PKAC1/2* genomic locus had been previously cloned in this laboratory (T.Klöckner, P.Hassan, unpublished). In addition to *PKAC1* and *PKAC2* it contains a gene for *PRP8* (a splice factor, Lücke *et al.*, 1997), for a putative *MCP* (mitochondrial carrier protein) and for a putative *RAB7* protein. Two open reading frames (*ORF1* and *ORF2*) show no homologies to any other proteins but are expressed (data not shown).

A) Names and positions of the phage clones C3 and CK34 that were used for the cloning T.Klöckner. In addition, the DNA of these phage clones was subcloned into the plasmids pC3-1, pC3-3, pC3-2, pCK34-1 and pCK34-2.

B) The positions of the probes used for hybridisation experiments in this work are shown. They were prepared from the corresponding plasmids (compare A) with the restriction enzymes as indicated.

C) Genes and putative genes of the *PKAC1/2* genomic locus. The systematic name (Acc. No), the size of the open reading frame and the characteristics of the corresponding proteins (size, molecular weight, isoelectric point) are indicated.



Attachment 2: Cytokinesis inhibition with vincristine

A) Growth of *T. brucei* WT cells in the presence of vincristine at different concentrations. The minimal vincristine concentration that caused a complete growth arrest of the cells was found to be $0.2 \mu\text{M}$. It was used for all further experiments.

B C D) Cell densities were measured 0, 2, 4, 6, and 8 hours after incubation with or without (control) $0.2 \mu\text{M}$ vincristine (B) The K/N configurations were analyzed for each time point, using 400 cells (C). Additionally, 2K2N cells (after 6 hours of vincristine incubation) were classified according to the stage of their division furrows (D).

Average values from three independent experiments are shown. Standard deviations are indicated by error bars.

E) Photographs of typical 2K2N cells and 4K2N cells after 6 hours of incubation with $0.2 \mu\text{M}$ vincristine. The cells are stained with DAPI. It can be seen that kinetoplast segregation was not inhibited.

T.brucei proteins with homology to PKARs:	1. The <i>T.brucei</i> genome data base was searched with cNMP binding domains of PKARs from:										2. Genbank was searched with the resulting putative <i>T.brucei</i> cNMP binding proteins and the proteins with the highest homologies are shown:			
	<i>T.brucei</i>		<i>S. cerevisiae</i>		<i>C.elegans</i>		<i>H.sapiens</i>		<i>D.melanogaster</i>		Protein	Organismus	% ID	overlap
	% ID	overlap	% ID	overlap	% ID	overlap	% ID	overlap	% ID	overlap				
TbPKAR	100	293	34	232	38	234	31	244	36	241	PKAR	<i>T. cruzi</i>	76	492
Tb10.70.1860	22	231	31	83	29	103	22	152	27	80	PKAR	<i>S. cerevisiae</i>	21	192
Tb08.26N11.680	26	103	29	92	26	67	21	95	23	81	PKAR	<i>T. brucei</i>	29	92
Tb11.01.7890	21	97	26	78	29	89	26	103	27	92	PKG	<i>A. mellifera</i>	33	114
Tb06.4M18.850	31	63	25	87	25	84	21	203	19	77	mucoicly inhibitor A	<i>P. aeruginosa</i>	24	169
Tb09.160.1310			27	117							putative transmembrane transport protein	<i>T. cruzi</i>	29	395
Tb09.211.1190			31	67							minichromosome maintenance family protein	<i>A. thaliana</i>	68	345
Tb11.22.0003			20	63							Phosphoglycerate kinase	<i>T. congolense</i>	32	512
Tb03.48K5.800					27	84			33	87	PKARI beta	<i>H. sapiens</i>	25	167
Tb06.2N9.830					25	104					adrenal gland protein ad-004 like	<i>C. elegans</i>	44	169
Tb927.1.1720					24	116					peptidyl-prolyl cis-trans isomerase, putative	<i>A. thaliana</i>	25	191
Tb03.5L5.210					36	68					cortical cytoskeleton component	<i>S. cerevisiae</i>	38	132
Tb07.26A24.610					27	69					RNA-dependent RNA polymerase	Little cherry virus 2	24	135
Tb07.22O10.620					24	114					GCN5-related N-acetyltransferase	<i>A. thaliana</i>	52	63
Tb11.01.7370					29	74	25	83			Predicted nucleotide-utilizing enzyme	<i>R. xylanophilus</i>	25	143
Tb04.24M18.120							23	154			similar to FYVE and collect-coil domain containing 1	<i>R. norvegicus</i>	22	742
Tb927.1.1530							23	121			MAP3Ka	<i>L. esculentum</i>	35	276
Tb11.01.5450							27	114			similar to protein tyrosine phosphatase PTP9Q22 isoform 1	<i>R. norvegicus</i>	36	325
Tb04.2H8.320							25	92			ESAG11	<i>T. brucei</i>	25	311
Tb11.02.4860							27	120			serine/threonine-protein kinase ssp1	<i>S. pombe</i>	36	313
Tb10.61.1060									30	89	possible RNA helicase-like protein	<i>L. major</i>	32	980

Attachment 3: *T.brucei* PKAR homologues

The *T.brucei* genome data base (<http://www.genedb.org/genedb/trypp/blast.jsp>, *T.brucei* predicted proteins, blastp, default parameters as set by the genedb server) was searched with the cNMP binding domains of *T.brucei* PKAR (246-488), *S.cerevisiae* (Acc No.: P07278,187-423), *C.elegans* (type I PKAR; Acc No.: OKKW1R, 134-374), *H.sapiens* (PKAR type II a, Acc No.: OKHU2R, 141-392) and *D.melanogaster* (type I PKAR, Acc No.: P16905, 134-376). All *T.brucei* proteins that had at least 60 amino acids sequence overlap to any of these PKAR-cNMP binding domains are indicated in the left column. The percentage of identical residues (% ID) and the number of overlapping residues to each of these PKAR-cNMP binding domains (overlap) is shown (left part of the table). Each of the resulting *T.brucei* PKAR homologue proteins was used to search the protein database nr at NCBI (<http://www.ncbi.nlm.nih.gov/BLAST/>, blastp) with default parameters as set by the NCBI server (right part of the table). The protein with the highest homology according to the stochastic model of Karlin and Altschul (1990) (e-value) is shown together with its organism and the number of identical residues and sequence overlap to the *T.brucei* homologue PKAR proteins. If possible, characterized proteins were chosen rather than putative ones, thus in some cases the protein with the second or third highest e-value is shown rather than a putative protein with the highest e-value. The known *Tb*PKAR subunit is marked orange, the *T.brucei* proteins with highest homologies to a PKA or PKG are shadowed blue.

Genotypes of recombinant *T. brucei* cell lines used in this study

No.	name of the cell line (used in this study)	<i>T. brucei</i> host strain	genotype of recombinants	targeting construct(s)	
				1st construct	2nd construct
1	MITat1.4 Ty1-PKAC1	MITat 1.4	Δ pkac1::BLD / PKAC1::ty1-pkac1 BLE	pTy1-PKAC1	p Δ PKAC1BSD
2	Ty1-T324	MITat 1.2 NY subclone	Δ pkac1::BLD / PKAC1::ty1-pkac1 BLE	p Δ PKAC1BSD	pTy1-PKAC1
3	Ty1-E324	MITat 1.2 NY subclone	Δ pkac1::BLD / PKAC1::ty1-pkac1(T324E) BLE	p Δ PKAC1BSD	pTy1-PKAC1-E324
4	Ty1-A324	MITat 1.2 NY subclone	Δ pkac1::BLD / PKAC1::ty1-pkac1(T324A) BLE	p Δ PKAC1BSD	pTy1-PKAC1-A324
5	T324	MITat 1.2 NY subclone	Δ pkac1::BLD / PKAC1::PKAC1 BLE	p Δ PKAC1BSD	pPKAC1-T324
6	A324	MITat 1.2 NY subclone	Δ pkac1::BLD / PKAC1::pkac1(T324A) BLE	p Δ PKAC1BSD	pPKAC1-A324
7	E324	MITat 1.2 NY subclone	Δ pkac1::BLD / PKAC1::pkac1(T324E) BLE	p Δ PKAC1BSD	pPKAC1-E324
8	HA-PKAC2	MITat 1.2 NY subclone	PKAC2::ha-pkac2 NEO	pTy1-PKAC1	
9	Ty1-PKAC1	MITat 1.2 NY subclone	PKAC1::ty1-pkac1 BLE	pTSArribTy1-PKAC3	
10	Ty1-PKAC3	MITat 1.2 NY subclone	RRNA::ty1-pkac3 HYG	pLew82Ty1-PKAR	
11	Ty1-PKAR	MITat 1.2 "single marker"	T7POL TETR NEO RDNA::ty1-pkar BLE	pTy1-PKAC1-dead	
12	Ty1-PKAC1-dead	MITat 1.2 NY subclone	PKAC1::ty1-pkac1(N165A) BLE	p Δ PKAC2HYG	p Δ PKAC2NEO
13	PKAC2 knock-out	MITat 1.2 NY subclone	Δ pkac2::NEO / Δ pkac2::HYG	p Δ PKAC2HYG	
14	PKAC2 hemizygote knock-out	MITat 1.2 NY subclone	Δ pkac2::HYG	p Δ PKAC1BSD	
15	PKAC1 hemizygote knock-out	MITat 1.2 NY subclone	Δ pkac1::BLD	p2T7 PKAR	
16	13-90 p2T7 PKAR	MITat 1.2 13-90	T7POL TETR NEO HYG RDNA::T7PRO PKAR BLE	p2T7TAbblue PKAC3	
17	1313-514 p2T7TAbblue PKAC3	MITat 1.2 1313-514	T7POL TETR NEO BLE RDNA::T7PRO PKAC3 HYG	pTSArribVASP	
18	VASP	MITat 1.2 NY subclone	RRNA::VASP HYG	p2T7TAbblue PKAC1/2	
19	1313-514p2T7TAbblue PKAC1/2	MITat 1.2 1313-514	T7POL TETR NEO BLE RDNA::T7PRO PKAC1 HYG		

Attachment 5: Overview about all recombinant *T. brucei* cell lines used in this Ph.D project

Each cell line is described in more detail in 2.1.1.2.. The cell lines have been named according to the nomenclature of Clayton *et al.* (1998). Strain 13-90 carrying T7POL TETR HYG NEO was kindly provided by G.A.M. Cross, New York (Wirtz *et al.*, 1999). Strain 1313-514 was kindly provided by Christine Clayton, Heidelberg (unpublished).